

**From the
Medical Clinic and Polyclinic I
of the University Hospital Bonn
Director:
Univ.-Prof. Dr. med. Christian P. Strassburg**

**Extracellular Vesicles,
a novel liquid biopsy marker in liver
pathophysiology**

Habilitation thesis
for obtaining the *venia
legendi* of the High
Faculty of Medicine
of the Rheinische Friedrich-Wilhelms-University
of Bonn for the teaching area
"Molecular Medicine"

presented by

Dr. rer. nat. Miroslaw Theodor Kornek

from Opole, Poland
appointed project leader GenTAnI 1831
at the Medical Clinic and Polyclinic I of the University of Bonn

Bonn 2023

Date of Habilitation Colloquium

4th of May 2023

Overview of own work used

The scientific work included in this cumulative postdoctoral thesis on "Extracellular Vesicles, a novel liquid biopsy marker in liver pathophysiology?" was performed from 2008 to 2021 at Harvard Medical School, Beth Israel Deaconess Medical Centre (BIDMC), MA, USA, at Saarland University Hospital, Homburg, Saarland, Germany, and in parts at the Medical Clinic I and III of Bonn University, North Rhine-Westphalia, Germany.

The published own original papers on which this habilitation thesis based are listed below:

Kornek M, Popov Y, Libermann TA, Afdhal NH and Schuppan D, *Human T cell microparticles circulate in blood of hepatitis patients and induce fibrolytic activation of hepatic stellate cells*, **Hepatology**. 2011 Jan;53(1):230-42 doi: 10.1002/hep.23999 **IF = 11.655** (2011)

Kornek M, Lynch M, Lai M, Exley M, Afdhal NH and Schuppan D, *Circulating microparticles: Inflammatory cell type specific biomarkers reflecting severity of inflammation in hepatitis C and NASH*, **GASTROENTEROLOGY**. 2012 Aug;143(2):448-58 doi: 10.1053/j.gastro.2012.04.031 **IF = 12.821** (2012)

Willms A, Müller C, Julich H, Klein N, Schwab R, Güsgen C, Richardsen I, Schaaf S, Krawczyk M, Krawczyk M, Lammert F, Schuppan D, Lukacs-Kornek V and **Kornek M**, *Tumour-associated circulating microparticles: a novel liquid biopsy tool for screening and therapy monitoring of colorectal carcinoma and other epithelial neoplasia*, **Oncotarget** 2016, 2016 Apr 26. doi: 10.18632/oncotarget.9018 **IF = 5.168** (2016)

Julich-Haertel H, Urban S K, Krawczyk M, Willms A, Jankowski K, Patkowski W, Kruk B, Krasnodębski M, Ligocka J, Schwab R, Richardsen I, Schaaf S, Klein A, Gehlert S, Casper M, Banales J M, Schuppan D, Milkiewicz P, Lammert F, Krawczyk M, *Lukacs-Kornek V and ***Kornek M**, *Cancer-associated circulating large extracellular vesicles in cholangiocarcinoma (CCA) and hepatocellular carcinoma (HCC)*, **J Hepatol**. 2017

Aug;67(2):282-292. doi: 10.1016/j.jhep.2017.02.024 **IF = 14.911** (2017)

*shared last author

Urban SK, Sanger H, Krawczyk M, Julich-Haertel H, Willms A, Ligocka J, Azkargorta M, Mocan T, Kahlert C, Kruk B, Jankowski K, Patkowski W, Krawczyk M, Zieniewicz K, Hołowko W, Krupa Ł, Rzucidło M, Gutkowski K, Wystrychowski W, Król R, Raszeja-Wyszomirska J, Słomka A, Schwab R, Wöhler A, Gonzalez-Carmona MA, Gehlert S, Sparchez Z, Banales JM, Strassburg CP, Lammert F, Milkiewicz P and **Kornek M**, *Synergistic effects of extracellular vesicle phenotyping and AFP in hepatobiliary cancer differentiation*, **Liver Int.** 2020 Jul 2., doi: 10.1111/liv.14585 **IF = 5.8** (2019)

Table of Contents

1	<i>Introduction</i>	6
1.1.	Liquid biopsies in Cancer	6
1.1.1.	History of liquid biopsies in Cancer	6
1.1.2.	CTCs, a liquid biopsy in use	9
1.1.3.	A brief overview of history of extracellular vesicles	11
1.1.4.	The pathophysiological role of extracellular vesicles	13
2	<i>Aims</i>	17
3	<i>Results</i>	18
3.1	EVs in chronic liver diseases	18
3.1.1	T-cell derived EVs were elevated in patients with active hepatic C virus infection	18
3.1.2	EVs derived from immune competent cells in differentiating HCV from NASH	24
3.2	EVs in cancer screening	32
3.2.1	EVs as a novel pan-cancer marker in CRC and other and other epithelial neoplasia	32
3.2.2	Diagnostic and prognostic role of circulating microparticles in hepatocellular carcinoma	39
3.2.3	Synergistic effect of two biomarkers in hepatobiliary cancer entities – A comeback of Alpha-fetoprotein (AFP).	49
4	<i>Discussion</i>	56
4.1.	Conclusion	56
4.2.	Outlook	67
5	<i>Summary</i>	68
6	<i>Acknowledgment</i>	69
7	<i>References</i>	70
8	<i>Appendix</i>	78
8.1.	Peer-reviewed publications as part of this habilitation thesis	78

1 Introduction

1.1. Liquid biopsies in Cancer

1.1.1. History of liquid biopsies in Cancer

The history of liquid biopsies in cancer is funded on a historical misunderstanding through many decades how the term *liquid biopsies* is actually defined vs. how it has been used nowadays as outlined by Todd M. Morgan in his review article from 2018 and by others. Dr. Morgan made his point that defining “what constitutes a liquid biopsy is important here.” [1](#). Furthermore, he wrote, that “[t]he term biopsy implies direct measurement of a tumo[u]r, so the liquid biopsy marker should be restricted to tests with specificity approaching that of a tissue biopsy”. In the light of this definition, it’s practically impossible to use the term *liquid biopsies* in association with extracellular vesicles (EVs) if going in line with Dr. Morgan. Probably, it should be substituted with the term personalized cancer diagnostics, or as Dr. Morgan suggested, “...the term *liquid biopsy* is becoming as commonplace as *precision medicine*, ”that's because it probably is.” [1](#).

Despite this interesting opinion, the majority of experts and their countless expert reviews including our own, original research titles and other peer-reviewed publications are still using and accepting the term *liquid biopsy* to define biomarkers that are non-invasive (urine sample, smear) or minimal-invasive (puncture to draw blood) to associate with patients’ health condition, present, past or prognostic [2](#).

One of the oldest reports on liquid biopsy that was published and is matching the widely used definition and isn’t a biopsy in the light that patient’s cell tissue was obtained and then eventually further cultured and finally analysed accordingly as done 1966 by Wichelhausen RN *et al.* [3](#), was eventually published 1990 and from far bigger ramification. Where Partin AW and colleagues reported the quantitative assessment of prostate specific antigen (PSA) in serum samples in association with prostate cancer tumour volume and differentiation and as benign prostatic hyperplasia volume [4](#). Interestingly, at that time the authors reported discrepancies between pathological stage and serum PSA that might be explained by a decrease in production of PSA with increasing histological grade according to authors of this

study. Few years later, 1991, the study results were repeated on a broader scale and published in *New England Journal of Medicine*, a highly respected and very influential clinical peer-review journal, hence, eventually becoming the gold standard in prostate cancer screening *via* a liquid biopsy [5](#). Going in line, 1994, US Food and Drug Administration (FDA) approved PSA in conjunction with a digital rectal exam (DRE) to test asymptomatic men for prostate cancer [6](#). PSA is potentially one of the first liquid biopsy marker as approved by the FDA. And probably a story of success saving countless of men lives.

Another liquid biopsy cancer biomarker was once regarded to be the one that might bring screening and diagnosis in case of hepatocellular carcinoma (HCC) to another level. This biomarker was even recommended to be included to several international and national guidelines as provided by various organizations as the American Association for the Study of Liver Disease (AASLD) and the European Association for the Study of the Liver (EASL) besides others [7-9](#) at that time. Due to the promising results, the 2003 HCC guidelines from the British Society of Gastroenterology recommended both this biomarker and abdominal ultrasound for HCC diagnosis [10](#). During the course of using this biomarker, several concerns regarding sensitivity and specificity and usefulness of cut-off values appeared, so that finally this marker was soon questioned and eventually dropped for HCC screening and wasn't recommended anymore until today by AASLD or EASL [11-13](#). The name of this promising biomarker was Alpha-fetoprotein (AFP). As indicated and very unfortunately, since it has been shown that AFP is relatively insensitive as it is only elevated in 40-60% of HCC cases, thus HCC patients exhibit normal AFP serum levels, particularly during early stage disease [14-15](#). Additionally, AFP levels can also be found elevated in non-HCC patients, including non-cancerous chronic liver diseases, intrahepatic cholangiocarcinoma and metastatic colon cancer [16](#). In sum clinical practice guidelines do not recommend AFP (or any other biomarker for that matter) for the diagnosis of HCC [12](#). However, we could demonstrate that AFP's limitations could be successfully substituted by utilizing dedicated large extracellular vesicle (IEVs) populations as published, some partially tumour derived or at least associated with liver progenitor cells by taking synergistic gains of both liquid biopsy cancer biomarkers [17](#) (in detail discussed in results part).

Besides these two proteins based liquid biopsy cancer biomarkers, some other methodical interesting liquid biopsy biomarker in cancer were actually studied, being somehow non-invasively taken as cervical smear that is routinely assessed and used to explore feasibility of experimental use of those samples for DNA testing using both Digene Hybrid Capture assay (DHCA) and polymerase chain reaction (PCR) techniques at that time, 2001, to detect high-risk human papillomaviruses (HPVs) DNA [18](#). From nowadays perspective probably to be regarded as another milestone in liquid biopsy in cancer.

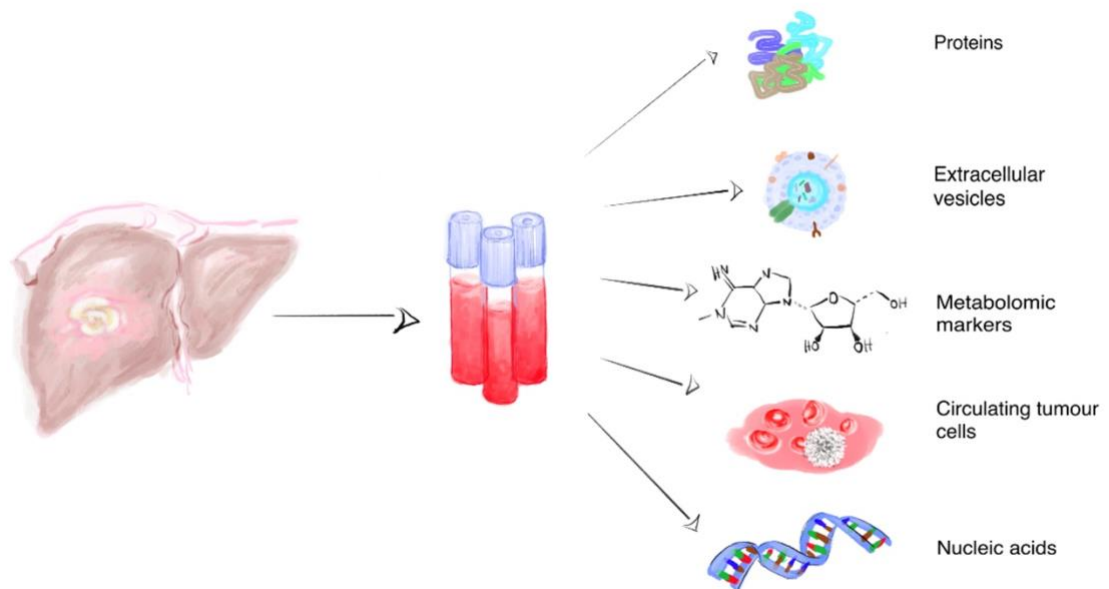


Figure 1: Liquid biopsy in HCC. Various forms of liquid biopsy, aiming at different tumour tracers, have been investigated in HCC. Some still not commercially available or approved for HCC, or are still under experimental research, including cell-free DNA and cell-free RNA (cfDNA and cfRNA, respectively), circulating tumour cells (CTCs), extracellular vesicles (EVs), and metabolomics. Figure published in *J Clin Med* by us [2](#).

Especially in the last 1 ½ decades, liquid biopsy biomarker in cancer took another spin, another boost by taking advantage of novel tracers of various tumours that might be potentially successfully utilized as summarized in figure 1. One of this liquid biopsy biomarker in cancer are circulating tumour cells (CTCs) as in detail outlined

in upcoming paragraph 1.1.2. and extracellular vesicles (EVs), paragraphs 1.1.3. and 1.1.4.. Both are somehow ancestors of the tumour mass itself, directly, being a tumour cell as CTCs are or indirectly, as being derived from a tumour cell as EVs are. One of the main differences between both markers is from numeric nature. Large quantities of tumour derived EVs vs. relative very low numbers of CTC. Therefore, we speculate that EVs might be considered as a multiplier in numbers compared to CTCs, and that EVs might be superior in liquid biopsy cancer screening and identification of the underlying cancer entity.

In the following paragraphs two of those, CTCs and EVs, will be introduced in depth since both are sharing some interesting common features regarding their analysis.

1.1.2. CTCs, a liquid biopsy in use

Circulating tumour cells (CTCs) are commonly a subset of malignant cells, that are typically disconnected from their primary tumour and circulating in peripheral blood of cancer bearing patients. CTCs can be phenotyped according their surface antigen status or analysed at their expression-, protein- and genomic level allowing their assessment of their dynamic status of the respective patients at different cancer stages and cancer heterogeneity [19:20](#). Noteworthy, CTCs were first time described by Ashworth TJ in 1869 in blood of a metastatic cancer patient indicating their role in cancer spread and by doing so paving the ground for modern CTC based diagnostics [21](#). Noteworthy, rarely, CTCs may also appear in premalignant conditions, under conditions where “potential” CTCs were detected without any molecular proof of malignancy at this stage [22](#). Nowadays, CTCs are regarded to be one of the most prominent kinds of liquid biopsy and their enumeration offers a simple, highly standardized and vigorous way to do precise medical disease pre-diagnosis, prognosis, and therapy response assessment [19:23:24](#). Several applications in various tumour entities had been published so far. Some of those, very compelling and therefor from readers interest and some are showing interesting conceptual extensions of the common CTC diagnostic routine. The authors covering certain aspects how CTCs could be potentially applied in pre-diagnosis, prognosis, and therapy response assessment have summarized those.

Considering the blood micro-environment in which CTC circulating, it is quite challenging to find a viable CTC maker to eliminate interference of billions of white blood cells, non-malignant endothelial cells, stem cells, or other blood cells as erythrocytes, thrombocytes, leucocytes etc.. This CTC marker/s should be at best located on the CTC cell membrane, therefore easily accessible and robust enough expressed on those CTCs without pathological inhibition. In other words, its shouldn't be present non-malignant cells, for example, epithelial markers which could be absent on mesenchymal cells but presented on cancer cells or *vice versa*, depending if CTC will be positive or negative selected [25](#). Newer CTC capturing strategies are either based on their physical properties as size (ISET: isolation by size of epithelial tumour cells) [26](#), as elasticity and deformability [27](#) and others that aren't depending on their surface tumour specific antigen profile. Therefore CTC isolation can be generally divided into label and label-free detection as reviewed in depth by Habli Z. *et al.* [27](#). Independent of such methodical advantages, the most established and most robust CTC capture methodology is probably the immunobead assay using epithelial cell adhesion molecules (EpCAM, CD 326) to select EpCAM⁺ CTCs (positive selection) and simultaneously to exclude CD45⁺ white blood cells (negative selection) [28](#). Keeping in mind that 1995 Gross H.J. *et al.* demonstrated that utilising flow cytometry could in fact discriminate rare cancer cells from other cells in blood and bone marrow introducing the usage of CD45 and “multiple markers, each identified by a separate colour of immunofluorescence (yellow and two shades of red) tri fluorochromes” [29](#). At that time a remarkable achievement in flow cytometry. Approximately one decade later, finally, in 2004 the CellSearchTM system was introduced and first data in Clinical Cancer Research published [28](#). The CellSearchTM system, as an only Food and Drug Administration (FDA)-cleared immunobead assay detecting EpCAM⁺CK⁺CD45⁻ CTCs has been designed to enumerate the number of CTCs in 7.5ml of whole blood under the assumption that under non-pathological conditions EpCAM⁺CK⁺CD45⁻ cells will be not present in the peripheral blood. The sensitivity exceeds 90% in metastatic breast, in metastatic prostate, and in metastatic colorectal carcinoma studies [28](#). Currently, the CellSearchTM is still regarded as the gold standard by many experts in the field. Typically, in brief, CTCs will be captured, enriched, and fluorescently stained by the automated autoprep system, and last

enumerated by the semi-automatic CellSpotter Analyzer [28](#)[30](#).

To date, inclusion of CTCs in clinical assessments for management of colorectal and breast cancers has not been accepted by the American Society of Clinical Oncology (ASCO) Tumour Marker Guidelines Committee. In 2007, CTCs and disseminated tumour cells (DTCs) were just cited in ASCOS's recommendations on cancer markers [31](#). On the contrary, lately, the American Joint Committee of Cancer (AJCC) proposed a new category for TNM staging in breast cancer M0(i+) as defined by CTCs or DTCs, if evidences of distant metastases are missing [32](#). Likewise, no other committees recommended CTC to diagnose cancer or make therapy decisions, but still possible all phases of CTC cancer guidelines will be formulated following the advantage of mature CTC techniques in the near future [33](#). Reasons might be manifold, limited possibility to detect cancer at an early time point under caveat of cancer screening. Some speculated that heterogeneity of clinical studies regarding patients/CTC donor selection might play a role asking for CTC guideline (CTC Guide) on study design and study report [33](#).

1.1.3. A brief overview of history of extracellular vesicles

54 years ago, 1967, Wolf P described something like as 'platelet dust' as a trivial by-product of cell degradation in his preparations [34](#). His electron microscopic data revealed lipid-rich particles that may originate from the osmophilic granules of platelets and interestingly the "liberation of this material" as he called, is the result of 'activation' [34](#). Nowadays, we call them extracellular vesicles (EVs) and typically activation is one of the major mechanisms *in vivo* and *in vitro* besides others to induce the release of small EVs (sEVs) or large EVs (IEVs) [35](#). 2011 we published that the induction of IEVs-release by various mechanisms as donor cell activation, as induction of apoptosis in donor cells might eventually result in IEVs differing in the capability to induce fibrolysis in recipient cells *in vitro* [36](#). At that time, we called those EVs 'microparticles' and others 'microvesicles' or 'ectosomes'. Today's International Society For Extracellular Vesicles (ISEV) guidelines, published by ISEV members as us, with the purpose to frame an urgent needed standardisation, actually agreed on to call them correctly as IEVs [37](#).

During the last decade EV research intensified by a lot, EV research caught finally attention of many research communities including liver research communities and others [38](#). Thus, advanced methodologies enabled to categorize EVs into sEVs, typically consistent of exosomes, and smallest microvesicles (MV). On the contrary, large EVs are consistent of microvesicles aka microparticles (MPs)/ectosomes [35:39:40](#). This careful differentiation implies already that distinction between sEVs and IEVs, isn't razor sharp and exactly defined by a size number. Some might say 100 nm might be the border, other 150 nm [37](#). However, exosomes and MPs/MVs can be distinguished clearly by their biogenesis. MPs/MVs could range in sizes from around 100 to 1000 nm and are shed directly from the cell membrane by a "budding process" during cellular activation or early apoptosis [35](#). Exosomes are the smallest vesicles, usually below 100 nm, and formed in endosomes and are stored within multi-vesicular bodies (MVB) that release their contents into intracellular space upon fusion with the cell membrane [41](#). Several markers for exosomes have been described including heat shock protein HSP70 and the integrins as CD63, CD9, CD8 [42-44](#). However, some of these might be expressed on MVs/MPs as CD9 and CD81 [45](#).

Apart from EV size and EV marker issues that are in detail unresolved, IEVs are somewhat representing its donor cell with its membrane-associated proteins on a smaller scale, making IEVs into an appealing field of research. sEVs and IEVs contain lipids, cytosolic proteins, some messenger RNAs and microRNAs [35:37](#). Once EVs were considered to be a kind of a cellular waste system, removing unneeded cytosolic proteins, some messenger RNAs and microRNAs [41](#). Apparently, EVs are more than that. EVs are orchestrating many physiological or pathological effects by their cargo and membrane composition and are a novel horizontal cell to cell communication route. Including the communication between tumour cell and tumour niche, inducing tumour tolerance. Apart from that, eventually its worth to highlight their potential for early cancer screening, cancer diagnosis, especially before metastasis takes place [46](#). Until now, not a single human body cell was reported to be incapacitated of the ability to release EVs including tumour cells, "underlining the attractiveness of these vesicles to use as novel minimal invasive biomarkers not only in liver tumours but also in non-malignant liver diseases" [40](#). In other words, EVs might be an outstanding tool as an integral part of a new generation of liquid biopsy cancer biomarkers.

1.1.4. The pathophysiological role of extracellular vesicles

The pathophysiological role of EVs is probably manifold. Many, many *in vitro* and *in vivo* animal experiments were done demonstrating a possible role of EVs in extracellular communication between cells proximal or distal, downstream pathway activation in EV recipient cells or even contributing to tumour tolerance [44-46](#). But, those reports could only give a glimpse that EVs, large EVs or small EVs, have actually a more pronounced pathophysiological role than thought and from far bigger clinical interest beyond cancer screening. Actually, 2017, Bernd Giebel and his group performed a first human interventional study where MSC-EVs were administered in case of steroid refractory graft-versus-host disease (GvHD) [47](#). How precisely MSC EVs did act was debatable, some thought that MSC EVs might be rather the source of a substance that was released by MSC. However, MSCs were isolated from bone marrow donors, expanded and conditioned supernatants were collected being potentially MSC-EV rich. A dose, 1 unit of MSC EVs was defined as the amount of MSC EVs released by 4×10^7 for patient's body weight. This highly cited publication demonstrated a successful experimental clinical application of MSC-EVs where MSC-EVs decreased probably indirectly numbers of patient-derived peripheral blood cells, which secreted pro-inflammatory cytokines IL-1 β , TNF α and IFN γ , likely contributing in modulating patient's immune status that led to significant improvement of clinical GvHD symptoms [47](#). Following this report, it is fair to conclude that EVs, here MSC derived EVs might play an important future role as a novel therapy option, e.g. in personalized medicine.

But the question remains, how EVs might actually contribute to pathophysiology? EVs, small or large EVs, are generally released into the extracellular space and can interact with their surroundings, mainly with neighbouring cells, somehow proximal, systemically/distal as so-called paracrine effectors [48](#) or in an autocrine way.

But in cases of hepatobiliary diseases and hepatobiliary disease models in animals, how does the role of EVs actually manifest pathophysiological or reverse pre-existing diseases?

Thus, sEVs, eventually derived from human umbilical cord MSCs reversed partially

CCl₄-induced liver fibrosis [49-50](#). Going in line that an anti-inflammatory effect of MSC EVs has been frequently reported [51-52](#). In general, EVs might be a suitable alternative to cell-based therapy, since EV donor cells could be potentially easier manipulated to fit certain therapeutic needs, including such as: EVs are typically stored easier, longer, and EV administration might be easier and without any major unwanted risk of host immune responses, as shown 2017 when MSC derived EVs were administered in case of steroid refractory graft-versus-host disease (GvHD), as discussed above [47](#).

Apart from making use of EVs with a positive effect in halting or reversing disease progression, it is therefore also important to consider depletion of EVs that have a proven harmful effect and are promoting in some disorders. There are multiple ways of preventing cell-to-cell communication *via* EVs. Inhibition of EV release has been demonstrated *in vitro* as well as *in vivo* by several studies. “Hirsova and colleagues administered rho-associated, coiled-coil-containing protein kinase 1 (ROCK1) inhibitor fasudil in a murine NASH model and observed a decrease in serum EVs, resulting in attenuation of disease progression [53](#). Chen *et al.* demonstrated an attenuation of fibrosis by preventing exosomal transfer of HSC-derived miR-214 [54](#). Another possibility to interrupt cell-to-cell communication *via* EVs is to block delivery of specific cargo, as demonstrated by Ibrahim and colleagues [55](#). They showed that toxic lipid-associated accumulation of CXCL10 in EVs is dependent on Mixed-lineage protein kinase 3 (MLK3) function, suggesting a way to reduce liver injury and inflammation. Furthermore, inhibition of EV uptake represents a promising target in disease-associated cell communication. Several molecular targets were identified and blocked to prevent liver endothelial cell-derived exosome uptake *in vivo*, resulting in attenuated fibrosis in murine CCl₄-induced liver fibrosis [56](#).” [40](#).

Moreover, it was shown by us *in vitro* that T-cell derived EVs successfully induce fibrolysis in TGF-beta activated hepatic stellate cells through a *cis* interaction between EMMPRIN (CD147) as present on T-cell derived EVs and their target cell, here hepatic stellate cells, that ultimately effected downstream ERK pathway-signalling [36](#). Interestingly, differences among EVs derived from PHA and apoptosis activated T-cells and between T-cell entities as CD4 and CD8 were noticeable,

indicating slide differences among EV depending on donor cell activation methodology. This might lead to the hypothesis of EV donor cell manipulation for therapeutics. In this case, would an overexpression of CD147 on EV donor cells result in a more pronounced fibrolytic effect on the target cells?

In fact, usage of EV as a novel vector for drug delivery isn't new. "Various loading techniques have been described in the past years and can be performed either before (by transfection or incubation of the donor cells [57-58](#) or after isolation of EVs from the donor cells. Simple methods such as incubation of EVs with the desired cargo molecules can be performed without the risk of membrane rupture but have a lower loading efficiency than extrusion, sonication or permeabilization with Saponin [59-61](#). Additional techniques include freeze-thawing and electroporation [59-62](#).

There is a broad variety of cargo molecules with which EVs can be packed. The most popular options are small nucleic acids such as miRNA and siRNA, which are protected from RNase-mediated degradation by the EV membrane. In liver disease, potential therapeutic options were implied by recent studies. Ota and colleagues demonstrated that miR30e can inhibit epithelial-mesenchymal transition (EMT) during CCA progression [63](#). A set of miRNAs contained in serum EVs of healthy patients was shown to elicit anti-fibrotic and anti-fibrogenic effects on activated HSCs and injured hepatocytes [64](#). Not only nucleic acids, but also proteins contained in EVs offer therapeutic options in liver diseases. It was demonstrated that heat shock protein (HSP)-enriched exosomes can increase the anti-tumour response of NK cells in HCC cells *in vitro* [65](#)." [40](#).

"Very promising research has been performed packing chemotherapeutic agents in EVs for HCC treatment. The advantages of EV-encapsulated drugs are their physiological and site-specific delivery and reduced toxicity to the recipient, but at the same time high efficiency. After packing MVs with methotrexate (MTX), the vesicles were internalized by HCC cells, inducing apoptosis in a considerable number of cancer cells and resulting in a second generation of tumour cell-killing vesicles released by the cells themselves [66](#). Notably, in this study, MVs packed with MTX induced tumour cell death with a much higher efficiency than the same amount of the freely administered drug. Tian and colleagues demonstrated that doxorubicin (Dox)-

loaded exosomes had an apoptotic effect on HCC cells *in vitro*, but observed no increase in efficacy compared to the free agent [67](#). “[40](#).

In sum, drug delivery *via* EVs might be a novel emerging research field, especially in the context that EVs might be stable enough to be first isolation, followed by a modulation step *in vitro* and finally administered back to the EV donor, potentially avoiding any MHC Class II mediated immunoreaction. Instead of EVs, of note patients' EV donor cells might be suitable as well and as described above modulated prior administration.

2 Aims

Since this habilitation work is written in a cumulative manner and spanning more than a decade of intense EV research by us, funded by German Cancer Foundation (German.: Deutsche Krebshilfe (DKH)) and German Research Foundation (DFG), aims are given in a retrospective approach and may differ in detail from original publications. However, the overall aim, the overall vision was to explore if large EVs (IEVs) may be beneficial in minimal invasive to non-invasive liver disease screening and diagnosis including hepatobiliary cancers being part of a novel type of liquid biopsy. This habilitation work summarizes our efforts to do so.

- I. Beginning with the question if T-cell derived EVs might have a fibrolysis inducing capability in hepatic fibrogenesis *in vitro* and may be elevated in chronic hepatitis C infection *in vivo*.
- II. Thus, proving if indicated IEVs subpopulation including T-cell and other immunocompetent cell derived IEVs may be capable to discriminate between chronic hepatitis C infection and NAFLD and healthy specimens under experimental conditions.
- III. Followed by the question if cancer cell derived IEVs, so called tumour associated large EVs (talEVs) could serve as a non-invasive biomarker in human cancer.
- IV. Furthermore, addressing the question if cancer entity depending surface antigen combination/s may be discovered aiding in the differentiation between human hepatobiliary cancer entities from hepatic cirrhosis e.g.,
- V. and ultimately separating HCC from CCA *via* IEVs in humans.

3 Results

3.1 EVs in chronic liver diseases

3.1.1 T-cell derived EVs were elevated in patients with active hepatic C virus infection

Hepatic cirrhosis is the end stage of persisting chronic liver diseases of various hepatic disorders as hepatitis A, B, C, D and E infections besides other viral infections and non-alcoholic liver steatosis or fatty liver and long-term alcohol abuse. A cure, here the reversal of hepatic cirrhosis is not yet within reach due to massive remodelling of the liver architecture from healthy organ towards an organ that lacks its multiple functions [68](#). Promising animal data does exist and indicated that in small rodent reversal of hepatic fibrosis or even cirrhosis might be possible as summarized by Kronborg, TM *et al.* [69](#). If this animal data might be translated to men, is debatable. Do small rodent hepatic fibrosis models resample sufficiently the situation in men, or are the differences between small rodent biology and humans too far apart?

Typically, liver transplantation is the only curative option left. Due to an excessive shortage of liver donors, transplantation is only available for a fraction of patients [70](#). Nowadays within Germany, liver transplantation situation did not improved pre-COVID19 pandemic and surely current pandemic did worsen the situation [71](#)[72](#). Therefore, then and now, we are still in favour that an advanced and novel antifibrotic treatment, which can prevent, halt or even reverse advanced fibrosis might be of high interest. Especially in context that already 1979 it was discussed that advanced experimental cirrhosis might be generally reversible in human and in small rodents if once pathogenic triggers will be dropped and sufficient time for recovery is given [73](#)[74](#).

Interestingly, others showed that lymphocytes derived microparticles might modulate fibroblasts in a non-cytokine-mediated manner and induce matrix-metalloproteases (MMP) that relevant in terms of collagen degradation *in vitro* [75](#). So called microparticles (MPs), nowadays named in accordance to the latest Minimal Information for Studies of Extracellular Vesicles (MISEV) guideline as extracellular vesicles (EVs) [37](#), here apparently a crude preparation of EVs derived from Jurkat T-

cells (an immortal lymphoma T-cell line) sufficiently induced in synovial fibroblast fibrolytic the expression of matrix-metalloproteases (MMP) [75](#). Those MMPs as MMP1 and as MMP3 and as MMP9 and as MMP13 were known to be capable of collagens degradation, a major component of the extracellular matrix (ECM) [76](#). ECM deposition is a cornerstone of fibrosis progression towards a cirrhotic organ. We were interested if those T-cell derived EVs might modulate fibrolysis *in vitro* and balance fibrosis in hepatic fibrogenic effector cells as activated hepatic stellate cells [36](#). And if certain EV populations could be found elevated in patients suffering from chronic liver infection as HCV [39](#).

Main Results: To address the first experimental question, Jurkat T-cells were used as potential EV donor cells and additionally primary human naïve CD4 and CD8 T-cells from healthy human specimens served as EV control donors to avoid an artificial effect that could be attributed to the use of Jurkat T-cells [36](#). Jurkat T-cells are in fact a lymphoma T-cell line isolated from a 14-year-old leukaemia patient [77](#). Additionally, these potential EV donor T-cells were activated with a mitogenic lectin as phytohemagglutinin (PHA) [78](#) to mirror a chronic inflamed organ environment or T-cell homing to liver (followed by T-cell apoptosis within the liver) according to grave yard hypothesis [79](#). Apoptosis of EV donor cells was induced with staurosporine (ST), a cell toxin [80](#). It is widely accepted that EV release could be stimulated, enhanced or triggered by EV donor cell activation and by EV donor cell apoptosis induction (here early phase of apoptosis prior cell fragmentation) [35](#). Several fractions of T-cell derived EVs were given to EV recipient cells, here hepatic stellate cells (HSCs), either the human HSC line LX2 or to primary rat hepatic stellate cells. The ratio between EVs and EV recipient cells was set to 50.000 EVs vs. 200.000 EV recipient cells. T-cell derived CD4⁺ small EVs (CD4 S100-MP) and CD8⁺ small EVs (CD8 S100-MP) were capable to induce MMPs as MMP1, MMP3, as MMP9, as MMP13 compared to large EVs (S10-MP) [36](#). Those MMPs are associated with fibrolytic processes [76](#). Nevertheless, differences were observed between EVs when EV donor cells were activated prior EV release or in the early phase of apoptosis during EV release, see please table 1.

Table 1: MMP-1, MMP-3, MMP-9, MMP-13, TIMP-1, and procollagen $\alpha 1(I)$ transcript levels were determined by way of quantitative RT-PCR in LX-2 hepatic stellate cells (HSCs; 2×10^5 cells per well) incubated with IEVs (S10-MP) or sEVs (S100-MP) for 24 hours. Only effects $>50\%$ were considered relevant. Up-regulation was categorized as follows: +++, more than four-fold; ++, more than two-fold; +, less than two-fold compared with plain medium without EVs or corresponding staurosporine control (ST); down-regulation was categorized as follows: ---, more than 75%; --, more than 50%; -, less than 50% compared with plain medium without EVs or ST; ~, not significant toward ST control. PHA= phytohemagglutinin (PHA), ST= staurosporine. Table published in *Hepatology* by us [36](#).

	Jurkat (ST)	Jurkat (PHA & ST)	Jurkat (PHA)	CD4+ (ST)	CD4+ (PHA & ST)	CD4+ (PHA)	CD8+ (ST)	CD8+ (PHA & ST)	CD8+ (PHA)
MMP-1	(++)	~	~	~	-	+	~	++	++
MMP-3	++	---	--	+	~	+	~	++	~
MMP-9	++	~	~	~	~	+	(+++)	+++	(++)
MMP-13	++	~	~	~	~	++	+	~	~
TIMP-1	~	~	~	~	~	~	~	~	~
Pro- collagen $\alpha 1(I)$	~	~	~	~	~	~	~	--	~

Overall, human primary activated T-cell derived EV were slightly more capable to inducing fibrolysis in EV recipient cells. Interestingly, T-cell derived EV dependence of observed fibrolytic modulation of the EV recipient HSCs could be further elaborated if CD54 expression was modulated with TNF-alpha prior incubation with pre-activated and apoptotic CD8⁺ derived small EVs (figure 2A). TNF-alpha had been known to stimulate the expression of CD54 on HSC. Assuming that CD54 is engaged by CD11a/CD18 on T-cell derived EVs, an increased HSC CD54 expression should enhance EV uptake [36](#). Hence, HSCs were stimulated with 10 ng/mL TNF-alpha, resulting in a significant 10-fold up-regulation of CD54 on HSCs. This pre-treatment led to a modest EV-induced increase of MMP-9, and MMP-13 expression in HSCs (figure 2A). A direct fibrolytic effect of TNF-alpha on HSCs was largely ruled out because TNF-alpha alone did not engage HSC MMP-3 mRNA upregulation. To elucidate further the result of a modulation of CD54 on HSCs by

TNF- α , HSCs were incubated with CD54 blocking or an isotype-matched control antibody 2 hours prior to addition of EVs. CD54 blocking resulted in a significant downregulation of MMP-3 and MMP-13 transcripts induced by MPs from Jurkat T cells (40% and 45%, respectively), see figure 2B.

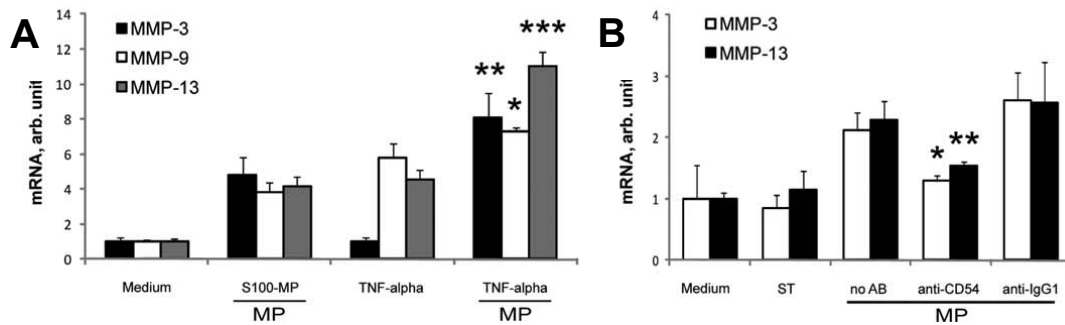


Figure 2: CD8 T cell derived small EVs interact with activated hepatic stellate cells (HSCs). A) EVs (S100-MPs) from activated and apoptotic human CD8⁺ T cells (EV donor cells) increased further indicated fibrolytic relevant matrix metalloproteases (MMP) as MMP-3, as MMP-9 and as MMP-13 in TNF- α pre-activated hepatic stellate cells (HSCs). Up-regulation of CD54 on HSC by TNF- α facilitated MMP induction after addition of EVs. *P < 0.05. **P < 0.04. ***P < 0.001. B) HSCs were incubated with CD54 blocking antibody (50 μ g/mL) or an IgG-matched control antibody for 2 hours, followed by addition of EVs from activated and apoptotic human CD8⁺ T cells for 24 hours. MMP-3 and MMP-13 transcripts were determined by way of quantitative RT-PCR. *P=0.02 **P=0.046. All experiments were performed at least twice (n=3/group). Results are expressed as arbitrary (arb.) units relative to β 2-microglobulin mRNA. Figure published in *Hepatology* by us [36](#).

This functional *in vitro* EV data supported the hypothesis of a physiological relevance of T-cell derived EVs in reversal of liver fibrosis *via* fibrolysis induction in EV recipient cells, here HSCs. Hence, T-cell derived EVs might be a possible future treatment option, since patient's own T-cells might be isolated, expanded and activated as a source of own T-cell derived EVs that may be given intravenously (i.v.) back to same patient, potentially avoiding any MCH class mismatch and rejection of those EVs. That EVs are in fact actually a suitable treatment option was demonstrated by the group of Bernd Giebel from the University Hospital Essen, Germany. In their work, Bernd Giebel and co-workers reported the successfully administration of MSC-EVs in case of steroid refractory graft-versus-host disease (GvHD) [47](#).

Prior their publication MSC were considered as an experimental therapy option in

severe therapy-refractory acute GvHD [81:82](#). How precisely MSCs did act was debatable, some thought that MSC might be rather the source of a substance that was released by MSC. Therefore, MSCs were isolated from bone marrow donors, expanded and conditioned supernatants were collected being potentially MSC-EV rich. A dose of 1 unit of MSC-EVs was defined as the amount of MSC-EVs released by 4×10^7 for patient's body weight. This highly cited publication demonstrated a successful experimental clinical application of MSC-EVs where administered MSC-EVs decreased numbers of patient-derived peripheral blood cells, which secreted the pro-inflammatory cytokines IL-1 β , TNF α and IFN γ , likely contributing modulating patient's immune status and led to significant improvement of clinical GvHD symptoms [47](#).

In spite of this hallmark publication by Bernd Giebel and co-workers demonstrating impressively that EVs might be from highest benefit as a novel treatment option, EV therapy for liver cirrhosis wait for further studies. Next, we asked ourselves, if 1st T-cell derived EVs may be detectable in patients with a chronic liver disease, speculating to balance hepatic fibrosis *via* fibrolysis or more likely to be simply activated by ongoing HBV infection. And 2nd, if T-cell derived EVs might be utilised as a minimal invasive novel biomarker.

At that time, 2011, our still preliminary finding indicated that in active hepatitis C virus infection (HCV), characterized by an ALT value above 100 IU/L, T-cell derived EVs were significantly elevated (figure 3B and C) compared to inactive HCV (ALT below 40 IU/L). Thus, those EVs, as shown for AnnV⁺CD8⁺ EVs (= CD8⁺ MPs) were probably released from activated CD8⁺ T cells, while those CD8⁺ EVs were additionally CD25⁺. AnnV (Annexin V) is a recommended EV marker [17:83-86](#). Hence only measured FACS events positive for AnnV were accounted as potential EVs. Corresponding AnnV FACS gate is depicted in figure 3A. In agreement, only triple positive large EVs as AnnV⁺CD8⁺CD25⁺ were accounted up to 80% while released from CD8 and CD25 activated T cells *in vivo* in HCV without a significant restriction to active or inactive HCV (figure 3D).

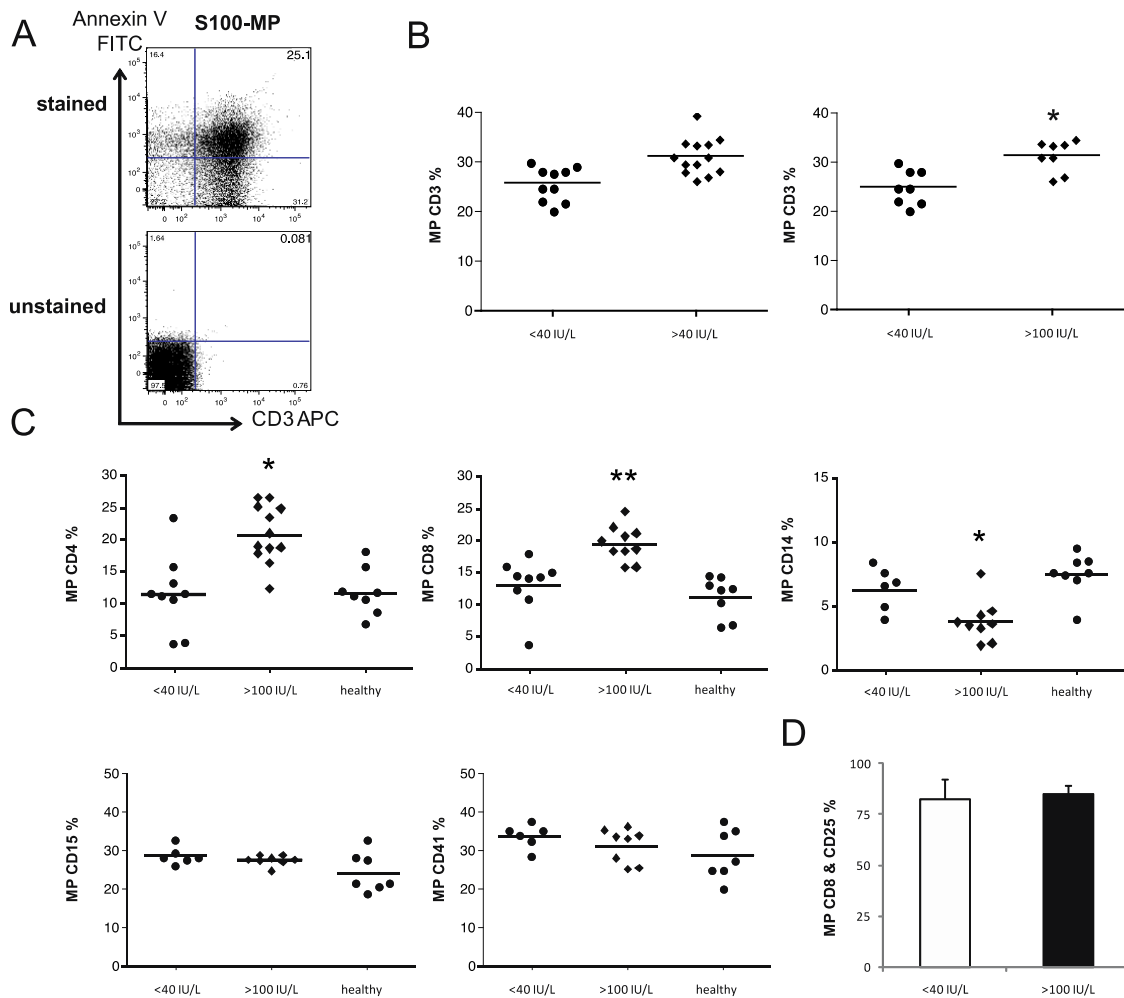


Figure 3: Plasma borne T cell-derived EVs (MPs) are elevated in patients with active hepatitis C (HCV). A) Representative FACS analysis of CD3-APC and Annexin V-fluorescein isothiocyanate double-positive EVs in healthy human T cell donor. B) Relative percentage of circulating AnnV⁺CD3⁺ EVs from patients with active HCV and normal ALT levels (<40 IU/L; n=10), elevated ALT levels (>40 IU/L; n=14), or high ALT levels (>100 IU/mL; n=8). C) AnnV⁺CD4⁺, AnnV⁺CD8⁺, AnnV⁺CD14⁺, AnnV⁺CD15⁺ and AnnV⁺CD41⁺ EV populations derived from T-cells, monocytes, neutrophils or potentially from platelets as detectable in plasma of active HCV patients with ALT >100 IU/L (n=9) compared with healthy controls and hepatitis C virus patients with ALT <40 IU/L (n=9). D) Percentage of AnnV⁺CD8⁺CD25⁺ EVs in active or inactive HCV *P < 0.05. **P < 0.005. Figure published in *Hepatology* by us [36](#).

3.1.2 EVs derived from immune competent cells in differentiating HCV from NASH

Showing first time in human HCV plasma specimens that EVs are present in active HCV, ALT >100 IU/L and elevated [36](#), we asked ourselves how EVs might be a contribution factor in personalized medicine as an novel and minimal invasive EV liquid biopsy marker. Such liquid biopsy could monitor disease progression without the need of an invasive liver biopsy [2](#). However, the next logical step towards a possible clinical translation was to design an experimental setting allowing us to assess designated EV populations in patients' plasma/serum and comparing healthy human specimens and chronic hepatitis C (CHC) patients and patients with non-alcoholic fatty liver (NAFL) or non-alcoholic steatohepatitis (NASH) to each other [85](#). This somewhat controlled experiment should prove that EVs, here certain populations, as T-cell derived, as monocyte derived, as neutrophils derived, as platelets derived and as invariant NK T-cells derived EVs being part of an EV based profile panel are capable to diagnose those liver diseases [85](#). The secondary question was, does the investigated EV populations correlate with clinical markers of hepatic diseases as ALT, AST, HCV virus load and furthermore with histological fibrosis stage and inflammatory grade as histologically assessed [85](#)?

Main Results: To assess the first main question two prevalent but mechanistically different chronic liver diseases, here CHC and NAFL/NASH were profiled and compared to each other and to healthy human specimens. Importantly, the selected EV profile panel consisting of CD4⁺ and CD8⁺ EVs (both T-cells derived EVs), CD14⁺ EVs (monocytes derived EVs), CD15⁺ (neutrophils derived EVs) EVs, CD41⁺ EVs (platelets derived EVs) and iNK T-cell derived EVs (iNKT EVs*), were investigated. Of note only AnnV⁺ EVs were accounted in our study at that time, which was in line with the “Minimal information for studies of extracellular vesicles 2018 (MISEV2018)” guidelines published few years later to which our lab contributed [37](#).

Overall, CHC and NAFL/ NASH were associated with increased percentage values of inflammatory EVs as AnnV⁺CD4⁺ and AnnV⁺CD8⁺ EVs. Actually, both T-cell derived EV populations were in CHC compared to healthy specimens elevated by 40% and 29%, respectively (figure 4). Thus, Similarly, AnnV⁺CD4⁺ and AnnV⁺CD8⁺ EVs were significantly increased in NAFL/NASH (56%) and in CHC (26%)

compared to healthy specimens (figure 4). T-cell derived EV clinical performance as measured by AUROC, sensitivity and specificity were modest (CD4 T-cell EVs: sensitivity 84%, specificity 47%, AUROC 0.56; CD8 T-cell EVs: sensitivity: 12%, specificity 97%, AUROC 0.65) [85](#). AnnV⁺CD4⁺ EVs and AnnV⁺CD8⁺ EVs did not discriminate between CHC and NAFL/NASH, both were probably due to the chronic inflammation and hence T-cell activation *per se* released and elevated [85](#).

From far more importance, monocyte derived EVs, AnnV⁺CD14⁺ EVs were in this experimental setting almost exclusively elevated in NAFL/NASH compared to CHC and associated with an AUROC value of 0.99 and a sensitivity of 100% and a specificity of 96% (cut-off: 9.71, $p < 0.0001$) [85](#).

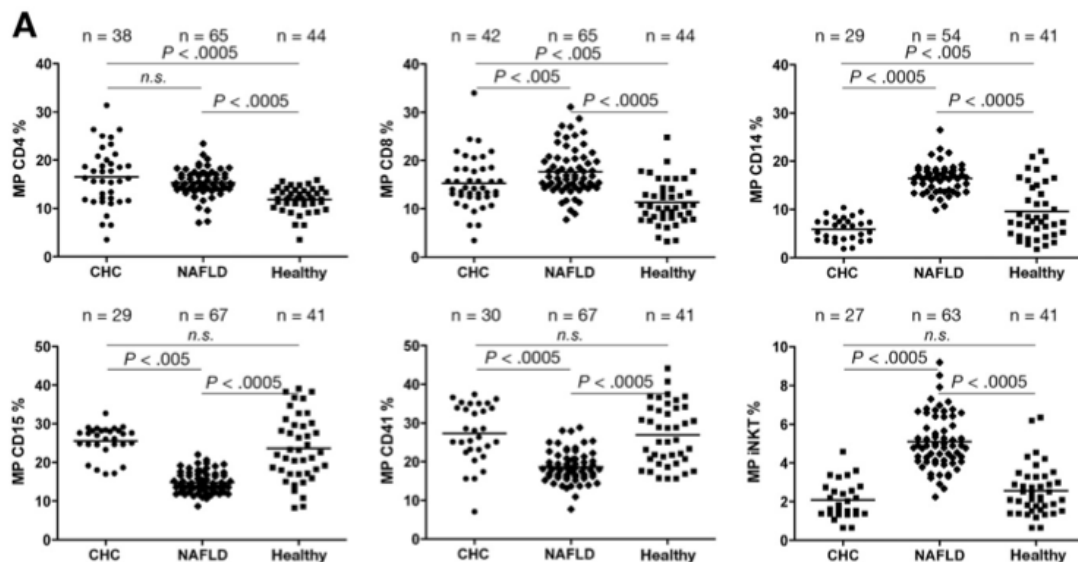


Figure 4: Profile given percentages of indicated EV populations in patients with NAFL, CHC, and in healthy controls. EVs were isolated by differential centrifugation and analysed by FACS as described in Materials and Methods [85](#). The overall P value for each EV population for the Kruskal–Wallis test was set at $P < 0.0001$ before assessing pairwise relationships by the post-hoc Dunn’s multiple comparisons approach to compare the 3 study cohorts (CHC, NAFL/NASH, and healthy controls). Figure published in *Gastroenterology* by us [85](#).

Going in line with the measured levels of monocyte derived EVs, iNKT EVs* were in NAFL/NASH increased as well, as compared to CHC and to healthy specimens (figure 4). Actually, as compared to CHC, the reported cut-off value was 3.6% with

an associated AUROC of 0.97. Overall, both AUROC values indicated clinical relevance of these two EV biomarkers in this experimental setting for the discrimination between CHC and NAFL/NASH. It would be interesting to extend this study with other liver diseases and compare these EV populations such as chronic hepatobiliary disease, as Primary Sclerosing Cholangitis (PSC), which is a long-term progressive disease of the liver or another chronic hepatic disease based on chronic hepatitis B (CHB). Nevertheless, these two EV donor cell populations, monocytes and invariant NK T-cells had been successfully linked to be key in NAFL/NASH pathogenesis [87:88](#). These immune cells derived EVs however could be associated with multiple other disease conditions. From today's perspective, 2021, we have unpublished preliminary data showing that Annexin⁺CD14⁺ EVs are actually elevated in poly trauma (Injury Severity Score >15), if internal organs are damaged such as in liver rupture and spleen rupture (own unpublished data).

In conclusion, in this experimental setting, performance of the indicated EV population was promising as a novel diagnostic tool, however their ability to perform as reported in a real clinical situation with patients of an unknown underlying hepatic diseases could be probably very well limited. Nevertheless, data obtained from the EV panel could shed light on the involvement of the EV donor cells in the pathogenesis in CHC and NAFL/NASH. Increased immune cell turnover during liver inflammation, independently if acute or chronically, and homing of those cells into the liver might contribute to elevated EV numbers of those immune competent cells [36:83:89](#). Additionally, it was reported that in fact “CD8⁺>CD4⁺ T-cell [90](#) as well as NKT cell populations [91](#) including iNKT cells [92](#) are major immune effectors in CHC, although histological inflammation of the liver appears to be better reflected by iNKT [EVs] than by blood iNKT cells. [91:92](#)”. Going in line that “iNKT cells have been implicated as major drivers of inflammation and fibrosis progression in NASH. [93:94](#)”. And that “CD14⁺ macrophages>monocytes appear to play a prominent role in peripheral adipose tissue inflammation, the associated metabolic syndrome, [95:96](#)”. Newest data on CD14⁺ immune competent cells supports our thesis that NASH is associated with CD14⁺ response, e.g. with increased CD14⁺ cell numbers if NASH is associated with fibrosis [97](#). These observations are in line that increased soluble CD14 values were associated with NAFLD [98](#). Interestingly,

AnnV⁺CD14⁺ EVs are elevated in organ damage as hepatic rupture and spleen rupture (own unpublished data) supporting our updated hypothesis that CD14⁺ EVs are not disease specifically released and discrimination between CHC and NAFL/NASH, might require additional disease controls for more accurate diagnosis. Typically, CD14⁺ macrophages are actually heavily involved in tissue repair in organ injury [99](#). Release of AnnV⁺CD4⁺ and AnnV⁺CD8⁺ EVs are universal and obviously not disease dependent but rather reflect if CD4 and CD8 cells were activated during disease progression or acute immune reaction [89](#).

The secondary question was probably besides the previously discussed diagnostic possibilities to discriminate liver diseases from a bigger clinical ramification and likely to be sooner translated. We have various Pearson correlations reported at that time as between indicated EV populations as AnnV⁺CD14⁺ EVs and as iNKT EVs with ALT and with other histological parameters. For example, in NAFL/NASH both AnnV⁺CD14⁺ EVs and iNKT EVs* correlated well with ALT ($r=0.63$; $P<0.0001$; $r=0.59$; $P<0.0001$, respectively). Sub analysis ruled out any gender bias in any correlations (data not shown).

On the contrary, in CHC, AnnV⁺CD4⁺ EVs and AnnV⁺CD8⁺ EVs correlated well with fibrosis stage ($r=0.63$; $P<0.0001$; $r=0.59$; $P<0.0002$, respectively). Unfortunately, those EV populations and iNKT EVs did not correlate with stage in NAFL/NASH (data not shown).

Interestingly, in CHC, the disease with the lowest expected sampling variability (approx. 25% and 33% for 1 Metavir grade and stage difference, respectively [100](#)), there was a good correlation of AnnV⁺CD4⁺ EVs or AnnV⁺CD8⁺ EVs with ALT, biopsy grade and stage (figures 5 and 6).

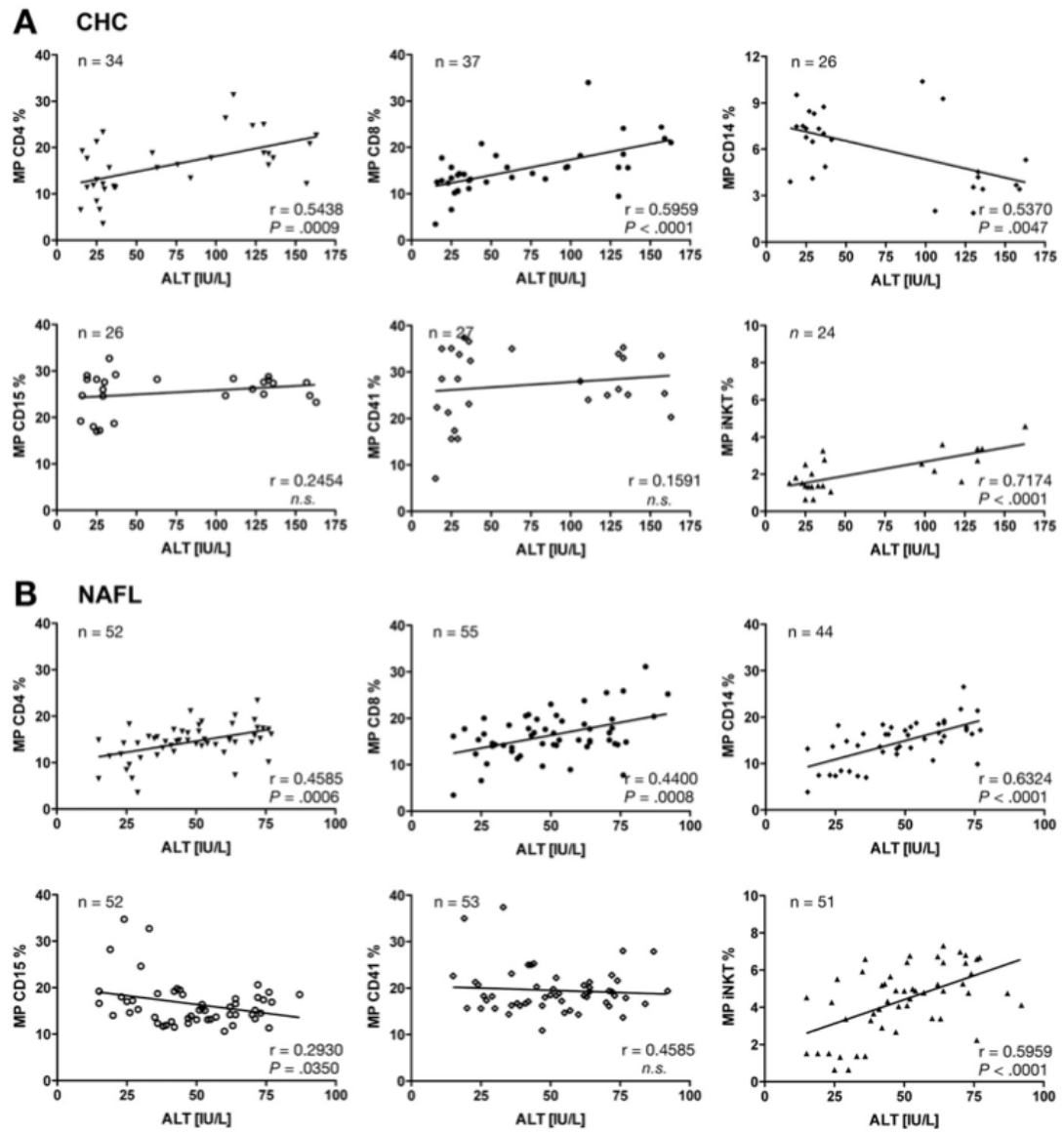


Figure 5: Correlations of investigated EV populations with ALT in CHC and NAFL. Correlations of AnnV⁺CD4⁺ EVs, AnnV⁺CD8⁺ EVs and AnnV⁺CD14⁺ and AnnV⁺iNKT⁺ EVs with patients' ALT values from blood samples used simultaneously for EV preparation and ALT determination. A) CHC, B) NAFL/NASH. Correlations were calculated using the Person algorithm with r values and P values shown in the lower right corner of each graph. Variations in numbers are due to limitations in serum. Figure published in *Gastroenterology* by us [85](#).

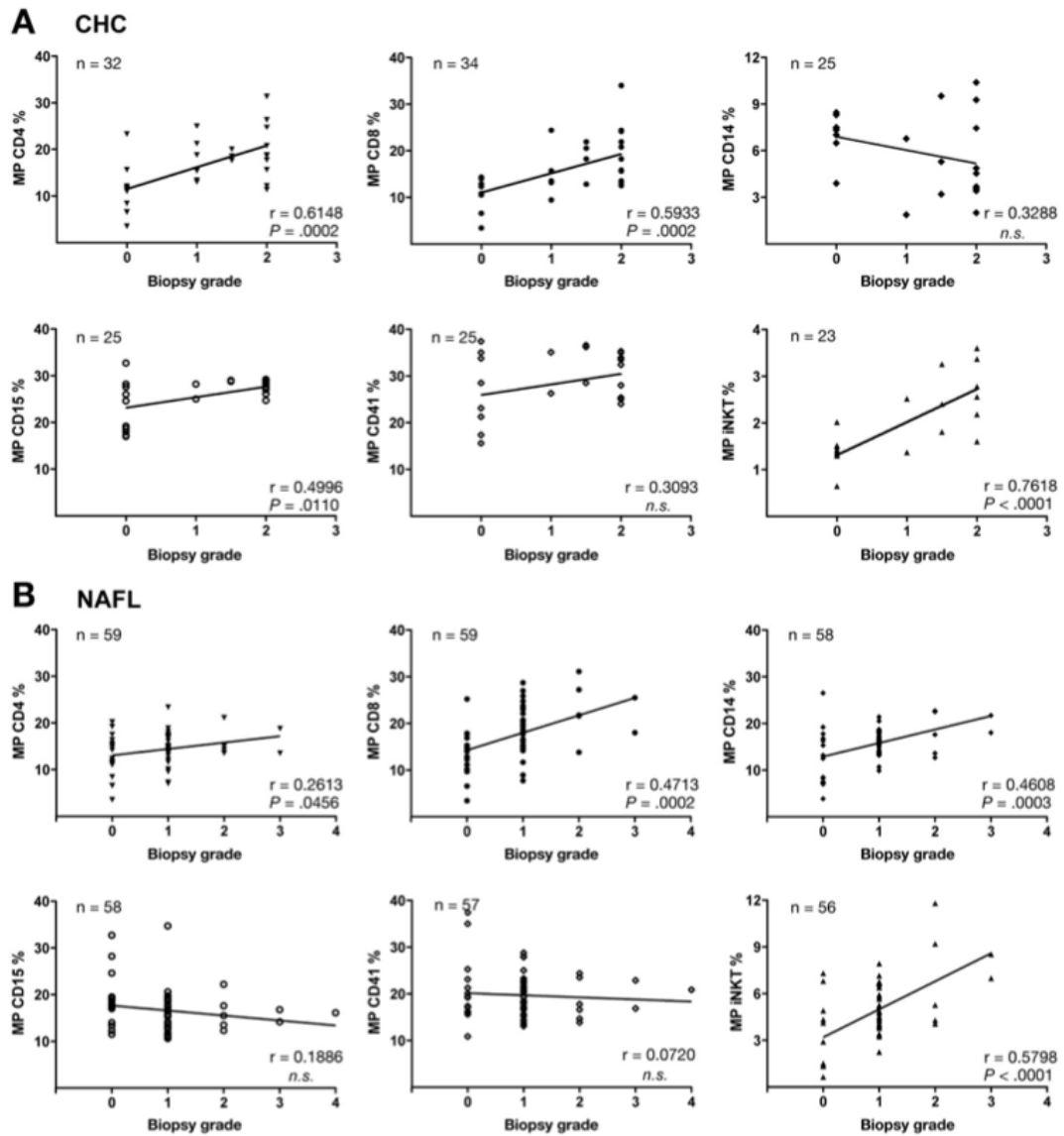


Figure 6: Correlations of investigated EV populations with biopsy grade in CHC and NAFL. Correlations of AnnV⁺CD4⁺ EVs, AnnV⁺CD8⁺ EVs and AnnV⁺CD14⁺ and AnnV⁺iNKT⁺ EVs were isolated from serum A) CHC patients, B) NAFL/NASH patients with paired biopsies. Correlations were calculated using the Person algorithm with r values and P values shown in the lower right corner of each graph. Variations in numbers are due to limitations in serum. Figure published in *Gastroenterology* by us [85](#).

Another important correlation we observed in CHC between AnnV⁺iNKT⁺ EVs and biopsy grade; $r=0.76$, $P<0.0001$, figure 6A. Additionally, the histological NAS score as considered as the gold standard for assessing/scoring NAFL, showed only a modest

correlation with AnnV⁺CD14⁺ and AnnV⁺iNKT⁺ EVs* ($r=0.60$; $P<0.0001$; figure 7). Analog to the existing sampling variability in CHC, for NAFL/NASH, sampling variability might be higher than in CHC as reported, approx. 40% for 1 Metavir grade or stage [100](#).

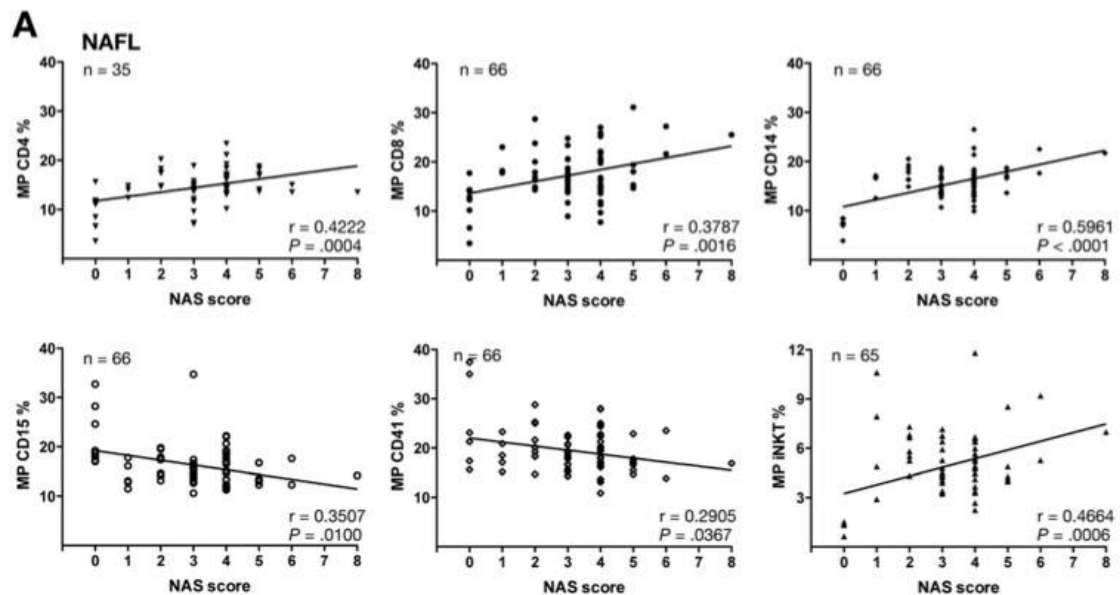


Figure 7: Correlations of investigated EV populations with NAS score NAFL. Correlations of AnnV⁺CD4⁺ EVs, AnnV⁺CD8⁺ EVs and AnnV⁺CD14⁺ and AnnV⁺iNKT⁺ EVs with NAS score using the Person algorithm with r values and P values shown in the lower right corner of each graph. Variations in numbers are due to limitations in serum. Figure published in *Gastroenterology* by us [85](#).

For example, 2012 the NAS score >4 rendered the best evidence for NASH, was consisting of 3 sub-scores for hepatic steatosis, lobular inflammation, and ballooning and was affected by significant sampling variability, especially for detection of hepatocellular ballooning, [101-102](#) which was missed in at least 50% of biopsies at that time [100](#). Additionally, due to its multicomponent character, the NAS score was influenced as probably today by the skill and experience of the reading pathologist, more than other histological scores, and was prone to intra- and inter-observer variability [103-104](#). Of note, newest research is aiming for to reduce as much as possible any intra- or inter-observer variability applying Artificial Intelligence/Machine Learning (AI/ML) resulting in promising numbers in case of reproducibility and sensitivity [105](#). However, a quantitative and objective diagnostic

test that can measure overall activation of a certain immune cell subset, such as circulating EVs, might circumvent biopsy sampling and observer variabilities in spite of recent AI/ML advances.

In sum, our correlation data between the indicated EV populations, namely AnnV⁺CD4⁺ EVs, AnnV⁺CD8⁺ EVs and AnnV⁺CD14⁺ and AnnV⁺iNKT⁺ EVs*, and stage, grade or even NAS score, could be weighted as a convincing argument that EV based liquid biopsy might be superior over conventional liver biopsy typically performed with a needle. Taking in account that liver biopsy isn't a convenient procedure, mostly associated with discomfort and requires typically an expert physician. Thus, liver biopsies are a tarnished gold standard due to high sampling variability as discussed above.

Nevertheless, this publication from 2012, might be seen as one of the frontrunners, showing the usefulness and feasibility of EV phenotyping of EV surface antigens by FACS in NAFL/NASH [85](#). Of note this was an experimental setting with two prevalent but mechanistically different chronic liver diseases, here CHC and NAFL/NASH. The usage of additional negative controls, probably other hepatobiliary diseases as PSC, organ damage as liver rupture, as biliary cancer entities would be beneficial from today's perspective. Due to the low methodological standardisation at that time, we consider a multi-centric approach with UpToDate methodology of EV isolation as SEC and EV phenotyping as currently done with the NanoView EVChip Reader R100 (NanoView Biosciences) would be of highest benefit. These should be considered if this finding should be considered for translation from bench to bed side.

Technical note: AnnV⁺iNKT⁺ EVs* are actually stained for the following antibodies including AnnV: Valpha24 and Vbeta11. Valpha24 and Vbeta11 are markers for invariant NK T-cells, hence Valpha24 and Vbeta11 double positive cells or EVs are iNKT origin [85-92](#).

3.2 EVs in cancer screening

3.2.1 EVs as a novel pan-cancer marker in CRC and other epithelial neoplasia

After showing that EVs and certain EV populations are actually beneficial in separating CHC from NALF/NASH, we addressed the next rational question, if our concept of utilizing EVs in disease diagnosis might actually be true in cancer diagnosis *per se*. Since hypothetically any cell, any cancer cell *in vitro* is capable to shed EVs. Furthermore, several hints were at time available indicating that EVs in cancer are a diagnostic option, but their scientific value is disputable due to technical limitations at that time [106-107](#). However, one limitation was due to missing negative controls, which biased experimental results. For example, “elevated levels of CD95L expressing large EVs have been found to be associated with oral squamous cell carcinoma (OSCC) [108](#). However, CD95L expressing large EVs have also been associated with pregnancy, pinpointing that the use of single surface markers is not sufficient to associate large EVs with specific diseases [108-109](#). In 2008, a hepatocellular carcinoma (HCC) pilot study was published, showing that the levels of endothelial (CD31⁺/CD42⁻) and hepatocyte (HepPar) derived large EVs in HCC liver transplant patients were altered after surgery and correlated with the clinical outcome [106](#)” [110](#). Therefore, we postulated if we may phenotype successfully EVs by a chosen set of antibodies against designated EV surface antigens, that are associated with cancer, we might succeed. The aim was at that time two-fold. 1st to identify an EV surface antigen or antigen combination that might be used as a pan cancer marker successfully indicating the presence of a cancer within the human body and 2nd to explore if the level of those cancer related EVs might reveal tumour burden (size of tumour).

Main results: Regarding the first aim, in 2016 we showed that AnnV⁺EpCAM⁺CD147⁺ IEVs were elevated in various cancer entities such as colorectal carcinoma (CRC), non-small cell lung carcinoma (NSCLC) and pancreatic carcinoma (PaCa) [111](#), see figure 8. IEVs were isolated by differential centrifugation of sera of 103 confirmed cancer patients. Median AnnV⁺EpCAM⁺ IEVs values were significantly elevated in patients with CRC, NSCLC, PaCa by an average of 2.3-fold

irrespective of the tumour entity and size (figure 8A) [111](#). Surprisingly, AnnV⁺EpCAM⁺ IEVs were also found elevated in thyroid nodules patients (short: struma) as compared to healthy controls by 1.9-fold [111](#).

To increase cancer specificity in that sense that obviously non-malignant thyroid nodules will be not falsely identified as a cancer entity, we extended our pan-cancer tumour associated antibody by EMMPRIN (CD147). CD147 was reported to be closely associated with cancer since some cancer entities are actually expressing CD147 [112-115](#). Therefore, as expected, our selected antigen combination of EpCAM and CD147 successfully detected *in vivo* derived AnnV⁺CD147⁺EpCAM⁺ IEVs in patients' serum derived EVs. AnnV⁺CD147⁺EpCAM⁺ IEVs median values significantly increased in cancer patients by an average of 4.8-fold (figure 8B) across all investigated tumour entities. Additionally, the CD147⁺EpCAM⁺ IEVs were significantly reduced compared to the elevated cancer IEVs values in thyroid nodules (figure 8B).

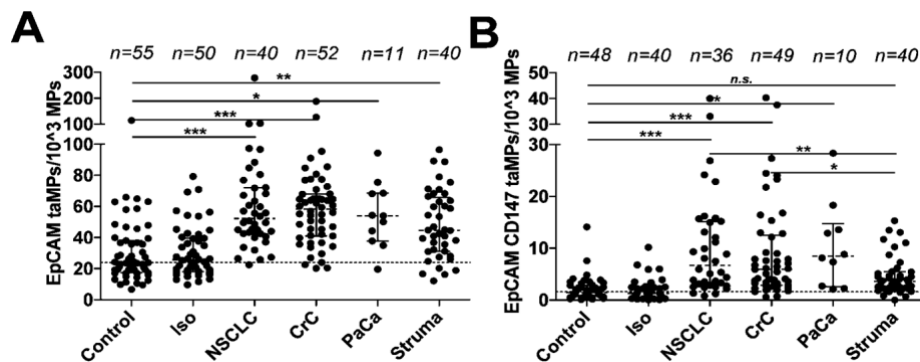


Figure 8: Detection of AnnV⁺EpCAM⁺ and AnnV⁺EpCAM⁺CD147⁺ large EVs in sera of indicated cancer patients. IEVs were isolated by differential centrifugation and analysed by FACS as described in our *Oncotarget* publication. The indicated p-value for each IEVs population, (A) AnnV⁺EpCAM⁺ IEVs and (B) AnnV⁺EpCAM⁺CD147⁺ IEVs as predictor of controls vs. cancer and control vs. *struma nodosa* (thyroid nodules; short: struma) was calculated by using one-way ANOVA test including multiple comparisons using Dunn's post test. Shown are medians with 25 and 95 percentiles. P-values are shown as indicated; *= $p < 0.05$, **= $p < 0.005$, ***= $p < 0.0005$ (one-way ANOVA test including multiple comparisons using Dunn's Multiple Comparison Test). Overall, an error level $p < 0.05$ was considered significant. Note: taMPs = tumour associated MPs = tumour derived IEVs. Figure published in *Oncotarget* by us [111](#).

These results highlighted both the potential advantage but also the limitations of this relative new technology at that time in 2015. By using multiple markers rather than a single tumour marker on the surface of IEVs we could overcome these limitations. Our approach suggests that tumours can be detected by quantification of AnnV⁺EpCAM⁺ IEVs, but it is far superior and more reliable when using a surface marker combination for AnnV⁺EpCAM⁺CD147⁺ IEVs independently of the underlying cancer entity [111](#).

Still, certain disease/health circumstances associated with epithelial damage, such as *struma nodosa* (thyroid nodules), do not allow to draw any conclusions based on only AnnV⁺EpCAM⁺ IEVs *per se*. Thus, disorders primary causing epithelial damage should be regarded as exclusion criteria if only EpCAM is used for IEV surface phenotyping. However, this observation led to the hypothesis that a cancer-entity specific antigen combination on IEVs might be feasible to find, and use to differentiate underlying cancer entity or cancer origin. In agreement, we evaluated AnnV⁺EpCAM⁺CD147⁺ IEVs as a specific “pan-cancer-EV” marker that could be used to screen for early cancer outbreak, particularly when conventional differential diagnostic tools would not yet indicate the presence of tumour or no indication is given to apply them.

In past decade, EpCAM (CD326) turned out to be a useful marker to detect circulating tumour cells (CTCs) or tumour stem cells [116-119](#). Although CTCs are rare, the optical detection of such EpCAM⁺ tumour cells as done with the CellSearch™ System is in clinical use for a limited number of cancer entities [119-121](#). This method depends on the metastatic spread of tumour cells from the primary tumour side and free floating of tumour cells in blood circulation [121](#). In contrast to these scarce CTCs, EpCAM⁺ EVs might be larger in numbers, a possible multiplier of EpCAM⁺ tumour cells *in vivo*. We showed that AnnV⁺EpCAM⁺CD147⁺ IEVs were far superior than EpCAM⁺ IEVs in terms of detecting and distinguishing cancer from other epithelial damage [111](#). More importantly, IEV shedding, including of AnnV⁺EpCAM⁺CD147⁺ IEVs, was not dependent on metastatic spread rather than activation and apoptosis [111](#). Thus, these tumour EVs might reach the circulation [122](#) as CTCs and not be restricted to metastatic tumour spread [110:123](#).

Of course, we asked ourselves, whether our IEV data was somewhat connected randomly to tumour load, or as previously reported for sEVs by Melo *et al.* were statistically significant [124](#). We and Melo *et al.* used R0 resection of full tumour load as a simplified and reproducible model of a typical curative cancer therapy. As Melo *et al.* for sEVs, we observed a significant drop of IEVs from day 7 postoperatively (post-OP) as compared IEVs values drawn preoperatively (pre-OP) (figure 9). Of note, drop of sEVs as reported by Melo *et al.* was inferior to our reported changes [124](#) and the observed decreased levels of IEVs compared between different tumour entities. We speculated in our publication that IEVs stay longer in circulation than sEVs and will drop from day 10 post-OP on [111](#). Nevertheless, and in spite of thinkable limitation, as how stable sEVs are compared to IEVs, we assume that tumour derived IEVs, from large or small EV entity, will drop after a complete tumour load removal (R01 resection) or tumour load shrinking due to an anti-tumoural therapy [111](#).

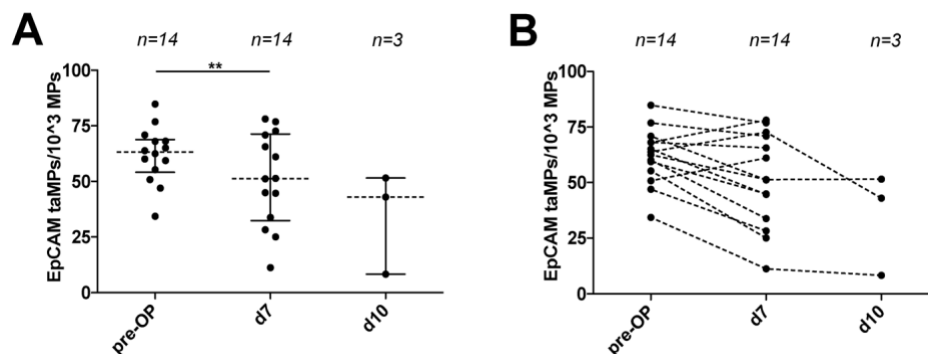


Figure 9: Detection of EpCAM⁺ large EVs in CRC sera patient samples post R0 resection. (A) Ann⁺EpCAM⁺ IEVs levels 7 days post CRC tumour resection and at day 10 post-OP. (B) Paired display of accompanied pre-OP and post-OP values of indicated IEVs populations. Shown are indicated median with 25 and 95 percentile including p-value as indicated; *= $p < 0.5$, **= $p < 0.005$, ***= $p < 0.0005$, n.s.= not significant (paired t-test with Wilcoxon matched pairs signed rank-test). Overall, an error level $p < 0.05$ was considered significant. Note: taMPs = tumour associated MPs = tumour derived IEVs. Figure published in *Oncotarget* by us [111](#).

Another aspect that was addressed, was the question if IEV levels do actually correlate with the total tumour load, as size of tumour given in cm³. Unfortunately, our data regarding this question showed clearly the limitation of IEVs in assessing

tumour load. In NSCLC we did not draw any correlation better than $r = 0.5$ between tumour volume and measured IEV levels (figure 10). In CRC, AnnV⁺EpCAM⁺CD147⁺ IEV levels were correlating with CRC tumour volume significantly ($r=0.7288$, $P<0.0001$, figure 10A). If CRC tumour volumes were divided into subgroups spanning from 0 (healthy controls), over 1–10 cm³, 10–50 cm³, 50–100 cm³ and above 100 cm³ of CRC tumour volume, we concluded that 10 cm³ of CRC volume might be the lower detection limit of our used methodology at that time (figure 10B) [111](#). Additionally, no correlations were observed between UICC scores or metastatic phenotype exceeding an r value of 0.5. Thus, matched sera CEA and CA19–9 sera values did not show any dependence ($p>0.05$) [111](#). We speculate that since EVs shed from tumour cells and generally interact with the tumour environment, with CAFs and with immunocompetent cells as T_{regs}, consequently not all EVs that had been shed by the tumour may reach the circulation and as observed for CTCs.

It's shown by others that in case of CTCs, especially in case of CTC clusters, CTC might get stacked in narrow capillaries and therefore potentially contribute to metastasis in highly vascularized organs such as liver and especially lung [125](#). Therefore, it is fair to speculate that most CTCs that enter a highly vascularized organ will not exit and therefore not being accounted or available for CTC diagnosis based. Whether measured tumour associated IEVs are prone to a similar bias as CTCs is still open. Nevertheless, a possible robust correlation between these IEVs and tumour load might depend on the selected antigens of tumour associated IEVs and on the investigated cancer entity. Notably, in CRC a correlation of $r=0.73$ is considered good and from clinical relevance [111](#).

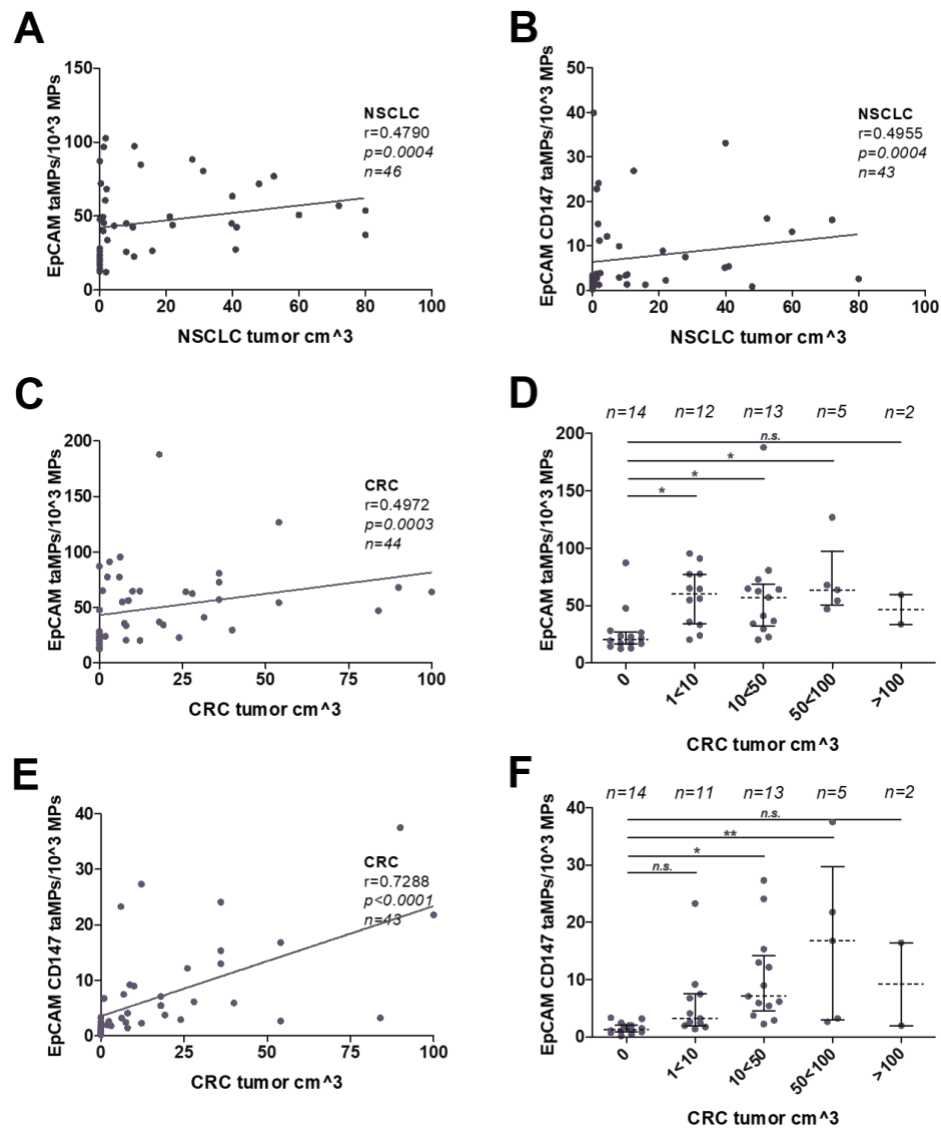


Figure 10: large EVs predict tumour volumes. Measured AnnV⁺EpCAM⁺ IEVs and AnnV⁺EpCAM⁺CD147⁺ IEVs were set in correlation (Spearman algorithm) to associate patient tumour volumes; (A/B): NSCLC; (C-F): CRC. Correlations were restricted to 100 cm³ of tumour volume. (D/F) Detail analysis of indicated tumour ranges revealing the possible lower and upper detection limit. Shown are indicated median with 25 and 95 percentile including p-value as indicated; *=p<0.5, **=p<0.005, ***=p<0.0005, n.s.= not significant (one-way ANOVA test including multiple comparisons using Dunn's Multiple Comparison Test). Overall, an error level p<0.05 was considered significant. Note: taMPs = tumour associated MPs = tumour derived IEVs. Figure published in *Oncotarget* by us [111](#).

In summary we provided evidences that tumour associated IEVs were successfully quantified by a set of tumour associated surface antigens that are present on those IEVs [111](#). Furthermore, we shown that IEVs have the same potential as sEVs in diagnosis as reported by Melo *et al.*. Of note, sensitivity and specificity are not comparable since Melo *et al.* reported a sensitivity of astonishing 100% and a specificity of 100%, too [124](#). But comparing both methodologies as used at that time, we see huge differences and probably at that time more potential in IEVs quantification in tumour diagnosis specially to discriminate tumour entities as shown by us in 2017 and in 2020 [17·84](#). Our methodology, using certain combination of surface antigens on IEVs allowed us to detect several antigens simultaneously on each IEV vesicles [126](#) whereas Melo *et al.* could detect only one antigen on each sEV at that time [124](#). This was the consequence of the facts that sEVs were not detectable by conventional flow cytometer devices due to their size [127](#), hence, sEVs were captured unspecific by latex beads first. These latex beads are in mean 2000 nm in size and are capable to bind an unknown number of various sEV populations originating from different cell types [124](#). Therefore, if two antigens would be stained on sEVs bound to the same latex bead, it would be impossible to know if both antigens were present on the same sEV or on two different sEVs. Consequently, the methodology of using latex beads for flow cytometer depending analysis of sEVs at that time were not suitable for a combinatoric approach as our one, to assess two, three or more antigens simultaneously on one IEVs as demonstrated for AnnV⁺EpCAM⁺ IEVs and AnnV⁺EpCAM⁺CD147⁺ IEVs. It is fair to say, that 2021, our current used methodology in the lab was further developed using the machine from NanoView Biosciences and it allows us to quantify four antigens simultaneously on sEVs (own unpublished data). Noteworthy, today the Amnis ImageStream device is capable to provide the needed resolution and sensitivity for sEV analysis too [128](#).

3.2.2 Diagnostic and prognostic role of circulating microparticles in hepatocellular carcinoma

After showing own scientific evidence that EVs might bear a bigger role as thought in cancer detection, in cancer surveillance as shown by Melo *et al.* and their work on Glypican1⁺ EVs in patients with pancreatic cancer [124](#), we hypothesize that a set of antigens being simultaneously present on the same IEV could lead to a cancer entity specific composition of those antigens [126](#). Furthermore, additionally we hypothesized that one EV surface antigen might be related to several cancer entities, and by adding more antigens in that fashion the specificity of cancer entity will be achieved [126](#). In figure 11 we depicted how increase of designated surface antigens may add to cancer entity specificity in order to differentiate HCC, CCA, CRC and NSCLC from each other. In fact, our next aim was to provide substantial evidence that a set of designated EV surface antigens simultaneously detectable on same IEV could achieve such cancer specific differentiation across the indicated cancer entities and controls such as non-malignant liver cirrhosis [84](#).

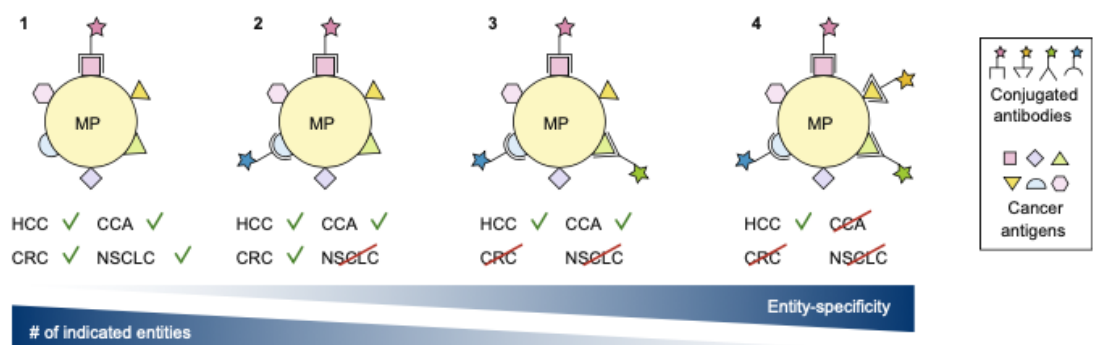
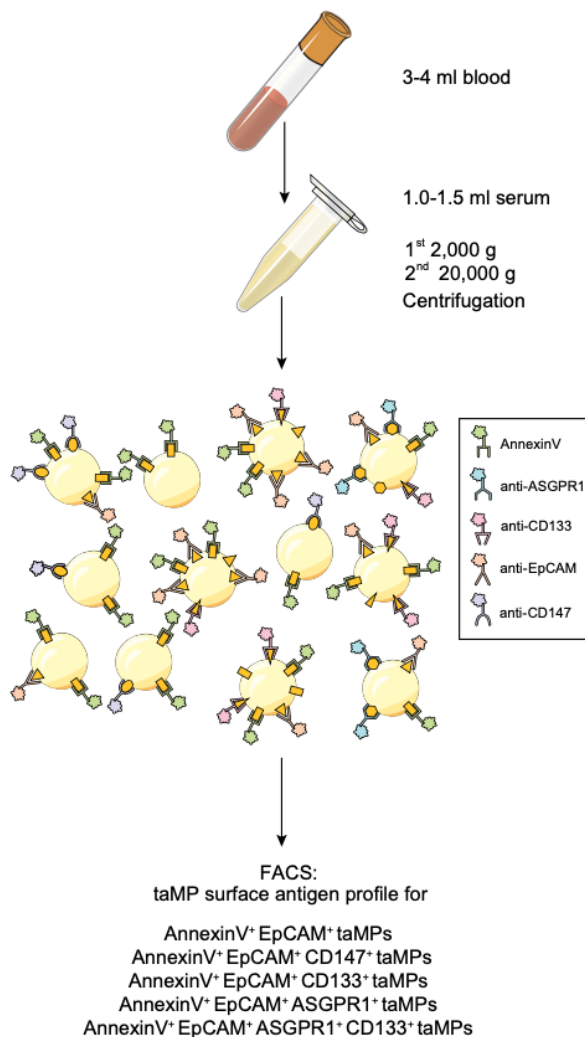


Figure 11: “Principle of entity-specific cancer detection by characterising combinations of surface antigens on [EVs]. The scheme illustrates the hypothesis that the number of antibodies incorporated into the analysis of surface antigens on [EVs] influences entity-specific detection of cancer. Hypothetically, an [EV] that is characterised by only one surface antigen is likely to be representative for more than one cancer entity, whereas an [EV] that is characterised by two or more antigens simultaneously will probably represent less entities, which is due to the heterogeneity of presented antigens on the respective entities. Thus, using a combinatorial approach of more than one antibody for characterisation of [EV] populations might likely increase the entity-specific detection of cancer. CCA, cholangiocarcinoma; CRC, colorectal carcinoma; [EV, extracellular vesicle;] HCC, hepatocellular carcinoma; NSCLC, non-small cell lung carcinoma.” Figure published in *Journal of Hepatology* by us [126](#).



Minimal invasive sampling

Isolation/Preparation

MP profiling

Figure 12: “ta[IEV] surface antigen profiling workflow. Schematic summary of the possible [IEV] profiling workflow is depicted based on the availability of 1 mL serum. [IEVs] will be enriched by sequential centrifugation resulting in an ultrapure [IEV] fraction. [IEV] profiling is performed by FACS analyses (fluorescence-activated cell sorting) for the indicated surface antigen combinations [as detailed in our *Oncotarget* publication]. Some of these combinations are present on [IEV] associated with liver cancer (AnnexinV⁺EpCAM⁺CD133⁺ [IEV], AnnexinV⁺ EpCAM⁺ ASGPR1⁺ CD133⁺ [IEV]) while some others are generally accompanying multiple cancer entities (AnnexinV⁺EpCAM⁺ [IEV] and AnnexinV⁺ EpCAM⁺ CD147⁺ [IEV]). The most likely antigen combinations are depicted consisting of the indicated antigens

e.g. CD133, ASGPR1 etc., plus AnnV, our general [IEV] marker. [IEVs] that are positive for all the listed antigen combinations will be evaluated by FACS. AnnexinV serves additionally as a general [IEV] quantification marker.” ta[IEV], tumour associated large extracellular vesicles. Note: taMPs = tumour associated MPs = tumour derived IEVs. Figure published in *Journal of Hepatology* by us [84](#).

Main goal was to explore a liver cancer specific combination of antigens simultaneously detectable on IEVs (at that time called microparticles (MPs) by us and others [35:36:39:66:75:80:85:106:111:122:126:129:130](#)) that will allow to discriminate healthy individuals from patients with a hepatic disorder and further on to dissect the underlying hepatic liver disorder either as non-malignant cirrhosis or hepatic cancer, here HCC or CCA. For that purpose, we have chosen besides AnnV, a general IEV

marker, other antigens of interest as CD133, as CD147, as EpCAM associated with cancer *per se* as shown previously by us [111](#) and as Asialoglycoprotein Receptor (ASGPR1) a hepatocyte specific antigen [131](#). Various combinations of interest of those antigens on same IEVs are depicted in figure 12. We hoped to achieve a liquid biopsy that in fact may substitute AFP or at best be far superior than AFP and other often used proteins as CA19-9 or CEA, that are considered not to be cancer specific for liver cancers and other malignancies *per se* [2:16](#).

Main results: We speculated that the use of additional antigens as CD133 and as ASGPR1 plus EpCAM, previously published tumour-associated antigen-combination [111](#)·[117](#)·[131-134](#), could probably identify liver malignancies as HCC and CCA. To do so, first, we examined expression levels of those antigens on commercially available tumour cell lines to check if those antigens could separate them. Hence, if selected surface antigens will separate successfully those cell lines by FACS methodology, it should be feasible to do so with IEVs too, since those surface antigens should be hypothetically expressed on IEVs as well [126](#).

In fact “EpCAM, CD147, CD133 and ASGPR1 as potential surface antigens for [IEVs] showed medium to high expression on human tumour cell lines (HCC: HUH7 [135](#); hepatoblastoma: HepG2 [136](#); liver adenocarcinoma: SK-HEP-1 [137](#)) *in vitro* with EpCAM ranging from 95 to 99% of all living cells, except on SK-HEP-1 cells; with CD147 ranging from 82 to 85%, except on HuH7 cells; with CD133 ranging from 93 to 99%, except on SK-HEP-1 cells, and with ASGPR1 ranging from 91 to 99% [(figure 13)]. Importantly, ASGPR1 was not detectable (<1.5%, $p < 0.005$, figure 13B) on human pancreas ductal adenocarcinoma cell lines Panc-1 [138](#) and Capan1/-2 [139](#)·[140](#), illustrating the importance of these antigens as possible cancer antigens and confirming ASGPR1 as a liver tumour restricted antigen. From these *in vitro* data we concluded that distinct cancer specific antigen combinations, on donor tumour cells and their tumour cell derived [IEVs] could specifically be associated with liver tumours.” [84](#).

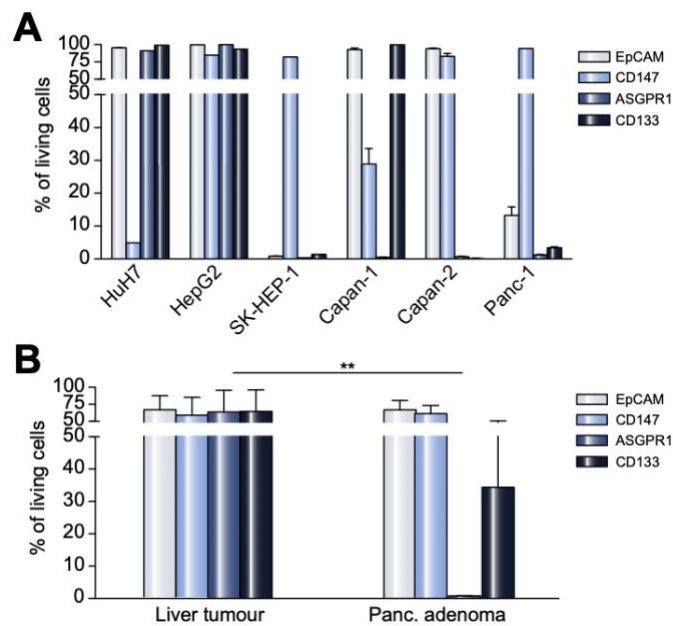


Figure 13: “Expression profiles of the surface antigens EpCAM, CD147, ASGPR1 and CD133 on human tumour cell lines. 16 to 24 hrs after serum starvation cells were harvested and fluorescently stained for their surface antigens, followed by FACS analysis. (A) Percentages of the antigen-bearing populations among living cells are depicted in each individual cell lines. (B) The summed marker expression present together in all three liver tumour cell lines (HuH7, HepG2 and SK-HEP-1) and the pancreatic adenoma cell lines (Capan-1, Capan-2 and Panc-1). A two-tailed Mann Whitney test was performed to compare the antigen expressing cell populations (* = $p < 0.05$, ** = $p < 0.005$, *** = $p < 0.0005$.)” [84](#). Note: taMPs = tumour associated MPs = tumour derived IEVs. Figure published in *Journal of Hepatology* by us [84](#).

Confirming our selected antigen candidates successfully on indicated tumour cell lines (figure 13), next we aimed to validate those selected antigens on IEVs in our human specimens (figure 14A, B, C). AUROC values, sensitivity and specificity scores indicated that the combination of EpCAM and CD133 as detectable on $\text{AnnV}^+\text{EpCAM}^+\text{CD133}^+$ IEVs and EpCAM, ASGPR1 and CD133 as present on $\text{AnnV}^+\text{EpCAM}^+\text{ASGPR1}^+\text{CD133}^+$ IEVs might be suitable to separate patients with a liver disorder (HCC and CCA and non-malignant cirrhosis) from healthy controls (figure 14 A, C, E). In detail, in “liver disorders cohort, consisting of patients with cirrhosis without malignancy and HCC or CCA, $\text{AnnV}^+\text{EpCAM}^+$ [IEVs] were in general significantly increased by 2.5-fold ($p < 0.0005$, one-way ANOVA with Dunn’s

test, [figure 14A]), with specific increases in patients with HCC by 2.7-fold, CCA by 2.7-fold and cirrhosis by 1.8-fold ($p < 0.005$, $p < 0.0005$, respectively). When the surface antigen combination was extended by CD133 [figure 14B] and AnnV⁺EpCAM⁺CD133⁺ [IEVs] were assessed, we observed a liver disorder (cirrhosis without malignancy, HCC and CCA combined) restricted increase of AnnV⁺EpCAM⁺CD133⁺ [IEVs] by 2.6-fold ($p < 0.005$, one-way ANOVA with Dunn's test), and individual increases for HCC by 2.6-fold, CCA by 3.3-fold, and cirrhosis by 2.3-fold ($p < 0.05$, $p < 0.005$, respectively). As mentioned earlier, no increased AnnV⁺EpCAM⁺CD133⁺ [IEVs] values were noted in patients with CRC, NSCLC and inguinal hernia as compared to CTRL. Whereas the accompanied levels of significance were not impressive for AnnV⁺EpCAM⁺CD133⁺ [IEVs], the separation between CTRL and liver tumours and cirrhosis markedly increased when staining was extended by ASGPR1. Overall, AnnV⁺EpCAM⁺CD133⁺ASGPR1⁺ [IEVs] in liver disorders were increased by 3.1-fold ($p < 0.0005$, one-way ANOVA with Dunn's test); individual increases were 3.1-fold for HCC, 3.7-fold for CCA, and 2.5-fold for cirrhosis ($p < 0.0005$, $p < 0.0005$, $p < 0.05$, respectively)." [84](#).

However, those IEVs populations somehow still failed to separate between liver disorders such as HCC, CCA and HCV/HBV induced non-malignant cirrhosis (F4). Of note, desired goal would have been to separate those liver disorders from each other or at least from non-malignant cirrhosis.

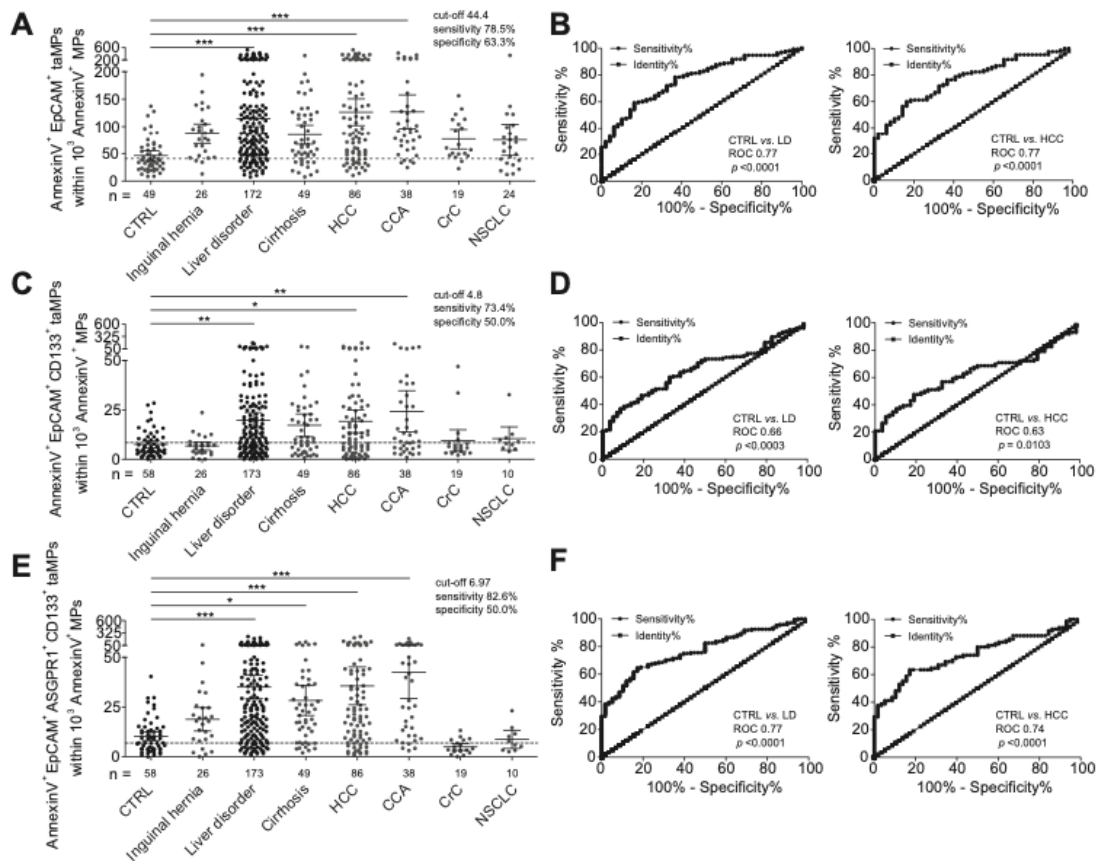


Figure 14: “Detecting EpCAM⁺CD133⁺ and EpCAM⁺ASGPR1⁺CD133⁺ [IEVs] in human serum samples patients with indicated liver disorders can be discriminated from controls. [IEVs] were isolated and characterised by FACS from the sera of cancer patients (HCC, CCA, CRC, NSCLC), controls (CTRL), patients with inguinal hernia and patients with cirrhosis (Cirrhosis). Cohort ‘Liver Disorder’ combines HCC, CCA and cirrhosis patients. (A-C) Visualises [IEVs] profile for each study cohort including EpCAM⁺ (A), EpCAM⁺CD133⁺ (C) and EpCAM⁺ASGPR1⁺CD133⁺ (E) populations given in mean with 95% CI. Dotted lines represent cut-off values. Differences were assessed by one-way analysis of variances (ANOVA) including Dunn's test. For each population the corresponding ROC curve and AUROC value is displayed in (B), (D) and (F) in order to analyse the diagnostic performance of the respective [IEVs] population. (*p<0.05, **p<0.005, ***p<0.0005).” [84](#). Note: taMPs = tumour associated MPs = tumour derived IEVs. Figure published in *Journal of Hepatology* by us [84](#).

Interestingly, to achieve the latter goal, another combination consisting of EpCAM and ASGPR1 as simultaneously detectable on AnnV⁺EpCAM⁺ASGPR1⁺ IEVs was highly associated with both liver cancer entities, here HCC and CCA, but not with non-malignant cirrhosis (figure 15A). Unfortunately, disallowing us a clear

separation between HCC and CCA. “Nevertheless, AnnexinV⁺EpCAM⁺ASGPR1⁺ [IEVs] were significantly elevated by 3.0-fold in [HCC and CCA] ($p < 0.0005$, one-way ANOVA with Dunn's test, Figure 14A), individually, HCC by 3.01-fold and CCA by 2.97-fold ($p < 0.005$, $p < 0.05$, respectively). The accompanied AUROC values were significant and indicated solid diagnostic performance.” [84](#) (figure 15B).

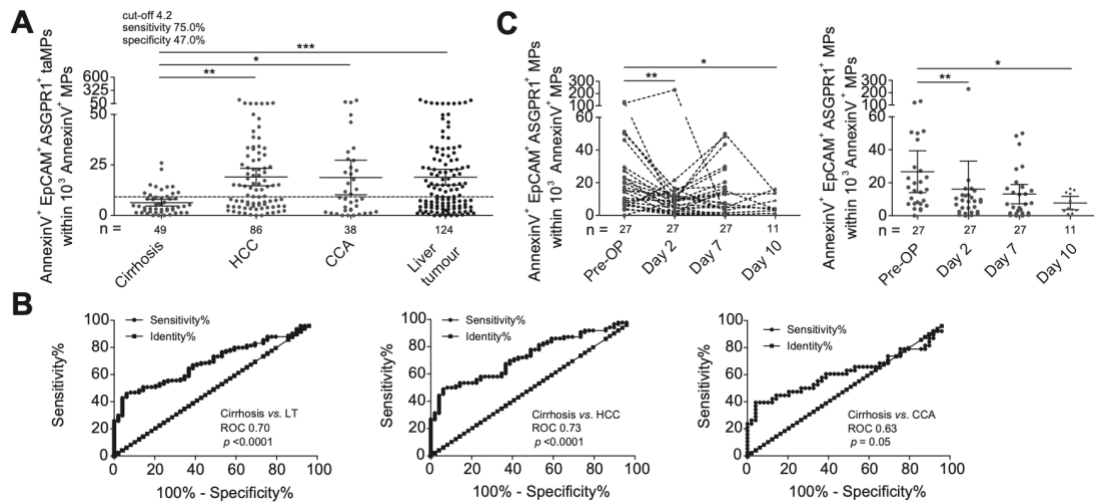


Figure 15: “EpCAM⁺ ASGPR1⁺ [IEVs] from human serum can separate patients with indicated liver tumours from patients with cirrhosis. [IEVs] were isolated and characterized by FACS from the sera of cancer patients (CCA, HCC) and patients with cirrhosis. The cohort ‘Liver Tumour’ combines both HCC and CCA patients. (A) Visualises EpCAM⁺ ASGPR1⁺ [IEVs] values for each study cohort given in mean with 95% CI. The dotted line represents the cut-off value for assessing the diagnostic accuracy of the population. Differences were assessed by one-way analysis of variances (ANOVA) including Dunn’s test. For each population the corresponding ROC curve and AUROC value is displayed in (B) in order to analyse the diagnostic performance of the respective [IEVs] population. (C) Progress of EpCAM⁺ ASGPR1⁺ [IEVs] values of liver tumour patients before surgical R0 tumour resection (pre-OP) and day 2, day 7 and day 10 after the resection. Only pre-OP values above the respective cut-off for liver tumours were included into analysis. Right panel, mean with 95% CI values of each day are depicted. [IEVs] levels for each post-OP day were compared to pre-OP values by applying a two-tailed Wilcoxon matched pairs signed rank test, resulting in significant p values. (* $p < 0.05$, ** $p < 0.005$, *** $p < 0.0005$).” [84](#). Note: taMPs = tumour associated MPs = tumour derived IEVs. Figure published in *Journal of Hepatology* by us [84](#).

Of note, if tumour mass was completely resected (R0), we could monitor a significant drop of AnnV⁺EpCAM⁺ASGRP1⁺ IEVs at day2 post resection (figure 15C), which

was expected since with the removal of the tumour load IEV donor cells were absent and hence remaining IEVs were cleared from the circulation in a timely manner. Precisely, mean pre-OP AnnV⁺EpCAM⁺ASGPR1⁺ [IEVs] levels of 26.7 AnnV⁺EpCAM⁺ASGPR1⁺ [IEVs] per 10³ AnnV⁺ [IEVs] dropped significantly at day 2 post-OP to 16.1 AnnV⁺EpCAM⁺ASGPR1⁺ [IEVs] per 10³ AnnV⁺ [IEVs] and remained low at day 10 post-OP at 7.7 AnnV⁺EpCAM⁺ASGPR1⁺ [IEVs] per 10³ AnnV⁺ [IEVs]. However, drop of those indicated IEVs were less pronounced as reported for sEVs after complete removal of pancreas cancer [124](#).

In summary, we reported that a separation between non-malignant cirrhosis (F4) and investigated liver cancer as HCC and CCA is achievable. However, indicated clinical values (reported AUROC and sensitivity and specificity) denied a clinical application for diagnosis without further validation by other clinical diagnostic means as CT/MRI or invasive liver biopsy. But rather a cancer screening at best, since AUROC and sensitivity and specificity was better than ultrasound and AFP measurement in HCC [141](#). Tzartzeva K *et al.* reported 2018 in their meta-analysis that “sensitivity of ultrasound with or without AFP for detection of HCC at any stage, sensitivity of ultrasound alone was 78% (95% CI 67%–86%) compared with 97% (95% CI 91%–99%) for ultrasound plus AFP.” [141](#). Specificity was not assessed in greater detail allowing us a direct comparison between our clinical values and calculated meta-analysis data. Of note, our cohort sizes were smaller than the above-mentioned study. Nevertheless, the fact that the smallest tumour diameters that was successfully detected by AnnV⁺EpCAM⁺ IEVs was of 9 and 10 mm was promising for relatively early detection [142](#). Notably, smaller diameters were not present in our cohort, thus it is possible that IEVs would provide even better sensitivity for detection.

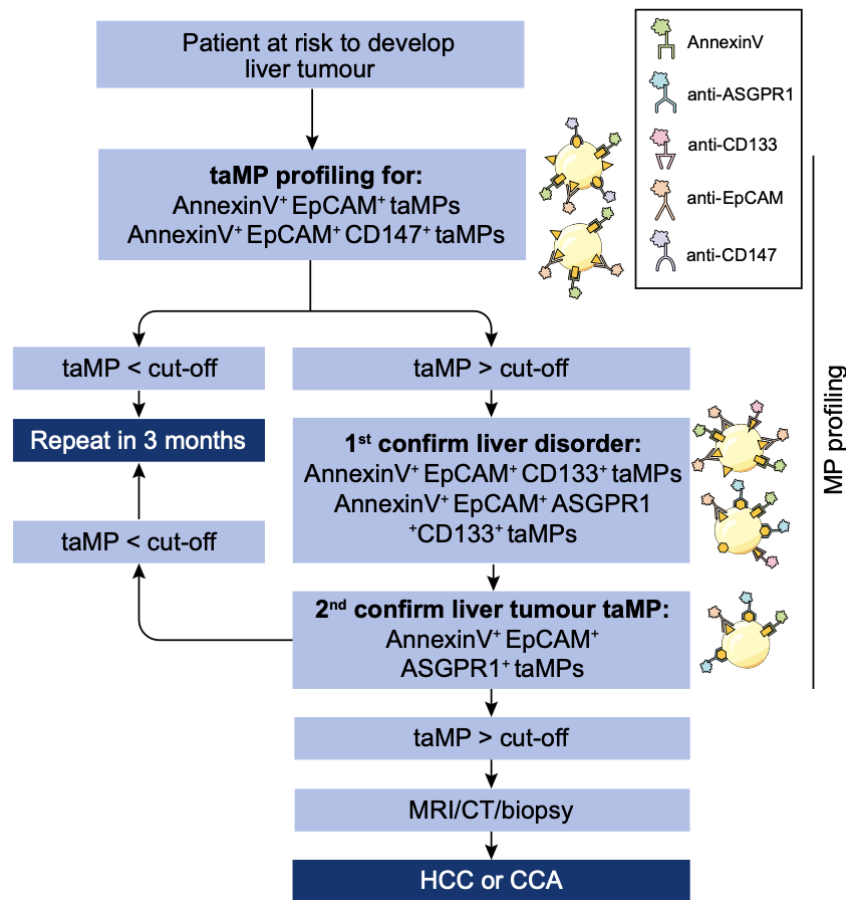


Figure 16: “Possible application as a diagnostic tool for detection of liver cancer. Overview of the application of the presented data is displayed as potential future detection guideline for non-invasive [IEVs] liver cancer assessment in patients at risk to develop liver cancer. This approach will consist of a general screening for elevated AnnexinV+EpCAM+ [IEVs] and AnnexinV+EpCAM+CD147+ [IEVs] indicating a liver disorder, here liver cancer or cirrhosis. Patients positively identified by elevated values above given cut-offs will follow a second step, where [IEVs] screening will consist of a validation and a differentiation step. 1st – Validation of liver cancer or cirrhosis – using the screening for AnnexinV+ EpCAM+CD133+ [IEVs] and AnnexinV+EpCAM+ASGPR1+CD133+ [IEVs]. 2nd – Final discrimination between liver tumours and cirrhosis – here, the presence of AnnexinV+EpCAM+ASGPR1+ [IEVs] will be evaluated. Patients identified with liver cancer will undergo finally tumour assessment with MRI/CT/biopsy.” [84](#). Note: taMPs = tumour associated MPs = tumour derived IEVs. Figure published in *Journal of Hepatology* by us [84](#).

Additionally, we embedded our findings in an overall scheme how to utilise it in liver cancer screening in liver cirrhotic patients being at risk to develop HCC (figure 16). Suggesting a two-step approach as outlined in figure 16.; 1st confirming presence of

malignant cirrhosis or non-malignant cirrhosis, hence liver disorders as HCC, as CCA or as cirrhosis and 2nd to differentiate between those, here between liver tumour-bearing vs. non-liver tumour-bearing patients.

From the methodologic point of view this work demonstrated that cancer entity specific antigen combination might be achievable on IEVs, a method which due to methodological shortages to detect several surface antigens simultaneously on exosomes (sEVs) was not attainable at that time. In 2015 Melo *et al.* took advantage of a simple and smart move to make sEVs detectable by FACS [124](#). In fact, sEVs are capable to bound unspecifically to latex beads. However, how many of those sEVs could potentially bind to one latex bead was shown exemplary for some sEVs by the authors, but overall sEV binding capability remained unknown to such latex beads as expressed in precise numbers [124](#). Hence, each exosome loaded latex bead generated only one accountable FACS event that was displayed as Glypican 1 positive sEVs. This methodology denied detection of two surface antigens simultaneously on same sEVs. Since signal A (antigen a) could originate from sEVs X and Y and signal B (antigen b) from Y or Z sEVs. Meaning a single latex bead positive for A and B, can potentially be loaded with 3 different sEV populations. sEV population X (only a), Y (a and b) and Z (only b). Newest developments in sEVs analysis permits now detection of several antigens simultaneously on same sEV by advanced FACS devices as Amnis ImageStream [128](#) or advanced microscopes as NanoView's ExoReader R100.

3.2.3 Synergistic effect of two biomarkers in hepatobiliary cancer entities – A comeback of Alpha-fetoprotein (AFP).

After demonstrating that a liver cirrhosis, here a non-malignant F4 cirrhosis (according to Scheuer PJ [143](#) and METAVIR [144](#) two frequently used 5-tier histological staging systems), are well distinguishable from hepatic malignancies as HCC or CCA *via* a set of antigens as detectable simultaneously on same patients' IEV, we aimed to achieve a separation between those hepatic malignancies as HCC and CCA, with an emphasize on intrahepatic CCA. Since ductular and extrahepatic CCA may be fairly well distinguished from HCC. Intrahepatic CCA (iCCA) remains challenging and requires ample of experience, operator hours, to distinguish HCC from iCCA [145](#) on the basis of morphology [146](#). In our experimental approach we actually excluded mix forms of HCC/CCA, which show both characteristics of HCC and CCA and represent another challenge.

Currently, few markers are used to identify liver progenitor cells (LPCs), such as CD24 (Cluster of differentiation 24) [147](#), Prominin-1 (CD133) [148](#), Stem cell antigen 1 (Sca-1) [148](#), Epithelial cell adhesion molecule (EpCAM) [147](#), ATP-binding cassette sub-family G member 2 (Abcg2), Leucine-rich repeat-containing G-protein coupled receptor 5 (Lgr5)[149](#), podoplanin / glycoprotein 38 (gp38) [148](#) and A6 antigen and Macrophage inhibitory cytokine-1-1C3 (MIC1-1C3) [150](#) besides others. Additionally, part of the periportal triad is besides the portal vein and the hepatic artery, the bile duct, which forms intrahepatic ductules and the canals of Hering lined by liver progenitor cells (LPCs) [145](#). Bile ducts and ductules are part of the biliary system and we assumed that LPCs due to their close location to the biliary system would be affected or activated in the presence of biliary cancer, here CCA or GbCA. Based on this assumption and well-funded on our previous publication on LPCs [148](#), we had chosen CD133 and gp38 as surface markers that could be simultaneously detectable on LPC derived IEVs helping us to differentiate between HCC and CCA including iCCA. Additionally, during study we observed that IEVs, even derived from LPCs wouldn't allow us a complete differentiation between HCC and CCA, therefore, we additionally investigated a possible synergistic effect of adding AFP to our differentiation protocol indicating a possible revival of AFP in case of hepatic malignancy screening and diagnosis in case of HCC and CCA.

Main results: In our previous publications on tumour associated IEVs we described surface antigen combinations on IEVs most likely derived from tumour cells directly. Since this approach somehow failed to differentiate between HCC and CCA (including iCCA), we addressed the question if IEVs indirectly associated with cancer *per se* but rather linked to LPCs might be beneficial in separating HCC from biliary cancer entities such as gallbladder cancer (GbCA) as extrahepatic CCA, and intrahepatic CCA. Following our typical approach, 1st we checked our surface antigen candidates on tumour cell lines *in vitro* (figure 17). EpCAM was highly expressed on all human tumour cell lines, on HCC cell lines as HUH7, HepG2 and Hep3B and on CCA cell lines as TFK-1, EGI-1 and CCC-5 too. CD133 stable on HCC cell lines as compared to CCA cell lines by 6.7-fold ($p \leq 0.0001$), whereas CD44v6 is increased by 5.0-fold ($p \leq 0.0001$) in CCA cell lines as compared to HCC cell lines. As expected neither tumour cell line expressed gp38. 2nd this preliminary *in vitro* data was repeated with human derived IEVs (explorative study, data not shown) [17](#).

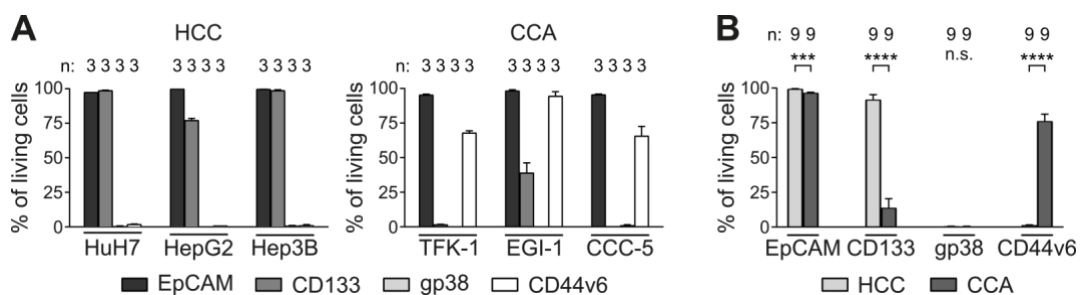


Figure 17: Human HCC and CCA cell lines show differential expression pattern of candidate markers. HCC tumour cells (HuH7, HepG2, Hep3B, each n=3) and CCA tumour cells (TFK-1, EGI-1, CCC-5, each n=3) were after starving for 16-24 hrs, cells harvested and EpCAM, CD133, gp38 and CD44v6 *via* FACS analysed. A two-tailed Mann-Whitney U test was performed with $p \leq 0.05$ considered statistically significant (* = $p \leq 0.05$, ** = $p \leq 0.01$, *** = $p \leq 0.001$, **** = $p \leq 0.0001$). n.s.: non-significant. Depicted are means with standard error of mean (SEM) for each HCC and CCA cell line individually. Figure published in *Liver International* by us [17](#).

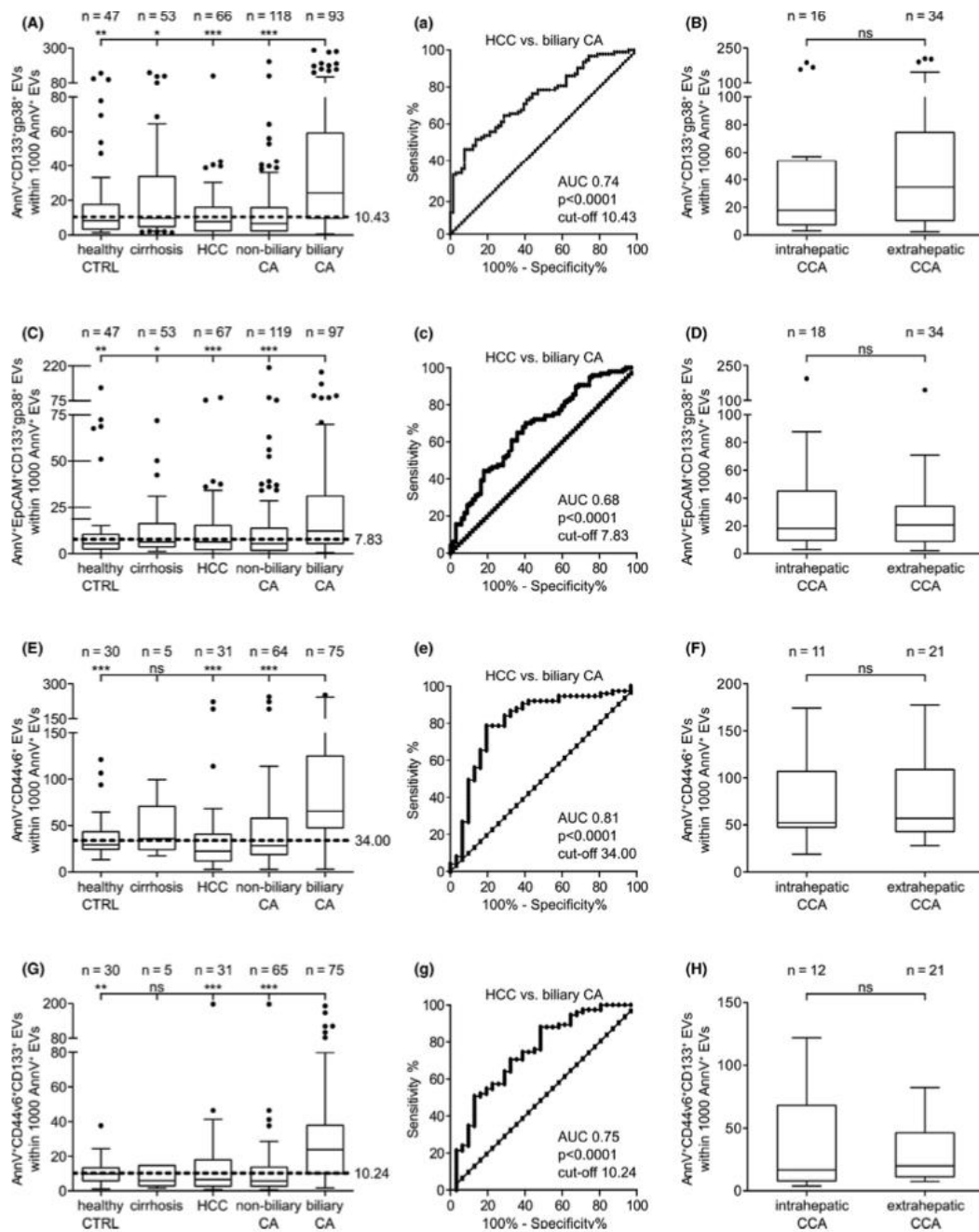


Figure 18: Validation study – CD133, gp38, EpCAM and CD44v6 positive extracellular vesicles are comprehensive biomarkers for biliary cancer. [Large] EVs were isolated and characterized by FACS from serum of indicated cancer patients and healthy donors. A, AnnV⁺CD133⁺gp38⁺ [I]EV profile for biliary (biliary CA) and non-biliary cancer patients (non-biliary CA) as well as for negative controls (HCC, cirrhosis and healthy CTRL). 'Biliary CA' combines GbCA and CCA patients. 'Non-biliary CA' comprises the cancer cohorts HCC, CRC and NSCLC. Data shown represent medians with interquartile range (IQR), whiskers represent $1.5 \times$ IQR (Tukey) with outliers plotted as dots. (A) depicts the corresponding ROC curve for AnnV⁺CD133⁺gp38⁺ EVs including AUC and P values as well as the diagnostic cut-off for biliary CA vs HCC. [I]EV profile for the populations

AnnV⁺EpCAM⁺CD133⁺gp38⁺ (C), AnnV⁺CD44v6⁺ (E) and AnnV⁺CD44v6⁺CD133⁺ (G) and their corresponding ROC curves (c, e, g, respectively) are depicted. Dotted lines indicate diagnostic cut-offs for discrimination between biliary CA and HCC for the respective [I]EV population. Statistical significance was assessed by Kruskal-Wallis nonparametric test with 3 df followed by Dunn's Multiple Comparison post hoc test ($p \leq 0.05$). AnnV⁺CD133⁺gp38⁺ (B), AnnV⁺EpCAM⁺CD133⁺gp38⁺ (D), AnnV⁺CD44v6⁺ (F) and AnnV⁺CD44v6⁺CD133⁺ (H) [I]EV profiles of intra- and extrahepatic CCA within the total CCA cohort are shown. Statistical significance was assessed by two-tailed Mann-Whitney U tests with $P \leq .05$ considered statistically significant" ($*p \leq 0.05$, $**P \leq .01$, $*** = P \leq .001$)" [17](#). Figure published in *Liver International* by us [17](#).

Our validation study (figure 18) revealed that a clear separation between HCC and biliary cancers (GbCA and CCA/iCCA) entities is most likely achievable associated with a sensitivity ranging between 72% and 91% and a specificity ranging between 58% and 69% between HCC specimens and biliary cancer specimens for the indicated IEVs, see table 2. Interestingly, and somehow against our own previous hypothesis, that only the combinations of multiple EV surface antigens simultaneously detectable on same tumour associated IEV (talEV) could be superior over a single EV surface antigen in diagnosis, we observed actually best AUROC value with CD44v6 as detectable on AnnV⁺CD44v6⁺ talEVs with an AUROC of 0.81 ($p < 0.0001$), see figure 17E. The investigated LPC derived IEVs, here AnnV⁺CD133⁺gp38⁺ IEVs and AnnV⁺EpCAM⁺CD133⁺gp38⁺ IEVs were inferior by their AUROC values (figure 18 and table 2).

Unfortunately, but somehow expected, our chosen IEV antigens failed to differentiate between iCCA from extrahepatic CCA (exCCA). Reasons could be manifold: expression arrays showed by others only distinct differences regarding classes associated with metabolism, proliferation, mesenchymal – and immunological status between those two cancer entities [151](#), and non-of those molecules are actually surface antigens. Hence, our methodology solely depending on surface antigens on IEVs might need additional component for successful diagnosis.

Table 2: “Diagnostic performance of the indicated EV populations individually and combined with AFP in biliary cancers (GbCA and CCA) as compared to HCC. Depicted are diagnostically relevant cut-offs (AFP: ng/mL, EVs: number per 10^3 AnnV⁺ EVs) as well as sensitivities, specificities, positive (PPV) and negative predictive values (NPV). n indicates cohort size, (*combined AUROC were not calculate.” [17](#). Table published in *Liver International* by us [17](#).

Progenitor cell-associated EVs (biliary CA: n = 73, HCC: n = 59)							
	AUROC	P-value	Cut-off	Sensitivity [%]	Specificity [%]	PPV [%]	NPV [%]
AnnV ⁺ CD133 ⁺ gp38 ⁺	0.74	<.0001	10.43	72.6	59.3	68.8	63.6
AnnV ⁺ EpCAM ⁺ CD133 ⁺ gp38 ⁺	0.68	<.0001	7.83	71.2	59.3	68.4	62.5
AFP	0.89	<.0001	20.00	98.6	54.2	72.7	97.0
AFP and AnnV ⁺ CD133 ⁺ gp38 ⁺	*	*	20.00 and 10.43	100.0	76.3	83.9	100.0
AFP and AnnV ⁺ EpCAM ⁺ CD133 ⁺ gp38 ⁺	*	*	20.00 and 7.83	100.0	76.3	83.9	100.0
Tumor-associated EVs (biliary CA: n = 60, HCC: n = 29)							
	AUROC	P-value	Cut-off	Sensitivity [%]	Specificity [%]	PPV [%]	NPV [%]
AnnV ⁺ CD44v6 ⁺	0.81	<.0001	34.00	91.7	69.0	85.9	80.0
AnnV ⁺ CD44v6 ⁺ CD133 ⁺	0.75	<.0001	10.24	81.7	58.6	80.3	60.7
AFP	0.95	<.0001	20.00	98.3	79.3	90.8	95.8
AFP and AnnV ⁺ CD44v6 ⁺	*	*	20.00 and 34.00	100.0	100.0	100.0	100.0
AFP and AnnV ⁺ CD44v6 ⁺ CD133 ⁺	*	*	20.00 and 10.24	100.0	96.6	98.4	100.0

Since a clear and complete separation up to 100% between HCC and biliary cancers had been not yet achieved by us with IEVs alone, we explored and evaluated a possible synergistic effect of investigated LPCs derived IEVs populations as AnnV⁺CD133⁺gp38⁺ IEVs and as AnnV⁺EpCAM⁺CD133⁺gp38⁺ IEVs and talEVs as AnnV⁺CD44v6⁺ talEVs and as AnnV⁺CD44v6⁺CD133⁺ talEVs with AFP (figure 19).

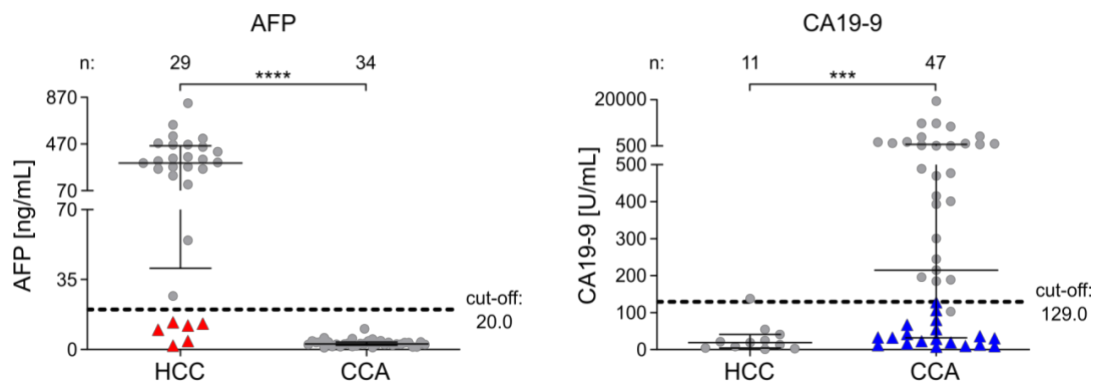


Figure 19: “Tumour-associated large EVs improve the diagnostic performance of AFP and CA19-9. After isolation of serum IEVs and flow cytometry characterization AFP values of HCC and CCA patients were combined analysed and depicted. Indicated in red triangles are patients that based on AFP levels are not classified as HCC patients (AFP < 20 ng/mL) but can positively be identified as

HCC by AnnV⁺CD44v6⁺ IEVs, left panel. Right panel, CA19-9 values of HCC and CCA patients are displayed. Indicated in blue are patients that based on CA19-9 levels are not classified as CCA patients (CA19-9 < 129 U/mL) but can positively be identified as CCA by AnnV⁺CD44v6⁺ gp38⁺ IEVs. Data is shown as scatter plots including median with interquartile range. n indicates number of patients. Dotted lines indicate recommended diagnostic cut-off of 20 ng/mL for AFP and 129 U/mL for CA19-9. Statistical significance was assessed by two-tailed Mann-Whitney U tests with $p \leq 0.05$ considered statistically significant. (*= $p \leq 0.05$, **= $p \leq 0.01$, ***= $p \leq 0.001$, ****= $p \leq 0.0001$). [17](#). Figure published in *Liver International* by us [17](#).

In order to do so, we assessed the diagnostic potential of two-IEV populations, LPCs-derived IEV and talEVs populations each plus AFP for separating HCC and biliary cancers. SOP was given as: HCC defined as: AFP >20 ng/mL or indicated IEVs levels below cut-offs; biliary cancer defined as: AFP <20 ng/mL or indicated IEV levels above the respective cut-offs. Patients were considered being positive for HCC if patients fulfilled at least one parameter, for example: if diagnosis was relying only on AFP we observed a typical outcome that only a certain percentage of HCCs had been associated with an elevated AFP value above 20 ng/mL and could be designated correctly as HCC.

Examining further this low AFP HCC tumours, we observed that some of those HCC samples were negative for our LPC IEVs and talEVs. And therefore, correctly designated as HCC accounting to the lacking LPC IEVs and tumour associated IEVs.

Vice versa, in case of biliary cancer entities, only one sample had been associated with AFP above 20 ng/mL and conclusively falsely considered to be an HCC. However, this high AFP⁺ biliary cancer specimen was however correctly associated with LPC IEVs and talEVs levels above calculated cut-offs indicating a biliary cancer entity. The detailed statistical examination (table 2) indicated that AFP and talEVs together, at least if one parameter/criteria is fulfilled (AFP low or talEVs high (here AnnV⁺CD44v6⁺)), achieved 100% correct separation between HCC and biliary cancer with a sensitivity of 100% and a specificity of 100%. AFP plus LPCs IEVs (AFP high or LPCs IEVs low, here AnnV⁺EpCAM⁺CD133⁺gp38⁺) resulted in a sensitivity of 100% and a specificity of 76.3%. Potentially and from relevance it is noteworthy to mention that either AFP in combination with CEA or CA19-9 did not led to a better separation between HCC and biliary cancer entities, indicating the

unique and versatile nature of tIEVs in cancer screening as a novel liquid biopsy [17](#). This synergistic effect of AFP and IEVs, that IEV's sensitivity is much improved if combined with AFP is somewhat surprising, but similar synergistic benefits were reported combining AFP and ultrasound. Tzartzeva K *et al.* reported that the actual sensitivity of ultrasound was advanced with AFP for detection of HCC at any stage. Sensitivity of ultrasound alone was 78% (95% CI 67%–86%) compared with 97% (95% CI 91%– 99%) for ultrasound plus AFP [141](#). Of note, our improvement is restricted to differentiating HCC from iCCA. Taking into account that typically CCA is not associated with AFP increase except for combined (or mixed) hepatocellular-cholangiocarcinoma (cHCC-CCA) [152](#) and usually 60% to 80% of HCCs cases are AFP positive [153](#), nearly 100% separation of those two liver cancer entities in this experimental setting must be validated in larger cohorts. However, in spite of that AFP lacks the capacity for clear HCC diagnosis, AFP is still interesting in combination with ultrasound as shown by Tzartzeva K *et al.* and in combination with IEVs as shown by us.

4 Discussion

4.1. Conclusion

More than a decade ago the role of large EV (IEVs) in context of hepatic pathophysiology wasn't well understood. Especially their role in fibrogenesis or from far bigger importance in fibrosis resolution of established hepatic fibrosis and cirrhosis (Aim I). Our *in vitro* data as published 2011 in *Hepatology* shed light on a possible role of T-cell derived EVs inducing fibrolysis in hepatic stellate cells [36](#). Additionally, then, we were strongly emphasizing a quality difference in EVs' capability to induce fibrolysis depending on how EV release was induced in EV donor T-cells, here with Staurosporine (apoptosis) vs. Phytohemagglutinin (activation), thus differences between EV donor cell origins as observed between primary CD4 T-cells vs. primary CD8 T-cells and vs. CD4 T-cell leukaemia cell line as EV donors (see please 3.1.1). Depending on EV donor cells and used methodology, EVs capacity to promote expression of fibrolytic active matrix-metalloproteins (MMPs) did differ as summarized in table 1. Readout was expression of MMP1 and MMP3 and MMP13 in EV recipient hepatic stellate cells *in vitro*. Our reported observation that it does matter how EV release was induced and the fact that certain T-cell types derived EVs had been associated with a bigger potential to induce fibrolysis *in vitro*, was from interest and might pave way to our hypothesis that chronic inflammation might promote tumour growth and metastatic spread *via* T-cell derived EVs. Since extracellular matrix (ECM) fibrolysis is key for a malignant cancer entity associated with tumour cell invasion, tumour cell spread and forming secondary tumours sites (metastasis) as reviewed by Kessenbrock K *et al.* [154](#). Actually, we observed alternated and enhanced tumour growth and intrahepatic metastatic spread *in vivo* in pre-fibrotic mice earlier [155](#)[156](#). But at that time, before 2008 we did not explore if T-cell derived EVs were causal to our observations. 2008 EVs weren't in focus or considered to play such a prominent role in pathophysiology as shown by others. Nevertheless, our hypothesis that EVs aren't equal by just being derived from the same donor cell type, but rather depending on associated EV release trigger mechanism might be well funded by us (see please 3.1.1) [36](#). Interestingly, most of T-cell derived IEV in human specimens were additionally CD25⁺, indicating that EV

donor T-cells were activated *in vivo* prior IEV release [36](#). However, this finding has to be repeated with newest methodology since we used at that time an LSR2 flow cytometer for IEV characterisation. A comparison across various commercially available FACS devices indicated that BD LSR2 are fine, bearing the needed sensitivity for IEV analysis if well maintained [127](#). Newer FACS devices might be very well superior, but still not capable to detect robustly single sEVs [127](#) except Amnis ImageStream device [128](#). With the access to our ExoView Reader from NanoView Biosciences, a microscope-based device for the numeration of immunological captured EVs, we aim to confirm this earlier done data in an multi-centric approach.

Independently of used EV flow cytometer, T-cell derived EVs' fibrolytic capacity was depending on EV uptake that was shown to be partly depending on a receptor ligand interaction and could be likely enhanced or prevented as shown by us at that time [36](#). Indicating that EVs aren't just an artefact or a release mechanism for intracellular stored 'garbage', no longer needed proteins, nucleotides etc, or other cellular waste. We showed a distinguished role of T-cell derived EVs in their interaction with hepatic stellate cells of the liver, the major driver of hepatic fibrogenesis more than a decade ago [36](#).

Additionally, we have to acknowledge and discuss that we used primary T-cells as EV donors, but CD4⁺ Jurkat cells as well. Jurkat cells are in fact leukaemia derived cancer cells. Thus, EV uptake of EMMPRIN (CD147) positive EVs, eventually resulting in an advantage in case of migration and metastatic spread as shown by others [157-158](#). In our study, Jurkat cell derived EVs induced downstream pathways as p38/MAPK signalling pathway [36](#) that could results in cancer metastatic spread in agreement that CD147 might be a likely direct driver of cancer cell metastasis due to CD147⁺ EVs [158](#). This could underline a hypothetical autocrine effect, that tumour cells might have a capability to increase metastatic spread by their own EVs if needed through such autocrine effect, probably as a response by any kind of disturbance such as undergoing anti-cancer therapy. Therefore, it would be from interest to explore the metastatic potential of tumour derived EVs and their effect after initiating cancer therapy as chemotherapy or radiofrequency ablation (RFA). In fact, we could show

that RFA might induce tumour cell proliferation that is temperature depending, restricted to a certain temperature and probably triggered by EMT [159](#). Lately EMT has been associated with EV uptake in Diethylnitrosamine (DEN)-induced HCC small rodent model [160](#). Additionally, in thyroid cancer too [161](#). Taking this in account, we might speculate that EV release could be a hint for a novel hypothetical tumour cell escape mechanism besides inflammatory mediated tumour tolerance.

Besides functional aspects of our *Hepatology* publication we observed that AnnV⁺CD4⁺ IEVs and as AnnV⁺CD8⁺ IEVs were present and elevated in active hepatitis C with ALT above 100 IU/L (figure 3) [36](#). This finding by us could be considered as the starting point of our diagnostic approach to utilize IEVs as a liquid biopsy biomarker in chronic hepatic disorders as HCV and NAFLD and hepatic cancer malignancies as published later on with great success in *Gastroenterology* [85](#) and *Journal of Hepatology* [84](#).

Our *Gastroenterology* work confirmed our preliminary data as published previously and demonstrated that that indicated EVs populations that are associated with the immune status in those diseases as AnnV⁺CD4⁺ EVs, as AnnV⁺CD8⁺ EVs and as AnnV⁺CD14⁺ and as AnnV⁺iNKT⁺ EVs* could be fairly well utilized to discriminate between healthy study controls and patients suffering from active HCV and NAFLD patients (Aim II) as discussed in 3.1.2 (figure 4). Besides our great success at that time and methodological limitations as seen from nowadays perspective, here using BD LSR2 FACS device, especially our experimental study design was flawed by the fact that we just included 3 human study cohorts, HCV patients, NAFLD patients and healthy volunteers as negative controls [85](#). As reported, we monitored differences between those three study cohorts, but the questions remained: what about other specimen entities, as hepatitis B, as IBD or as gluten sensitivity? We have unpublished data showing that T-cell derived EVs were elevated in those diseases too, as well AnnV⁺CD14⁺ EVs. However, our aims of this earlier human study were to elaborate if profiling of IEVs in those chronic hepatic disease as part of a minimal invasive liquid biopsy, one puncture for blood sampling instead of an invasive liver biopsy is a) capable to differentiate among HCV and NAFLD and healthy controls and b) somehow superior than a conventional liver biopsy which is quite invasive and

associated with some risks. As discussed in 3.1.2, we found good arguments to fund our hypothesis, that profiling of EVs somehow reflecting the immune status in this chronic liver diseases might be of interest. Not only from a screening/diagnostic standpoint, but it might shed light which immune competent cells, which immune cascades might be involved assuming that activated immune competent cells will release EVs upon activation. Many data acquired by others do hint that EVs play a crucial role in the pathophysiology of inflammation-associated disorders as reviewed by us [89](#).

Learning from this short coming in our study design, we decided to emphasize strongly on using negative controls in case of our following cancer studies in near future.

Our next publications on IEVs potentially derived directly from cancer cells, we heavily shed emphasises on using additional cancer entities. And we aimed to explore antigens on cancer derived IEVs that might be suitable as a general pan cancer marker (Aim III).

In the past decade, EpCAM (CD326) turned out to be a useful marker in detecting circulating tumour cells (CTCs) or tumour stem cells [116-119](#). Although CTCs are rare, optical detection of such EpCAM⁺ tumour cells as done with the CellSearch™ System is in clinical use for a limited number of cancer entities [25,120,121](#). US Food and Drug Administration (FDA) so far only approved this method for metastatic epithelial tumours in the United States. In contrast to these scarce CTCs, EpCAM⁺ IEVs might be larger in numbers, a possible multiplier of EpCAM⁺ tumour cells *in vivo*. 2015 we published that EpCAM⁺CD147⁺ IEVs were far superior than EpCAM⁺ IEVs in terms of detecting and distinguishing cancer from other epithelial damage (Aim III, figure 8) [111](#). Equal important EV shedding, including of EpCAM⁺CD147⁺ IEVs, wasn't dependent on metastatic spread [111](#).

So far, we have shown that AnnV⁺EpCAM⁺CD147⁺ IEVs are elevated in NSCLC, CrC, PaCa (figure 8) [111](#) and CCA and HCC [84](#). Unfortunately, as shown in our *Journal of Hepatology* publication in hepatic cirrhosis partially too [84](#). This isn't surprising, since EpCAM and CD147 are associated with liver progenitor cells (LPCs) and hepatic stellate cells (HSCs) that are activated in liver fibrogenesis too

[148](#)·[162](#)·[163](#). Emphasising a likely limitation of AnnV⁺EpCAM⁺CD147⁺ IEVs to distinguish between liver disorders that are associated with hepatic cancerogenesis or hepatic fibrogenesis. Or rather an exclusion factor for our cancer liquid biopsy if only based on AnnV⁺EpCAM⁺CD147⁺ IEVs. But, if hepatic cirrhosis and hepatic malignancies are bound, as they are, how we should detect liver malignancies typically with underlying cirrhosis and discriminate them from non-malignant cirrhosis?

Proceeding with those thoughts, we concluded, that a specific set of antigens simultaneously detectable on the same IEVs and consisting of typical HCC cancer surface antigens could permit such desired distinction between HCC on the background of cirrhosis and non-malignant cirrhosis (Aim IV) [84](#).

Following our hypothesis, we investigated couple of common cancer markers and hepatocyte markers on commercially available HCC cell lines as HUH7, HepG2, SK-Hep1 (figure 13). Our negative control were actually pancreatic cancer cell lines. Finally, we identified some commonly shared antigens on both cancer entity cell lines. Interestingly, an expected difference was confirmed that asialoglycoprotein receptor 1 (ASGPR1). ASGPR1 was restricted to HCC cell lines only (figure 13) [84](#). This allowed us to investigate various plausible antigen combinations on IEVs that are highly associated with HCC or at least with hepatic cancer entities as HCC and CCA as AnnV⁺EpCAM⁺ASGPR1⁺ IEVs and as AnnV⁺EpCAM⁺ASGPR1⁺CD133⁺ IEVs (figure 12) [84](#). This approach resulted in some IEV antigen combinations that a) could separate hepatic malignancies from non-malignant cirrhosis and additionally from patients bearing CrC or NSCLC or as healthy patients with inguinal hernia (figure 14), representing an epithelial tissue damage and of note from healthy volunteers. Second set of IEV antigens could b) separate between hepatic malignancies and non-malignant cirrhosis (figure 15), proofing that our previous assumption that individual IEV antigen combinations for certain cancers are feasible, however, our data as published 2017 in *Journal of Hepatology* [84](#), underlined that restrictions how far our hypothesis is valid are given. As discussed earlier, we failed to differentiate HCC specimens from CCA specimens (figure 15), two cancer entities closely associated regarding several aspects including the associated organ, here

liver, and expression profiles and histological markers especially in cases of iCCA and cHCC-CCA [164-165](#).

Our next aim (Aim V) was to discover a robust IEV antigen combination that would allow us to separate HCC from biliary cancer entities as hepatic CCA, ductular CCA and gall bladder cancer (GbCA). In contrast to our previous approach, we focused now on IEVs derived not directly from cancer cells *per se*, but rather from cells that had been associated with hepatic organ regeneration, thus likely contributing to cancer growth by forming cancer's niche. As published by us elsewhere, co called liver progenitor cells (LPCs) could be such IEV donor cells [148](#).

As mentioned before in 3.2.3, few surface markers were considered and selected to identify liver progenitor cells (LPCs) derived IEVs, as Prominin-1 (CD133) [148](#), as Epithelial cell adhesion molecule (EpCAM) [147](#), podoplanin / glycoprotein 38 (gp38) [148](#) and A6 antigen and Macrophage inhibitory cytokine-1-1C3 (MIC1-1C3) [150](#) besides others. Based on our previous publication on LPCs [148](#), we had chosen CD133 and gp38 as promising surface antigens that might be simultaneously detectable on LPC derived IEVs. In short, we could associate AnnV⁺CD133⁺gp38⁺ IEVs and AnnV⁺CD133⁺EpCAM⁺gp38⁺ IEVs with the presence of biliary cancers, here CCA and GbCA, allowing us to differentiate between those biliary cancers vs HCC (figure 18).

Examining various publications on GbCA or CCA on useful markers, CD44 draw our attention [166-167](#) and its isoform CD44v6 [168](#). CD44v6 was found on CCA cancer cell lines as TFK-1, EGI-1 and CCC-5 but not on HCC cell lines by us (figure 17). Against our earlier published hypothesis that a combination of antigens on the same IEVs will give us needed power to separate cancer entities [126](#), we checked CD44 in those biliary cancer patients. First, it wasn't conclusive. Other reported that actually isoform CD44v6, could potentially aid in [168](#). In fact AnnV⁺CD44v6⁺ talEVs and AnnV⁺CD44v6⁺CD133⁺ talEVs could discriminated between biliary cancer entities and HCC and cirrhosis as published by us, but failed to distinguish between extrahepatic (exCCA) and intrahepatic CCA (iCCA) [17](#). Until now we have to admit that we failed constantly to separate between exCCA and iCCA. A challenge that might be set as the biggest hurdle for any liquid biopsy-based approach.

Nevertheless, our reported discrimination between HCC and CCA (exCCA and iCCA) wasn't that remarkable in numbers as expressed in AUROC, sensitivity and specificity, positive and negative prediction value (see table 2). Probably better than other used clinical serum marker as AFP, CEA and CA19-9, but not good enough as desired. However, EV based methodology should be suitable for routinely done liver cancer screening, requiring moderate operator skills and being better in terms of sensitivity, specificity, costs and patients' convenience.

So, we picked up again an old friend, AFP. AFP was once regarded as the liquid biopsy marker in HCC for diagnosis and screening. Guidelines were based and recommended use of AFP once, probably more than decade ago. Nowadays AFP isn't recommended for diagnosis by the associated professional NGO as AASLD or EASL [7-9](#), two of the biggest and most influential organisations promoting and setting guidelines in case of hepatic disorders. Though, AFP is still used for screening [13](#), since its cheap and convenient. It's simple available. Therefore, we separated our two cancer patient collectives, HCC and CCA according to their measured AFP value. AFP cut-off was 20 ng/mL indicating HCC [13](#). As expected some HCC were so called AFP negative HCC entities. Hence, missed if screening or diagnosis would only depended on AFP. But, those AFP negative HCC specimens were successfully separated from CCA based on indicated IEVs populations (see table 2). Overall, if AFP and AnnV⁺CD44v6⁺ talEVs data was combined a positive synergy was observed resulting in a 100% separation between HCC and CCA (exCCA and iCCA) (table 2). Associated combined sensitivity and specificity were 100%. This data, clearly demonstrated that IEVs alone might not bear the needed power, needed robustness in terms of clinical usefulness, being used instead of AFP but in combination with AFP, it might be from interest and worth to be explored further in much larger numbers, repeated in an multi-centric study approach.

The remaining question might be are EV superior over CTCs or *vice versa*? To our knowledge up to now CTC and EVs were not isolated from the same tumour bearing patient isolated and quantified and their clinical performance directly compared. Hence, we may only make assumptions and that matter based on reported data and general limitation given by each methodology and under which circumstances CTC

might be superior over EVs or EVs over CTCs. However, some methodological similarities might be found, more from conceptual point of view.

Though CTCs and EVs are very different in many ways, living material, ongoing metabolism and proliferative capacity vs. non-living material, possessing small traces of cells, besides obviously being different in size, macro vs nano-sized. Nevertheless both, CTCs and EVs, share some methodical similarities how to be identified, some minor conceptual and mythological differences how to be phenotyped. In common, both are taking advantage of utilizing surface antigens as available on their membrane surface [169](#). The widely used CellSearch™ is designed using surface antigens such as EpCAM or CK and others as discussed as a kind of positive selection and CD45 for negative selection of leucocytes, besides DAPI, an intracellular nucleus staining as discussed before [28](#). This nucleus staining capability of CTCs is in EVs obviously not given, since EVs are lacking a nucleus and larger genomic material except minor genomic fragments [170-171](#). Additionally, and probably one of the biggest differences is that an intracellular staining in case of EVs, likely to be called an intravesicular staining, wasn't reported so far to our knowledge, since an intracellular staining relies generally speaking "to poke holes" into the cell membrane using mild membrane solubilizers as Tween 20, as Saponin, as Digitonin and as Leucoperm (0.5% v/v in PBS) [172](#). However, a very recent publication demonstrated that EVs bound to a coverslip overnight at 4 degrees Celsius were fixed with paraformaldehyde and were permeabilized using 0.1% Saponin for downstream imaging purposes [173](#). Without fixation, such detergence will eventually destroy as reported for sodium dodecyl sulfate (SDS), an anionic detergent, the structural integrity of nano-sized EVs and random those to be useless for quantification efforts [174](#).

Typically, both type of liquid biomarker, CTCs and EVs, had been phenotyped by flow cytometry by several researchers around the globe using various available models of flow cytometers including advanced imaging flow cytometry as with various resolutions regarding lower detectable size boarder [128-175-177](#). 2015 Melo et al. published eventually the so far most promising publication and the most recognised publication and a kind of kick off in EV based cancer diagnosis [124](#). On the contrary, 2004 can be regarded as the year when CTCs had their breakthrough by

recognition and approval by the FDA. Nevertheless, the usage of small EVs in prostate cancer diagnosis received FDA acknowledgment by granting Breakthrough Device Designation to Bio-Techne ExoDx Prostate IntelliScore (EPI) test, [28:178](#). Nevertheless, CTCs had been so far researched for a longer time period than EVs as a kind of cancer liquid biopsy biomarker in patients' blood. Hence it is not surprising that the methodology of CTC isolation and phenotyping is more advanced and to a higher degree standardized. Including FDA approved for the detection of several metastatic cancer entities in the USA. In contrast, the EV research field is somehow still exploring and elaborating the usefulness of EVs in cancer diagnosis and especially with a strong emphasis on prognosis [24](#). EVs are still somewhat experimental and guidelines were given to the EV field by the International Society for Extracellular Vesicles (ISEV) 2014 and 2018 [179:180](#). Of note CTC methodology is not final set, neither in case of EVs. New combinations of CTC antigens have been investigated allowing diagnosis and prognosis in case of additional cancer entities, yet not FDA approved [176](#).

Hypothetically, there is actually an overlap given of used antigens on CTCs and EVs and being specific for cancer entities. The classical CellSearch™ pan cancer marker is EpCAM, reliably used for the detection of CTCs in co-junction with CD45 and DAPI and others (experimental) [24:28:117](#). Interestingly, EpCAM on IEVs as shown by us, was insufficient in discrimination between investigated cancer entities as colorectal-, as non-small cell lung-, as pancreas carcinoma and thyroid nodules, kind of abnormal growth of thyroid cells forming a lump within the thyroid gland, typically non- malignant (figure 8A). Only combination of antigens being simultaneously present on the same IEV were sufficient to separate patients suffering from thyroid gland and cancers (figure 8B). Additionally, other combinations were reported being specific to a certain extent for biliary malignancies, including the EV based differentiation of HCC from CCA including intrahepatic CCA as shown by us and discussed above in greater detail. Applying cancer entity specific antigens on CTCs was meanwhile achieved by taking advantage of hepatocyte markers as Glypican 3 and ASGPR1, in combination with EpCAM utilizing flow cytometry for experimental purpose [176:181](#).

Some researchers didn't rely on initial EpCAM-based capture of CTCs allowing them to identify additional CTC populations being associated with cancer progression. Armstrong A.J. et al. explored not only CTCs in patients with metastatic CRPC co-expressing EpCAM or CK, but rather E-cadherin, mesenchymal proteins as Vimentin, as N-cadherin and O-cadherin, thus CD133 as well [182](#). All of them eventually missed by the FDA- approved CellSearch™ methodology and other on CTC isolation and numeration depending methods heavily relying on EpCAM. Armstrong's *et al.* data suggests that CTCs from common epithelial malignancies co-express epithelial and mesenchymal markers, suggesting that EMT/MET transitions is likely contributing to metastatic progression. From importance is, that EpCAM is lost earlier than cytokeratin during the epithelial-to-mesenchymal transition resulting in escape from EpCAM-based CTC capture [183](#). To our best knowledge EMT/MET transitions surface antigens on EVs were not explored yet.

Another flow cytometric advantage and applicable only on CTCs, eventually isn't yet reproduced on EVs, the so-called discrimination of high expressing and low expressing CTCs [184](#), up to date not achieved on EVs. Scientist around the world can easily providing ample of examples where it does matter if a cell's antigen is high or low/dim expressing [148:185](#). No reports are available if CellSearch™ is capable to do so would be off-label usage. In an experimental setting the blood waste enriched with cancer cell line cells, that blood waste discarded by CellSearch™, was collected and passed through a micro sieves and accounted. In fact, the CellSearch™ cartridge effectively recovered EpCAM^{high} tumour cells, whereas the EpCAM^{low} cells are mainly recovered by micro sieve [186](#). This might be from relevance, since EU-FP7 CTC-Trap program suggested that CTCs expressing high levels of epithelial cell adhesion molecule, EpCAM^{high} compared to EpCAM^{low} CTCs were associated with a different clinical outcome as given in median survival in metastatic prostate and breast cancer patients. In favour of EpCAM^{high} CT, those were strongly related to shorter survival [184](#).

As shown, EpCAM plays a prominent role in the FDA approved CellSeach™ system. The hypothetical question that must appear, is obviously, if the CellSearch™ System and others immunoaffinity – positive selection/enrichment based systems will evolve

further into a system that is more capable to detect specific cancer entities by utilising another selection of antigens present on cancer derived CTCs, for example ASGPR1 and CD133 on liver cancer derived CTCs. Of note such move has successfully to pass the clinical phases prior FDA approval and clinical use. Would such evaluation of the CellSearch™ system give physicians an advantage in liver cancer diagnosis and prognosis? It is debatable and financial interest might play a role.

But how about EVs, is a pre-enrichment of EpCAM⁺ EVs feasible including a subsequently analysis for other tumour associated antigens on those enriched EpCAM⁺ EVs? Indeed sEVs may be enriched with anti-EpCAM beads as done by Ostenfeld MS *et al.* and subsequently analysed for a specific miRNA profiles in CRC [187](#).

As discussed, CTC and EVs are somewhat similar how to be used in cancer screening and eventually in cancer diagnosis. Newest advances in EV analysis, lifting given limitations as restricting sEVs analysis to only one surface antigen per sEVs might allow to try out our reported cancer entity specific surface antigen combinations as reported on IEVs on sEVs, providing the needed edge over CTC. The current advantage of CTC is surely the higher degree of standardisation that is in our EV field not reached. Therefore, it is from our point of view way too early to decide if CTC or EVs are superior in cancer screening and diagnosis.

4.2. Outlook

Over the past decade, we provided evidences that large EVs might have the capacity to be a useful tool for liver cancer screening. We are capable to detect a liver tumour with a fair sensitivity and specificity and if we use AFP data we might separate HCC from CAA entities including intrahepatic CCA (iCCA). Further, we have published that IEVs numbers will decrease with tumour removal [84·111](#). Hence, we speculate that EVs might bear the potential to separate anti-cancer therapy responders from non-responders. And if so, we hope that such differentiation between responders and non-responders will be feasible fairly early after therapy start with current line of anti-cancer drugs as Sorafenib and checkpoint inhibitors as PDL-1. Others have shown that CTCs levels do respond to anti-cancer therapies and might be a robust indicator for anti-tumour therapy success and to draw overall survival prognosis. Therefore, we postulate the following hypothesis that liver tumour specific IEVs will differentiating hepatocellular and intrahepatic cholangiocarcinoma from each other and from other cancer entities, and might be a perfect screening tool for tumour relapse as frequently observed in HCC. Furthermore, we expect that EVs will be very likely a robust biomarker to evaluate current anti-cancer therapies, such as transarterial chemoembolisation (TACE) or microwave ablation (MWA). This could give the chance to change used anti-cancer therapy regime in time at beginning of therapy, and use another anti-cancer therapy approach. Further modern proteomic and genomic tools could give additional marker combinations for better cancer entity differentiation and follow-up. Additionally, a direct comparison between CTC and EVs regarding cancer screening, diagnosis and therapy monitoring is needed too in the future.

5 Summary

This habilitation thesis is actually spanning more than a decade of successful and high-profile laboratory research published accordingly in high cited journals as *Hepatology*, *Gastroenterology* and *Journal of Hepatology*. During more than a decade, 2008-2021, the developments in EV science are actually well reflected by our publication track record, e.g. as applying correct wording for investigated EV populations in accordance with EV mainstream understanding at that timepoint. Framing IEVs as *microparticles* by us during first few years at Harvard Medical School, probably raising unintentionally an idea of *microparticles* being non-organic particles. Later developments encouraged us to use the more correct term of *microvesicles*. Microvesicles had been correctly associated with vesicles that are typically organic origin. However, *micro* still did not and does not imply the correct nano-size nature of microvesicles, but, somehow still correctly emphasizing that microvesicles are overall very little in size. Pursuing standardization in our EV research field, 2018, my lab contributed to the publication of the revised Minimal Information for Studies of Extracellular Vesicles (MISEV) guidelines, which uniformly called these entities microparticles/microvesicles. Additionally, we distinguished between *large extracellular vesicles* (IEVs) separating them from *small extracellular vesicles* (sEVs, commonly referred as exosomes). This standardization approach to name EVs correctly took more than a decade, as this habilitation thesis did. However, from more importance was the research content during this decade presented in this work. Among them was how IEVs were used as a tool to profile HCV, later even to differentiate HCV from NAFLD. Moreover, IEVs were regarded as a pan-cancer biomarker tool and finally were used to screen liver cancers in valuable collectives being at risk to develop liver cancer. And recently our work revived Alpha-fetoprotein (AFP) as a biomarker in order to distinguish HCC from CCA including iCCA and exCCA with a pinpoint accuracy of 100% sensitivity and 100% specificity. Actually, this habilitation thesis shows the development of an idea that was born at BIDMC, Harvard Medical School and which was completed in Bonn, Germany.

6 Acknowledgment

My great and sincere thanks go to all the patients, all the cancer patients who, despite their cancer diagnosis, often associated with a poor prognosis, have consented to support with their blood, their serum, our studies on which this habilitation thesis is based without any self-interest. This deserves highest recognition and thanks. I bow to you.

At the same time, I would like to thank our co-authors involved, especially those of the research groups to which I belonged previously and my own research group. Especially to the students who helped to build up my research group in Homburg/Saar, especially in our first year.

Then, I would like to thank the German Cancer Aid (Deutsche Krebshilfe e.V.) and the German Research Foundation (Deutsche Forschungsgemeinschaft, DFG), who have placed their trust in me in the form of third-party funding.

I would also like to thank the BwZKrhs Koblenz, the management of the hospital, as well as the lead of the department 2, the project lead as well as the whole department 2 for their support, after my return to Germany.

Last but not least to my spouse, Veronika. The years in Homburg/Saar, where we led a joint laboratory at the UKS, like Marie and Pierre Curie, were, next to our time at Harvard Medical School, Boston, MA, USA, among the most beautiful that scientists may experience in the context of our research activities. Thank you for that!

7 References

- 1 Morgan, T. M. Liquid biopsy: Where did it come from, what is it, and where is it going? *Investig Clin Urol* **60**, 139-141, doi:10.4111/icu.2019.60.3.139 (2019).
- 2 Mocan, T. *et al.* Liquid Biopsies in Hepatocellular Carcinoma: Are We Winning? *J Clin Med* **9**, doi:10.3390/jcm9051541 (2020).
- 3 Wichelhausen, R. N., McLean, R. L. & Lowrey, F. B. Reinforcement of diagnostic value of pleural biopsies by culture in liquid medium. *Am Rev Respir Dis* **93**, 288-290, doi:10.1164/arrd.1966.93.2.288 (1966).
- 4 Partin, A. W. *et al.* Prostate specific antigen in the staging of localized prostate cancer: influence of tumor differentiation, tumor volume and benign hyperplasia. *J Urol* **143**, 747-752, doi:10.1016/s0022-5347(17)40079-6 (1990).
- 5 Catalona, W. J. *et al.* Measurement of prostate-specific antigen in serum as a screening test for prostate cancer. *N Engl J Med* **324**, 1156-1161, doi:10.1056/NEJM199104253241702 (1991).
- 6 Kouriefs, C., Sahoyl, M., Grange, P. & Muir, G. Prostate specific antigen through the years. *Arch Ital Urol Androl* **81**, 195-198 (2009).
- 7 Bruix, J., Sherman, M. & American Association for the Study of Liver, D. Management of hepatocellular carcinoma: an update. *Hepatology* **53**, 1020-1022, doi:10.1002/hep.24199 (2011).
- 8 Bruix, J. *et al.* Clinical management of hepatocellular carcinoma. Conclusions of the Barcelona-2000 EASL conference. European Association for the Study of the Liver. *J Hepatol* **35**, 421-430, doi:10.1016/s0168-8278(01)00130-1 (2001).
- 9 Omata, M. *et al.* Asian Pacific Association for the Study of the Liver consensus recommendations on hepatocellular carcinoma. *Hepatol Int* **4**, 439-474, doi:10.1007/s12072-010-9165-7 (2010).
- 10 Ryder, S. D. & British Society of, G. Guidelines for the diagnosis and treatment of hepatocellular carcinoma (HCC) in adults. *Gut* **52 Suppl 3**, iii1-8 (2003).
- 11 Giannini, E. G. *et al.* Alpha-fetoprotein has no prognostic role in small hepatocellular carcinoma identified during surveillance in compensated cirrhosis. *Hepatology* **56**, 1371-1379, doi:10.1002/hep.25814 (2012).
- 12 European Association for the Study of the Liver. Electronic address, e. e. e. & European Association for the Study of the, L. EASL Clinical Practice Guidelines: Management of hepatocellular carcinoma. *J Hepatol* **69**, 182-236, doi:10.1016/j.jhep.2018.03.019 (2018).
- 13 Marrero, J. A. *et al.* Diagnosis, Staging, and Management of Hepatocellular Carcinoma: 2018 Practice Guidance by the American Association for the Study of Liver Diseases. *Hepatology* **68**, 723-750, doi:10.1002/hep.29913 (2018).
- 14 Marrero, J. A. *et al.* Des-gamma carboxyprothrombin can differentiate hepatocellular carcinoma from nonmalignant chronic liver disease in american patients. *Hepatology* **37**, 1114-1121, doi:10.1053/jhep.2003.50195 (2003).
- 15 Zhou, L., Liu, J. & Luo, F. Serum tumor markers for detection of hepatocellular carcinoma. *World J Gastroenterol* **12**, 1175-1181 (2006).
- 16 Zamcheck, N. & Pusztaszeri, G. CEA, AFP and other potential tumor markers. *CA Cancer J Clin* **25**, 204-214 (1975).
- 17 Urban, S. K. *et al.* Synergistic effects of extracellular vesicle phenotyping and AFP in hepatobiliary cancer differentiation. *Liver Int* **40**, 3103-3116, doi:10.1111/liv.14585 (2020).
- 18 Brennan, M. M. *et al.* Detection of high-risk subtypes of human papillomavirus in cervical swabs: routine use of the Digene Hybrid Capture assay and polymerase chain reaction analysis. *Br J Biomed Sci* **58**, 24-29 (2001).
- 19 Pantel, K. & Speicher, M. R. The biology of circulating tumor cells. *Oncogene* **35**, 1216-1224, doi:10.1038/onc.2015.192 (2016).
- 20 Tellez-Gabriel, M., Heymann, M. F. & Heymann, D. Circulating Tumor Cells as a Tool for Assessing Tumor Heterogeneity. *Theranostics* **9**, 4580-4594 (2019).
- 21 Ashworth, T. R. A case of cancer in which cells similar to those in the tumours were seen in the blood after death.
- 22 Lopresti, A. *et al.* Sensitive and easy screening for circulating tumor cells by flow cytometry. *JCI Insight* **5** (2019).
- 23 Pantel, K. & Alix-Panabières, C. The clinical significance of circulating tumor cells. *Nat Clin Pract Oncol* **4**, 62-63, doi:10.1038/nponc0737 (2007).
- 24 Cristofanilli, M. *et al.* Circulating tumor cells, disease progression, and survival in metastatic breast cancer. *N Engl J Med* **351**, 781-791, doi:10.1056/NEJMoa040766 (2004).

- 25 Alix-Panabières, C. & Pantel, K. Challenges in circulating tumour cell research. *Nat Rev Cancer* **14**, 623-631, doi:10.1038/nrc3820 (2014).
- 26 Marquette, C. H. *et al.* Circulating tumour cells as a potential biomarker for lung cancer screening: a prospective cohort study. *Lancet Respir Med* **8**, 709-716, doi:10.1016/s2213-2600(20)30081-3 (2020).
- 27 Osmulski, P. *et al.* Nanomechanical biomarkers of single circulating tumor cells for detection of castration resistant prostate cancer. *Prostate* **74**, 1297-1307 (2014).
- 28 Allard, W. J. *et al.* Tumor cells circulate in the peripheral blood of all major carcinomas but not in healthy subjects or patients with nonmalignant diseases. *Clin Cancer Res* **10**, 6897-6904, doi:10.1158/1078-0432.ccr-04-0378 (2004).
- 29 Gross, H. J., Verwer, B., Houck, D., Hoffman, R. A. & Recktenwald, D. Model study detecting breast cancer cells in peripheral blood mononuclear cells at frequencies as low as $10(-7)$. *Proc Natl Acad Sci U S A* **92**, 537-541 (1995).
- 30 Riethdorf, S., O'Flaherty, L., Hille, C. & Pantel, K. Clinical applications of the CellSearch platform in cancer patients. *Adv Drug Deliv Rev* **125**, 102-121, doi:10.1016/j.addr.2018.01.011 (2018).
- 31 Harris, L. *et al.* American Society of Clinical Oncology 2007 update of recommendations for the use of tumor markers in breast cancer. *J Clin Oncol* **25**, 5287-5312, doi:10.1200/jco.2007.14.2364 (2007).
- 32 Rossi, E. & Fabbri, F. CTCs 2020: Great Expectations or Unreasonable Dreams. *Cells* **8** (2019).
- 33 Bünger, S., Zimmermann, M. & Habermann, J. K. Diversity of assessing circulating tumor cells (CTCs) emphasizes need for standardization: a CTC Guide to design and report trials. *Cancer Metastasis Rev* **34**, 527-545, doi:10.1007/s10555-015-9582-0 (2015).
- 34 Wolf, P. The nature and significance of platelet products in human plasma. *Br J Haematol* **13**, 269-288, doi:10.1111/j.1365-2141.1967.tb08741.x (1967).
- 35 Beyer, C. & Pisetsky, D. S. The role of microparticles in the pathogenesis of rheumatic diseases. *Nat Rev Rheumatol* **6**, 21-29, doi:10.1038/nrrheum.2009.229 (2010).
- 36 Kornek, M., Popov, Y., Libermann, T. A., Afdhal, N. H. & Schuppan, D. Human T cell microparticles circulate in blood of hepatitis patients and induce fibrolytic activation of hepatic stellate cells. *Hepatology* **53**, 230-242, doi:10.1002/hep.23999 (2011).
- 37 They, C. *et al.* Minimal information for studies of extracellular vesicles 2018 (MISEV2018): a position statement of the International Society for Extracellular Vesicles and update of the MISEV2014 guidelines. *J Extracell Vesicles* **7**, 1535750, doi:10.1080/20013078.2018.1535750 (2018).
- 38 Banales, J. M. *et al.* Extracellular Vesicles in Liver Diseases: Meeting Report from the International Liver Congress 2018. *Hepatol Commun* **3**, 305-315, doi:10.1002/hep4.1300 (2019).
- 39 Kornek, M. & Schuppan, D. Microparticles: Modulators and biomarkers of liver disease. *J Hepatol* **57**, 1144-1146, doi:10.1016/j.jhep.2012.07.029 (2012).
- 40 Urban, S. K., Mocan, T., Sanger, H., Lukacs-Kornek, V. & Kornek, M. Extracellular Vesicles in Liver Diseases: Diagnostic, Prognostic, and Therapeutic Application. *Semin Liver Dis* **39**, 70-77, doi:10.1055/s-0038-1676122 (2019).
- 41 They, C., Zitvogel, L. & Amigorena, S. Exosomes: composition, biogenesis and function. *Nature reviews. Immunology* **2**, 569-579, doi:10.1038/nri855 (2002).
- 42 Kowal, J. *et al.* Proteomic comparison defines novel markers to characterize heterogeneous populations of extracellular vesicle subtypes. *Proc Natl Acad Sci U S A* **113**, E968-977, doi:10.1073/pnas.1521230113 (2016).
- 43 Mathieu, M. *et al.* Specificities of exosome versus small ectosome secretion revealed by live intracellular tracking of CD63 and CD9. *Nat Commun* **12**, 4389, doi:10.1038/s41467-021-24384-2 (2021).
- 44 Kalluri, R. & LeBleu, V. S. The biology, function, and biomedical applications of exosomes. *Science* **367**, doi:10.1126/science.aau6977 (2020).
- 45 Crescitelli, R. *et al.* Distinct RNA profiles in subpopulations of extracellular vesicles: apoptotic bodies, microvesicles and exosomes. *J Extracell Vesicles* **2**, doi:10.3402/jev.v2i0.20677 (2013).
- 46 Willms, E., Cabanas, C., Mager, I., Wood, M. J. A. & Vader, P. Extracellular Vesicle Heterogeneity: Subpopulations, Isolation Techniques, and Diverse Functions in Cancer Progression. *Front Immunol* **9**, 738, doi:10.3389/fimmu.2018.00738 (2018).
- 47 Kordelas, L. *et al.* MSC-derived exosomes: a novel tool to treat therapy-refractory graft-versus-host disease. *Leukemia* **28**, 970-973, doi:10.1038/leu.2014.41 (2014).

- 48 Bruno, S., Kholia, S., Deregibus, M. C. & Camussi, G. The Role of Extracellular Vesicles as Paracrine Effectors in Stem Cell-Based Therapies. *Adv Exp Med Biol* **1201**, 175-193, doi:10.1007/978-3-030-31206-0_9 (2019).
- 49 Li, T. *et al.* Exosomes derived from human umbilical cord mesenchymal stem cells alleviate liver fibrosis. *Stem Cells Dev* **22**, 845-854, doi:10.1089/scd.2012.0395 (2013).
- 50 Jiang, W. *et al.* Human Umbilical Cord MSC-Derived Exosomes Suppress the Development of CCl4-Induced Liver Injury through Antioxidant Effect. *Stem Cells Int* **2018**, 6079642, doi:10.1155/2018/6079642 (2018).
- 51 Fouraschen, S. M. *et al.* Secreted factors of human liver-derived mesenchymal stem cells promote liver regeneration early after partial hepatectomy. *Stem Cells Dev* **21**, 2410-2419, doi:10.1089/scd.2011.0560 (2012).
- 52 Tamura, R., Uemoto, S. & Tabata, Y. Immunosuppressive effect of mesenchymal stem cell-derived exosomes on a concanavalin A-induced liver injury model. *Inflamm Regen* **36**, 26, doi:10.1186/s41232-016-0030-5 (2016).
- 53 Hirsova, P. *et al.* Lipid-Induced Signaling Causes Release of Inflammatory Extracellular Vesicles From Hepatocytes. *Gastroenterology* **150**, 956-967, doi:10.1053/j.gastro.2015.12.037 (2016).
- 54 Chen, L. *et al.* Epigenetic regulation of connective tissue growth factor by MicroRNA-214 delivery in exosomes from mouse or human hepatic stellate cells. *Hepatology* **59**, 1118-1129, doi:10.1002/hep.26768 (2014).
- 55 Ibrahim, S. H. *et al.* Mixed lineage kinase 3 mediates release of C-X-C motif ligand 10-bearing chemotactic extracellular vesicles from lipotoxic hepatocytes. *Hepatology* **63**, 731-744, doi:10.1002/hep.28252 (2016).
- 56 Wang, R. *et al.* Exosome Adherence and Internalization by Hepatic Stellate Cells Triggers Sphingosine 1-Phosphate-dependent Migration. *J Biol Chem* **290**, 30684-30696, doi:10.1074/jbc.M115.671735 (2015).
- 57 Zhang, Y. *et al.* Secreted monocytic miR-150 enhances targeted endothelial cell migration. *Mol Cell* **39**, 133-144, doi:10.1016/j.molcel.2010.06.010 (2010).
- 58 Akao, Y. *et al.* Microvesicle-mediated RNA molecule delivery system using monocytes/macrophages. *Mol Ther* **19**, 395-399, doi:10.1038/mt.2010.254 (2011).
- 59 Haney, M. J. *et al.* Exosomes as drug delivery vehicles for Parkinson's disease therapy. *J Control Release* **207**, 18-30, doi:10.1016/j.jconrel.2015.03.033 (2015).
- 60 Kim, M. S. *et al.* Development of exosome-encapsulated paclitaxel to overcome MDR in cancer cells. *Nanomedicine* **12**, 655-664, doi:10.1016/j.nano.2015.10.012 (2016).
- 61 Sun, D. *et al.* A novel nanoparticle drug delivery system: the anti-inflammatory activity of curcumin is enhanced when encapsulated in exosomes. *Mol Ther* **18**, 1606-1614, doi:10.1038/mt.2010.105 (2010).
- 62 Wahlgren, J. *et al.* Plasma exosomes can deliver exogenous short interfering RNA to monocytes and lymphocytes. *Nucleic Acids Res* **40**, e130, doi:10.1093/nar/gks463 (2012).
- 63 Ota, Y. *et al.* Extracellular vesicle-encapsulated miR-30e suppresses cholangiocarcinoma cell invasion and migration via inhibiting epithelial-mesenchymal transition. *Oncotarget* **9**, 16400-16417, doi:10.18632/oncotarget.24711 (2018).
- 64 Chen, L. *et al.* Therapeutic effects of serum extracellular vesicles in liver fibrosis. *J Extracell Vesicles* **7**, 1461505, doi:10.1080/20013078.2018.1461505 (2018).
- 65 Lv, L. H. *et al.* Anticancer drugs cause release of exosomes with heat shock proteins from human hepatocellular carcinoma cells that elicit effective natural killer cell antitumor responses in vitro. *J Biol Chem* **287**, 15874-15885, doi:10.1074/jbc.M112.340588 (2012).
- 66 Tang, K. *et al.* Delivery of chemotherapeutic drugs in tumour cell-derived microparticles. *Nat Commun* **3**, 1282, doi:10.1038/ncomms2282 (2012).
- 67 Tian, Y. *et al.* A doxorubicin delivery platform using engineered natural membrane vesicle exosomes for targeted tumor therapy. *Biomaterials* **35**, 2383-2390, doi:10.1016/j.biomaterials.2013.11.083 (2014).
- 68 Gines, P. *et al.* Liver cirrhosis. *Lancet* **398**, 1359-1376, doi:10.1016/S0140-6736(21)01374-X (2021).
- 69 Kronborg, T. M., Ytting, H., Hobolth, L., Moller, S. & Kimer, N. Novel Anti-inflammatory Treatments in Cirrhosis. A Literature-Based Study. *Front Med (Lausanne)* **8**, 718896, doi:10.3389/fmed.2021.718896 (2021).
- 70 Schuppan, D. & Afdhal, N. H. Liver cirrhosis. *Lancet* **371**, 838-851, doi:10.1016/S0140-

- 6736(08)60383-9 (2008).
- 71 Otto, G. Donor Shortage in Germany: Impact on Short- and Long-Term Results in Liver Transplantation. *Visc Med* **34**, 449-452, doi:10.1159/000493891 (2018).
- 72 Phipps, M. M. & Verna, E. C. Coronavirus Disease 2019 and Liver Transplantation: Lessons from the First Year of the Pandemic. *Liver Transpl* **27**, 1312-1325, doi:10.1002/lt.26194 (2021).
- 73 Perez-Tamayo, R. Cirrhosis of the liver: a reversible disease? *Pathol Annu* **14 Pt 2**, 183-213 (1979).
- 74 Ellis, E. L. & Mann, D. A. Clinical evidence for the regression of liver fibrosis. *J Hepatol* **56**, 1171-1180, doi:10.1016/j.jhep.2011.09.024 (2012).
- 75 Distler, J. H. *et al.* The induction of matrix metalloproteinase and cytokine expression in synovial fibroblasts stimulated with immune cell microparticles. *Proc Natl Acad Sci U S A* **102**, 2892-2897, doi:10.1073/pnas.0409781102 (2005).
- 76 Roderfeld, M. Matrix metalloproteinase functions in hepatic injury and fibrosis. *Matrix Biol* **68-69**, 452-462, doi:10.1016/j.matbio.2017.11.011 (2018).
- 77 Chanput, W., Mes, J. J. & Wichers, H. J. THP-1 cell line: an in vitro cell model for immune modulation approach. *Int Immunopharmacol* **23**, 37-45, doi:10.1016/j.intimp.2014.08.002 (2014).
- 78 Valentine, M. A., Tsoukas, C. D., Rhodes, G., Vaughan, J. H. & Carson, D. A. Phytohemagglutinin binds to the 20-kDa molecule of the T3 complex. *Eur J Immunol* **15**, 851-854, doi:10.1002/eji.1830150821 (1985).
- 79 Crispe, I. N., Dao, T., Klugewitz, K., Mehal, W. Z. & Metz, D. P. The liver as a site of T-cell apoptosis: graveyard, or killing field? *Immunol Rev* **174**, 47-62, doi:10.1034/j.1600-0528.2002.017412.x (2000).
- 80 Ullal, A. J. & Pisetsky, D. S. The release of microparticles by Jurkat leukemia T cells treated with staurosporine and related kinase inhibitors to induce apoptosis. *Apoptosis* **15**, 586-596, doi:10.1007/s10495-010-0470-3 (2010).
- 81 von Bonin, M. *et al.* Treatment of refractory acute GVHD with third-party MSC expanded in platelet lysate-containing medium. *Bone Marrow Transplant* **43**, 245-251, doi:10.1038/bmt.2008.316 (2009).
- 82 Resnick, I. B. *et al.* Treatment of severe steroid resistant acute GVHD with mesenchymal stromal cells (MSC). *Am J Blood Res* **3**, 225-238 (2013).
- 83 van Niel, G., D'Angelo, G. & Raposo, G. Shedding light on the cell biology of extracellular vesicles. *Nat Rev Mol Cell Biol* **19**, 213-228, doi:10.1038/nrm.2017.125 (2018).
- 84 Julich-Haertel, H. *et al.* Cancer-associated circulating large extracellular vesicles in cholangiocarcinoma and hepatocellular carcinoma. *J Hepatol* **67**, 282-292, doi:10.1016/j.jhep.2017.02.024 (2017).
- 85 Kornek, M. *et al.* Circulating microparticles as disease-specific biomarkers of severity of inflammation in patients with hepatitis C or nonalcoholic steatohepatitis. *Gastroenterology* **143**, 448-458, doi:10.1053/j.gastro.2012.04.031 (2012).
- 86 Bratseth, V. *et al.* Annexin V(+) Microvesicles in Children and Adolescents with Type 1 Diabetes: A Prospective Cohort Study. *J Diabetes Res* **2020**, 7216863, doi:10.1155/2020/7216863 (2020).
- 87 Peiseler, M. & Tacke, F. Inflammatory Mechanisms Underlying Nonalcoholic Steatohepatitis and the Transition to Hepatocellular Carcinoma. *Cancers (Basel)* **13**, doi:10.3390/cancers13040730 (2021).
- 88 Parker, R. *et al.* CC chemokine receptor 2 promotes recruitment of myeloid cells associated with insulin resistance in nonalcoholic fatty liver disease. *Am J Physiol Gastrointest Liver Physiol* **314**, G483-G493, doi:10.1152/ajpgi.00213.2017 (2018).
- 89 Slomka, A., Urban, S. K., Lukacs-Kornek, V., Zekanowska, E. & Kornek, M. Large Extracellular Vesicles: Have We Found the Holy Grail of Inflammation? *Front Immunol* **9**, 2723, doi:10.3389/fimmu.2018.02723 (2018).
- 90 Spengler, U. & Nattermann, J. Immunopathogenesis in hepatitis C virus cirrhosis. *Clin Sci (Lond)* **112**, 141-155, doi:10.1042/CS20060171 (2007).
- 91 Durante-Mangoni, E. *et al.* Hepatic CD1d expression in hepatitis C virus infection and recognition by resident proinflammatory CD1d-reactive T cells. *J Immunol* **173**, 2159-2166, doi:10.4049/jimmunol.173.3.2159 (2004).
- 92 Lucas, M. *et al.* Frequency and phenotype of circulating Valpha24/Vbeta11 double-positive natural killer T cells during hepatitis C virus infection. *J Virol* **77**, 2251-2257, doi:10.1128/jvi.77.3.2251-2257.2003 (2003).
- 93 Syn, W. K. *et al.* Accumulation of natural killer T cells in progressive nonalcoholic fatty liver disease. *Hepatology* **51**, 1998-2007, doi:10.1002/hep.23599 (2010).
- 94 Park, O. *et al.* Diverse roles of invariant natural killer T cells in liver injury and fibrosis induced by

- carbon tetrachloride. *Hepatology* **49**, 1683-1694, doi:10.1002/hep.22813 (2009).
- 95 Odegaard, J. I. & Chawla, A. Mechanisms of macrophage activation in obesity-induced insulin resistance. *Nat Clin Pract Endocrinol Metab* **4**, 619-626, doi:10.1038/ncpendmet0976 (2008).
- 96 Bouloumie, A. *et al.* Role of macrophage tissue infiltration in metabolic diseases. *Curr Opin Clin Nutr Metab Care* **8**, 347-354, doi:10.1097/01.mco.0000172571.41149.52 (2005).
- 97 Fukushima, H. *et al.* Changes in Function and Dynamics in Hepatic and Splenic Macrophages in Non-Alcoholic Fatty Liver Disease. *Clin Exp Gastroenterol* **13**, 305-314, doi:10.2147/CEG.S248635 (2020).
- 98 Ogawa, Y. *et al.* Soluble CD14 levels reflect liver inflammation in patients with nonalcoholic steatohepatitis. *PLoS One* **8**, e65211, doi:10.1371/journal.pone.0065211 (2013).
- 99 Vannella, K. M. & Wynn, T. A. Mechanisms of Organ Injury and Repair by Macrophages. *Annu Rev Physiol* **79**, 593-617, doi:10.1146/annurev-physiol-022516-034356 (2017).
- 100 Regev, A. *et al.* Sampling error and intraobserver variation in liver biopsy in patients with chronic HCV infection. *Am J Gastroenterol* **97**, 2614-2618, doi:10.1111/j.1572-0241.2002.06038.x (2002).
- 101 Wieckowska, A. & Feldstein, A. E. Diagnosis of nonalcoholic fatty liver disease: invasive versus noninvasive. *Semin Liver Dis* **28**, 386-395, doi:10.1055/s-0028-1091983 (2008).
- 102 Kleiner, D. E. *et al.* Design and validation of a histological scoring system for nonalcoholic fatty liver disease. *Hepatology* **41**, 1313-1321, doi:10.1002/hep.20701 (2005).
- 103 Kleiner, D. E. *et al.* Design and validation of a histological scoring system for nonalcoholic fatty liver disease. *Hepatology* **41**, 1313-1321, doi:10.1002/hep.20701 (2005).
- 104 Younossi, Z. M. *et al.* Nonalcoholic fatty liver disease: assessment of variability in pathologic interpretations. *Mod Pathol* **11**, 560-565 (1998).
- 105 Taylor-Weiner, A. *et al.* A Machine Learning Approach Enables Quantitative Measurement of Liver Histology and Disease Monitoring in NASH. *Hepatology* **74**, 133-147, doi:10.1002/hep.31750 (2021).
- 106 Brodsky, S. V. *et al.* Dynamics of circulating microparticles in liver transplant patients. *J Gastrointest Liver Dis* **17**, 261-268 (2008).
- 107 Wang, W., Li, H., Zhou, Y. & Jie, S. Peripheral blood microvesicles are potential biomarkers for hepatocellular carcinoma. *Cancer Biomark* **13**, 351-357, doi:10.3233/CBM-130370 (2013).
- 108 Kim, J. W. *et al.* Fas ligand-positive membranous vesicles isolated from sera of patients with oral cancer induce apoptosis of activated T lymphocytes. *Clin Cancer Res* **11**, 1010-1020 (2005).
- 109 Abrahams, V. M., Straszewski-Chavez, S. L., Guller, S. & Mor, G. First trimester trophoblast cells secrete Fas ligand which induces immune cell apoptosis. *Mol Hum Reprod* **10**, 55-63, doi:10.1093/molehr/gah006 (2004).
- 110 Julich, H., Willms, A., Lukacs-Kornek, V. & Kornek, M. Extracellular vesicle profiling and their use as potential disease specific biomarker. *Frontiers in Immunology* **5**, doi:10.3389/fimmu.2014.00413 (2014).
- 111 Willms, A. *et al.* Tumour-associated circulating microparticles: A novel liquid biopsy tool for screening and therapy monitoring of colorectal carcinoma and other epithelial neoplasia. *Oncotarget* **7**, 30867-30875, doi:10.18632/oncotarget.9018 (2016).
- 112 Liu, M. *et al.* CD147 expression is associated with poor overall survival in chemotherapy treated triple-negative breast cancer. *J Clin Pathol* **71**, 1007-1014, doi:10.1136/jclinpath-2018-205342 (2018).
- 113 Tian, X. *et al.* Expression of CD147 and matrix metalloproteinase-11 in colorectal cancer and their relationship to clinicopathological features. *J Transl Med* **13**, 337, doi:10.1186/s12967-015-0702-y (2015).
- 114 Xu, X. Y., Lin, N., Li, Y. M., Zhi, C. & Shen, H. Expression of HAb18G/CD147 and its localization correlate with the progression and poor prognosis of non-small cell lung cancer. *Pathol Res Pract* **209**, 345-352, doi:10.1016/j.prp.2013.02.015 (2013).
- 115 Zhang, W. *et al.* Expression of extracellular matrix metalloproteinase inducer (EMMPRIN/CD147) in pancreatic neoplasm and pancreatic stellate cells. *Cancer Biol Ther* **6**, 218-227, doi:10.4161/cbt.6.2.3623 (2007).
- 116 Schulze, K. *et al.* Presence of EpCAM-positive circulating tumor cells as biomarker for systemic disease strongly correlates to survival in patients with hepatocellular carcinoma. *Int J Cancer* **133**, 2165-2171, doi:10.1002/ijc.28230 (2013).
- 117 Sun, Y. F. *et al.* Circulating stem cell-like epithelial cell adhesion molecule-positive tumor cells indicate poor prognosis of hepatocellular carcinoma after curative resection. *Hepatology* **57**, 1458-

- 1468, doi:10.1002/hep.26151 (2013).
- 118 Konigsberg, R. *et al.* Circulating tumor cells in metastatic colorectal cancer: efficacy and feasibility of different enrichment methods. *Cancer Lett* **293**, 117-123, doi:10.1016/j.canlet.2010.01.003 (2010).
- 119 Riethdorf, S. *et al.* Detection of circulating tumor cells in peripheral blood of patients with metastatic breast cancer: a validation study of the CellSearch system. *Clin Cancer Res* **13**, 920-928, doi:10.1158/1078-0432.CCR-06-1695 (2007).
- 120 Paterlini-Brechot, P. & Benali, N. L. Circulating tumor cells (CTC) detection: clinical impact and future directions. *Cancer Lett* **253**, 180-204, doi:10.1016/j.canlet.2006.12.014 (2007).
- 121 Alix-Panabieres, C. & Pantel, K. Circulating tumor cells: liquid biopsy of cancer. *Clin Chem* **59**, 110-118, doi:10.1373/clinchem.2012.194258 (2013).
- 122 Thomas, G. M. *et al.* Cancer cell-derived microparticles bearing P-selectin glycoprotein ligand 1 accelerate thrombus formation in vivo. *J Exp Med* **206**, 1913-1927, doi:10.1084/jem.20082297 (2009).
- 123 Mego, M., Mani, S. A. & Cristofanilli, M. Molecular mechanisms of metastasis in breast cancer--clinical applications. *Nat Rev Clin Oncol* **7**, 693-701, doi:10.1038/nrclinonc.2010.171 (2010).
- 124 Melo, S. A. *et al.* Glypican-1 identifies cancer exosomes and detects early pancreatic cancer. *Nature* **523**, 177-182, doi:10.1038/nature14581 (2015).
- 125 Au, S. H. *et al.* Clusters of circulating tumor cells traverse capillary-sized vessels. *Proc Natl Acad Sci U S A* **113**, 4947-4952, doi:10.1073/pnas.1524448113 (2016).
- 126 Urban, S. K. *et al.* Reply to: "Diagnostic and prognostic role of circulating microparticles in hepatocellular carcinoma". *J Hepatol*, doi:10.1016/j.jhep.2017.08.022 (2017).
- 127 van der Pol, E., Sturk, A., van Leeuwen, T., Nieuwland, R. & Coumans, F. Standardization of extracellular vesicle measurements by flow cytometry through vesicle diameter approximation. *J Thromb Haemost* **16**, 1236-1245, doi:10.1111/jth.14009 (2018).
- 128 Görgens, A. *et al.* Optimisation of imaging flow cytometry for the analysis of single extracellular vesicles by using fluorescence-tagged vesicles as biological reference material. *J Extracell Vesicles* **8**, 1587567 (2019).
- 129 Qu, M. *et al.* Platelet-derived microparticles enhance megakaryocyte differentiation and platelet generation via miR-1915-3p. *Nat Commun* **11**, 4964, doi:10.1038/s41467-020-18802-0 (2020).
- 130 Kuhn, S. *et al.* Mononuclear-cell-derived microparticles attenuate endothelial inflammation by transfer of miR-142-3p in a CD39 dependent manner. *Purinergic Signal* **14**, 423-432, doi:10.1007/s11302-018-9624-5 (2018).
- 131 Shi, B., Abrams, M. & Sepp-Lorenzino, L. Expression of asialoglycoprotein receptor 1 in human hepatocellular carcinoma. *J Histochem Cytochem* **61**, 901-909, doi:10.1369/0022155413503662 (2013).
- 132 Wu, L. J. *et al.* Capturing circulating tumor cells of hepatocellular carcinoma. *Cancer Lett* **326**, 17-22, doi:10.1016/j.canlet.2012.07.024 (2012).
- 133 Leung, E. L. *et al.* Non-small cell lung cancer cells expressing CD44 are enriched for stem cell-like properties. *PLoS One* **5**, e14062, doi:10.1371/journal.pone.0014062 (2010).
- 134 Cui, F., Wang, J., Chen, D. & Chen, Y. J. CD133 is a temporary marker of cancer stem cells in small cell lung cancer, but not in non-small cell lung cancer. *Oncol Rep* **25**, 701-708, doi:10.3892/or.2010.1115 (2011).
- 135 Nakabayashi, H., Taketa, K., Miyano, K., Yamane, T. & Sato, J. Growth of human hepatoma cells lines with differentiated functions in chemically defined medium. *Cancer Res* **42**, 3858-3863 (1982).
- 136 Lopez-Terrada, D., Cheung, S. W., Finegold, M. J. & Knowles, B. B. Hep G2 is a hepatoblastoma-derived cell line. *Hum Pathol* **40**, 1512-1515, doi:10.1016/j.humpath.2009.07.003 (2009).
- 137 Heffelfinger, S. C., Hawkins, H. H., Barrish, J., Taylor, L. & Darlington, G. J. SK HEP-1: a human cell line of endothelial origin. *In Vitro Cell Dev Biol* **28A**, 136-142 (1992).
- 138 Lieber, M., Mazzetta, J., Nelson-Rees, W., Kaplan, M. & Todaro, G. Establishment of a continuous tumor-cell line (panc-1) from a human carcinoma of the exocrine pancreas. *Int J Cancer* **15**, 741-747 (1975).
- 139 Fogh, J., Fogh, J. M. & Orfeo, T. One hundred and twenty-seven cultured human tumor cell lines producing tumors in nude mice. *J Natl Cancer Inst* **59**, 221-226 (1977).
- 140 Shiu, M. H., Cahan, A., Fogh, J. & Fortner, J. G. Sensitivity of xenografts of human pancreatic adenocarcinoma in nude mice to heat and heat combined with chemotherapy. *Cancer Res* **43**, 4014-4018 (1983).

- 141 Tzartzeva, K. *et al.* Surveillance Imaging and Alpha Fetoprotein for Early Detection of Hepatocellular Carcinoma in Patients With Cirrhosis: A Meta-analysis. *Gastroenterology* **154**, 1706-1718.e1701, doi:10.1053/j.gastro.2018.01.064 (2018).
- 142 Llovet, J. M., Bru, C. & Bruix, J. Prognosis of hepatocellular carcinoma: the BCLC staging classification. *Semin Liver Dis* **19**, 329-338, doi:10.1055/s-2007-1007122 (1999).
- 143 Scheuer, P. J. Classification of chronic viral hepatitis: a need for reassessment. *J Hepatol* **13**, 372-374, doi:10.1016/0168-8278(91)90084-o (1991).
- 144 Bedossa, P. & Poynard, T. An algorithm for the grading of activity in chronic hepatitis C. The METAVIR Cooperative Study Group. *Hepatology* **24**, 289-293, doi:10.1002/hep.510240201 (1996).
- 145 Moeini, A., Haber, P. K. & Sia, D. Cell of origin in biliary tract cancers and clinical implications. *JHEP Rep* **3**, 100226, doi:10.1016/j.jhepr.2021.100226 (2021).
- 146 Kendall, T. *et al.* Anatomical, histomorphological and molecular classification of cholangiocarcinoma. *Liver Int* **39 Suppl 1**, 7-18, doi:10.1111/liv.14093 (2019).
- 147 Lu, W. Y. *et al.* Hepatic progenitor cells of biliary origin with liver repopulation capacity. *Nat Cell Biol* **17**, 971-983, doi:10.1038/ncb3203 (2015).
- 148 Eckert, C. *et al.* Podoplanin discriminates distinct stromal cell populations and a novel progenitor subset in the liver. *Am J Physiol Gastrointest Liver Physiol* **310**, G1-12, doi:10.1152/ajpgi.00344.2015 (2016).
- 149 Lin, Y. *et al.* HGF/R-spondin1 rescues liver dysfunction through the induction of Lgr5(+) liver stem cells. *Nat Commun* **8**, 1175, doi:10.1038/s41467-017-01341-6 (2017).
- 150 Dorrell, C. *et al.* Prospective isolation of a bipotential clonogenic liver progenitor cell in adult mice. *Genes Dev* **25**, 1193-1203, doi:10.1101/gad.2029411 (2011).
- 151 Montal, R. *et al.* Molecular classification and therapeutic targets in extrahepatic cholangiocarcinoma. *J Hepatol* **73**, 315-327, doi:10.1016/j.jhep.2020.03.008 (2020).
- 152 Yano, Y. *et al.* Combined hepatocellular and cholangiocarcinoma: a clinicopathologic study of 26 resected cases. *Jpn J Clin Oncol* **33**, 283-287, doi:10.1093/jjco/hyg056 (2003).
- 153 Galle, P. R. *et al.* Biology and significance of alpha-fetoprotein in hepatocellular carcinoma. *Liver Int* **39**, 2214-2229, doi:10.1111/liv.14223 (2019).
- 154 Kessenbrock, K., Plaks, V. & Werb, Z. Matrix metalloproteinases: regulators of the tumor microenvironment. *Cell* **141**, 52-67, doi:10.1016/j.cell.2010.03.015 (2010).
- 155 Kornek, M. *et al.* Accelerated orthotopic hepatocellular carcinomas growth is linked to increased expression of pro-angiogenic and prometastatic factors in murine liver fibrosis. *Liver Int* **28**, 509-518, doi:10.1111/j.1478-3231.2008.01670.x (2008).
- 156 Kornek, M. *et al.* 1,2-dioleoyl-3-trimethylammonium-propane (DOTAP)-formulated, immunostimulatory vascular endothelial growth factor a small interfering RNA (siRNA) increases antitumoral efficacy in murine orthotopic hepatocellular carcinoma with liver fibrosis. *Mol Med* **14**, 365-373, doi:10.2119/2008-00003.Kornek (2008).
- 157 Aoki, M., Koga, K., Hamasaki, M., Egawa, N. & Nabeshima, K. Emmprin, released as a microvesicle in epithelioid sarcoma, interacts with fibroblasts. *Int J Oncol* **50**, 2229-2235, doi:10.3892/ijo.2017.3986 (2017).
- 158 Menck, K. *et al.* Tumor-derived microvesicles mediate human breast cancer invasion through differentially glycosylated EMMPRIN. *J Mol Cell Biol* **7**, 143-153, doi:10.1093/jmcb/mju047 (2015).
- 159 Yoshida, S. *et al.* Sublethal heat treatment promotes epithelial-mesenchymal transition and enhances the malignant potential of hepatocellular carcinoma. *Hepatology* **58**, 1667-1680, doi:10.1002/hep.26526 (2013).
- 160 Alzahrani, F. A. *et al.* Potential Effect of Exosomes Derived from Cancer Stem Cells and MSCs on Progression of DEN-Induced HCC in Rats. *Stem Cells Int* **2018**, 8058979, doi:10.1155/2018/8058979 (2018).
- 161 Hardin, H. *et al.* Thyroid cancer stem-like cell exosomes: regulation of EMT via transfer of lncRNAs. *Lab Invest* **98**, 1133-1142, doi:10.1038/s41374-018-0065-0 (2018).
- 162 So, J., Kim, A., Lee, S. H. & Shin, D. Liver progenitor cell-driven liver regeneration. *Exp Mol Med* **52**, 1230-1238, doi:10.1038/s12276-020-0483-0 (2020).
- 163 Zhang, D. W. *et al.* HAb18G/CD147 promotes activation of hepatic stellate cells and is a target for antibody therapy of liver fibrosis. *J Hepatol* **57**, 1283-1291, doi:10.1016/j.jhep.2012.07.042 (2012).
- 164 Stavrouka, C., Rush, H. & Ross, P. Combined hepatocellular cholangiocarcinoma (cHCC-CC): an update of genetics, molecular biology, and therapeutic interventions. *J Hepatocell Carcinoma* **6**, 11-

- 21, doi:10.2147/jhc.S159805 (2019).
- 165 Rodrigues, P. M. *et al.* Pathogenesis of Cholangiocarcinoma. *Annu Rev Pathol* **16**, 433-463, doi:10.1146/annurev-pathol-030220-020455 (2021).
- 166 Miwa, T., Nagata, T., Kojima, H., Sekine, S. & Okumura, T. Isoform switch of CD44 induces different chemotactic and tumorigenic ability in gallbladder cancer. *Int J Oncol* **51**, 771-780, doi:10.3892/ijo.2017.4063 (2017).
- 167 He, Y. *et al.* CD44 is overexpressed and correlated with tumor progression in gallbladder cancer. *Cancer Manag Res* **10**, 3857-3865, doi:10.2147/cmar.S175681 (2018).
- 168 Padthaisong, S. *et al.* Overexpression of a panel of cancer stem cell markers enhances the predictive capability of the progression and recurrence in the early stage cholangiocarcinoma. *J Transl Med* **18**, 64, doi:10.1186/s12967-020-02243-w (2020).
- 169 Ferreira, M. M., Ramani, V. C. & Jeffrey, S. S. Circulating tumor cell technologies. *Mol Oncol* **10**, 374-394 (2016).
- 170 Cai, J. *et al.* Extracellular vesicle-mediated transfer of donor genomic DNA to recipient cells is a novel mechanism for genetic influence between cells. *J Mol Cell Biol* **5**, 227-238 (2013).
- 171 Raposo, G. & Stoorvogel, W. Extracellular vesicles: exosomes, microvesicles, and friends. *J Cell Biol* **200**, 373-383 (2013).
- 172 Jamur, M. C. & Oliver, C. Permeabilization of cell membranes. *Methods Mol Biol* **588**, 63-66, doi:10.1007/978-1-59745-324-0_9 (2010).
- 173 Maire, C. L. *et al.* Genome-wide methylation profiling of glioblastoma cell-derived extracellular vesicle DNA allows tumor classification. *Neuro Oncol*, doi:10.1093/neuonc/noab012 (2021).
- 174 Kumeda, N. *et al.* Characterization of Membrane Integrity and Morphological Stability of Human Salivary Exosomes. *Biol Pharm Bull* **40**, 1183-1191, doi:10.1248/bpb.b16-00891 (2017).
- 175 Bhagwat, N. *et al.* An integrated flow cytometry-based platform for isolation and molecular characterization of circulating tumor single cells and clusters. *Sci Rep* **8**, 5035 (2018).
- 176 Ogle, L. F. *et al.* Imagestream detection and characterisation of circulating tumour cells - A liquid biopsy for hepatocellular carcinoma? *J Hepatol* **65**, 305-313, doi:10.1016/j.jhep.2016.04.014 (2016).
- 177 Urban, S. K. *et al.* Synergistic effects of extracellular vesicle phenotyping and AFP in hepatobiliary cancer differentiation. *Liver Int*, doi:10.1111/liv.14585 (2020).
- 178 Yekula, A. *et al.* From laboratory to clinic: Translation of extracellular vesicle based cancer biomarkers. *Methods* **177**, 58-66 (2020).
- 179 Lötval, J. *et al.* Minimal experimental requirements for definition of extracellular vesicles and their functions: a position statement from the International Society for Extracellular Vesicles. *J Extracell Vesicles* **3**, 26913 (2014).
- 180 Théry, C. *et al.* Minimal information for studies of extracellular vesicles 2018 (MISEV2018): a position statement of the International Society for Extracellular Vesicles and update of the MISEV2014 guidelines. *J Extracell Vesicles* **7**, 1535750 (2018).
- 181 Li, J. *et al.* Detection of circulating tumor cells in hepatocellular carcinoma using antibodies against asialoglycoprotein receptor, carbamoyl phosphate synthetase 1 and pan-cytokeratin. *PLoS One* **9**, e96185 (2014).
- 182 Armstrong, A. J. *et al.* Circulating tumor cells from patients with advanced prostate and breast cancer display both epithelial and mesenchymal markers. *Mol Cancer Res* **9**, 997-1007 (2011).
- 183 Gorges, T. M. *et al.* Circulating tumour cells escape from EpCAM-based detection due to epithelial-to-mesenchymal transition. *BMC Cancer* **12**, 178 (2012).
- 184 de Wit, S. *et al.* EpCAM(high) and EpCAM(low) circulating tumor cells in metastatic prostate and breast cancer patients. *Oncotarget* **9**, 35705-35716 (2018).
- 185 Darlington, P. J. *et al.* Natural Killer Cells Regulate Th17 Cells After Autologous Hematopoietic Stem Cell Transplantation for Relapsing Remitting Multiple Sclerosis. *Front Immunol* **9**, 834 (2018).
- 186 de Wit, S. *et al.* The detection of EpCAM(+) and EpCAM(-) circulating tumor cells. *Sci Rep* **5**, 12270 (2015).
- 187 Ostefeld, M. S. *et al.* miRNA profiling of circulating EpCAM(+) extracellular vesicles: promising biomarkers of colorectal cancer. *J Extracell Vesicles* **5**, 31488, doi:10.3402/jev.v5.31488 (2016).

8 Appendix

8.1. Peer-reviewed publications as part of this habilitation thesis

Human T Cell Microparticles Circulate in Blood of Hepatitis Patients and Induce Fibrolytic Activation of Hepatic Stellate Cells

Mirosław Kornek,¹ Yury Popov,¹ Towia A. Libermann,² Nezam H. Afdhal,¹ and Detlef Schuppan¹

Microparticles (MPs) are small cell membrane vesicles that are released from cells during apoptosis or activation. Although circulating platelet MPs have been studied in some detail, the existence and functional role of T cell MPs remain elusive. We show that blood from patients with active hepatitis C (alanine aminotransferase [ALT] level >100 IU/mL) contains elevated numbers of T cell MPs compared with patients with mild hepatitis C (ALT <40 IU/mL) and healthy controls. T cell MPs fuse with cell membranes of hepatic stellate cells (HSCs), the major effector cells for excess matrix deposition in liver fibrosis and cirrhosis. MP uptake is partly intercellular adhesion molecule 1–dependent and leads to activation of nuclear factor kappa B and extracellular signal-regulated kinases 1 and 2 and subsequent up-regulation of fibrolytic genes in HSCs, down-regulation of procollagen $\alpha 1(I)$ messenger RNA, and blunting of profibrogenic activities of transforming growth factor $\beta 1$. *Ex vivo*, the induced fibrolytic activity is evident in MPs derived from activated CD4+ T cells and is highest in MPs derived from activated and apoptotic CD8+ T cells. Mass spectrometry, fluorescence-activated cell sorting analysis, and function blocking antibodies revealed CD147/Emmprin as a candidate transmembrane molecule in HSC fibrolytic activation by CD8+ T cell MPs. **Conclusion:** Circulating T cell MPs are a novel diagnostic marker for inflammatory liver diseases, and *in vivo* induction of T cell MPs may be a novel strategy to induce regression of liver fibrosis. (HEPATOLOGY 2011;53:230-242)

Abbreviations: ALT, alanine aminotransferase; ERK1/2, extracellular signal-regulated kinases 1 and 2; FACS, fluorescence-activated cell sorting; FBS, fetal bovine serum; HSC, hepatic stellate cell; ICAM-1, intercellular adhesion molecule 1; IgG, immunoglobulin G; MMP, matrix metalloprotease; MP, microparticle; mRNA, messenger RNA; NF κ B, nuclear factor kappa B; PHA, phytohemagglutinin; RT-PCR, reverse-transcription polymerase chain reaction; ST, staurosporine; TGF $\beta 1$, transforming growth factor β ; TIMP-1, tissue inhibitor of metalloproteinase 1; TNF α , tumor necrosis factor α .

From the ¹Division of Gastroenterology and ²BIDMC Genomics and Proteomics Center, Beth Israel Deaconess Medical Center and Harvard Medical School, Boston, MA.

Received July 1, 2010; accepted September 13, 2010.

Part of the data were presented in abstract form (Popov Y, Zaks J, Grall F, Liebermann T, Afdhal NH, Schuppan D. T cell derived membrane microparticles containing EMMPRIN induce profibrolytic activation in hepatic stellate cells. HEPATOLOGY 2007;46(Suppl):717A; Popov Y, Millonig G, Schuppan D. T-cell derived membrane microparticles fuse with hepatic stellate cells and induce a profibrolytic phenotype. Gastroenterology 2007;132:A825–A826).

Address reprint requests to: Detlef Schuppan, M.D., Ph.D., Division of Gastroenterology, Beth Israel Deaconess Medical Center, Harvard Medical School, 330 Brookline Avenue, Boston, MA 02215. E-mail: dschuppa@bidmc.harvard.edu; fax: 617-667-2767.

Copyright © 2010 by the American Association for the Study of Liver Diseases.

View this article online at wileyonlinelibrary.com.

DOI 10.1002/hep.23999

Potential conflict of interest: Nothing to report.

Additional Supporting Information may be found in the online version of this article.

Cirrhosis is a complication of many forms of chronic liver disease. Due to a shortage of donors, liver transplantation is available to only a fraction of patients. Consequently, there is an urgent need for antifibrotic treatments, which can prevent, halt, or even reverse advanced fibrosis.¹ Significant progress has been made in our understanding of hepatic fibrosis, which is now viewed as a dynamic process characterized by an excess of extracellular matrix production (i.e., fibrogenesis) over its degradation (i.e., fibrolysis), which eventually leads to distortion of the hepatic architecture (i.e., cirrhosis) and loss of organ function.^{1,2}

In hepatic fibrosis, excessive extracellular matrix is produced by activated mesenchymal cells, which resemble myofibroblasts. Mesenchymal cells derive from quiescent hepatic stellate cells (HSCs) and periportal or perivenular fibroblasts, hereafter referred to collectively as HSCs. Activation of HSCs by several profibrogenic cytokines and growth factors, especially by transforming growth factor $\beta 1$ (TGF- $\beta 1$), is a general feature of fibrosis progression.² These factors are mainly produced by activated macrophages or cholangiocytes, but also by liver infiltrating lymphocytes.³

Several studies have suggested that advanced experimental and possibly human liver fibrosis can regress once pathogenic triggers are eliminated and sufficient time for recovery is available.^{4,5} Interestingly, the same cells that drive fibrogenesis (HSCs) can become major effectors of fibrolysis through the production and activation of certain matrix metalloproteinases (MMPs). This has been shown *in vitro* when dermal fibroblasts are plated from a two-dimensional cell culture dish into a three-dimensional collagen gel,^{6,7} allowing them to contract, thereby up-regulating MMPs and down-regulating procollagen I production.

A recent report suggested that lymphocytes can modulate fibroblasts in a different, non-cytokine-mediated manner.⁸ Thus a crude microparticle (MP) preparation released from the membranes of Jurkat T cells (an immortal lymphoma T cell line) during activation and early apoptosis could induce synovial fibroblast fibrolytic MMP expression. However, the mechanisms by which these MPs exert their fibrolytic effects remain unclear. Moreover, the effect of T cell-derived MPs on the activation of fibrogenic effector cells of a major organ such as the liver, where lymphocyte-driven inflammation frequently occurs, has not been addressed.¹ Finally, such MPs were not demonstrated in the circulation.

We report that T cell MPs circulate in blood and are elevated in patients with active chronic hepatitis C. Further, MPs derived both from CD8+ and CD4+ T cells can induce a fibrolytic phenotype in HSCs. This activity depends on fusion of the MPs with HSC membranes and transfer of T cell membrane molecules such as CD147 (Emmprin) to HSCs in a partly CD54 (intercellular adhesion molecule 1 [ICAM-1])-dependent manner. We conclude that T cell MPs may become a novel diagnostic tool and could be used therapeutically to mitigate (hepatic) inflammation and fibrosis.

Materials and Methods

Cell Lines. Jurkat T cells (ATCC#: CRL-2570, Manassas, VA) were grown in 10% fetal bovine serum (FBS) in Roswell Park Memorial Institute 1640 medium, and LX-2 were grown in 2.5% FBS in Dulbecco's modified Eagle's medium (Cellgrow, Manassas, VA). THP-1 monocytes (American Type Culture Collection No. TIB-202) were grown in 10% FBS in Dulbecco's modified Eagle's medium (Cellgrow) and were differentiated into macrophages by way of incubation with 0.05 $\mu\text{g}/\text{mL}$ phorbol myristate acetate for 24 hours.⁹

Lymphocyte Isolation. Human peripheral blood was collected in heparinized tubes from healthy volun-

teers within a protocol approved by Children's Hospital (Boston, MA). Mononuclear cells were isolated by way of centrifugation over Ficoll-Paque Premium (GE Healthcare, Uppsala, Sweden). After three washes in Hank's balanced salt solution, CD4+ and CD8+ T cells were isolated by way of negative selection using magnetic beads (Miltenyi Biotec, Auburn, CA).

Isolation of MPs from Activated or Apoptotic T Cells and Monocytes/Macrophages. For induction of apoptosis, T cells or monocytes/macrophages were treated with 4 $\mu\text{mol}/\text{mL}$ staurosporine (ST) (Cell Signaling Technology, Danvers, MA) for 4 hours. T cells were activated with 5 $\mu\text{g}/\text{mL}$ phytohemagglutinin (PHA) (Roche, Mannheim, Germany) for 24 hours, and 3 days later restimulated. During stimulation with PHA, T cell cultures were supplemented with 5 ng/mL interleukin-2 (PeproTech, Rocky Hill, NJ). Three days after restimulation, cells were pelleted and cell-free supernatants were centrifuged at 10×10^3g for 20 minutes yielding S10-MPs, whereas the resultant supernatant was centrifuged at 100×10^3g for 90 minutes to yield purified, biologically active S100-MPs.

Characterization and Quantification of MPs. The MP preparations were characterized by way of fluorescence-activated cell sorting (FACS) with an LSR2 sorter (Becton Dickinson, San Jose, CA) and cytometric data was analyzed with FlowJo 8.8.6 software (Tree Star, Inc., Ashland, Oregon). MP particles were gated on forward and sidescatter acquired from runs including 500 standard beads (Becton Dickinson, San Jose, CA). The number of CD3 (CD11a, CD14, CD147) and AnnexinV (eBioscience, San Diego, CA; GeneTex Inc., Irvine, CA for CD147) double-positive events were calculated relative to the number of beads added to the samples. To avoid unspecific antibody binding, Fc receptors on MPs and target cells were blocked with FcR Blocking Reagent (Miltenyi Biotec). Antibody solutions were centrifuged prior to FACS to avoid artifacts due to aggregation.

Isolation of T Cell MPs from Human Plasma and Liver Histology. Human peripheral blood was collected in citrate-containing tubes (BD Vacutainer, Buff. Na. Citrate [9NC]; BD, Franklin Lakes, NJ) from patients and healthy controls (protocol approved by the Beth Israel Deaconess Medical Center, approval no. 2004-P-000318). MPs were isolated by way of differential centrifugation, and S100-MPs were characterized by way of FACS using staining for Annexin V, CD3, CD4, CD8, CD14, CD15, CD41, and CD25 (eBioscience) as detailed above. Levels of T cell MPs were correlated with liver histology as detailed in the Supporting Materials and Methods.

Incubation of HSCs with T Cell-Derived or Monocyte/Macrophage-Derived MPs and Quantitative Polymerase Chain Reaction. HSCs (200×10^3 /well) were seeded into six-well culture plates and serum-starved for 24 hours, followed by incubation with 1×10^3 or 50×10^3 S10-MPs or S100-MPs for 24 hours, and RNA extraction using TRIzol reagent (Invitrogen, Carlsbad, CA). ST ($0.04 \mu\text{M}/\text{mL}$) or plain medium served as controls. One microgram of RNA was reverse-transcribed using random primers and Superscript RNase H-reverse transcriptase (Invitrogen). Primers and probes are listed in Supporting Table 2. Relative transcript levels were quantified on a LightCycler 1.5 (Roche, Mannheim, Germany) using the TaqMan methodology.

Labeling of MPs. MP membranes were labeled with the PKH26 lipid dye (Sigma-Aldrich, St. Louis, MO). Labeled S10-MPs and S100-MPs were coincubated with LX-2 cells for 0-1, 30, and 60 minutes, washed extensively, and fixed with 2% paraformaldehyde for 15 minutes at room temperature.

Quantification of CD3 Receptor Transfer. HSCs (200×10^3 /well) were seeded into six-well cell culture plates (BD Labware, Franklin Lakes, NJ) for 12 hours, serum-starved for 24 hours, followed by incubation with 100×10^3 S100-MPs for 1 minute up to 24 hours. Cells were then washed with phosphate-buffered saline and collected using trypsin/ethylene diamine tetraacetic acid (Cellgrow, Manassas, VA), and single-cell suspensions stained with anti-CD3-APC were followed by FACS analysis.

ICAM-1 Up-regulation of HSCs by TNF α . Tumor necrosis factor α (TNF α) (PeproTech) was added to HSC cultures, and ICAM-1 expression assessed after 2, 4, and 24 hours by FACS using anti-ICAM-1 PE (eBioscience, San Diego, CA).

Comparative Proteomic Analysis. A detailed description of the comparative proteomic analysis is provided in the Supporting Materials and Methods. A total of $20 \mu\text{g}$ of S-100 MP protein from ST-treated Jurkat T cells and Huh-7 hepatoma cells was extracted and denatured with 0.1% (vol/vol) sodium dodecyl sulfate in phosphate-buffered saline, reduced and alkylated, digested with trypsin, and labeled with isobaric tags (4-plex iTRAQ; Applied Biosystems, Foster City, CA). The two digested extracts were pooled and subjected to two-dimensional peptide fractionation and analyzed for their comparative proteomic signature by way of matrix-assisted laser desorption ionization/time of flight mass spectrometry.¹⁰

CD54 (ICAM-1) and CD147 (EMMPRIN) Blocking Studies. Subconfluent, serum-starved HSCs were preincubated with monoclonal blocking anti-human CD54 or isotype-matched (immunoglobulin G1 [IgG1]) control antibody ($50 \mu\text{g}/\text{mL}$; GeneTex Inc., Irvine, CA) for 120 minutes, washed, and incubated with Jurkat T cell-derived S100-MPs. S100-MPs were incubated with monoclonal blocking anti-human CD147 (Abcam, Cambridge, MA) or IgG1 control antibody ($50 \mu\text{g}/\text{mL}$; GeneTex Inc.) for 60 minutes prior to their addition to HSCs.

P65 Nuclear Factor kappa B Translocation. HSCs were serum-starved for 24 hours, then washed with phosphate-buffered saline and fixed in cold methanol for 10 minutes. Nuclear translocation of p65 nuclear factor kappa B (NF κ B) was detected by incubating cells with polyclonal p65 antibody (1:100; Delta Biolabs) for 30 minutes followed by TRITC-conjugated anti-rabbit IgG (1:200, Dako, Germany). Representative images were documented using a scanning confocal microscope (Carl Zeiss, Germany).

Signaling Pathway Inhibition. Serum-starved HSCs were incubated with the inhibitors SB203580 (p38 MAPK), U0126 (extracellular signal-regulated kinases 1 and 2 [ERK1/2]), and LY294002 (phosphatidylinositol-3 kinase) (LC Labs, Woburn, MA) as described.¹¹ The proteasome inhibitor MG132 (Rockland Inc.) was used to block NF κ B nuclear translocation and activity.

Statistical Analysis. All data are presented as the mean \pm SD. Differences between independent experimental groups were analyzed using a two-tailed Student *t* test. $P < 0.05$ was considered statistically significant. Correlations of MP levels with histological grade and stage were calculated by best-fit linear regression analysis based on a 95% confidence interval. All calculations were performed with Prism 4 (GraphPad Software, Inc.).

Results

T Cell-Derived MPs Circulate in the Blood Plasma of Healthy Controls and Are Increased in Patients with Active Hepatitis C. We searched for T cell-derived MPs in human plasma from normal controls and patients with chronic hepatitis. Pure S100-MPs that carried the MP marker Annexin V^{12,13} and the T cell marker CD3 were present in human plasma (Fig. 1A). Their percentage increased significantly from 25% in healthy controls and patients with serologically mild hepatitis C (alanine aminotransferase [ALT] $<40 \text{ IU}/\text{mL}$) to 31% in patients with

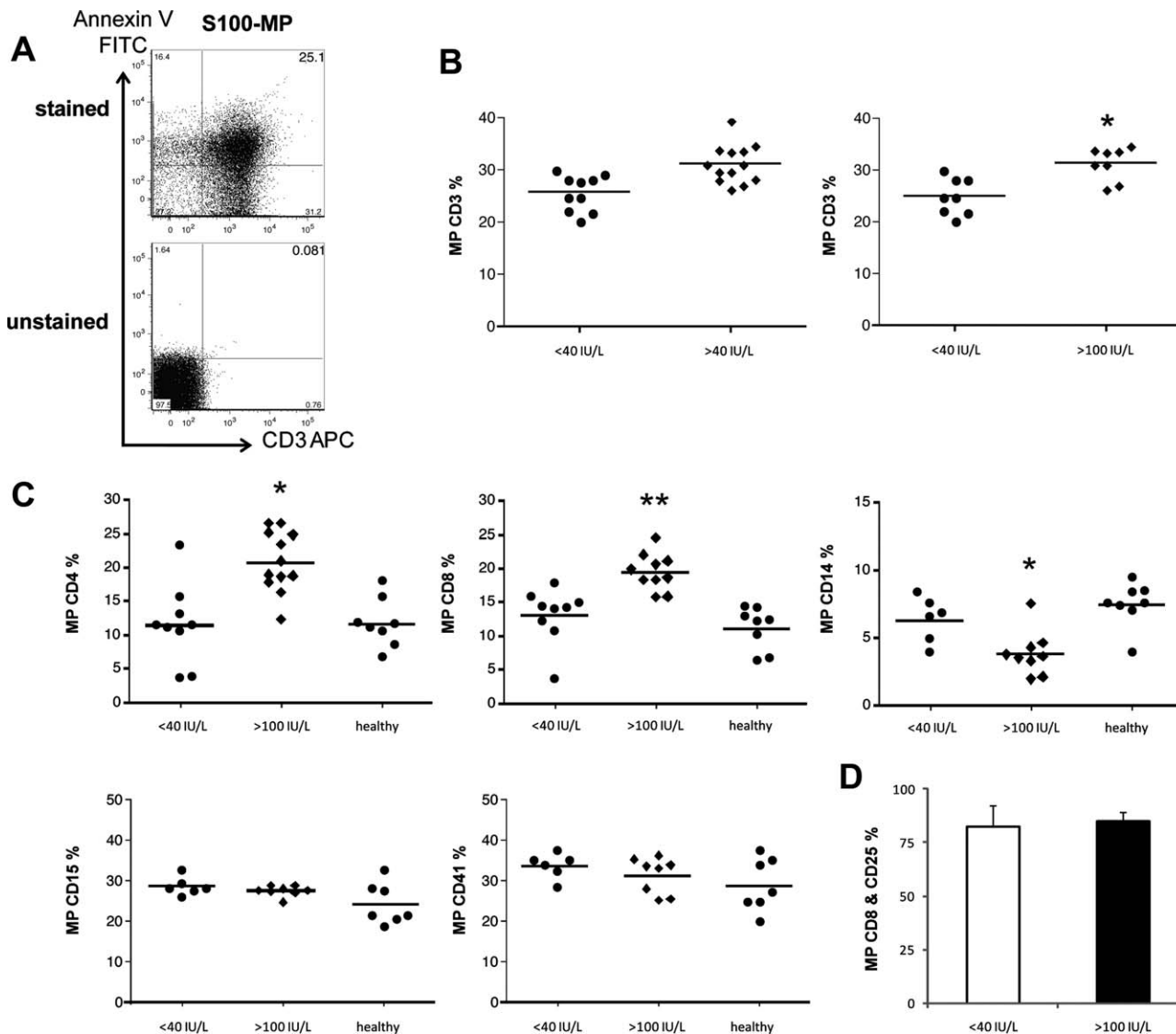


Fig. 1. T cell-derived MPs are found in plasma and are elevated in patients with active hepatitis C. (A) Representative FACS analysis of CD3-APC and Annexin V-fluorescein isothiocyanate double-positive S100-MPs in a plasma sample from a healthy human donor. (B) Relative percentage of circulating CD3 and Annexin V double-positive S100-MPs from patients with hepatitis C and normal ALT levels (<40 IU/L; n = 4), elevated ALT levels (>40 IU/L; n = 10), or high ALT levels (>100 IU/mL; n = 7). (C) CD4/Annexin V and CD8/Annexin V double-positive, CD14/Annexin V, CD15/Annexin V, and CD41/Annexin V double-positive S100-MPs in the plasma of patients with ALT >100 IU/L (n > 9) compared with healthy controls and hepatitis C virus patients with ALT <40 IU/L (n > 9). (D) CD8+ S100-MPs are ≈80% positive for CD25. *P < 0.05. **P < 0.005.

serologically active hepatitis C (ALT >40 IU/mL and ALT >100 IU/mL) (Fig. 1B). The higher percentages were paralleled by a higher mean fluorescence intensity for CD3 (data not shown). Of note, looking at T cell subsets, patients with active hepatitis C had a significant increase in circulating MPs derived from CD4+ as well as CD8+ T cells (two- and 1.5-fold versus patients with mild hepatitis C and healthy controls, respectively). Furthermore, 80% of CD8+ MPs were additionally CD25+, a T cell activation marker.¹² Levels of MPs derived from other cells,¹⁴ such as CD41+ MPs (from platelets) and CD15+ MPs (from neutrophils), were unchanged, whereas CD14+ MPs

(from monocytes, macrophages, and dendritic cells) were reduced by nearly 50% in patients with active hepatitis C (P = 0.015) (Fig. 1C). When patients' liver histology was matched with MP plasma levels using linear regression analysis, both histological grade and stage showed a significant correlation with CD4+ and CD8+ MPs (Fig. 2).

Isolation and Characterization of T Cell-Derived MPs. Due to the low numbers of circulating MPs, initial characterization and functional analyses were performed with T cell MPs released from the human Jurkat T cell line and from peripheral blood of healthy human donors. We stimulated MP release either by

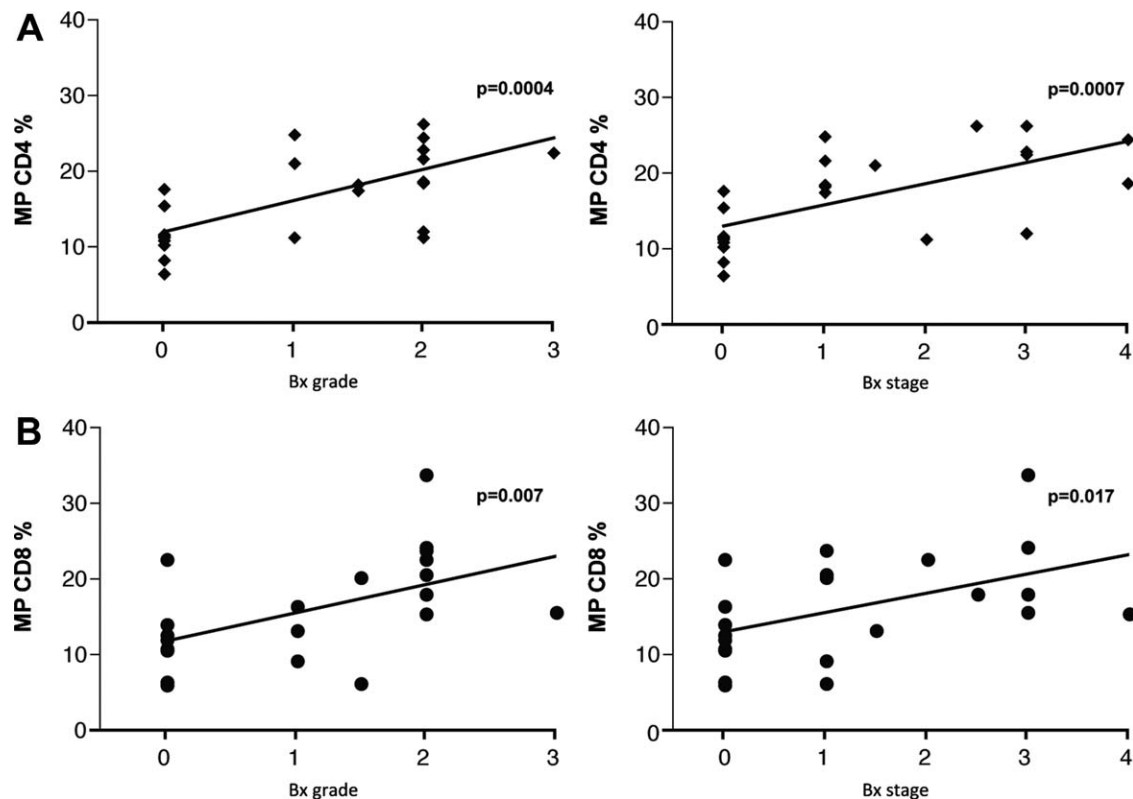


Fig. 2. Levels of circulating T cell-derived S100-MPs correlate with histological grade and stage in patients with hepatitis C. Correlations of plasma CD4⁺ and CD8⁺ S100-MPs with patient biopsy specimens were performed as detailed in the Supporting Materials and Methods. Patients with normal and elevated ALT levels were included. CD8⁺ analysis did not work in one patient with biopsy (Bx) stage 4.

activation with PHA,^{15,16} or by induction of apoptosis using the tyrosine kinase inhibitor ST.⁸ Whereas the Jurkat S100-MP fraction was Annexin V^{low} and CD3^{low}, the Jurkat S100-MP fraction was Annexin V^{high} and CD3^{high} (Supporting Fig. 1A), which was confirmed by analysis of mean fluorescence intensity (Supporting Fig. 1B). This difference between S100-MPs and S10-MPs was found regardless of the mode of generation (by way of PHA, ST, or PHA and ST combined) (Supporting Fig. 1B).

Electron microscopic images from both fractions demonstrated that S10-MPs were heterogeneous in size and contained electron dense material, indicating debris of intracellular organelles, whereas S100-MPs showed a more homogeneous structure, being surrounded by a double-layered cell membrane and being electron-lucent, with a variable diameter ranging from 30 nm to 700 nm (Fig. 3A). Fig. 3B shows a typical FACS scatter plot that characterizes the S-100 MPs along with 3- μ m marker beads and intact T cells.

CD3 T Cell Receptor Transfer from S100-MPs to Cell Membranes of Human HSCs. The exclusive expression of transmembrane CD3 on T cells allowed us to monitor the transfer of CD3 from S100-MPs to

human LX-2 HSCs. Six hours of incubation with S100-MPs, the transfer of CD3 from MPs to HSCs peaked, with 17% of the HSCs being positive for CD3 (Fig. 3C,D). In support of the FACS data, fluorescence microscopy demonstrated that S100-MPs labeled with the membrane-dye PKH26 began to attach to HSC membranes at 30 minutes, generating a punctate red-fluorescent membrane pattern, and a diffuse membrane staining, indicative of membrane fusion, from 60 minutes onward (Fig. 3E). Membrane fusion was not found with PKH26-labeled S10-MPs (Supporting Fig. 1C).

T Cell Derived S100-MP Do Not Induce Apoptosis of HSCs. Because MMPs, especially MMP-3, are up-regulated in cells undergoing apoptosis,¹⁷ and because our data show that S100-MPs derived from apoptotic T cells prominently up-regulated MMP-3 in HSCs, we evaluated apoptosis induction by S100-MPs using Annexin V and 7-amino-actinomycin D staining as a readout (Supporting Fig. 1D,E). Jurkat T cell-derived S100-MPs did not induce enhanced apoptosis or necrosis in HSCs after 24 hours of incubation, which also ruled out a significant ST contamination in our MP preparations.

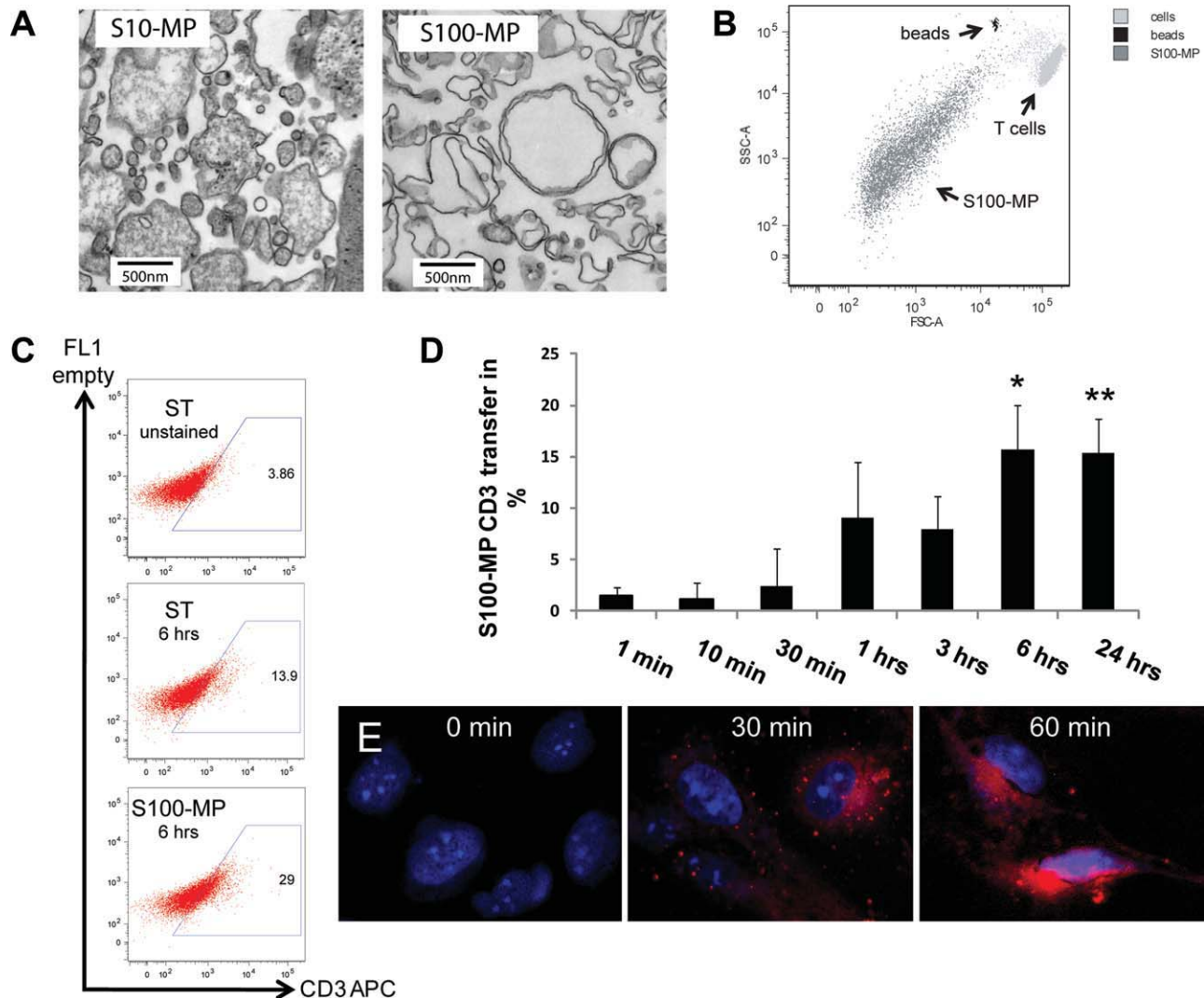


Fig. 3. Characteristics of T cell-derived S100-MPs and S10-MPs and demonstration of their fusion with HSC membranes. (A) Ultrastructural analysis of the two subfractions of MPs generated from apoptotic Jurkat T cells. Magnification $\times 51,000$. (B) Representative forward and side-scatter profiles of events in blood-derived S100-MPs after addition of beads and intact T cells. (C) FACS analysis demonstrating CD3 receptor transfer from S100-MPs to HSCs. A total of 2×10^5 LX-2 cells were incubated with 10^5 Jurkat T cell-derived S100-MPs and CD3-positive LX-2 HSCs were quantified after 6 hours. Unstained HSCs and HSCs incubated with $0.04 \mu\text{M}/\text{mL}$ ST served as controls. (D) Time-dependent uptake of CD3 S100-MPs by HSCs assessed by way of FACS analysis, demonstrating maximal MP uptake (15%-17%) after 6 hours ($n = 3$ events; mean \pm SD). * $P = 0.003$. ** $P = 0.01$. (E) Fluorescence microscopy confirming S100-MP uptake and membrane fusion with HSCs. S100-MPs were labeled with PKH26 membrane dye and incubated with LX-2 HSCs.

Effect of S100 T Cell MPs on Fibrosis-Related Gene Expression by HSCs. Fibrosis related transcripts were measured in LX-2 HSCs 24 hours after addition of 1×10^3 or 50×10^3 S100-MP from Jurkat T cells using quantitative reverse-transcription polymerase chain reaction (RT-PCR). S10-MPs, plain medium, and ST alone served as controls. MPs were obtained from PHA-activated and/or apoptotic (ST-treated) Jurkat T cells. After induction of T cell apoptosis, significant changes in fibrosis-related transcripts were found with 50×10^3 S100-MP, whereas equivalent amounts of S10-MPs had no effect (Fig. 4A). S100-MPs induced a significant (2.05- to 4.9-fold) up-regu-

lation of fibrolytic genes (MMP-1, MMP-3, MMP-9, MMP-13) in HSCs, whereas transcript levels of the profibrogenic genes tissue inhibitor of metalloproteinase 1 (TIMP-1) and procollagen $\alpha 1(\text{I})$ were unaffected (Fig. 4A). Similar results were obtained when S100-MPs were incubated with freshly isolated primary rat HSCs. Here, the human S100-MPs induced MMP-3 even nine-fold (Supporting Fig. 2). S100-MPs from apoptotic T cells that had been preactivated by PHA did not induce up-regulation of MMPs in human HSCs, but rather down-regulated MMP-3 (Supporting Fig. 4). A similar response was found with S100-MPs derived from merely PHA-activated T

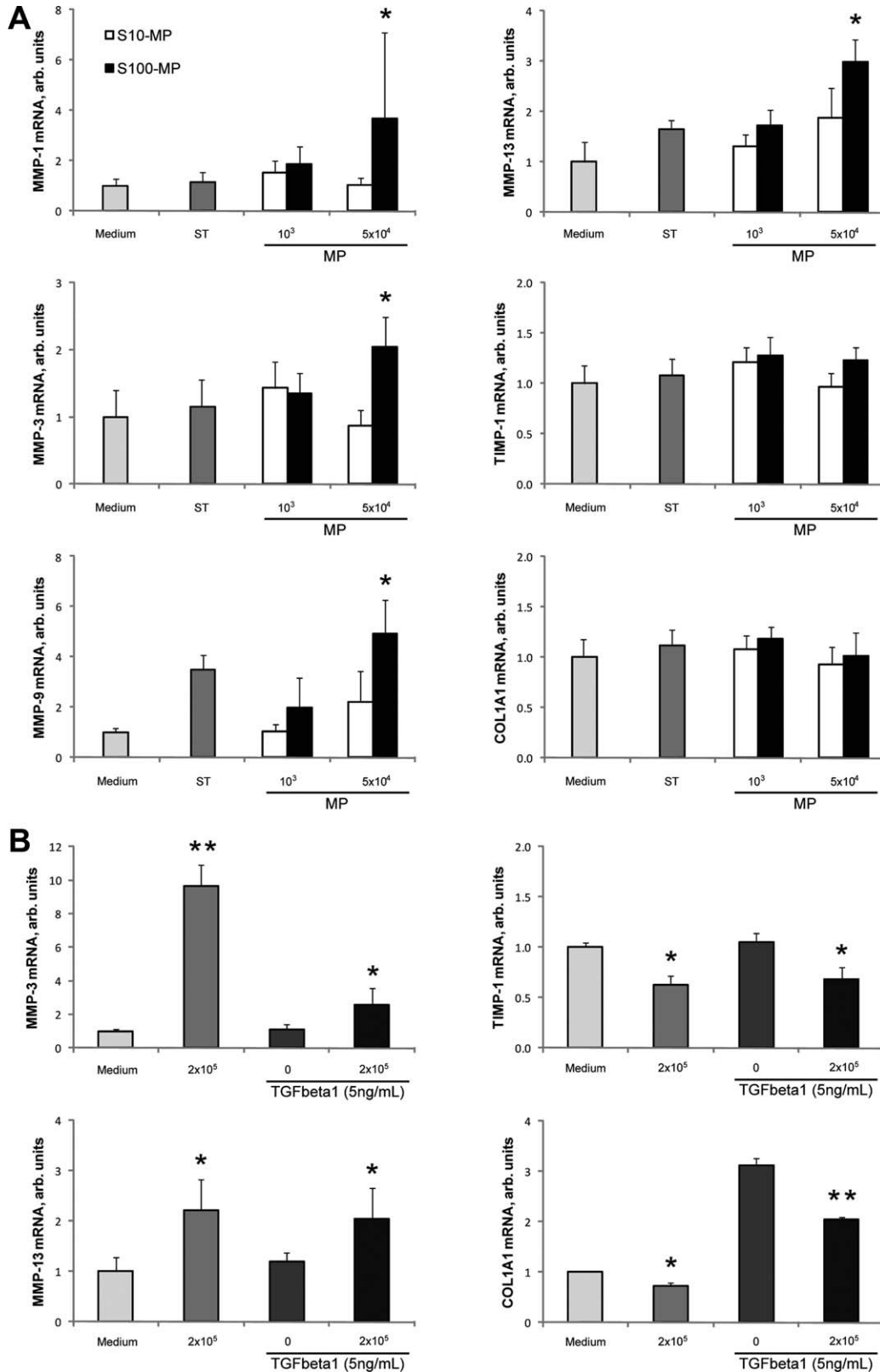


Fig. 4. S100-MPs from Jurkat T cells elicit antifibrogenic responses in HSCs. (A) MMP-1, MMP-3, MMP-9, MMP-13, TIMP-1, and procollagen $\alpha 1(I)$ transcripts were determined by quantitative RT-PCR in LX-2 HSCs (2×10^5 cells per well in 12-well plates) that were incubated with 10^3 or 5×10^4 S10-MPs or S100-MPs from apoptotic Jurkat T cells suspended in 350 μ L medium for 24 hours. ST (0.04 μ M/mL) or plain medium served as controls. (B) Induction of fibrolytic and inhibition of fibrogenic genes in TGF β 1 (5 ng/mL)-activated HSCs when incubated with S100-MPs (2×10^5 MPs suspended in 350 μ L medium) for 24 hours. All experiments were performed at least twice ($n = 3-4$ /group). Results (mean \pm SD) are expressed as arbitrary (arb.) units relative to $\beta 2$ -microglobulin mRNA. * $P < 0.05$ versus medium control. ** $P < 0.005$.

cells (data not shown). As non-T cell controls, MPs derived from THP-1 monocytes and macrophages did not induce significant changes in MMP, TIMP-1, or procollagen $\alpha 1(I)$ transcript levels, except for induction of MMP-3 and TIMP-1 by macrophage-derived MPs (Supporting Fig. 4).

S100-MPs Abrogate HSC Profibrogenic Responses to TGF β 1. Human HSCs were exposed to 5 ng/mL TGF β 1, which elicits a strong fibrogenic response. Jurkat T cell-derived S100-MPs not only blunted the TGF β 1 response by reducing procollagen $\alpha 1(I)$ expression, they induced fibrolytic MMP transcripts beyond the levels produced by unstimulated HSCs (Fig. 4B). Therefore, TGF β 1 enhanced HSC procollagen $\alpha 1(I)$ expression 2.7-fold, which after MP addition was reduced by almost 40%, and MPs increased the expression of MMP-3 and MMP-13 almost 2.5- and 2.1-fold, respectively. In addition, both in TGF β 1-treated and TGF β 1-untreated HSCs the addition of S100-MPs significantly reduced profibrogenic TIMP-1 expression by 30%-35% (Fig. 4B).

Comparison of the Effect of S100-MPs Derived from CD4+ and CD8+ T Cells. Overall, apoptotic CD4+ T cell-derived MPs induced MMP expression in HSCs much less efficiently than MPs from CD8+ T cells, irrespective of their mode of generation (with or without prior activation by PHA). Therefore, MPs from CD4+ T cells did not significantly affect MMP-1, MMP-3, MMP-9, MMP-13, TIMP-1, or procollagen $\alpha 1(I)$ expression (data not shown). If MPs were induced only by CD4+ T cell activation with PHA, a significant induction was observed for MMP-1, MMP-3, and MMP-9 messenger RNA (mRNA) (between 1.7- and three-fold), whereas procollagen $\alpha 1(I)$ and TIMP-1 transcript levels remained unchanged (Supporting Fig. 5). S100-MPs derived from apoptotic CD8+ T cells did not affect fibrosis-related gene expression (Supporting Fig. 6), whereas S100-MPs from CD8+ T cells that were only preactivated by PHA increased MMP-1 transcripts 1.9-fold and reduced procollagen $\alpha 1(I)$ transcripts by 30% (data not shown). S100-MPs from apoptotic CD8+ T cells that were preactivated by PHA produced the strongest fibrolytic effects in HSCs, also reducing procollagen $\alpha 1(I)$ mRNA significantly by 45% (Fig. 5A).

CD54 (ICAM-1)-Dependent Uptake of S100-MPs. It remains to be shown what cell membrane molecules or receptors mediated attachment and uptake of S100-MPs by HSCs. Our FACS analysis revealed that >60% of S100-MPs were highly positive for the CD54 ligand CD11a (Fig. 5B). Assuming that ICAM-1 expressed by the recipient HSCs is engaged by

CD11a/CD18 on the S100-MPs, an increased HSC CD54 expression should enhance MP uptake. We therefore incubated HSCs with 10 ng/mL TNF α , a strong inducer of CD54,¹⁸ which induced a robust (>10-fold) up-regulation (Fig. 5C). This pretreatment led to a further significant MP-induced increase of MMP-3, MMP-9, and MMP-13 expression in HSCs (Fig. 5D). A direct fibrolytic effect of TNF α on HSCs was largely ruled out, because TNF α alone did not enhance HSC MMP-3 mRNA, and alone modestly induced HSC MMP-9 and MMP-13 expression (Fig. 5D).

To corroborate that the observed effects were indeed due to an engagement of CD54 on HSCs, HSCs were incubated with CD54 blocking or an isotype-matched control antibody 2 hours prior to addition of S100-MPs. CD54 blocking resulted in a significant down-regulation of MMP-3 and MMP-13 transcripts induced by MPs from Jurkat T cells (40% and 45%, respectively) (Fig. 5E).

Emmprin (CD147) Is Involved in MP-Induced MMP Induction in HSCs. Comparative quantitative proteomics of T cell versus control (Huh7 hepatoma) cell S100-MPs using iTRAQ isobaric tagging yielded three candidate cell (membrane)-associated molecules, other than growth factor or cytokine receptors, namely nodal modulator 1 and 2 (molecules involved in the inhibition of TGF β signaling and Emmprin/Basigin (CD147) (Supporting Table 1). FACS analysis showed that T cell-derived S100-MPs as well as HSCs were highly positive for CD147 (>70% and 99%, respectively), a molecule that requires homodimeric interaction for MMP induction (Fig. 6A). Blocking of CD147 on S100-MPs (CD8+ T cell-derived after induction with PHA and ST) resulted in a significant reduction of MMP-3 and MMP-9 transcripts (35% and 30%, respectively) (Fig. 6B), confirming the functional involvement of CD147.

Fibrolytic Activation of HSCs by S100-MPs Depends on NF κ B and ERK1/2 Pathways. HSC MMP-3 induction by T cell MPs was completely abrogated by inhibition of p42/p44 mitogen-activated protein kinase (ERK1/2), to a modest degree by inhibition of p38 or NF κ B, and remained unaffected by inhibition of phosphatidylinositol-3 kinase/Akt (Fig. 6C). >10% of HSC showed NF κ B relocation to the nucleus after incubation with S100-MP, confirming modest activation of the NF κ B pathway (Fig. 6D).

Discussion

We have shown that CD4+ and CD8+ T cell-derived MPs can be detected in human plasma, and

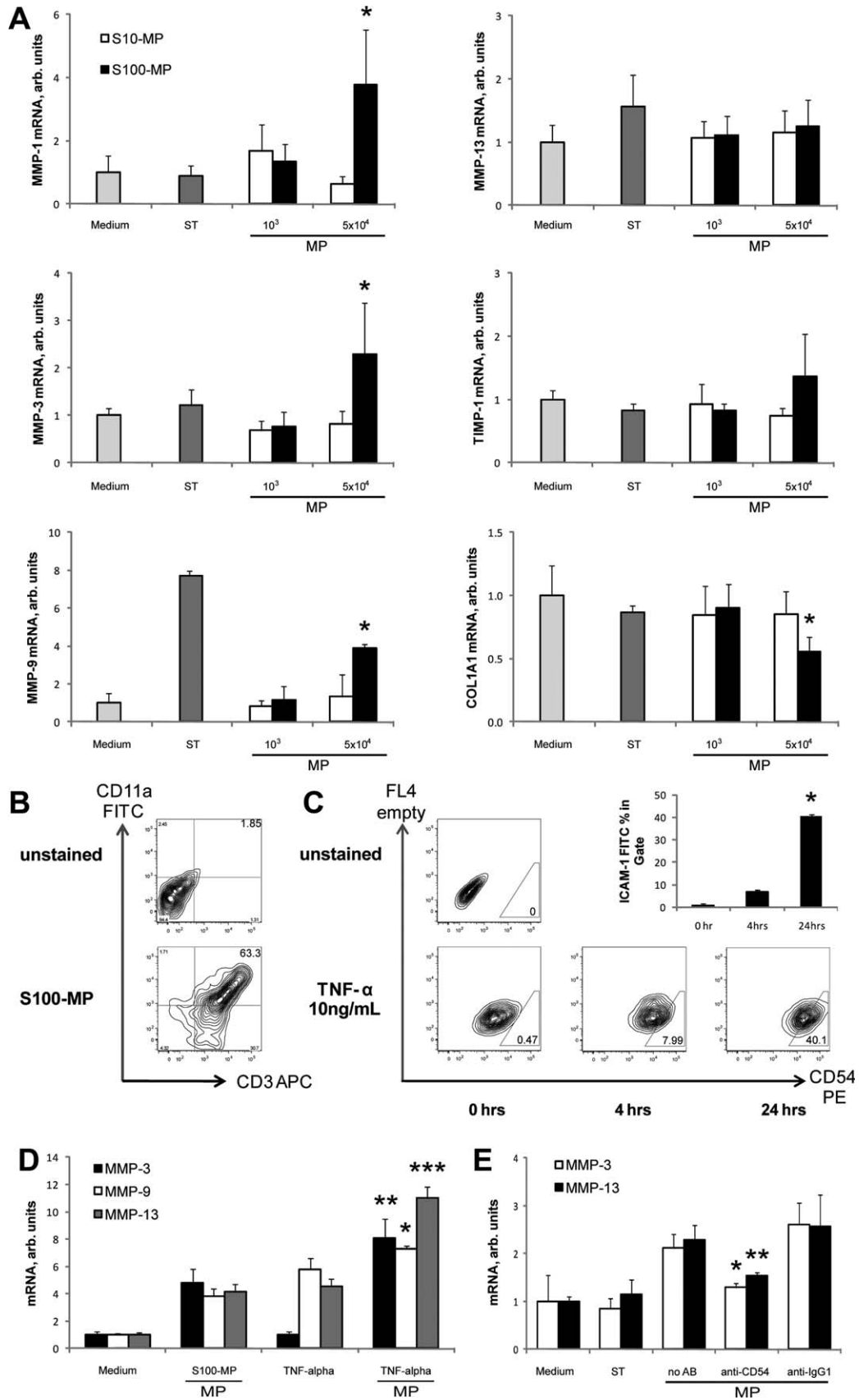


Fig. 5. S100-MPs from activated and apoptotic human CD8⁺ T cells increase MMP and reduce procollagen $\alpha 1(I)$ gene expression in HSCs in a partly CD54-dependent manner. (A) Transcript levels were determined in LX-2 HSCs (2×10^5 cells/mL per well) incubated with S10-MPs or S100-MPs (10^3 or 5×10^4) from PHA-activated and apoptotic CD8⁺ T cells for 24 hours by way of quantitative RT-PCR. ST (0.04 μ M/ml) or plain medium served as controls. * $P < 0.05$ versus medium control. (B) FACS analysis revealed that 64% of the S100-MPs were CD11a and Annexin V double-positive. (C) HSCs were stimulated with TNF α (10 ng/mL) for 0, 4, and 24 hours, resulting in a 40% up-regulation of CD54. * $P < 0.001$. (D) Up-regulation of CD54 on the surface of HSCs by TNF α facilitated MMP induction after addition of S100-MPs. * $P < 0.05$. ** $P = 0.04$. *** $P = 0.001$. (E) HSCs were incubated with a CD54 blocking antibody (50 μ g/mL) or an IgG-matched control antibody for 2 hours, followed by addition of S100-MPs for 24 hours. MMP-3 and MMP-13 transcripts were determined by way of quantitative RT-PCR. * $P = 0.02$. ** $P = 0.046$. All experiments were performed at least twice ($n = 3$ /group). Results (mean \pm SD) are expressed as arbitrary (arb.) units relative to $\beta 2$ -microglobulin mRNA.

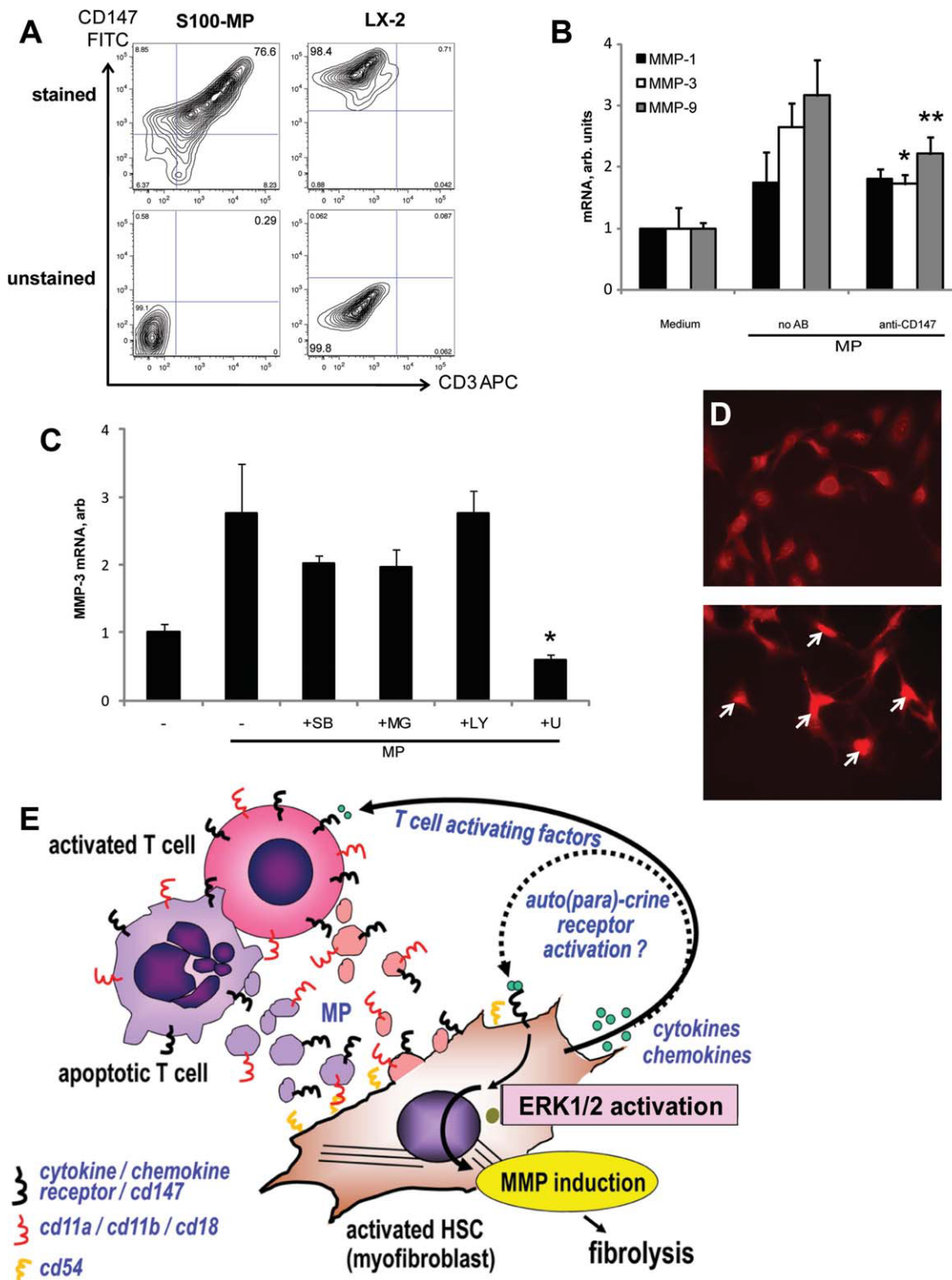


Fig. 6. T cell MPs engage CD147 (EMMPRIN) on HSCs and elicit MMP expression by way of ERK1/2. (A) FACS analyses of CD147 expression on S100-MPs and LX-2 HSCs (CD147 positivity 77% and 99%, respectively). (B) CD8+ T cell-derived S100-MPs (PHA+ST treatment) were incubated with CD147 blocking antibody (50 μ g/mL) for 1 hour, followed by addition to LX-2 HSCs for 24 hours. CD147 blocking significantly decreased MMP-3 (by 35%, * $P = 0.007$) and MMP-9 (30%, ** $P = 0.03$) induction as determined by way of quantitative RT-PCR. Experiments were performed twice ($n = 3$ /group). Results (mean \pm SD) are expressed as arbitrary (arb.) units relative to β 2-microglobulin mRNA. (C) Induction of MMP-3 by T cell MPs in HSCs. There was a lack of inhibition by the phosphatidylinositol-3 kinase inhibitor LY294002 (LY, 5 μ g/mL). Abrogation of MMP-3 induction by the ERK1/2 inhibitor U0126 (U, 5 μ g/mL), and 50% inhibition by the p38 kinase inhibitor SB203580 (SB, 5 μ g/mL) and the proteasome (NF κ B) inhibitor MG132 (MG, 15 μ g/mL). * $P = 0.02$. Comparison with untreated S100-MP-stimulated controls. (D) Nuclear translocation of NF κ B p65 in LX-2 HSCs exposed to S100-MPs from Jurkat T cells for 60 minutes. Representative micrograph from three similar experiments. (E) Sketch illustrating the transfer of T cell-derived membrane-associated molecules including CD147 to HSC membranes by way of shredded MPs. These MPs fuse with the HSC membrane, which is facilitated by CD54. The transferred receptors can activate novel signaling pathways or autocrine/paracrine signaling loops in HSCs that favor a switch toward a fibrolytic phenotype by way of mitogen-activated protein kinase and/or NF κ B pathway activation and subsequent induction of MMPs.

Table 1. Summary of Observed Fibrolytic Effects on HSCs Induced by S100-MPs Derived from Activated and/or Apoptotic Human T Cells

	Jurkat			CD4+			CD8+		
	ST	PHA+ST	PHA	ST	PHA+ST	PHA	ST	PHA+ST	PHA
MMP-1	(++)	~	~	~	-	+	~	++	++
MMP-3	++	---	--	+	~	+	~	++	~
MMP-9	++	~	~	~	~	+	(+++)	+++	(++)
MMP-13	++	~	~	~	~	++	+	~	~
TIMP-1	~	~	~	~	~	~	~	~	~
Pro-collagen $\alpha 1(I)$	~	~	~	~	~	~	~	-	~

MMP-1, MMP-3, MMP-9, MMP-13, TIMP-1, and procollagen $\alpha 1(I)$ transcript levels were determined by way of quantitative RT-PCR in LX-2 HSCs (2×10^5 cells per well) incubated with (active) S-100 or (inactive) S-100 MPs for 24 hours. Only effects $\geq 50\%$ were considered relevant. Up-regulation was categorized as follows: +++, more than four-fold; ++, more than two-fold; +, less than two-fold compared with plain medium without MPs or ST; down-regulation was categorized as follows: ---, more than 75%; --, more than 50%; -, less than 50% compared with plain medium without MPs or ST; ~, not significant toward ST control.

that their percentages were significantly elevated in patients with active hepatitis C, as reflected by high ALT levels. *In vitro*, S100-MPs are released from human T cells after activation (and apoptosis) and fuse with the cell membranes of HSCs and transfer membrane molecules (CD147, Emmprin), which triggers up-regulation of fibrolytic MMP-1, MMP-3, MMP-9, and MMP-13. Of note, the circulating CD4+ and CD8+ S100-MPs found in patients' plasma mainly derive from activated T cells, and their equivalent generated *ex vivo* by PHA stimulation of donor CD4+ and CD8+ T cells most strongly up-regulated putatively fibrolytic MMPs in HSCs (Table 1). This finding will likely have relevance *in vivo*, because activated HSCs are the principal driving force of liver fibrogenesis.

MPs were described as a product of various kinds of cell types, including T cells, as a product of activation or early apoptosis. However, characterization of the biological effects of these MPs has been limited. A prior study implicated MPs from the Jurkat T cell line in fibrolytic activation of synovial fibroblasts.⁸ Questions relevant to liver disease or diseases of other epithelial-mesenchymal organs have not been addressed.

We demonstrated that increased T cell activation (and apoptosis) in active hepatitis C¹⁹ is paralleled by excess release of T cell-derived MPs, which can be detected in the circulation. Using T cell subpopulations and HSCs, both of which are key players in liver inflammation and fibrogenesis, we demonstrated the functional relevance of these MPs *in vitro*. Therefore, T cell MPs ameliorated or even blunted the fibrogenic response that is usually prevalent in chronic hepatitis,¹ including the neutralization of fibrogenic activation of HSCs by TGF $\beta 1$, the strongest profibrogenic cytokine in hepatic fibrosis and other fibrotic diseases.²

Of note, not all T cell-derived MPs were equally potent inducers of fibrolytic MMP expression in

HSCs. Therefore, MPs derived from apoptotic and activated CD8+ T cells were the strongest inducers compared with MPs from activated CD4+ T cells or from the CD4-expressing Jurkat T cell line (Table 1). In this regard, it is noteworthy that CD8+ cells predominate in livers with hepatitis C, and the presence of CD8+ rather than CD4+ T cells has been correlated with the progression of liver fibrosis.²⁰⁻²² These contrast with circulating MPs in inflammatory intestinal diseases where CD4+ T cell-derived MPs predominate (unpublished data). Therefore, MPs derived from activated (and apoptotic) CD8+ and CD4+ T cells may represent a negative feedback loop that counteracts the yet ill-defined profibrogenic activity of T cells once they become highly stimulated (as reproduced *in vitro* with PHA) with or without subsequent deletion by apoptosis. Human T cell-derived MPs could also potently induce MMP expression in primary HSCs from rats, suggesting a conserved mechanism, which is working beyond species boundaries. MPs from THP-1 monocytes and macrophages did not significantly induce fibrosis or fibrolysis-related transcripts, except for an induction of MMP-3 and TIMP-1 in macrophages, underlining the unique properties of T cell-derived MPs.

As a prominent adhesion molecule in T cell interactions, we evaluated the role of CD54 (ICAM-1). CD54 is needed for the adhesion of lymphocytes to antigen-presenting cells for immune priming and for the interaction between T cells and HSCs.^{3,23} We showed that both the fusion of and biological effects elicited by T cell-derived MPs were at least partly mediated through CD54. In addition, proteomic analysis revealed several membrane and intracellular molecules in the S100-MP preparation from Jurkat T cells that were absent in the S100-MP fraction from inactive control cells (Supporting Table 1). A primary candidate molecule in this search was the transmembrane MMP inducer Emmprin/Basigin (CD147). CD147 is expressed

on monocytes, stromal fibroblasts, platelets, cardiac myocytes, and on tumor epithelia including hepatocellular cancer cells.²⁴⁻²⁷ Homodimerization of CD147 by interaction of neighboring cells elicits signaling pathways that lead to expression of MMP-1, MMP-2, MMP-3, MMP-9, and MMP-11.²⁸⁻³⁰ Of note, CD147-CD147 interactions were found between tumor cells³¹ and suggested between tumor cells and surrounding fibroblasts.³² CD147 activation on monocytes was reported to activate the NF κ B pathway and induce MMP-9 expression,³³ and to stimulate the ERK1/2³⁴ and p38 MAPK pathways.³⁵ By using a CD147 blocking antibody, we confirmed the functional involvement of this molecule (MMP down-regulation by 30%-35%). Additional fibrolytic mechanisms may be engaged in HSCs by S100-MPs, which involve mainly ERK1/2 and NF κ B activation. Furthermore, although not the focus of the present study, transfer of bioactive soluble molecules within MPs (e.g., cytokines, microRNAs, or effectors of hedgehog signaling) may occur.³⁶

To date, the generation of MPs in general and of T cell-derived MPs in particular for *in vivo* therapeutic use remains elusive. So far, only one group infused tumor cell-derived MPs under well-defined conditions *in vivo* to accelerate arteriolar occlusion.¹³ The reasons are several, including potential difficulties to induce MPs specifically in CD8+ T cells as the major fibrolytically active T cell subset, or to prevent undesired side effects when using cytokines, biological agents, or proapoptotic agents. Alternatively, MPs could be generated *ex vivo* to be infused or even injected into the target organ.

In conclusion, we demonstrated a novel mechanism by which activated (and apoptotic) T cells induce fibrolytic activation of HSCs, the most relevant fibrogenic effector cells in the liver. The proposed mechanisms are schematically illustrated in Fig. 6E. We assume that similar mechanisms likely apply to cells of other organs once T cell infiltration dominates the inflammation. We identified CD54 and CD147 as important mediators of MP fusion with HSC membranes and MMP induction, but we anticipate that additional molecular players will be discovered. T cell-derived MPs may give rise to their exploitation as novel diagnostic markers and potential antifibrotic agents.

Acknowledgment: LX-2 HSCs were kindly donated by Scott L. Friedman. We thank Gunda Millonig (Beth Israel Deaconess Medical Center) and Veronika Lukacs-Kornek (Dana-Farber Cancer Institute) for help with initial FACS experiments and Franck Grall (Beth Israel Deaconess Medical Center) for help with mass spectroscopy.

References

- Schuppan D, Afdhal NH. Liver cirrhosis. *Lancet* 2008;371:838-851.
- Friedman SL. Mechanisms of hepatic fibrogenesis. *Gastroenterology* 2008;134:1655-1669.
- Muhanna N, Doron S, Wald O, Horani A, Eid A, Pappo O, et al. Activation of hepatic stellate cells after phagocytosis of lymphocytes: a novel pathway of fibrogenesis. *HEPATOLOGY* 2008;48:963-977.
- Dienstag JL, Goldin RD, Heathcote EJ, Hann HW, Woessner M, Stephenson SL, et al. Histological outcome during long-term lamivudine therapy. *Gastroenterology* 2003;124:105-117.
- Issa R, Zhou X, Constantinou CM, Fallowfield J, Millward-Sadler H, Gaca MD, et al. Spontaneous recovery from micronodular cirrhosis: evidence for incomplete resolution associated with matrix cross-linking. *Gastroenterology* 2004;126:1795-1808.
- Langholz O, Rockel D, Mauch C, Kozłowska E, Bank I, Krieg T, et al. Collagen and collagenase gene expression in three-dimensional collagen lattices are differentially regulated by alpha 1 beta 1 and alpha 2 beta 1 integrins. *J Cell Biol* 1995;131:1903-1915.
- Mauch C, Adelman-Grill B, Hatamochi A, Krieg T. Collagenase gene expression in fibroblasts is regulated by a three-dimensional contact with collagen. *FEBS Lett* 1989;250:301-305.
- Distler JH, Jungel A, Huber LC, Seemayer CA, Reich CF 3rd, Gay RE, et al. The induction of matrix metalloproteinase and cytokine expression in synovial fibroblasts stimulated with immune cell microparticles. *Proc Natl Acad Sci USA* 2005;102:2892-2897.
- Whatling C, Bjork H, Gredmark S, Hamsten A, Eriksson P. Effect of macrophage differentiation and exposure to mildly oxidized LDL on the proteolytic repertoire of THP-1 monocytes. *J Lipid Res* 2004;45:1768-1776.
- Li Y, Liu B, Dillon ST, Fukudome EY, Kheirbek T, Sailhamer EA, et al. Identification of a novel potential biomarker in a model of hemorrhagic shock and valproic acid treatment. *J Surg Res* 2010;159:474-481.
- Popov Y, Patsenker E, Bauer M, Niedobitek E, Schulze-Krebs A, Schuppan D. Halofuginone induces matrix metalloproteinases in rat hepatic stellate cells via activation of p38 and NF κ B. *J Biol Chem* 2006;281:15090-15098.
- Beyer C, Pisetsky DS. The role of microparticles in the pathogenesis of rheumatic diseases. *Nat Rev Rheumatol* 2010;6:21-29.
- Thomas GM, Panicot-Dubois L, Lacroix R, Dignat-George F, Lombardo D, Dubois C. Cancer cell-derived microparticles bearing P-selectin glycoprotein ligand 1 accelerate thrombus formation *in vivo*. *J Exp Med* 2009;206:1913-1927.
- Boilard E, Nigrovic PA, Larabee K, Watts GF, Coblyn JS, Weinblatt ME, et al. Platelets amplify inflammation in arthritis via collagen-dependent microparticle production. *Science* 2010;327:580-583.
- Ceuppens JL, Baroja ML, Lorre K, Van Damme J, Billiau A. Human T cell activation with phytohemagglutinin. The function of IL-6 as an accessory signal. *J Immunol* 1988;141:3868-3874.
- O'Flynn K, Russul-Saib M, Ando I, Wallace DL, Beverley PC, Boylston AW, et al. Different pathways of human T-cell activation revealed by PHA-P and PHA-M. *Immunology* 1986;57:55-60.
- Wetzel M, Rosenberg GA, Cunningham LA. Tissue inhibitor of metalloproteinases-3 and matrix metalloproteinase-3 regulate neuronal sensitivity to doxorubicin-induced apoptosis. *Eur J Neurosci* 2003;18:1050-1060.
- Hellerbrand, Wang SC, Tsukamoto H, Brenner DA, Rippe RA. Expression of intracellular adhesion molecule 1 by activated hepatic stellate cells. *HEPATOLOGY* 1996;24:670-676.
- Ishii S, Koziel MJ. Immune responses during acute and chronic infection with hepatitis C virus. *Clin Immunol* 2008;128:133-147.
- Muhanna N, Horani A, Doron S, Safadi R. Lymphocyte-hepatic stellate cell proximity suggests a direct interaction. *Clin Exp Immunol* 2007;148:338-347.

21. Safadi R, Ohta M, Alvarez CE, Fiel MI, Bansal M, Mehal WZ, et al. Immune stimulation of hepatic fibrogenesis by CD8 cells and attenuation by transgenic interleukin-10 from hepatocytes. *Gastroenterology* 2004;127:870-882.
22. Holt AP, Salmon M, Buckley CD, Adams DH. Immune interactions in hepatic fibrosis. *Clin Liver Dis* 2008;12:861-882.
23. Parameswaran N, Suresh R, Bal V, Rath S, George A. Lack of ICAM-1 on APCs during T cell priming leads to poor generation of central memory cells. *J Immunol* 2005;175:2201-2211.
24. Siwik DA, Kuster GM, Brahmabhatt JV, Zaidi Z, Malik J, Ooi H, et al. EMMPRIN mediates beta-adrenergic receptor-stimulated matrix metalloproteinase activity in cardiac myocytes. *J Mol Cell Cardiol* 2008;44:210-217.
25. Zhu P, Ding J, Zhou J, Dong WJ, Fan CM, Chen ZN. Expression of CD147 on monocytes/macrophages in rheumatoid arthritis: its potential role in monocyte accumulation and matrix metalloproteinase production. *Arthritis Res Ther* 2005;7:R1023-R1033.
26. Pennings GJ, Yong AS, Kritharides L. Expression of EMMPRIN (CD147) on circulating platelets in vivo. *J Thromb Haemost* 2010;8:472-481.
27. Mamori S, Nagatsuma K, Matsuura T, Ohkawa K, Hano H, Fukunaga M, et al. Useful detection of CD147 (EMMPRIN) for pathological diagnosis of early hepatocellular carcinoma in needle biopsy samples. *World J Gastroenterol* 2007;13:2913-2917.
28. Gabison EE, Mourah S, Steinfels E, Yan L, Hoang-Xuan T, Watsky MA, et al. Differential expression of extracellular matrix metalloproteinase inducer (CD147) in normal and ulcerated corneas: role in epithelial-stromal interactions and matrix metalloproteinase induction. *Am J Pathol* 2005;166:209-219.
29. Gabison EE, Hoang-Xuan T, Mauviel A, Menashi S. EMMPRIN/CD147, an MMP modulator in cancer, development and tissue repair. *Biochimie* 2005;87:361-368.
30. Haffner C, Frauli M, Topp S, Irmeler M, Hofmann K, Regula JT, et al. Nicalin and its binding partner Nomo are novel Nodal signaling antagonists. *EMBO J* 2004;23:3041-3050.
31. Sun J, Hemler ME. Regulation of MMP-1 and MMP-2 production through CD147/extracellular matrix metalloproteinase inducer interactions. *Cancer Res* 2001;61:2276-2281.
32. Nabeshima K, Suzumiya J, Nagano M, Ohshima K, Toole BP, Tamura K, et al. Emmprin, a cell surface inducer of matrix metalloproteinases (MMPs), is expressed in T-cell lymphomas. *J Pathol* 2004;202:341-351.
33. Schmidt R, Bultmann A, Fischel S, Gillitzer A, Cullen P, Walch A, et al. Extracellular matrix metalloproteinase inducer (CD147) is a novel receptor on platelets, activates platelets, and augments nuclear factor kappaB-dependent inflammation in monocytes. *Circ Res* 2008;102:302-309.
34. Boulos S, Meloni BP, Arthur PG, Majda B, Bojarski C, Knuckey NW. Evidence that intracellular cyclophilin A and cyclophilin A/CD147 receptor-mediated ERK1/2 signalling can protect neurons against in vitro oxidative and ischemic injury. *Neurobiol Dis* 2007;25:54-64.
35. Lim M, Martinez T, Jablons D, Cameron R, Guo H, Toole B, et al. Tumor-derived EMMPRIN (extracellular matrix metalloproteinase inducer) stimulates collagenase transcription through MAPK p38. *FEBS Lett* 1998;441:88-92.
36. Witek RP, Yang L, Liu R, Jung Y, Omenetti A, Syn WK, et al. Liver cell-derived microparticles activate hedgehog signaling and alter gene expression in hepatic endothelial cells. *Gastroenterology* 2009;136:320-330.

Circulating Microparticles as Disease-Specific Biomarkers of Severity of Inflammation in Patients With Hepatitis C or Nonalcoholic Steatohepatitis

MIROSLAW KORNEK,* MICHAEL LYNCH,* SHRUTI H. MEHTA,[†] MICHELLE LAI,* MARK EXLEY,[§] NEZAM H. AFDHAL,* and DETLEF SCHUPPAN*^{||}

*Division of Gastroenterology, Beth Israel Deaconess Medical Center and Harvard Medical School, Boston, Massachusetts; [†]Johns Hopkins Bloomberg School of Public Health, Johns Hopkins University, Baltimore, Maryland; [§]Cancer Biology Program, Hematology-Oncology Division, Beth Israel Deaconess Medical Center and Harvard Medical School, Boston, Massachusetts; and ^{||}Division of Molecular and Translational Medicine, Department of Medicine I, University of Mainz Medical School, Mainz, Germany

BACKGROUND & AIMS: Microparticles released into the bloodstream upon activation or apoptosis of CD4⁺ and CD8⁺ T cells correlate with inflammation as determined by histologic analysis in patients with chronic hepatitis C (CHC). Patients with nonalcoholic fatty liver (NAFL) or nonalcoholic steatohepatitis (NASH) can be differentiated from those with CHC based on activation of distinct sets of immune cells in the liver. **METHODS:** We compared profiles of circulating microparticles from patients with NAFL and NASH (n = 67) to those of CHC (n = 42), with healthy individuals (controls) using flow cytometry; the profiles were correlated with inflammation grade and fibrosis stage based on histologic analyses. We assessed the ability of the profiles to determine the severity of inflammation and fibrosis based on serologic and histologic analyses. **RESULTS:** Patients with CHC had increased levels of microparticles from CD4⁺ and CD8⁺ T cells; the levels correlated with disease severity based on histologic analysis and levels of alanine aminotransferase. Patients with NAFL or NASH had significant increases in numbers of microparticles from invariant natural killer T cells and macrophages/monocytes (CD14⁺), which mediate pathogenesis of NASH. Microparticles from CD14⁺ and invariant natural killer T cells correlated with levels of alanine aminotransferase and severity of NASH (based on histology). Levels of microparticles could differentiate between patients with NAFL or NASH and those with CHC, or either group of patients and controls (area under the receiver operating characteristic curves ranging from 0.56 to 0.99). **CONCLUSIONS: Quantification of immune cell microparticles from serum samples can be used to assess the extent and characteristics of hepatic inflammation in patients with chronic liver disease.**

Keywords: Noninvasive Assay; Lymphocyte; Serum Assay; Biomarker Assay.

Cell membrane-derived microparticles (MP) represent a novel route of horizontal communication between different cells. These MP are generated through a process of cell membrane blebbing (ectosome shedding) during cellular activation or early apoptosis in vitro and in vivo.¹ Of note, MP resemble their cell of origin on a smaller scale, with many parental cell characteristics, such as surface receptors, integral membrane and certain cytosolic

proteins, some messenger RNAs, and even microRNAs.¹ MP can transfer complete cell surface receptor signaling pathways into the recipient cell that are specific for the MP releasing cell, exchange genetic information,¹ or transfer antigen via major histocompatibility complex class II molecules.² We have shown that T-cell–derived MP could transfer CD147 (the matrix metalloproteinase inducer EMMPRIN) to hepatic stellate cells (HSC) leading to up-regulation of fibrolytic matrix metalloproteinases in HSC, and that the process of MP fusion with HSC membranes was intercellular adhesion molecule 1–dependent.³ Others have demonstrated successful rescue of CXCR4 and CD81-deficient cells by transfer of MP carrying these surface receptors.^{4,5} Furthermore, biliary MP were shown to contain biologically active Hedgehog ligand.⁶

However, data on the presence of inflammatory cell MP and their role in vivo are scarce. Only the role of platelet (CD41⁺) derived MP was explored in some detail in vitro and in vivo, such as an elevation of CD41⁺ MP in synovial fluid and blood plasma of patients with rheumatoid arthritis,⁷ human immunodeficiency virus infection,⁸ or severe malaria.⁹

We demonstrated that CD4⁺ and CD8⁺ T-cell–derived MP are elevated in the plasma of patients with chronic hepatitis C (CHC), a disease that is dominated by CD8⁺>CD4⁺ hepatic T-cell infiltration, and that levels of these MP correlated with histological severity (grade and stage).³ Based on these data, we reasoned that other liver diseases might have a disease-specific MP signature. We therefore focused on patients with nonalcoholic fatty liver (NAFL) and included patients with simple steatosis (NAFLD activity score [NAS] score <3) or NASH (NAS score >4). To this aim, we studied an extended panel of MP surface markers, including CD14⁺ (monocytes/macrophages, and myeloid dendritic cells), CD15⁺ (neutrophils), CD41⁺ (platelets and endothelial cells), and Vα24/

Abbreviations used in this paper: ALT, alanine aminotransferase; AUROC, areas under the receiver operating characteristics; CHC, chronic hepatitis C; FACS, fluorescence-activated cell sorting; HSC, hepatic stellate cells; iNKT, invariant natural killer T; MP, microparticle; NAFL, nonalcoholic fatty liver; NAS, NAFLD activity score; NASH, nonalcoholic steatohepatitis.

© 2012 by the AGA Institute
0016-5085/\$36.00

<http://dx.doi.org/10.1053/j.gastro.2012.04.031>

Vβ11 (invariant natural killer T [iNKT] cells). We found that MP derived from CD14⁺ and iNKT cells, 2 cell populations that have been implicated as being central to adipose tissue inflammation,^{10,11} were uniquely and characteristically elevated in patients with NAFL and further increased in patients with histologically severe NASH, but not in CHC. We conclude that circulating MP might qualify as a novel tool to quantify the underlying type and extent of inflammation in NAFL/NASH.

Material and Methods

Human Study Cohort

The Committee for Clinical Investigations at the Beth Israel Deaconess Medical Center approved the study, and all patients gave their informed consent before participation. Forty-two patients with CHC, 67 patients with histologically proven NAFL or NASH, and 44 healthy controls were enrolled. Ten of the CHC patients from our earlier study were included to increase the power of this group.³ All patients were followed up in the Beth Israel Deaconess Medical Center Liver Center and received physical examinations, regular blood draws, and a diagnostic liver biopsy as part of their standard care. Both patient cohorts had comparable mean age (55 and 49 years, respectively; $P > .05$) and sex (Table 1). Patients with a major second known comorbidity that could affect immune cell activation, such as human immunodeficiency virus infection, autoimmune diseases, or another hepatitis virus infection were excluded. Patients with CHC were characterized as HCV antibody and RNA positive for >6 months, and patients with NAFL/NASH by standard clinical criteria confirmed by liver biopsy with the absence of other liver diseases.¹² The criteria used for assessing the health of the each participant are summarized in Supplementary Table 1.

Isolation of T-Cell MP From Human Serum and Plasma

From controls, both plasma and serum were drawn at the same time point, in order to compare results for MP isolation between the 2 methods. Additionally, to assess changes in MP profiles in short-term follow-up, healthy controls were subjected to serial blood sampling 7 days apart. For plasma, blood

was collected in citrate-containing tubes and for serum, blood was collected in standard Vacutainers (both BD Vacutainer; BD, Franklin Lakes, NJ, USA) and left for 1 hour at 37°C to allow to clot, followed by centrifugation at 4000 rpm for 20 min at 4°C. Clot palettes were carefully separated and plasma or serum supernatants were stored at -80°C for further MP isolation. MP were isolated by differential centrifugation between 10,000g and 100,000g as described,³ and S100-MP sedimenting at 100,000g were characterized by fluorescence-activated cell sorter (FACS) using staining for Annexin V, CD1c, CD3, CD4, CD8, CD14, CD16, CD15, CD41, CD147, Va24/Vβ11 (eBioscience, San Diego, CA; BioLegend; Becton Dickinson, San Jose, CA). Notably, these surface markers were not described on exosomes,¹³ another class of membrane-coated vesicles. All antibodies were titrated against the matching isotype control before use on patient's samples, as shown in detail in Supplementary Figure 1. MP preparations were characterized on an LSR2 FACS sorter (Becton Dickinson), and cytometric data were analyzed with FlowJo 8.8.6 software for MAC OSX (Tree Star, Inc, Ashland, OR). MP were gated on forward and sideward scatter. A detailed overview of our gating strategy is shown in Supplementary Figure 2. To avoid nonspecific antibody binding, Fc receptors on MP and target cells were blocked with FcR Blocking Reagent (Miltenyi Biotec, Auburn, CA). Antibody solutions were centrifuged before FACS to avoid artifacts due to aggregation.

Liver Histology

Liver biopsies were performed with an 18-gauge Menghini needle for clinical indications and encompassed at least 8 portal tracts. Biopsy specimens were formalin-fixed, paraffin-embedded, sectioned, and stained with H&E, Masson's trichrome, reticulin, and periodic acid-Schiff stains. Two experienced histopathologists graded and staged the liver samples according to Metavir (CHC and NAFL/NASH)¹⁴ and NAS score (NAFL/NASH).¹⁵ Only specimens predating the MP isolation from the patients' serum by no more than 12 months were used for comparisons.

Statistical Analysis

All data are arithmetic means with SD. Differences between independent experimental groups (NAFL/NASH, CHC,

Table 1. Summary of Demographic, Biochemical, and Histological Parameters of Patients With CHC and NAFL/NASH

	CHC	NAFL, total	NAS score 0–3	NAS score 4–8
Patients, n ^a	42	67	33	34
Female, % ^b	31 (13)	38.8 (26)	36.4 (12)	41.2 (14)
Male, % ^b	69 (29)	61.2 (41)	64.6 (21)	58.8 (20)
Age, y, mean (range)	55.1 (30–81)	48.7 (28–73)	47.9 (28–73)	49.4 (31–68)
ALT, IU/L, mean (range)	89.7 (16–291)	70.1 (13–201)	64.3 (13–201)	75.8 (36–165)
Biopsy grade, mean (range)	1.63 (0–3)	48 (0–4)	26 (0–2)	22 (1–4)
Biopsy stage, mean (range)	1.61 (0–4)	1.07 (0–4)	0.39 (0–4)	1.76 (0–4)
NAS score, mean (range)	NA	3.46 (0–8)	2.45 (0–8)	4.5 (0–8)
African American, % ^b	4.8	3.1	6.5	0
Asian, % ^b	4.8	10.8	12.9	8.8
Caucasian, % ^b	83.2	69.2	61.2	76.5
Hispanic, % ^b	4.8	10.8	6.5	14.7
Others, % ^b	2.4	6.2	12.9	0

NOTE. NAFL/NASH patients were subdivided according to their NAS score as indicated.

NA, not applicable.

^aTotal number of patients in each cohort.

^bPercentage of sex distribution (absolute numbers in parentheses).

and controls) were characterized using the Kruskal-Wallis test with subsequent pairwise comparisons and adjustment for multiple comparisons using Dunn's Multiple Comparison Test. Differences between plasma and serum MP levels were analyzed using the Mann-Whitney test. A pairwise Pearson algorithm was used for correlation analysis of MP levels with blood cells, alanine aminotransferase (ALT), histological grade and stage, and the NAS score. Scatterplots of the pairwise data are presented with corresponding linear regression lines. To assess the predictive ability of the 6 MP populations (CD4⁺, CD8⁺, CD14⁺, CD15⁺, CD41⁺, and iNKT) for discriminating between individuals with CHC and NAFL/NASH, we calculated sensitivity, specificity, and areas under the receiver operating characteristics (AUROC) curve. All calculations were done with Prism 5 software (GraphPad Software, Inc, La Jolla, CA). An error level $P < .05$ was considered significant.

Results

MP Isolated From Plasma and Serum Yield Comparable Results

We previously described MP from plasma.³ In order to test if (stored) serum could be used for MP quantification as well, we compared matched plasma-serum pairs from a subset of patients and healthy controls. When comparing relative levels of S100-MP (in the following simply termed MP) populations in serum vs plasma, both serum CD15⁺ (neutrophil) and CD41⁺ (platelet-derived) MP were reduced, the latter reported previously by others,¹⁶ CD4⁺ MP were slightly decreased and CD8⁺ MP were significantly increased, whereas CD14⁺ and iNKT S100-MP remained unchanged (Figure 1). At present, we cannot explain these minor to moderate differences of certain MP populations in serum vs plasma,

but the profiling of those MP turned out not to be relevant for the present study on patients with NAFL and NASH, or their differentiation from CHC patients. We also found some variation in percentages of MP in some individuals, but overall this was not significant (Supplementary Figure 3A). Such changes can result from slight alterations of immune activation in individual patients, eg, due to minor (subclinical) infection or by physical activity.^{1,17-19}

Additionally, we did not observe a significant correlation between blood cell counts and corresponding MP percentages, as demonstrated for monocytes (CD14⁺), neutrophils (CD15⁺), or platelets (CD41⁺) (see Supplementary Figure 3B). These results are in line with our previous findings in patients with CHC, and support the hypothesis that it is activated cells within affected organs (such as the liver) that are the source of plasma membrane MP and not the majority of nonactivated circulating blood cells.^{3,18}

Patients With CHC and NAFL/NASH Show Characteristic MP Profiles

Sixty-seven and 42 patients with NASH/NAFL and CHC, respectively, were included in the study (Table 1). MP results are summarized in Figure 2A and Supplementary Table 2, and AUROC curves are shown in Figure 2B and Supplementary Figure 4A and B. CHC and NAFL/NASH were associated with increased percentages of CD4⁺ MP compared to healthy controls (40% and 29%, respectively). Similarly, levels of CD8⁺ MP were significantly higher in NAFL/NASH (56%) and in CHC (26%) compared to healthy controls. However, CD4⁺ and CD8⁺ S100-MP did not discriminate between CHC and NAFL/NASH, with low AUROC values of 0.71 and 0.59, respec-

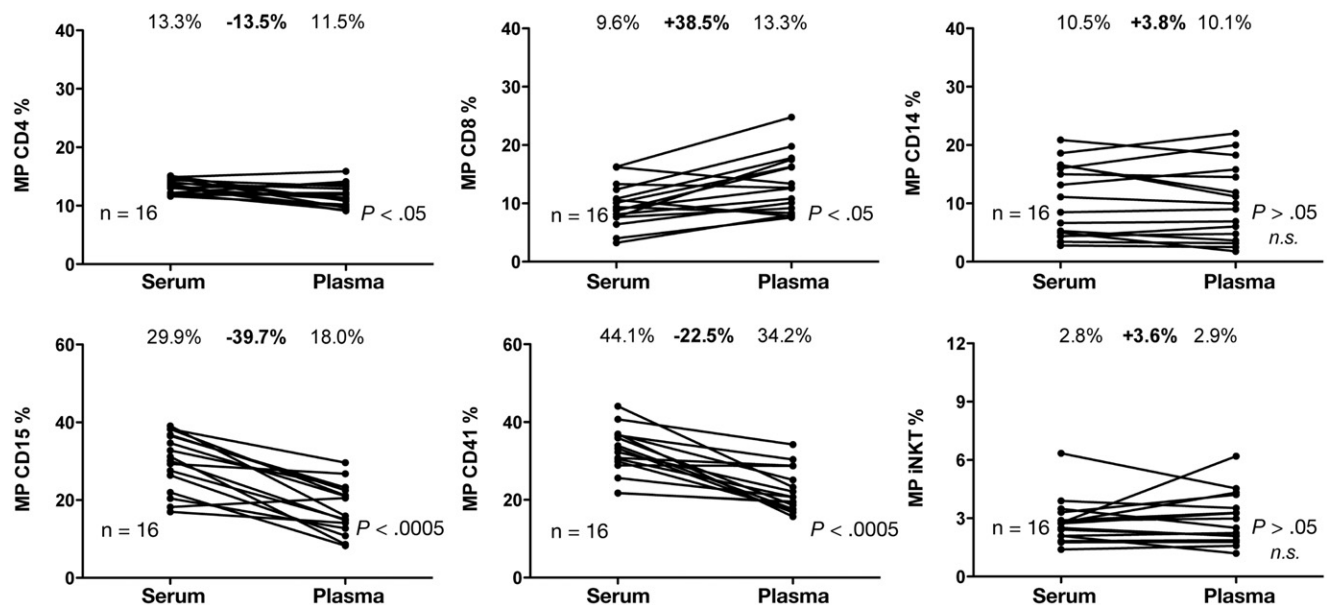


Figure 1. Comparison of S100-MP determinations from serum and plasma. FACS analysis revealed that both fresh plasma and stored serum samples can be used reliably to determine the levels of CD4⁺, CD14⁺, and iNKT MP. In agreement with previous reports, levels of platelet-derived MP (CD41⁺) were significantly decreased in serum.¹⁶ n, number of serum/plasma pairs; the *bold* number is the difference (in percent) between the means (*not bold*) of the measured MP population in serum vs plasma. Differences (percent *in bold*) between serum and plasma were calculated using the following formula: (mean plasma MP – mean serum MP)/mean serum MP.

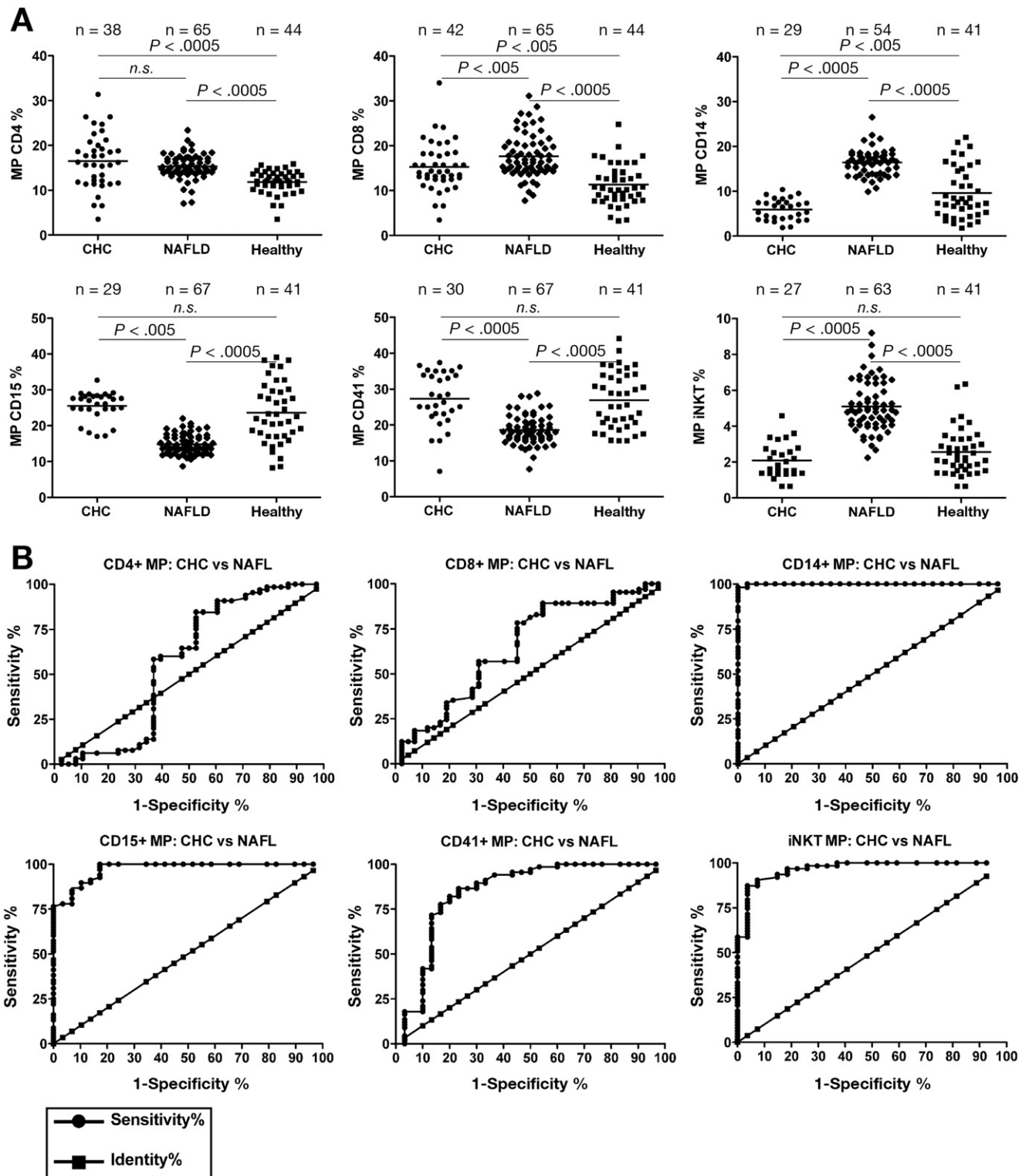


Figure 2. Gross overview/profile of the percentages of different S100-MP populations in patients with NAFL, CHC, and in healthy controls. (A) MP were isolated by differential centrifugation and analyzed by FACS as described in Materials and Methods. The overall *P* value for each MP population for the Kruskal–Wallis test was set at *P* < .0001 before assessing pairwise relationships by the post-hoc Dunn’s multiple comparisons approach to compare the 3 study cohorts (CHC, NAFL/NASH, and healthy controls). (B) AUROC curves were created using those cut-off values that yielded the highest likelihood to differentiate between CHC, NAFL, and healthy controls (see also Supplementary Table 1). n, number of patients in each MP analysis. Occasional missing data points are due to limitation of serum. Ten additional patients with CHC for whom only CD4⁺ and CD8⁺ MP were available were included (see Table 1).

tively (Supplementary Table 2). In contrast, the exclusive elevation of CD14⁺ and iNKT MP in NAFL/NASH compared to CHC led to AUROC values of >0.99 and 0.97, respectively. At cutoffs of 9.7% and 3.6%, respectively, we observed sensitivity and specificity values >87% for differentiation from CHC. Of note, these 2 cell populations have recently been implicated as being central to NAFL/NASH pathogenesis.^{11,20} In NAFL/NASH CD15⁺ and CD41⁺, MP levels were reduced significantly by 42% and 32%, respectively, compared to CHC. This reduction for CD15⁺ and CD41⁺ MP percentages was also associated with a high specificity score, >96%, but with lower sensitivity scores of 78% and 18%, respectively.

Figure 3A shows an MP analysis for the extremes of ALT values of the 2 liver disease cohorts focusing on T cell and iNKT MP. Here, we confirmed our earlier finding that patients with CHC and an ALT >100 IU/L (termed *active*) had significantly elevated levels of circulating CD4⁺ MP as compared to CHC patients with ALT <40 IU/L (termed *mild*) and to healthy controls. In contrast, NAFL/NASH patients with both low and high ALT levels were characterized by only a minor elevation of CD4⁺ MP (28%) compared to healthy controls, although this was statistically significant. CD8⁺ MP were also increased in NAFL/

NASH, especially in the high ALT group, similar to serologically active vs inactive CHC.

There was only a nonsignificant ($P > .05$) increase of iNKT MP in CHC, either with low or with high ALT values, vs healthy controls. However, in all patients with NAFL/NASH, iNKT MP were strikingly elevated (NAFL/NASH with high ALT [>100 IU/L]: by 124% vs normal controls; NAFL/NASH with ALT <100 IU/L: by 114% vs CHC with high ALT).

CD14⁺ MP Subgroup Analysis in NASH

Recently, a link between chronic liver disease progression and CD14⁺ CD16⁻ and CD14⁺CD16⁺ cells was reported.²¹ In a representative cohort of NAFL/NASH patients (ALT range, 31–109 IU/L), we found comparable percentages of MP from CD14⁺ CD16⁻ (classical), CD14⁺CD16⁺ (nonclassical, proinflammatory) monocytes, and CD14⁺CD1c⁺ myeloid dendritic cells (Figure 3B).

Correlation Between ALT and MP in Patients With NAFL/NASH and CHC

Correlations are shown in Figure 4. As expected, CD4⁺ and CD8⁺ MP correlated slightly better with ALT levels in patients with CHC (Figure 4A) as compared to

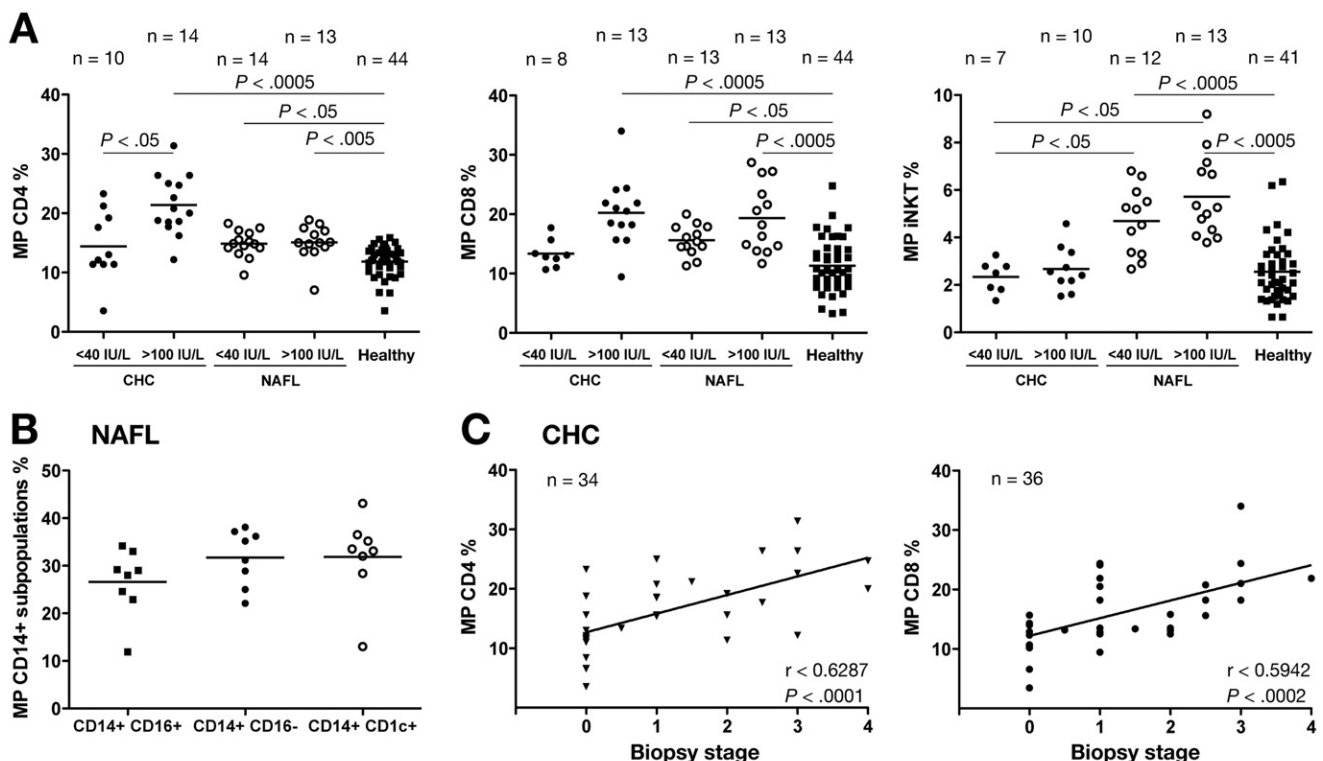


Figure 3. MP levels in relation to normal and high ALT values and biopsy stage, and analysis CD14⁺ MP subsets. (A) MP levels in CHC or NAFL/NASH patients with normal ALT values (<40 IU/mL, numbers as indicated) or high ALT values (>100 IU/mL, numbers as indicated) as a surrogate of hepatic inflammation, and in comparison to S100-MP populations from healthy controls. The overall P value for each MP population for the Kruskal–Wallis test was set at $P < .0001$ before assessing pairwise relationships by the post-hoc Dunn’s multiple comparisons approach to compare the 3 study cohorts (CHC, NAFL/NASH, and healthy controls). (B) Analysis of CD14⁺ S100-MP subpopulations in a representative cohort of NAFL/NASH patients. CD14⁺ CD16⁻: “classically activated” monocytes; CD14⁺CD16⁺: “nonclassically activated, inflammatory” monocytes, CD14⁺CD1c⁺: myeloid DCs. (C) In CHC CD4⁺ and CD8⁺, MP correlated well with fibrosis stage as we described previously in a smaller cohort³ ($r = 0.63$; $P < .0001$; $r = 0.59$; $P = .0002$, respectively). However, CD4⁺, CD8⁺, CD14⁺, and iNKT MP levels did not correlate with stage in NAFL/NASH (data not shown). Variations in numbers are due to limitation of serum.

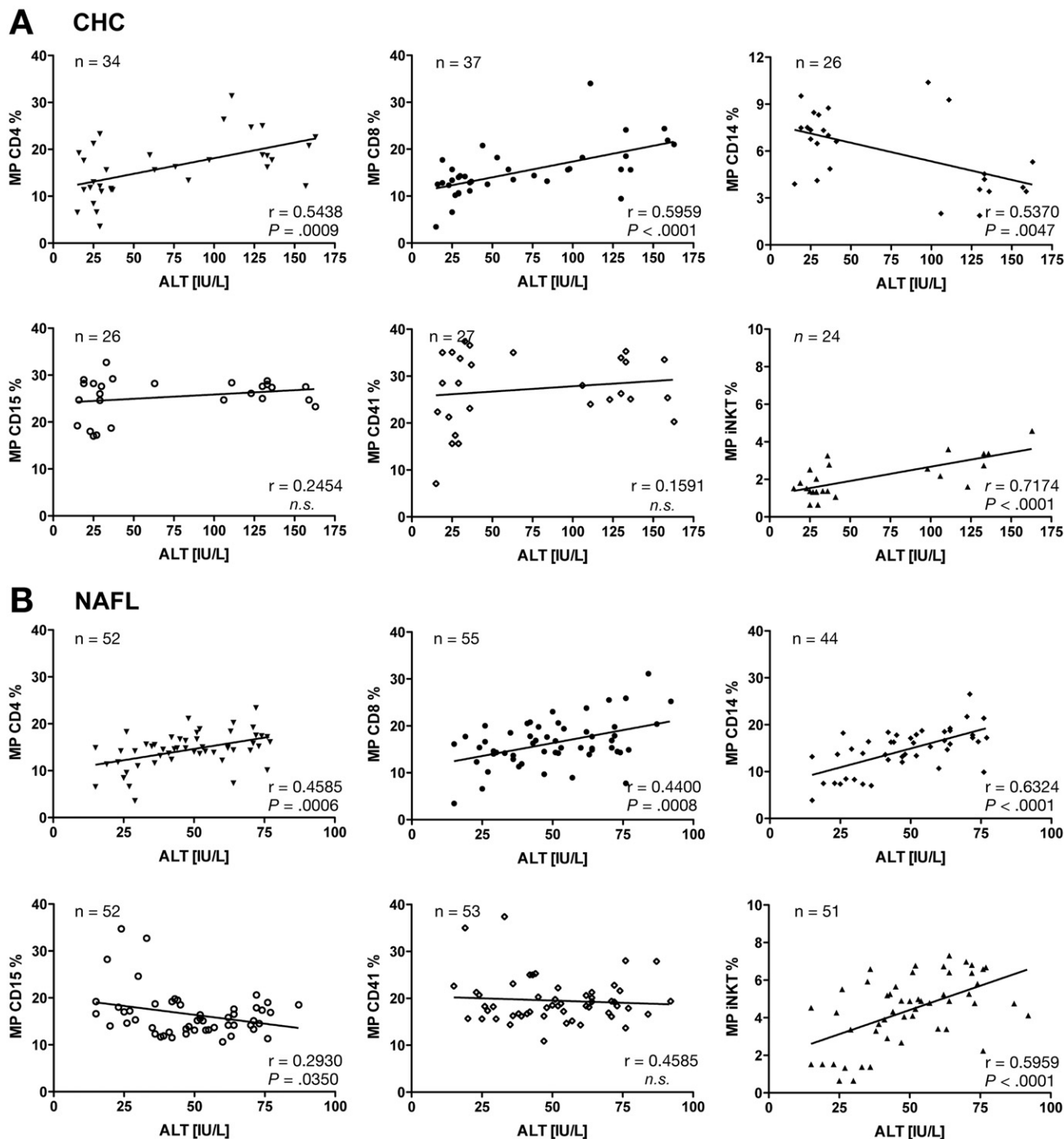


Figure 4. Correlations of circulating S100-MP with ALT. Correlations of CD4⁺, CD8⁺, CD14⁺, and iNKT S100-MP with patients' ALT values from blood samples used simultaneously for S100-MP isolation and ALT determination. (A) CHC, (B) NAFL/NASH. Correlations were calculated using the Pearson algorithm, with *r* values and *P* values shown in the lower right corner of each graph. Variations in numbers are due to limitation of serum.

NAFL/NASH (Figure 4B). However, the good correlations for all MP subpopulations with ALT in NAFL/NASH were lost when patients with ALT >80 IU/mL were included (data not shown) and improved with ALT <80 IU/L. The best correlations were found between ALT levels of patients with NAFL/NASH and their circulating CD14⁺ and iNKT MP (*r* = 0.63; *P* < .0001; *r* = 0.59; *P* = .0001). Interestingly, for CD8⁺, CD15⁺, and CD41⁺ MP, no clinically relevant correlations were found (*r* < 0.5), although

the correlations for CD8⁺ and CD15⁺ MP were statistically significant. Subanalysis ruled out a sex effect for all correlations (data not shown).

Circulating MP as Predictors of Histological Grade in CHC and NAFL/NASH

We confirmed our earlier findings of a good correlation between circulating CD4⁺ and CD8⁺ MP and histological inflammation grade in CHC.³ In addition,

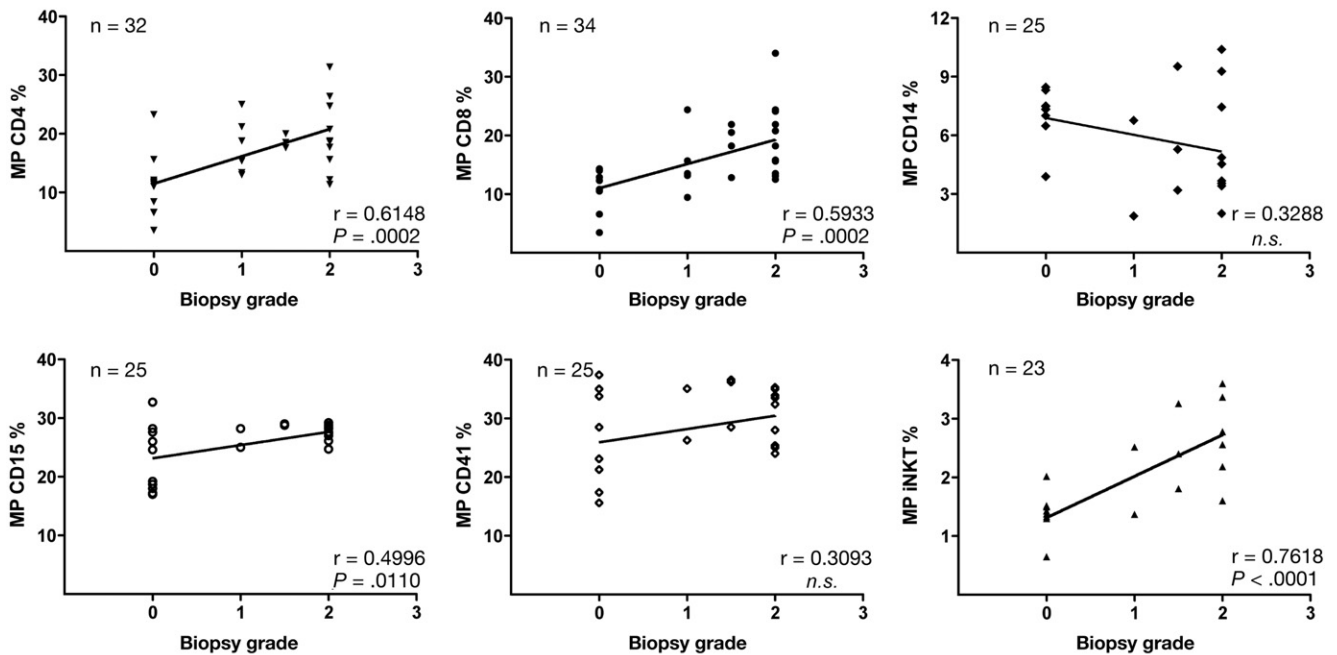
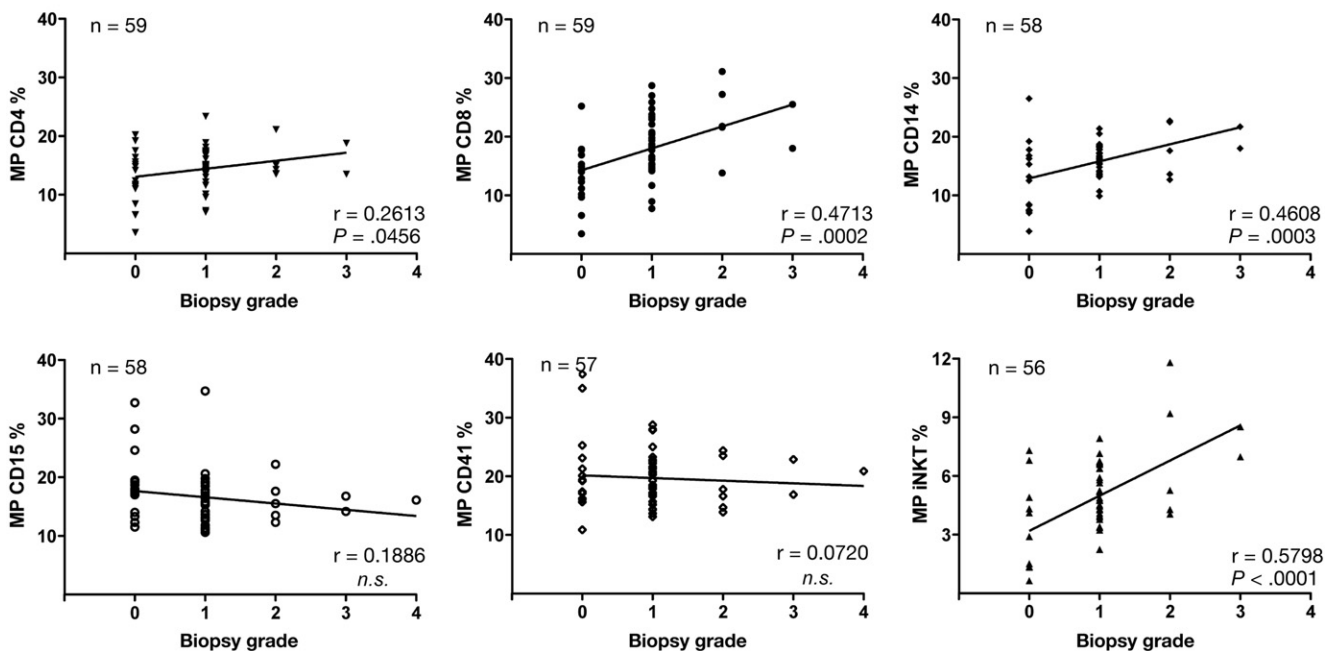
A CHC**B NAFL**

Figure 5. Correlations of circulating S100-MP with histological grade. S100-MP populations were isolated from the serum of CHC (A) or NAFL/NASH patients (B) with paired biopsies. Grading was done as detailed in Material and Methods. Correlations were calculated using Pearson's algorithm. Variations in numbers are due to limitation of serum.

iNKT MP correlated even better with histological grade in patients with CHC than CD4⁺ and CD8⁺ MP ($r = 0.76$; $P < .0001$, Figure 5A). Although CD14⁺, CD15⁺, and CD41⁺ MP did statistically correlate with grade in CHC, this was considered clinically irrelevant ($r < 0.5$). In NAFL/NASH, iNKT MP correlated well with histological grade ($r = 0.58$; $P < .0001$), and this correlation must be considered as clinically relevant (Figure 5B). Other corre-

lations, even when statistically significant, turned out to be clinically irrelevant ($r < 0.5$).

Correlation Between Biopsy Stage and MP in Patients With NAFL/NASH and CHC

In CHC, CD4⁺ and CD8⁺ MP correlated well with fibrosis stage, as described by us earlier in a smaller cohort³ ($r = 0.63$; $P < .0001$; $r = 0.59$; $P = .0002$, respec-

tively, Figure 3C). However, CD4⁺, CD8⁺, CD14⁺, and iNKT MP levels did not correlate well with stage in NAFL/NASH (data not shown). In addition, no correlations for either CHC or NAFL/NASH were found with circulating CD15⁺ and CD41⁺ MP (data not shown).

Circulating MP as Predictors of the Histological Severity in NAFL/NASH

MP were correlated with the NAFLD activity score (NAS), currently considered the gold standard for the assessment of the severity of inflammation and apoptosis in NAFL/NASH (Figure 6A). Although statistically significant, CD4⁺ and CD8⁺ MP correlated only weakly (therefore lacking clinical relevance) with the NAS score ($r = 0.42$; $P = .0004$; $r = 0.38$; $P = .0016$, respectively), as did iNKT MP ($r = 0.47$; $P = .0006$). As previously noted, CD14⁺ MP, derived from cells that play a particular role in NASH pathogenesis correlated best with the NAS score ($r = 0.60$; $P < .0001$).

Notably, CD14⁺ MP correlated strongly with iNKT MP in all patients with NAFL/NASH ($r = 0.7$; $P < .0001$) (Figure 6B), far exceeding correlations between all other combinations, and supporting the hypothesis that these 2 MP populations are not only uniquely released in NAFL, but also linked in pathogenesis.

Discussion

Cell-derived MP are recently discovered vehicles of intercellular communication and emerging tools to quantitate cell-specific pathological processes. Several publications describe MP shedding in inflammatory conditions, such as malaria (platelet-, red blood cell-, and monocyte-derived MP),⁹ heart failure (endothelium-derived MP),²² arthritis,⁷ human immunodeficiency virus infection,⁸ end-stage renal failure,²³ in coagulation disorders (platelet-derived MP),²⁴ and even after moderate exercise.¹⁹ We recently showed that T-cell S100-MP, which are found at

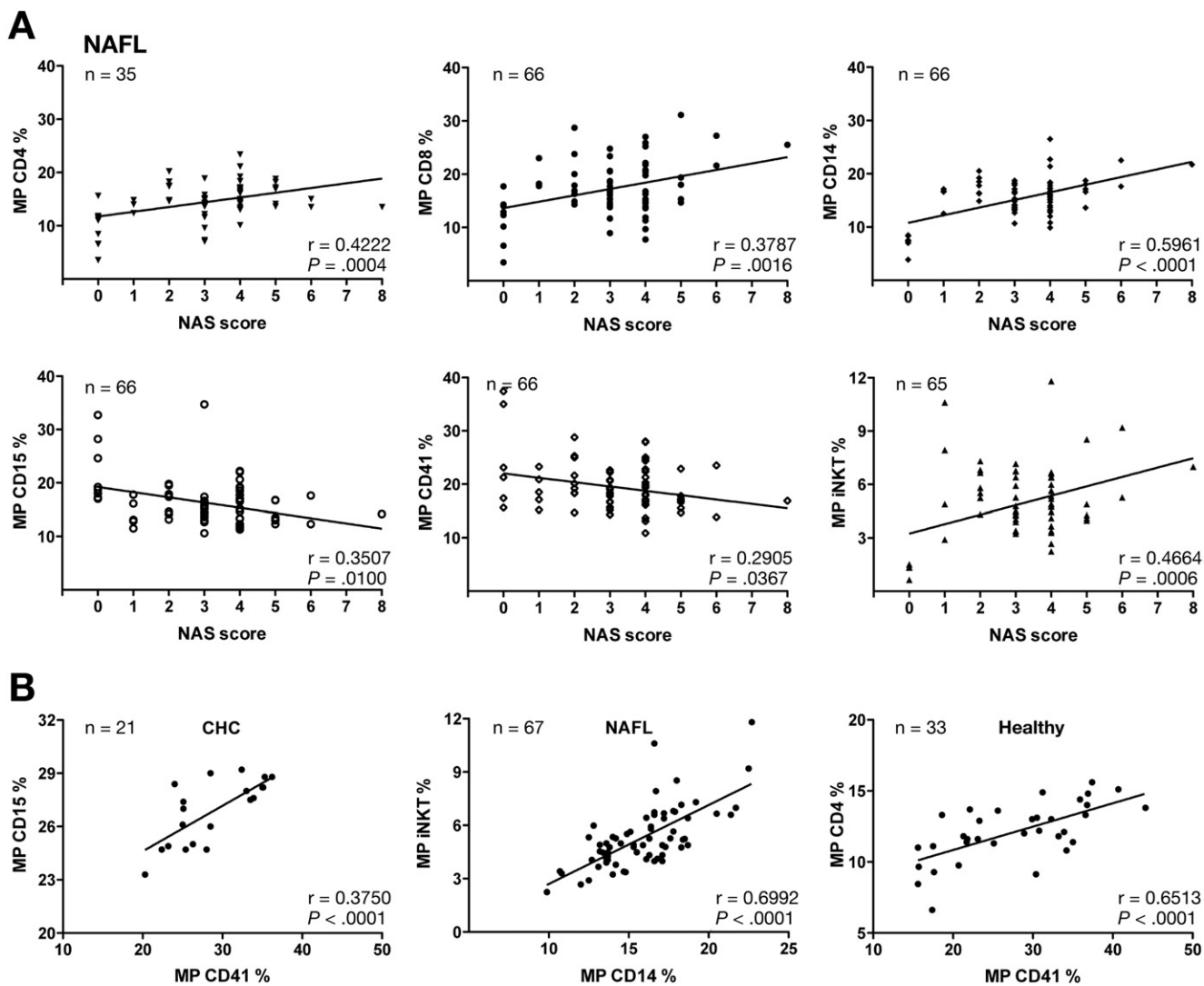


Figure 6. Correlations of circulating S100-MP populations with the NAS score and between MP populations. (A) Correlations of CD4⁺, CD8⁺, CD14⁺, CD15⁺, CD41⁺, and iNKT ($V\alpha 24/V\beta 11$ double-positive) S100-MP with the NAS score using the Pearson algorithm. (B) The strongest correlations between S100-MP subsets for each liver disease are shown. The strong correlation between CD14⁺ and iNKT S100-MP supports a tight functional link between these inflammatory cell types in NAFL/NASH. Variations in numbers are due to limitation of serum.

increased levels in the plasma of patients with CHC, can fuse with HSC plasma membranes via intercellular adhesion molecule 1 and consequently up-regulate HSC fibrolytic gene expression by transfer of CD147, suggesting a possible functional role of inflammatory cell MP in chronic liver diseases.³

The aim of this study was to explore if 2 prevalent but mechanistically different chronic liver diseases, CHC and NAFL/NASH, can be distinguished by their S100-MP profiles, if these profiles are biologically plausible, and if they could serve as novel plasma or serum biomarkers of disease activity.

Typically, hepatic fibrosis progression and acute hepatitis require activation of various immunological competent cells, such as T cells, NKT cells, dendritic cells, and macrophages (Kupffer cells).²⁵ Because activation or early apoptosis of cells can result in shedding of MP, levels of certain MP originating from different cell types can be measured by FACS in healthy subjects and in patients with different diseases.^{1,3,18}

By analyzing serum MP for 6 cell surface markers representing major immune cell populations that are involved in hepatic inflammation and fibrogenesis (CD4⁺/8⁺ T cells, CD14⁺ monocytes/macrophages/dendritic cells, CD15⁺ neutrophils, CD41⁺ platelets, and V α 24/V β 11-positive iNKT cells^{3,7,9,18}), we could identify S100-MP profiles that are highly characteristic for either NAFL/NASH or CHC. CHC was dominated by CD8⁺ and CD4⁺ MP, and NAFL/NASH patients showed a unique elevation of CD14⁺ and iNKT MP and a decrease in CD15⁺ and CD41⁺ MP, irrespective of ALT levels or histological markers of disease activity. The S100-MP patterns allowed an almost complete separation of patients with CHC or NASH and healthy controls.

These findings are not only in excellent agreement with the pathophysiology of both diseases, but also reveal novel insights into disease pathogenesis, as also published in recent studies. First, the homing of circulating immune cells to the liver and their turnover increases during hepatic inflammation, likely increasing circulating MP released during their activation or apoptosis.¹ Second, CD8⁺>CD4⁺ T cell,²⁶ as well as NKT cell populations²⁷ including iNKT cells,²⁸ are major immune effectors in CHC, although histological inflammation of the liver appears to be better reflected by iNKT MP than by blood iNKT cells.^{27,28} Third, iNKT cells have been implicated as major drivers of inflammation and fibrosis progression in NASH.^{20,29} Fourth, CD14⁺ macrophages>monocytes appear to play a prominent role in peripheral adipose tissue inflammation, the associated metabolic syndrome,^{30,31} and hepatic necroinflammation in NASH.³² In the latter context, inflammatory CD14⁺ CD16⁺ monocytes are linked to disease progression and fibrogenic activation of HSCs,²¹ as has been shown for a variety of inflammatory diseases, including rheumatoid arthritis, diabetes, atherosclerosis, and bacterial infections.³³ Our CD14⁺ S100-MP subgroup analysis revealed that CD14⁺ S100-MP in NAFL/NASH originated in equal proportions from

CD16⁻ (classical monocytes or macrophages), CD1c⁺ (myeloid dendritic cells), and CD16⁺ (inflammatory monocytes or macrophages). Because the latter cell population is lower in normal subjects (7.5%), the relative quantity of elevated count of CD14⁺CD16⁺ S100-MP in patients with NAFL/NASH indicates activation of inflammatory monocytes/macrophages.²¹ In addition, there was an excellent correlation between CD14⁺ and iNKT MP in patients with NAFL/NASH, which underscores a functional link between activation of these immune cells in patients with fatty liver and NASH.

Although inflammatory cell S100-MP correlated with ALT levels and histological staging/grading, these correlations were limited. This is expected, because ALT is a suboptimal surrogate of hepatic inflammation, apoptosis, or necrosis,³⁴ and biopsy is a tarnished gold standard due to high sampling variability.³⁵⁻³⁷ In CHC, the disease with the lowest expected sampling variability (~25% and 33% for 1 Metavir grade and stage difference, respectively³⁷), there was a good correlation of CD4⁺ or CD8⁺ MP with ALT and biopsy grade and stage. In NAFL/NASH, which incurs a higher biopsy sampling variability (~40% for 1 Metavir grade or stage³⁸), CD14⁺ and iNKT MP only correlated well with ALT up to 80 IU/L, but poorly with fibrosis stage. The histological NAS score, considered the gold standard for the diagnosis of NASH, showed only a modest correlation with CD14⁺ and iNKT MP. Although a positive NAS score >4 renders the best evidence for NASH, a borderline or negative score does not exclude its presence because this score, which consists of 3 subscores for hepatic steatosis, lobular inflammation, and ballooning, is affected by significant sampling variability, especially for detection of hepatocellular ballooning,³⁹ which is missed in at least 50% of biopsies.³⁸ Additionally, due to its multicomponent character, the NAS score is influenced by the skill and experience of the reading pathologist, more than other histological scores, and is prone to intra- and inter-observer variability.^{15,40} In contrast, a quantitative diagnostic test that can measure overall activation of a certain immune cell subset, such as circulating MP, might circumvent biopsy sampling and observer variabilities. In addition, it might rather reflect current disease activity compared with a more static picture as reflected by biopsy assessment, permitting, for example, the "real-time" monitoring of disease-specific anti-inflammatory therapies. However, at present we cannot present evidence that S100-MP quantification is superior to state of the art diagnostics for NAFL/NASH, which will require future large prospective and follow up studies. It will be particularly interesting to follow up MP profiles in patients with NASH who undergo treatment with, for example, insulin sensitizers or antioxidants, or who begin to favorably change their lifestyle.⁴¹⁻⁴³

In conclusion, by analyzing circulating S100-MP, a systemic profile of immune cell subsets that are prominently involved in CHC or NAFL/NASH can be obtained. MP profiling corroborates the in vivo significance of pathophysiological hypotheses on immune-mediated liver dis-

eases; as shown here for CHC and NAFL/NASH, S100-MP appear to represent a novel diagnostic tool to assess overall disease severity and especially activity, with the advantage of being specific, noninvasive, and quantitative.

Supplementary Material

Note: To access the supplementary material accompanying this article, visit the online version of *Gastroenterology* at www.gastrojournal.org, and at <http://dx.doi.org/10.1053/j.gastro.2012.04.031>.

References

- Beyer C, Pisetsky DS. The role of microparticles in the pathogenesis of rheumatic diseases. *Nat Rev Rheumatol* 2010;6:21–29.
- Thery C, Ostrowski M, Segura E. Membrane vesicles as conveyors of immune responses. *Nat Rev Immunol* 2009;9:581–593.
- Kornek M, Popov Y, Libermann TA, et al. Human T cell microparticles circulate in blood of hepatitis patients and induce fibrolytic activation of hepatic stellate cells. *Hepatology* 2011;53:230–242.
- Fritzsching B, Schwer B, Kartenbeck J, et al. Release and intercellular transfer of cell surface CD81 via microparticles. *J Immunol* 2002;169:5531–5537.
- Rozmyslowicz T, Majka M, Kijowski J, et al. Platelet- and megakaryocyte-derived microparticles transfer CXCR4 receptor to CXCR4-null cells and make them susceptible to infection by X4-HIV. *AIDS* 2003;17:33–42.
- Witek RP, Yang L, Liu R, et al. Liver cell-derived microparticles activate Hedgehog signaling and alter gene expression in hepatic endothelial cells. *Gastroenterology* 2009;136:320–330 e2.
- Boilard E, Nigrovic PA, Larabee K, et al. Platelets amplify inflammation in arthritis via collagen-dependent microparticle production. *Science* 2010;327:580–583.
- Corrales-Medina VF, Simkins J, Chirinos JA, et al. Increased levels of platelet microparticles in HIV-infected patients with good response to highly active antiretroviral therapy. *J Acquir Immune Defic Syndr* 2010;54:217–218.
- Pankoui Mfonkeu JB, Gouado I, Fotso Kuate H, et al. Elevated cell-specific microparticles are a biological marker for cerebral dysfunctions in human severe malaria. *PLoS One* 2010;5:e13415.
- Day CP. From fat to inflammation. *Gastroenterology* 2006;130:207–210.
- Karlmark KR, Weiskirchen R, Zimmermann HW, et al. Hepatic recruitment of the inflammatory Gr1+ monocyte subset upon liver injury promotes hepatic fibrosis. *Hepatology* 2009;50:261–274.
- Vuppalanchi R, Chalasani N. Nonalcoholic fatty liver disease and nonalcoholic steatohepatitis: selected practical issues in their evaluation and management. *Hepatology* 2009;49:306–317.
- Mathivanan S, Simpson RJ. ExoCarta: a compendium of exosomal proteins and RNA. *Proteomics* 2009;9:4997–5000.
- Poynard T, Bedossa P, Opolon P. Natural history of liver fibrosis progression in patients with chronic hepatitis C. The OBSVIRC, METAVIR, CLINIVIR, and DOSVIRC groups. *Lancet* 1997;349:825–832.
- Kleiner DE, Brunt EM, Van Natta M, et al. Design and validation of a histological scoring system for nonalcoholic fatty liver disease. *Hepatology* 2005;41:1313–1321.
- George JN, Thoi LL, McManus LM, et al. Isolation of human platelet membrane microparticles from plasma and serum. *Blood* 1982;60:834–840.
- Burnier L, Fontana P, Kwak BR, et al. Cell-derived microparticles in haemostasis and vascular medicine. *Thromb Haemost* 2009;101:439–451.
- Roos MA, Gennero L, Denysenko T, et al. Microparticles in physiological and in pathological conditions. *Cell Biochem Funct* 2010;28:539–548.
- Sossdorf M, Otto GP, Claus RA, et al. Cell-derived microparticles promote coagulation after moderate exercise. *Med Sci Sports Exerc* 2011;43:1169–1176.
- Syn WK, Oo YH, Pereira TA, et al. Accumulation of natural killer T cells in progressive nonalcoholic fatty liver disease. *Hepatology* 2010;51:1998–2007.
- Zimmermann HW, Seidler S, Nattermann J, et al. Functional contribution of elevated circulating and hepatic non-classical CD14CD16 monocytes to inflammation and human liver fibrosis. *PLoS One* 2010;5:e11049.
- Nozaki T, Sugiyama S, Sugamura K, et al. Prognostic value of endothelial microparticles in patients with heart failure. *Eur J Heart Fail* 2010;12:1223–1228.
- Amabile N, Guerin AP, Leroyer A, et al. Circulating endothelial microparticles are associated with vascular dysfunction in patients with end-stage renal failure. *J Am Soc Nephrol* 2005;16:3381–3388.
- Falati S, Liu Q, Gross P, et al. Accumulation of tissue factor into developing thrombi in vivo is dependent upon microparticle P-selectin glycoprotein ligand 1 and platelet P-selectin. *J Exp Med* 2003;197:1585–1598.
- Hernandez-Gea V, Friedman SL. Pathogenesis of liver fibrosis. *Annu Rev Pathol* 2011;6:425–456.
- Spengler U, Nattermann J. Immunopathogenesis in hepatitis C virus cirrhosis. *Clin Sci (Lond)* 2007;112:141–155.
- Durante-Mangoni E, Wang R, Shaulov A, et al. Hepatic CD1d expression in hepatitis C virus infection and recognition by resident proinflammatory CD1d-reactive T cells. *J Immunol* 2004;173:2159–2166.
- Lucas M, Gadola S, Meier U, et al. Frequency and phenotype of circulating Valpha24/Vbeta11 double-positive natural killer T cells during hepatitis C virus infection. *J Virol* 2003;77:2251–2257.
- Park O, Jeong WI, Wang L, et al. Diverse roles of invariant natural killer T cells in liver injury and fibrosis induced by carbon tetrachloride. *Hepatology* 2009;49:1683–1694.
- Odegaard JI, Chawla A. Mechanisms of macrophage activation in obesity-induced insulin resistance. *Nat Clin Pract Endocrinol Metab* 2008;4:619–626.
- Bouloumie A, Curat CA, Sengenès C, et al. Role of macrophage tissue infiltration in metabolic diseases. *Curr Opin Clin Nutr Metab Care* 2005;8:347–354.
- Xu H, Barnes GT, Yang Q, et al. Chronic inflammation in fat plays a crucial role in the development of obesity-related insulin resistance. *J Clin Invest* 2003;112:1821–1830.
- Ziegler-Heitbrock L. The CD14+ CD16+ blood monocytes: their role in infection and inflammation. *J Leukoc Biol* 2007;81:584–592.
- Green RM, Flamm S. AGA technical review on the evaluation of liver chemistry tests. *Gastroenterology* 2002;123:1367–1384.
- Ratziu V, Charlotte F, Heurtier A, et al. Sampling variability of liver biopsy in nonalcoholic fatty liver disease. *Gastroenterology* 2005;128:1898–1906.
- Schuppan D, Afdhal NH. Liver cirrhosis. *Lancet* 2008;371:838–851.
- Regev A, Berho M, Jeffers LJ, et al. Sampling error and intraobserver variation in liver biopsy in patients with chronic HCV infection. *Am J Gastroenterol* 2002;97:2614–2618.
- Ratziu V, Charlotte F, Heurtier A, et al. Sampling variability of liver biopsy in nonalcoholic fatty liver disease. *Gastroenterology* 2005;128:1898–1906.
- Wieckowska A, Feldstein AE. Diagnosis of nonalcoholic fatty liver disease: invasive versus noninvasive. *Semin Liver Dis* 2008;28:386–395.
- Younossi ZM, Gramlich T, Liu YC, et al. Nonalcoholic fatty liver disease: assessment of variability in pathological interpretations. *Mod Pathol* 1998;11:560–565.

41. Dowman JK, Armstrong MJ, Tomlinson JW, et al. Current therapeutic strategies in non-alcoholic fatty liver disease. *Diabetes Obes Metab* 2011;13:692–702.
42. Sanyal AJ, Chalasani N, Kowdley KV, et al. Pioglitazone, vitamin E, or placebo for nonalcoholic steatohepatitis. *N Engl J Med* 2010;362:1675–1685.
43. Schuppan D, Gorrell MD, Klein T, et al. The challenge of developing novel pharmacological therapies for non-alcoholic steatohepatitis. *Liver Int* 2010;30:795–808.

Reprint requests

Address requests for reprints to: Detlef Schuppan, MD, PhD, Division of Gastroenterology, Beth Israel Deaconess Medical Center, Harvard Medical School, 330 Brookline Avenue, Boston,

Massachusetts 02215, USA. e-mail: dschuppa@bidmc.harvard.edu; fax: (617) 667-2767.

Conflicts of interest

The authors disclose no conflicts.

Funding

This work was supported by National Institute of Diabetes and Digestive and Kidney Diseases grant 1 R21 DK075857-01A2 to D.S., CA143748 to M.E., and DFG fellowship grant KO4103/1-1 to M.K. Part of this work was presented as oral presentation by M.K. during the European Association for the Study of the Liver Annual Meeting 2011 in Berlin, Germany, and as a poster at Digestive Disease Week 2011, Chicago, Illinois.

Tumour-associated circulating microparticles: A novel liquid biopsy tool for screening and therapy monitoring of colorectal carcinoma and other epithelial neoplasia

Arnulf Willms¹, Clara Müller², Henrike Julich², Niklas Klein², Robert Schwab¹, Christoph GÜsgen¹, Ines Richardsen¹, Sebastian Schaaf¹, Marcin Krawczyk^{2,3}, Marek Krawczyk⁴, Frank Lammert², Detlef Schuppan⁵, Veronika Lukacs-Kornek², Mirosław Kornek^{1,2}

¹Department of General, Visceral and Thoracic Surgery, German Armed Forces Central Hospital, Koblenz, Germany

²Department of Medicine II, Saarland University Medical Center, Homburg/Saar, Germany

³Laboratory of Metabolic Liver Diseases, Department of General, Transplant and Liver Surgery, Medical University of Warsaw, Warsaw, Poland

⁴Department of General, Transplant and Liver Surgery, Medical University of Warsaw, Warsaw, Poland

⁵Institute of Translational Immunology and Research Center for Immune Therapy, Institute of Translational Immunology, University Medical Center, Johannes Gutenberg University, Mainz, Germany

Correspondence to: Mirosław Kornek, **e-mail:** miroslawkornek@web.de

Keywords: biomarker, CD147, CD326, CRC, diagnosis

Received: March 07, 2016

Accepted: April 02, 2016

Published: April 26, 2016

ABSTRACT

Up to date, novel tools for low-cost, minimal invasive cancer surveillance, cancer screening and treatment monitoring are in urgent need. Physicians consider the so-called liquid biopsy as a possible future tool successfully achieving these ultimate goals. Here, we aimed to identify circulating tumour-associated MPs (taMPs) that could aid in diagnosing minimal-invasively the presence and follow up treatment in non-small cell lung carcinoma (NSCLC), colorectal carcinoma (CRC) and pancreas carcinoma (PaCa). Tumour-associated MPs (taMPs) were quantified after isolation by centrifugation followed by flow cytometry analysis from the serum of cancer patients with CRC ($n = 52$), NSCLC ($n = 40$) and PaCa ($n = 11$). Healthy subjects ($n = 55$) or patients with struma nodosa (thyroid nodules) ($n = 43$) served as negative controls. In all three types of tumour entities, the presence of tumour was associated with an increase of circulating EpCAM⁺ and EpCAM⁺CD147⁺ taMPs. The presence of CD147⁺EpCAM⁺ taMPs were specific to tumour-bearing patients thus allowing the specific distinction of malignancies from patients with thyroid nodules. Increased level of EpCAM single positive MPs were, in turn, also detected in patients with thyroid nodules. Importantly, EpCAM⁺CD147⁺ taMPs correlated with the measured tumour-volume in CRC patients. EpCAM⁺ taMPs decreased at 7 days after curative R0 tumour resection suggesting a close dependence with tumour presence. AUROC values (up to 0.85 and 0.90), sensitivity/specificity scores, and positive/negative predictive values indicated a high diagnostic accuracy of EpCAM⁺CD147⁺ taMPs. Taken together, EpCAM⁺CD147⁺ double positive taMPs could potentially serve as novel promising clinical parameter for cancer screening, diagnosis, surveillance and therapy monitoring.

INTRODUCTION

Large cell membrane derived extracellular vesicles (EVs), known as microparticles (MPs), microvesicles (MVs) or ectosomes, have recently emerged as novel vehicles for

a horizontal crosstalk between different cells and cell types, especially in the setting of inflammatory conditions [1–6]. In brief, MPs are extruded cell membrane coated vesicles with diameters between ~100–1000 nm that are formed and shedded during cellular activation or in early stages of

apoptosis and that are released into the extracellular space. MPs can be isolated from human fluids such as whole blood, plasma, serum or e.g. synovial fluid [1–6]. They carry the surface signature of their cell of origin and the quantification of MP subsets using FACS sorting permits a non-invasive assessment of cell specific pathologies, especially in inflammation [7–10]. MPs have to be differentiated and separated from exosomes, which are derived from intracellular vesicles and do not carry cell surface markers of their origin, and from the larger fragments of apoptotic bodies [2, 3]. So far, only a few and technically limited studies have been performed on putative cancer-derived MPs or microvesicles identified by single surface marker [11–13]. Therefore, we explored the diagnostic potential of tumour-associated MPs (taMPs) and MP subtypes in thoroughly characterised patients with various underlying cancer entities such as colorectal carcinoma, non-small cell lung carcinoma and pancreas carcinoma.

RESULTS

Patients with CRC, other neoplasia or thyroid nodules (struma nodosa) show characteristic MP profiles

Based on literature research various cancer markers were considered for the detection of taMPs expressing common cancer antigens as EpCAM and CD147. Corresponding cancer lines were screened for the chosen surface antigens (data not shown). Indeed, EpCAM and CD147 were identified on the surface of cancer cell lines of colorectal (CRC), lung (NSCLC) and pancreas (PaCa) (data not shown). MPs were isolated by differential centrifugation of sera of total 103 confirmed cancer patients. Median EpCAM⁺ taMPs values were significantly elevated (one-way ANOVA) in patients with CRC ($n = 52$), NSCLC ($n = 40$), PaCa ($n = 11$) by an average of 2.3 fold irrespective of the tumour entity and size (Figure 1A and Table 1). Surprisingly, EpCAM⁺ taMPs were also found elevated in thyroid nodules patients (short: struma, $n = 40$) as compared to healthy controls by 1.9 fold ($p < 0.05$). Nevertheless, the antigen combination of EpCAM and CD147, successfully detected *in vivo* derived CD147⁺EpCAM⁺ taMPs and their median values significantly increased in cancer patients by an average of 4.8 fold (Figure 1B and Table 1) across all investigated tumour entities. Additionally, the CD147⁺EpCAM⁺ taMPs were significantly reduced compared to the elevated cancer taMPs values (Figure 1B). However, *in vivo*, putative carcinoma derived single positive taMPs (CD147⁺EpCAM⁻) levels were not significantly distributed in our study (Figure 1C).

Diagnostic performance (AUROC)

For all investigated MP types, accompanied cut-off values were calculated based on their associated AUROC

values (Table 1). The diagnostic performance of all three investigated taMPs populations (EpCAM⁺ taMPs, EpCAM⁺CD147⁺ taMPs and CD147⁺ taMPs) were assessed by their corresponding receiver operating characteristic (ROC) curves. The ROC curve is a plot of sensitivity versus 1- specificity for all possible cutoff values (Figure 1A–1C). Index of accuracy is the area under the ROC curve (AUROC). AUROC values reaching 1.0 indicating a high diagnostic accuracy. AUROC curves are given in Figure 1A–1C. EpCAM⁺CD147⁺ taMPs AUROC values were in general superior than the calculated AUROC value of EpCAM⁺ taMPs in this study (Table 1). CD147⁺ taMPs showed only a poor diagnostic relevance (AUROC data not shown).

Positive (PPV) and negative predictive values (NPV) across cancer entities

Based on the overall cut-off value of 23.91 EpCAM⁺ taMPs/10³MPs, 99 out of 103 investigated cancer patients disregarding their cancer entity were correctly as tumour bearer identified and 90 out of 95 were identified as cancers by a cut-off value of 1.605 EpCAM⁺CD147⁺ taMPs/10³MPs. The overall positive (PPV) and negative predictive values (NPV) across the investigated cancer entities (NSCLC, CRC and PaCa) for EpCAM⁺ taMP were: 79.03% (PPV) and 85.29% (NPV), respectively, with an overall sensitivity of 95.15% and specificity of 52.73%. Individual sensitivities and specificities are depicted in Table 1. EpCAM⁺CD147⁺ taMPs were associated with a slightly higher overall positive predictive values for the investigated tumour entities: 80.36% (PPV) and 83.87% (NPV), respectively, with an overall sensitivity of 94.74% and specificity of 54.17%.

Correlations between taMPs and CRC tumour load

While taMPs could aid in of the detection of the investigated tumour entities, the questions remained if taMPs, EpCAM⁺ taMPs and especially EpCAM⁺CD147⁺ taMPs could reflect tumour burden. However, in NSCLC we did not observe any correlation better than $r = 0.5$ between tumour volume and measured taMPs (Figure 2A–2B). In CRC, EpCAM⁺ taMPs were not indicating a sufficient correlation ($r = 0.4972$, Figure 2C–2D). But, as expected double positive taMPs, EpCAM⁺CD147⁺ taMPs, were correlating with CRC tumour volume significantly ($r = 0.7288$, $p < 0.0001$, $n = 43$) (Figure 2E). If CRC tumour volumes were broken up in meaningful tumour volume groups spanning from 0 (healthy controls), over 1–10 cm³, 10–50 cm³, 50–100 cm³ and above 100 cm³ CRC tumour volume, ANOVA analysis revealed that 10 cm³ of CRC volume might be the lower detection limit (Figure 2F). While a significant correlation between EpCAM⁺CD147⁺ taMPs and CRC tumour volume was observed, a good correlation exceeding $r = 0.5$ between EpCAM⁺CD147⁺

taMPs and EpCAM⁺ taMPs with the commonly used UICC scores for CRC were not reached (Figure 3A–3B). Leading to the further question whether was the shedding of taMPs from parental CRC tumour cells in fact dependent on the metastatic phenotype? Our data clearly indicated, that such dependence on the metastatic CRC phenotype

wasn't given, there were no observed differences measured between EpCAM⁺ or EpCAM⁺CD147⁺ taMPs isolated from metastatic CRC patients samples or non metastatic CRC samples (Figure 3C–3D). Matched sera CEA and CA 19–9 sera parameters in those CRC samples from patients suffering metastatic or non-metastatic CRC showed

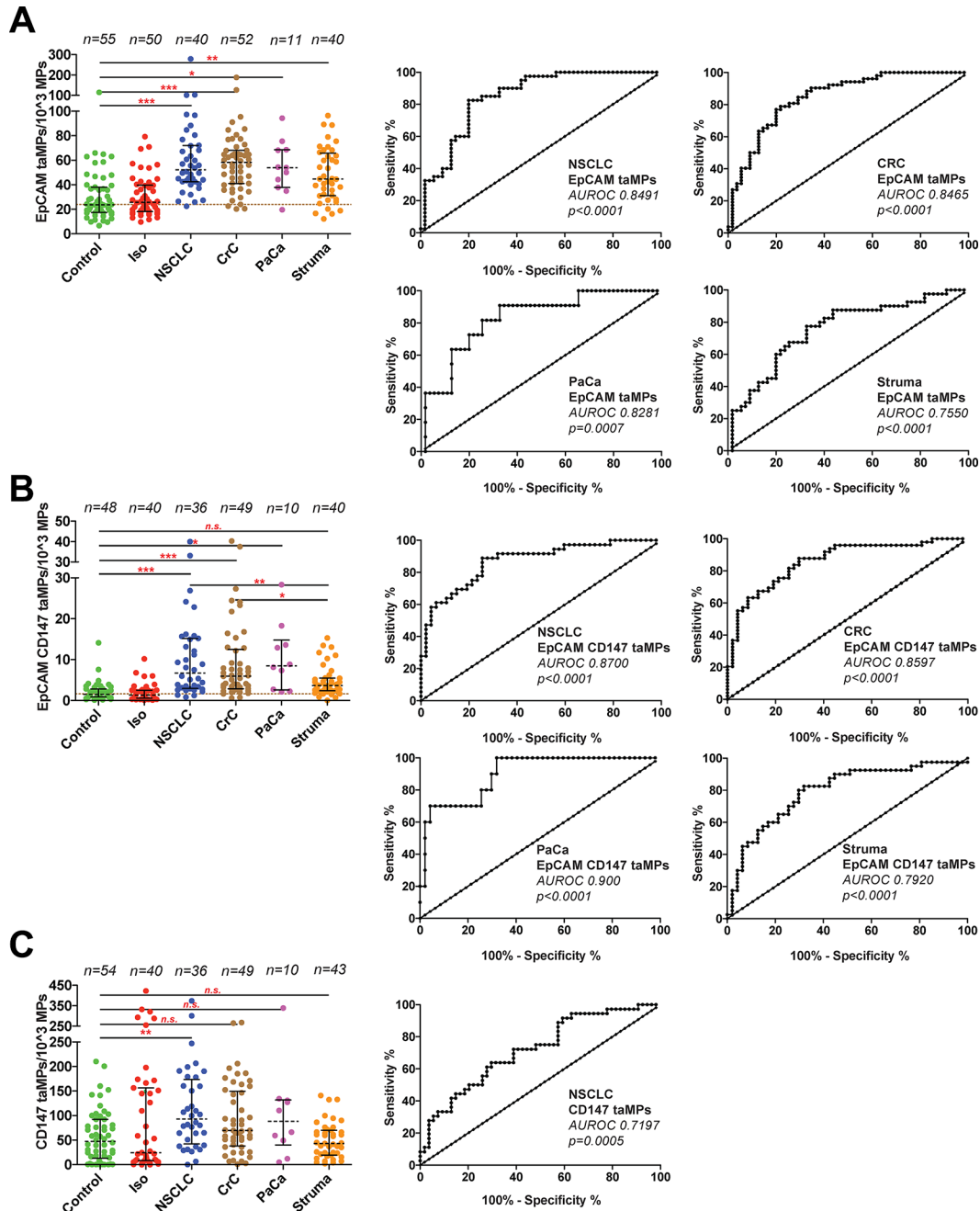


Figure 1: Detection of EpCAM⁺ and EpCAM⁺CD147⁺ and CD147⁺EpCAM⁻ tumour-associated microparticles (taMPs) in sera of indicated cancer patients. (A–C) MPs were isolated by differential centrifugation and analysed by FACS as described in Supplementary. Materials and Methods. The indicated *p*-value for each MP population as predictor of controls vs. cancer and control vs. struma nodosa (thyroid nodules; short: struma) was calculated by using one-way ANOVA test including multiple comparisons using Dunn's post test. Shown are medians with 25 and 95 percentile. Additionally, accompanied areas under the receiver operating characteristics (AUROC) curves and values including accompanied *p*-values are shown as indicated; * = *p* < 0.05, ** = *p* < 0.005, *** = *p* < 0.0005, n.s. = not significant. Overall, an error level *p* < 0.05 was considered significant. Calculations were done with Prism 5 (GraphPad Software, Inc., USA).

Table 1: Summary of predicted cut-off values, medians and other AUROC curve associated values of the indicated cancer entities

Cancer entity	Cut-Off taMPs/10 ³ MPs	Median taMPs/10 ³ MPs	Sensitivity [%]	Specificity [%]	AUROC	SD	p-Value
NSCLC	23.72*	52.28	97.50	50.91	0.8491	0.0388	< 0.0001
CRC	23.91*	58.21	94.23	52.73	0.8465	0.0373	< 0.0001
PaCa	23.72*	53.95	90.91	50.91	0.8281	0.0637	0.0007
Control		23.56					

Cancer entity	Cut-Off taMPs/10 ³ MPs	Median taMPs/10 ³ MPs	Sensitivity [%]	Specificity [%]	AUROC	SD	p-Value
NSCLC	1.611#	6.72	91.67	55.32	0.8700	0.0392	< 0.0001
CRC	1.605#	5.93	95.92	55.32	0.8597	0.03771	< 0.0001
PaCa	1.611#	8.472	100.0	55.32	0.900	0.0479	0.0005
Control		1.48					

NOTE: Calculations were done with Prism 5 (GraphPad Software, Inc., USA) based on the measured individual taMP data of the indicated taMP populations. Overall, an error level $p < 0.05$ was considered significant.

*for EpCAM⁺ taMPs/1k MPs.

#for EpCAM⁺CD147⁺ taMPs/1k MPs.

no significant differences ($p > 0.05$) (Figure 3E–3F). Additionally no significant correlations between CRC tumour volumes and matched CEA ($r = 0.2422$, $p = 0.06$) or CA 19–9 ($r = 0.059$, $p = 0.3601$) sera values were observed.

taMPs levels decrease after surgical CRC R0 resection

Furthermore, EpCAM⁺ taMPs values were evaluated in serum of CRC patients at pre- and post-surgery stages (pre-OP, usually the day before the planned R0 CRC resection, $n = 14$; d7, post-operative day 7, $n = 14$; d10, post-operative day 10, $n = 3$). In total, 11 out of 14 resected CRC patients with longitudinal blood collections showed a significant decrease from pre-OP 61 EpCAM⁺ taMPs per 10³ AnnexinV⁺ MPs to 51 EpCAM⁺ taMPs per 10³ AnnexinV⁺ MPs (Figure 4A–4B). On the contrary, EpCAM⁺CD147⁺ taMP and CD147⁺EpCAM⁻ MPs were at day 7 post-OP in median not differing compared to respective pre-OP values ($p > 0.05$) (Figure 4C–4D).

DISCUSSION

A recent study demonstrated that analysis of blood exosomes, another kind of small sized extracellular vesicles of 30–100 nm size that do not entirely share the same surface markers with MPs, might help to diagnose non invasively patients with pancreatic ductal adenocarcinoma (PADC) [14]. Based on the well founded hypothesis that cell specific MPs (200–1000 nm in size) are released into the circulation as a result of activation and/or apoptosis of their parent cell type [7], we searched for EpCAM⁺, CD147⁺

or EpCAM⁺CD147⁺ double positive taMPs that could indicate cancer presence.

Depending on the overall cut-off value 99 out of 103 investigated cancer patients disregarding their cancer entity were correctly as tumour bearer identified and 90 out of 95 were identified as cancers by EpCAM⁺CD147⁺ taMPs. Additionally, the calculated overall positive (PPV) and negative predictive values (NPV) across the investigated cancer entities (NSCLC, CRC and PaCa) for EpCAM⁺CD147⁺ taMPs distinguishing CRC and other neoplasia from healthy controls and from thyroid nodules (*struma nodosa*). These results suggest that tumours can be reliably detected with taMP profiling including EpCAM⁺ taMPs and EpCAM⁺CD147⁺ taMPs independently of the underlying cancer entity. However, certain disease/health circumstances associated with epithelial damage such as struma nodosa (thyroid nodules) does not permit to draw conclusions only on EpCAM taMPs. Thus, such disorders causing epithelial damage should be regarded as exclusion criteria in MP-based studies.

Next, we investigated whether both taMP populations, would reflect the tumour volume. For NSCLC only poor correlations ($r < 0.5$) were observed between the investigated taMPs populations and the tumour volume (Figure 2A–2B). EpCAM⁺ taMPs could not indicate tumour volume in CRC (Figure 2C). However, EpCAM⁺CD147⁺taMPs were greatly mirroring tumour volume with a significant dependence ($r = 0.73$; Figure 2E). Furthermore the detailed analysis revealed that in CRC the tumour volume of less than 10 cm³, (~2 cm in diameter) might be the lowest taMP detection limit (Figure 2F).

EpCAM is currently used as pan-cancer marker and their expression is also associated with stem cells [15, 16]. Additionally, EpCAM is a prominent cell surface antigen for detection of circulating tumour cells (CTCs) and part of the commercially available CellSearch™ system (Veridex LLC, Raritan, NJ, USA). Of note, the US Food and Drug Administration (FDA) approve this test only for the detection of certain metastatic cancers [17–19] whereas in our novel approach we cannot observe such limitation for either of the investigated taMPs subpopulations (Figure 3C–3D).

Next we explored whether total tumour R0 resection could alter taMPs. Based on the previously published results [14], we expected that taMPs should decrease after tumour removal. Indeed, we documented a significant decrease of the median values at day 7 post-OP from pre-OP 61 EpCAM⁺ taMPs per 10³ AnnexinV⁺ MPs to 51 EpCAM⁺ taMPs per 10³ AnnexinV⁺ MPs (Figure 4A–4B). While EpCAM⁺ taMPs did not decrease totally towards the healthy control levels. We assumed that the clearance of EpCAM⁺ taMPs might need longer time period as in the case of the

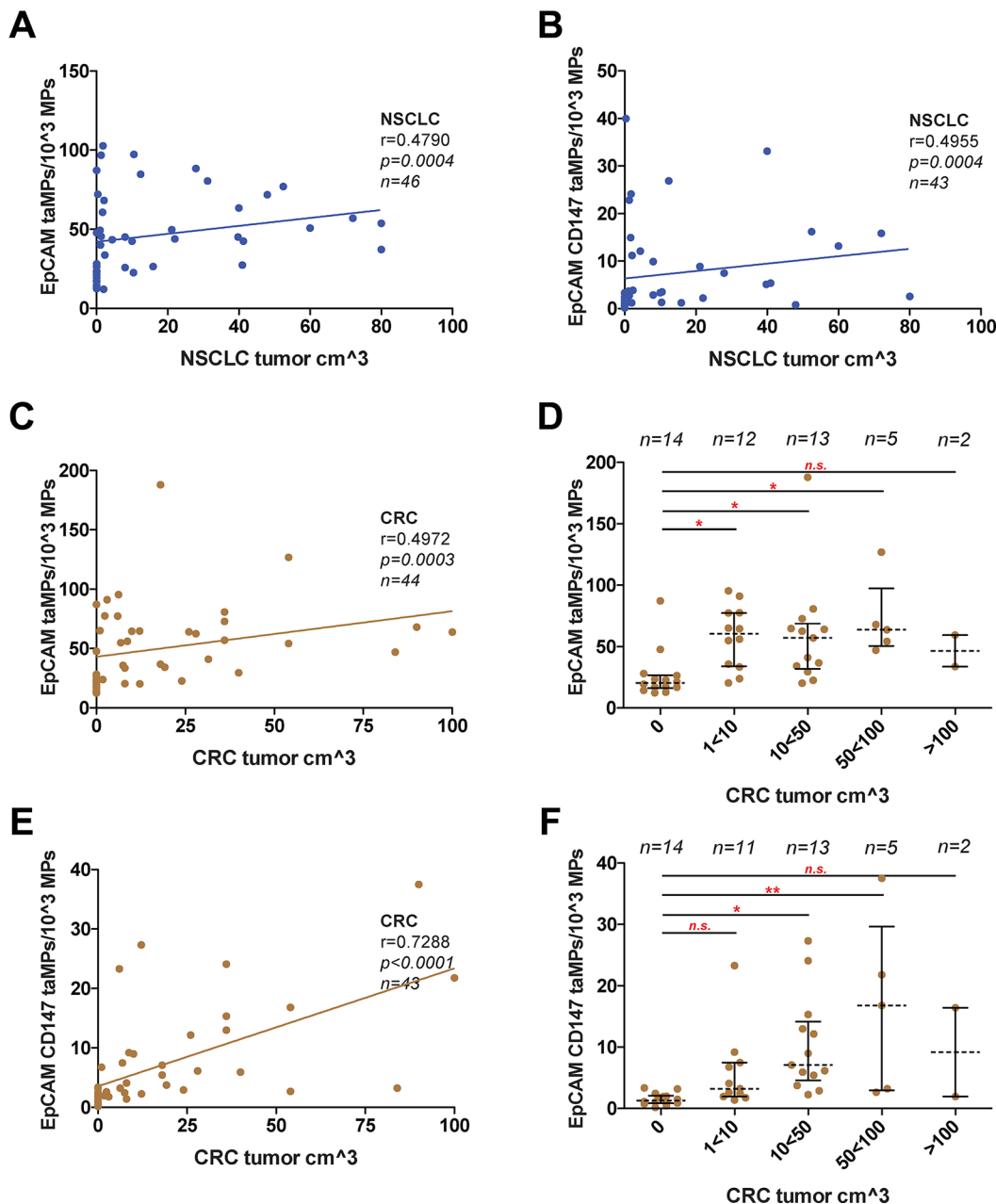


Figure 2: taMPs predict tumour volumes. Measured EpCAM⁺ taMP and EpCAM⁺CD147⁺ taMP values were set in dependence (Spearman algorithm) to associate patient tumour volumes of indicated cancer entities; (A–B): NSCLC; (C–F): CRC. Correlations were restricted to 100 cm³ of tumour volume. (D/F) Detail analysis of indicated tumour ranges revealing the possible lower and upper detection limit. Shown are indicated median with 25 and 95 percentile including p -value as indicated; * = $p < 0.05$, ** = $p < 0.005$, *** = $p < 0.0005$, n.s. = not significant (one-way ANOVA test including multiple comparisons using Dunn’s Multiple Comparison Test). Overall, an error level $p < 0.05$ was considered significant. Calculations were done with Prism 5 (GraphPad Software, Inc., USA).

clearance of Glypican-1 positive exosomes [14]. On the contrary, EpCAM⁺CD147⁺ taMP and CD147⁺EpCAM⁻ MPs were at day 7 post-OP in median not differing compared to respective pre-OP values (Figure 4C–4D). We speculate that CD147⁺EpCAM⁻ MPs were shed from fibroblast, T-cells, stroma cells, epithelial cells during tumour resection indicating tissue remodelling, migration and cancer cell invasion in which EMMPRIN/CD147 might play role as suggested by others [7, 20, 21].

Taken together, *in vivo* cancer cells shed distinct taMP populations with a unique pan-cancer MPs-based signature. Even if each tumour is composed of a mixture of heterogeneous tumour cells, the released EpCAM⁺ and EpCAM⁺CD147⁺ taMPs can be reliably detected in the circulation in both primary and metastatic tumour-bearing patients (Figure 4E). EpCAM⁺ and EpCAM⁺CD147⁺ taMPs might serve as an early indicator of cancer growth and monitor successful anti-tumour therapy and might be used as

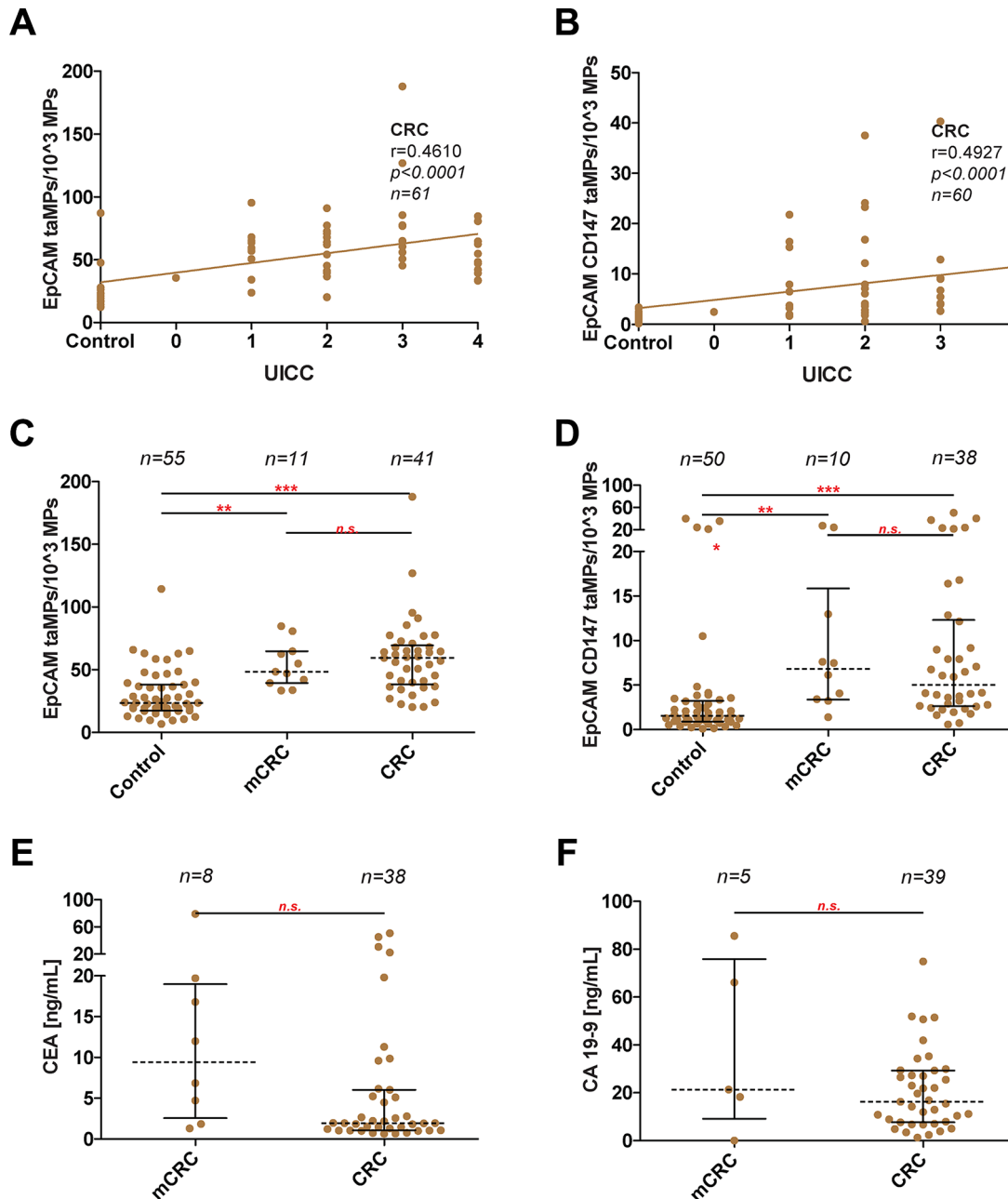


Figure 3: Discrimination between metastatic and non-metastatic phenotype in CRC. (A–B) Measured EpCAM⁺ taMP and EpCAM⁺CD147⁺ taMP values were set in dependence (Spearman algorithm) to associate patient UICC values. (C–D) Direct comparison of indicated taMPs population in metastatic CRC (mCRC) vs. non-metastatic CRC and healthy controls. (E/F) Direct comparison of measured CEA and CA 19-9 values in ng/mL in metastatic CRC (mCRC) vs. non-metastatic CRC. Shown are indicated median with 25 and 95 percentile including p -value as indicated; * = $p < 0.05$, ** = $p < 0.005$, *** = $p < 0.0005$, n.s. = not significant (one-way ANOVA test including multiple comparisons using Dunn’s Multiple Comparison Test (C/D) or unpaired Mann-Whitney test (E/F)).

important liquid biopsy tool to differentiate between therapy responders and therapy non-responders. Importantly, our data clearly indicate that it is far more beneficial to explore specific individual taMP subpopulations using multiple surface marker combination in order to distinguish cancer

from non-cancer patients. Our results demonstrate that the analysis of taMP can help to identify patients with cancer from healthy individuals but also to pinpoint the presence of specific MP subtype in epithelial damage and subtype exclusively associated with tumour.

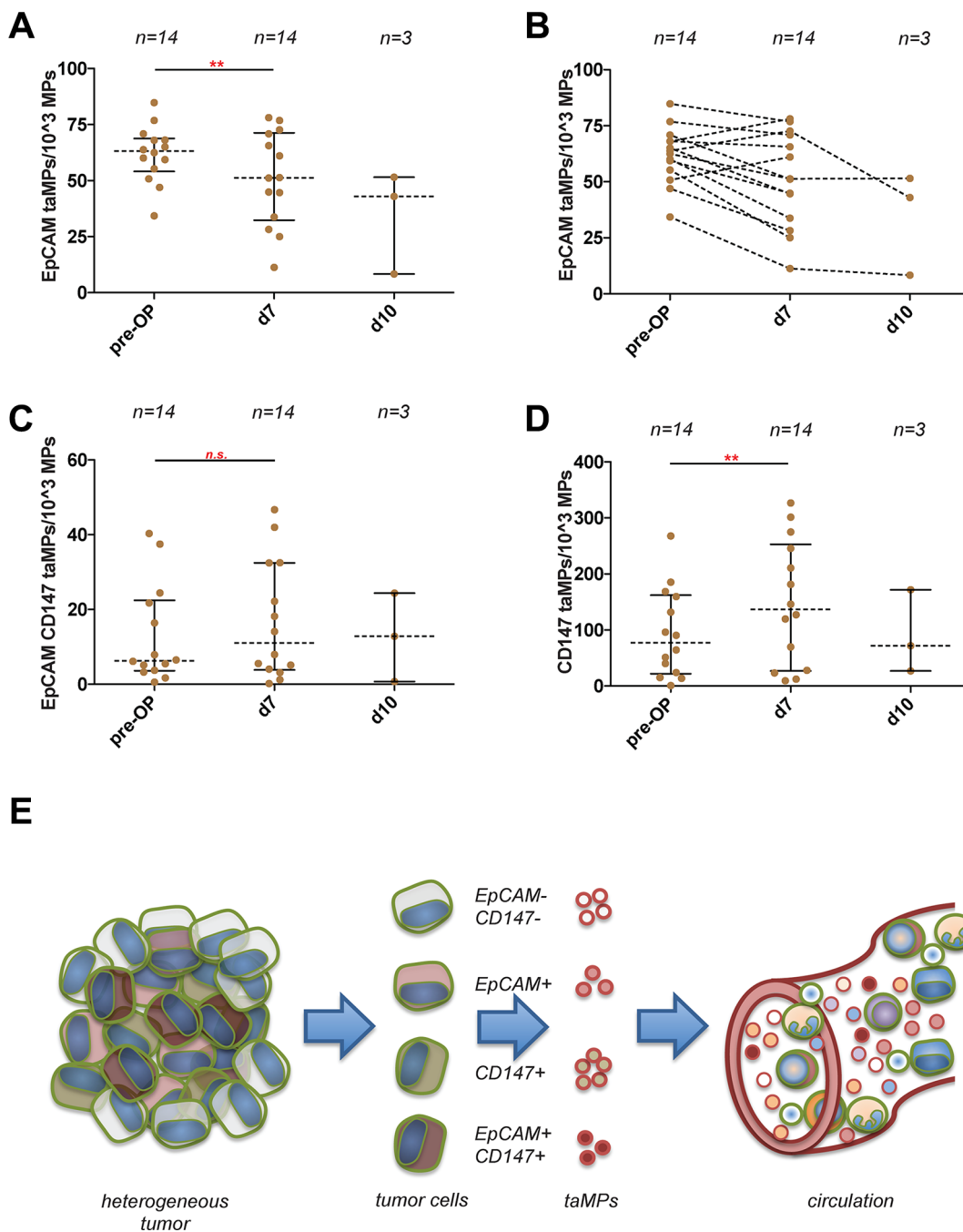


Figure 4: Detection of EpCAM⁺ and EpCAM⁺CD147⁺ and CD147⁺EpCAM⁻ tumour associated microparticles (taMPs) in CRC sera patient samples. (A) EpCAM⁺ taMPs levels 7 days post CRC tumour resection and at day 10 post-OP. (B) Paired display of accompanied post-OP and post-OP values of indicated taMP populations. (C) EpCAM⁺CD147⁺ taMPs levels 7 days post CRC tumour resection and at day 10 post-OP. (D) CD147⁺EpCAM⁻ taMPs levels 7 days post CRC tumour resection and at day 10 post-OP. Shown are indicated median with 25 and 95 percentile including *p*-value as indicated; * = *p* < 0.05, ** = *p* < 0.005, *** = *p* < 0.0005, n.s. = not significant (paired *t*-test with Wilcoxon matched pairs signed rank-test). Overall, an error level *p* < 0.05 was considered significant. (E) Sketch illustrating the heterogeneous tumour composition and tumour antigens used in the current study. Tumour cells shed multiple MP subpopulations carrying a distinguishing set of surface markers. These shedded taMPs can be detected in the sera of cancer patients.

MATERIALS AND METHODS

Human study cohort

The Ethics Commission of the State Chamber of Medicine in Rhineland-Palatinate approved the current study (approval number: 837.151.13 (8836-F)) and all patients gave their informed consent prior to participation. Patients with a major second or third known comorbidity that could affect immune cell activation such as acute inflammation, chronic inflammation, autoimmune diseases or viral infections, were excluded. Additionally, patients who underwent chemotherapy or were receiving chemotherapy or were subjected to any other anti-tumoural therapy during the time blood samples were taken were excluded, too. Characteristics of patients are summarized in Supplementary Table 1.

Isolation of cell derived microparticles from human serum

Blood was collected in standard S-Monovette® 7.5 ml, Serum Gel with Clotting Activator (Sarstedt AG & Co., Nümbrecht, Germany) and left for 30 minutes at 37°C to allow for clot formation followed by centrifugation at 4000 rpm for 20 min at 4°C. Clots were carefully separated and supernatants stored at -80°C for further MP isolation. MPs from serum samples were isolated by differential centrifugation between 2,000 and 20,000 g as described by us and others [4, 5, 7]. MPs sedimenting at 20,000 g were characterized by FACS using staining for AnnexinV, CD147, EpCAM (eBioscience™, San Diego, CA; BioLegend; Miltenyi Biotec, Bergisch Gladbach, Germany, respectively). All antibodies were titrated against the matching isotype control on patient's samples prior to use. MP preparations were characterized on a MACSquant 10 Analyser (Miltenyi Biotec, Bergisch Gladbach, Germany) and cytometric data was analysed with FlowJo X software for MAC OSX (Tree Star, Inc., Ashland, Oregon). To avoid non-specific antibody binding, Fc receptors on MPs and target cells were blocked with FcR Blocking Reagent (eBioscience™, San Diego, CA, USA). Additionally, MPs were dialyzed overnight against AnnexinV binding buffer containing 0.05% BSA (Miltenyi Biotec, Bergisch Gladbach, Germany). Used antibodies and BSA blocking solution were centrifuged prior to FACS to avoid artefacts due to aggregation. No differences regarding the total amount of MPs isolated were observed between healthy and cancer samples (Supplementary Figure 2).

Statistical analysis

All data are medians with their percentile. Differences between independent experimental groups (NSCLC, CRC and controls) were characterized using the one-way ANOVA test. As a post-hoc test, a Dunn's test was applied for multiple comparisons of subgroups when the one-way ANOVA test was positive and succeeded Bartlett's test for equal variance. A two-tailed Wilcoxon matched pairs signed rank-test was

applied to assay differences between patients who underwent a total R0 tumour resection between pre-operative and postoperative sera samples. To assess the predictive ability of the two taMP populations (EpCAM⁺ and EpCAM⁺CD147⁺ taMPs) and for discriminating between individuals with cancer, struma nodosa (thyroid nodules) and controls, we calculated sensitivity, specificity, PPV and NPV and AUROC values. These calculations were done with Prism 5 (GraphPad Software, Inc., USA). Overall, $p < 0.05$ was considered significant. The overall power (1- β err prob) of the study was calculated post-hoc with GPower (Version 3.1.9.2) assuming a minimum effect size of $f = 0.5$ with an α err prob = 0,05 for 5 groups, indicating that the minimum total sample size of 80 is needed to reach a power of 0.95 (1- β err prob).

Abbreviations

AUROC: Area under the Receiver Operating Characteristic; CTC: circulating tumour cell; CRC: colorectal carcinoma; EpCAM: epithelial cell adhesion molecule; MP: microparticle; NPV: negative predictive value; PPV: positive predictive value.

ACKNOWLEDGMENTS

The authors thank the leaders, patients and staff of the German Armed Forces Central Hospital for their continuous support and interest in our MP based cancer differentiation study. Part of this work was orally presented at AASLD 2015, SF, CA, USA.

CONFLICTS OF INTEREST

No potential conflicts of interest were disclosed.

GRANT SUPPORT

This work was supported by a Deutsche Krebshilfe grant (111184) to Miroslaw Kornek, a German Armed Forces SoFo grant (SoFo11K1-S-101416) to Arnulf Willms, Robert Schwab and Miroslaw Kornek. And by the Alexander von Humboldt Foundation, Sofja Kovalevskaja Award to Veronika Lukacs-Kornek.

Author's contributions

Conception and design: Arnulf Willms, Detlef Schuppan, Veronika Lukacs-Kornek and Miroslaw Kornek. Development of methodology: Clara Müller, Henrike Julich and Miroslaw Kornek. Acquisition of data (provided animals, acquired and managed patients, provided facilities, etc.): Arnulf Willms, Clara Müller, Henrike Julich, Niklas Klein, Robert Schwab, Christoph GÜsgen, Ines Richardsen, Sebastian Schaaf, Marcin Krawczyk, Marek Krawczyk, Frank Lammert, Detlef Schuppan, Veronika Lukacs-Kornek and Miroslaw Kornek. Analysis and interpretation of data (e.g., statistical analysis, biostatistics, computational analysis): Arnulf Willms, Detlef Schuppan, Veronika

Lukacs-Kornek and Mirosław Kornek. Writing, review, and/or revision of the manuscript: Arnulf Willms, Marcin Krawczyk, Marek Krawczyk, Detlef Schuppan, Veronika Lukacs-Kornek and Mirosław Kornek. Administrative, technical, or material support (i.e., reporting or organizing data, constructing databases): Arnulf Willms, Clara Müller, Henrike Julich, Niklas Klein, Robert Schwab, Christoph GÜsgen, Ines Richardsen, Sebastian Schaaf, Marcin Krawczyk, Marek Krawczyk, Frank Lammert, Detlef Schuppan, Veronika Lukacs-Kornek and Mirosław Kornek. Study supervision: Mirosław Kornek.

REFERENCES

1. Thery C, Ostrowski M, Segura E. Membrane vesicles as conveyors of immune responses. *Nat Rev Immunol.* 2009; 9:581–593.
2. Julich H, Willms A, Lukacs-Kornek V, Kornek M. Extracellular vesicle profiling and their use as potential disease specific biomarker. *Front Immunol.* 2014; 5.
3. Kornek M, Schuppan D. Microparticles: Modulators and biomarkers of liver disease. *J Hepatol.* 2012; 57:1144–1146.
4. Kornek M, Lynch M, Mehta SH, Lai M, Exley M, Afdhal NH, Schuppan D. Circulating microparticles as disease-specific biomarkers of severity of inflammation in patients with hepatitis C or nonalcoholic steatohepatitis. *Gastroenterology.* 2012; 143:448–458.
5. Witwer KW, Buzas EI, Bemis LT, Bora A, Lasser C, Lotvall J, Nolte-’t Hoen EN, Piper MG, Sivaraman S, Skog J, Thery C, Wauben MH, Hochberg F. Standardization of sample collection, isolation and analysis methods in extracellular vesicle research. *J Extracell Vesicles.* 2013; 2.
6. Yanez-Mo M, Siljander PR, Andreu Z, Zavec AB, Borrás FE, Buzas EI, Buzas K, Casal E, Cappello F, Carvalho J, Colas E, Cordeiro-da Silva A, Fais S, et al. Biological properties of extracellular vesicles and their physiological functions. *J Extracell Vesicles.* 2015; 4:27066.
7. Kornek M, Popov Y, Libermann TA, Afdhal NH, Schuppan D. Human T cell microparticles circulate in blood of hepatitis patients and induce fibrolytic activation of hepatic stellate cells. *Hepatology.* 2011; 53:230–242.
8. Nieuwland R, Berckmans RJ, McGregor S, Boing AN, Romijn FP, Westendorp RG, Hack CE, Sturk A. Cellular origin and procoagulant properties of microparticles in meningococcal sepsis. *Blood.* 2000; 95:930–935.
9. Canault M, Leroyer AS, Peiretti F, Leseche G, Tedgui A, Bonardo B, Alessi MC, Boulanger CM, Nalbone G. Microparticles of human atherosclerotic plaques enhance the shedding of the tumor necrosis factor- α converting enzyme/ADAM17 substrates, tumor necrosis factor and tumor necrosis factor receptor-1. *Am J Pathol.* 2007; 171:1713–1723.
10. Boilard E, Nigrovic PA, Larabee K, Watts GF, Coblyn JS, Weinblatt ME, Massarotti EM, Remold-O’Donnell E, Farndale RW, Ware J, Lee DM. Platelets amplify inflammation in arthritis via collagen-dependent microparticle production. *Science.* 2010; 327:580–583.
11. Julich H, Willms A, Lukacs-Kornek V, Kornek M. Extracellular vesicle profiling and their use as potential disease specific biomarker. *Front Immunol.* 2014; 5:413.
12. Roca E, Lacroix R, Judicone C, Laroumagne S, Robert S, Cointe S, Muller A, Kaspi E, Roll P, Brisson AR, Tantucci C, Astoul P, Dignat-George F. Detection of EpCAM-positive microparticles in pleural fluid: A new approach to minimally identify patients with malignant pleural effusions. *Oncotarget.* 2016; 7:3357–66. doi: 10.18632/oncotarget.6581.
13. Biggs CN, Siddiqui KM, Al-Zahrani AA, Pardhan S, Brett SI, Guo QQ, Yang J, Wolf P, Power NE, Durfee PN, MacMillan CD, Townson JL, Brinker JC, et al. Prostate extracellular vesicles in patient plasma as a liquid biopsy platform for prostate cancer using nanoscale flow cytometry. *Oncotarget.* 2016; 7:8839–49. doi: 10.18632/oncotarget.6983.
14. Melo SA, Luecke LB, Kahlert C, Fernandez AF, Gammon ST, Kaye J, LeBleu VS, Mittendorf EA, Weitz J, Rahbari N, Reissfelder C, Pilarsky C, Fraga MF, et al. Glypican-1 identifies cancer exosomes and detects early pancreatic cancer. *Nature.* 2015; 523:177–182.
15. Sun YF, Xu Y, Yang XR, Guo W, Zhang X, Qiu SJ, Shi RY, Hu B, Zhou J, Fan J. Circulating stem cell-like epithelial cell adhesion molecule-positive tumor cells indicate poor prognosis of hepatocellular carcinoma after curative resection. *Hepatology.* 2013; 57:1458–68. doi: 10.1002/hep.26151.
16. Yoon SM, Gerasimidou D, Kuwahara R, Hytioglou P, Yoo JE, Park YN, Theise ND. Epithelial cell adhesion molecule (EpCAM) marks hepatocytes newly derived from stem/progenitor cells in humans. *Hepatology.* 2011; 53:964–973.
17. Cristofanilli M, Budd GT, Ellis MJ, Stopeck A, Matera J, Miller MC, Reuben JM, Doyle GV, Allard WJ, Terstappen LW, Hayes DF. Circulating tumor cells, disease progression, and survival in metastatic breast cancer. *N Engl J Med.* 2004; 351:781–791.
18. Cohen SJ, Alpaugh RK, Gross S, O’Hara SM, Smirnov DA, Terstappen LW, Allard WJ, Bilbee M, Cheng JD, Hoffman JP, Lewis NL, Pellegrino A, Rogatko A, et al. Isolation and characterization of circulating tumor cells in patients with metastatic colorectal cancer. *Clin Colorectal Cancer.* 2006; 6:125–132.
19. Okegawa T, Nutahara K, Higashihara E. Prognostic significance of circulating tumor cells in patients with hormone refractory prostate cancer. *J Urol.* 2009; 181:1091–1097.
20. Xiong L, Edwards CK, 3rd, Zhou L. The biological function and clinical utilization of CD147 in human diseases: a review of the current scientific literature. *Int J Mol Sci.* 2014; 15:17411–17441.
21. Menck K, Scharf C, Bleckmann A, Dyck L, Rost U, Wenzel D, Dhople VM, Siam L, Pukrop T, Binder C, Klemm F. Tumor-derived microvesicles mediate human breast cancer invasion through differentially glycosylated EMMPRIN. *J Mol Cell Biol.* 2015; 7:143–153.

Cancer-associated circulating large extracellular vesicles in cholangiocarcinoma and hepatocellular carcinoma

Henrike Julich-Haertel^{1,†}, Sabine K. Urban^{1,†}, Marcin Krawczyk^{1,2,†}, Arnulf Willms^{3,†}, Krzysztof Jankowski⁴, Waldemar Patkowski⁵, Beata Kruk², Maciej Krasnodebski⁵, Joanna Ligocka⁵, Robert Schwab³, Ines Richardsen³, Sebastian Schaaf³, Angelina Klein³, Sebastian Gehlert⁶, Hanna Sanger¹, Markus Casper¹, Jesus M. Banales⁷, Detlef Schuppan⁸, Piotr Milkiewicz^{9,10}, Frank Lammert¹, Marek Krawczyk⁵, Veronika Lukacs-Kornek^{1,‡}, Mirosław Kornek^{1,3,*,‡}

¹Department of Medicine II, Saarland University Medical Center, Saarland University, Homburg, Germany; ²Laboratory of Metabolic Liver Diseases, Department of General, Transplant and Liver Surgery, Medical University of Warsaw, Warsaw, Poland; ³Department of General, Visceral and Thoracic Surgery, German Armed Forces Central Hospital, Koblenz, Germany; ⁴Department Internal Medicine and Cardiology, Medical University of Warsaw, Warsaw, Poland; ⁵Department of General, Transplant and Liver Surgery, Medical University of Warsaw, Warsaw, Poland; ⁶Department of Molecular and Cellular Sport Medicine, Institute of Cardiovascular Research and Sport Medicine, German Sport University Cologne, Cologne, Germany; ⁷Department of Liver and Gastrointestinal Diseases, Biodonostia Health Research Institute – Donostia University Hospital, University of the Basque Country (UPV/EHU), CIBERehd, Ikerbasque, San Sebastian, Spain; ⁸Institute of Translational Immunology and Research Center for Immune Therapy, University Medical Center, Johannes Gutenberg University, Mainz, Germany; ⁹Liver and Internal Medicine Unit, Department of General, Transplant and Liver Surgery, Medical University of Warsaw, Warsaw, Poland; ¹⁰Translational Medicine Group, Pomeranian Medical University, Szczecin, Poland

Background & Aims: Large extracellular vesicles, specifically AnnexinV⁺ EpCAM⁺ CD147⁺ tumour-associated microparticles (taMPs), facilitate the detection of colorectal carcinoma (CRC), non-small cell lung carcinoma (NSCLC) as well as pancreas carcinoma (PaCa). Here we assess the diagnostic value of taMPs for detection and monitoring of hepatocellular carcinoma (HCC) and cholangiocarcinoma (CCA). Specifically, the aim of this study was to differentiate liver taMPs from other cancer taMPs, such as CRC and NSCLC.

Methods: Fluorescence-activated cell scanning (FACS) was applied to detect various taMP populations in patients' sera that were associated with the presence of a tumour (AnnexinV⁺ EpCAM⁺ CD147⁺ taMPs) or could discriminate between cirrhosis (due to HCV or HBV) and liver cancers (AnnexinV⁺ EpCAM⁺ ASGPR1⁺ taMPs). In total 172 patients with liver cancer (HCC or CCA), 54 with cirrhosis and no liver neoplasia, and 202 control subjects were enrolled.

Results: The results indicate that AnnexinV⁺ EpCAM⁺ CD147⁺ taMPs were elevated in HCC and CCA. Furthermore, AnnexinV⁺

EpCAM⁺ ASGPR1⁺ CD133⁺ taMPs allowed the distinction of liver malignancies (HCC or CCA) and cirrhosis from tumour-free individuals and, more importantly, from patients carrying other non-liver cancers. In addition, AnnexinV⁺ EpCAM⁺ ASGPR1⁺ taMPs were increased in liver cancer-bearing patients compared to patients with cirrhosis that lacked any detectable liver malignancy. The smallest sizes of successfully detected cancers were ranging between 11–15 mm. AnnexinV⁺ EpCAM⁺ ASGPR1⁺ taMPs decreased at 7 days after curative R0 tumour resection suggesting close correlations with tumour presence. ROC values, sensitivity/specificity scores and positive/negative predictive values (>78%) indicated a potent diagnostic accuracy of AnnexinV⁺ EpCAM⁺ ASGPR1⁺ taMPs.

Conclusion: These data provide strong evidence that AnnexinV⁺ EpCAM⁺ ASGPR1⁺ taMPs are a novel biomarker of HCC and CCA liquid biopsy that permit a non-invasive assessment of the presence and possible extent of these cancers in patients with advanced liver diseases.

Lay summary: Microparticles (MPs) are small vesicles that bleb from the membrane of every cell, including cancer cells, and are released to circulate in the bloodstream. Since their surface composition is similar to the surface of their underlying parental cell, MPs from the bloodstream can be isolated and by screening their surface components, the presence of their parental cells can be identified. This way, it was possible to detect and discriminate between patients bearing liver cancer and chronic liver cirrhosis.

© 2017 European Association for the Study of the Liver. Published by Elsevier B.V. All rights reserved.

Keywords: ASGPR1; Biomarker; Cancer; CCA; CD147; CD326; EMMPRIN; EpCAM; Extracellular vesicles; HCC; Microparticles; Microvesicles.

Received 16 January 2017; received in revised form 22 February 2017; accepted 23 February 2017; available online 6 March 2017

* Corresponding author. Address: Department of Medicine II, Saarland University Medical Center, Saarland University, Kirrberger Str., 100, Homburg 66421, Germany.

E-mail address: miroslawkornek@web.de (M. Kornek).

[†] These authors contributed equally and shared first co-authorship.

[‡] These authors contributed equally and shared last authorship.



ELSEVIER

Introduction

A decade ago extracellular vesicles (EVs) raised little attention in the scientific communities around the globe. Nowadays, EV research has become intense and acquired more attention, including within the liver research community.^{1,2} Over the years, researchers explored the likely role of EVs, including small EVs as exosomes (50–100 nm in diameter)³ and large EVs, e.g. microvesicles/microparticles (MVs/MPs; 100–1000 nm in diameter).⁴ Rarely, MVs/MPs were referred to as ‘ectosomes’.⁵ However, the underlying biogenesis of exosomes and MVs/MPs is different and unique.⁶ It was reported that EVs play a role in the horizontal communication between cells.⁷ In fact, it was also shown that tumours prepare their own tumour niches via the release of EVs,⁸ including a possible suppression of the immune system and the activation of tumour neo-angiogenesis.^{9,10} Additionally, EVs are present in all body fluids such as urine,¹¹ blood serum/plasma,^{12,13} and bile.¹⁴ These facts made the isolation, quantification and characterization of circulating EVs a very promising and attractive potential clinical tool,¹⁵ and several methodologies have been established for these purposes.¹⁶ We demonstrated in the past that fluorescence-activated cell scanning (FACS) is accurate and reliable to detect MPs isolated from human serum and plasma.^{12,13,17} Additionally, we reported that MP profiling for distinct MP populations that are associated with chronic liver diseases robustly discriminates between non-alcoholic fatty liver disease and chronic hepatitis C virus (HCV) infection,¹² thus providing a novel liquid biopsy tool based on serum analyses. Since almost every cell can release EVs upon stimuli, it is likely that tumour cells release EVs that reach the peripheral blood flow or other body fluids and that these particles might reveal the presence of a tumour.^{15,18} We took advantage of this hypothesis and showed that tumour-released MPs carry one, two or multiple tumour-associated antigens simultaneously and could indeed indicate the presence of tumours.¹⁷ Furthermore, we showed that EpCAM⁺ and CD147⁺ tumour-associated MPs (taMPs) accurately detected colorectal, non-small cell lung, and pancreatic cancers.¹⁷ Additionally, we reported that cell-derived taMP release was independent of a metastatic phenotype.¹⁷ Glypican1⁺ exosomes have been used for the detection of pancreatic and breast cancer, but have failed to discriminate between these two entities.¹⁹ Nevertheless, few publications are available showing the diagnostic potential of EVs for cancer detection by exploring surface antigens on EVs. Importantly, based on our multiplex surface staining strategy, we successfully differentiated hepatocellular carcinoma (HCC) and cholangiocarcinoma (CCA) from chronic diseases without liver tumours.

Material and methods

Cell culture

All tissue culture work was performed under sterile conditions in a laminar flow hood. Cells were invariably incubated at 37°C and 5% CO₂ in a CO₂ incubator. The culture medium used throughout all tissue culture work consisted of Roswell Park Memorial Institute (RPMI) 1640 medium (Gibco by Life Technologies, Paisley, UK) supplemented with 10% (v/v) fetal bovine serum (FBS, Gibco by Life Technologies, Paisley, UK) and 1% (v/v) penicillin-streptomycin (P/S; 10,000 U/ml, Gibco by Life Technologies, Paisley, UK) dissolved in phosphate buffered saline (PBS, Sigma Aldrich, Steinheim, Germany) containing 4 mM ethylenediaminetetraacetic acid (EDTA; Invitrogen by Life Technologies, Paisley, UK).

Human cancer cell lines

The human HCC cell lines HuH7 (CLS Cell Lines Service GmbH, Eppelheim, Germany, #300156) and HepG2 (CLS Cell Lines Service GmbH, Eppelheim, Germany, #300198) and the human hepatic adenocarcinoma cell line SK-HEP-1 (CLS Cell Lines Service GmbH, Eppelheim, Germany, #300334) were used as an *in vitro* liver cancer model for surface antigen validation. Additionally, the human pancreas ductal adenocarcinoma cell lines Panc-1 (CLS Cell Lines Service GmbH, Eppelheim, Germany, #300228) and the human pancreatic adenocarcinoma cell lines Capan-1 (CLS Cell Lines Service GmbH, Eppelheim, Germany, #300143) and Capan-2 (CLS Cell Lines Service GmbH, Eppelheim, Germany, #300144) were utilized as an *in vitro* negative control.

Surface staining of human cancer cell lines

For the surface staining of human cancer cells 10⁵ freshly harvested cells were used for each staining. After determining the cell count the corresponding volume of the cell suspension was transferred to a fresh 1.5 ml reaction tube and the cells were centrifuged at 300 g for 5 min at 4°C. The supernatant was discarded and the cells were resuspended in 50 µl Fc Block Mix containing 47.5 µl FACS buffer and 2.5 µl Fc Block (unfiltered) for each staining. Samples were then incubated for 5 min on ice. After the incubation, 50 µl of the Multi Antibody Mix 1 (EpCAM/CD147) or Multi Antibody Mix 2 (EpCAM/ASGPR1/CD133) containing 50 µl FACS buffer and 1 µl (pre-dilution necessary) of the corresponding antibodies according to Table S1 were added to each staining and the samples were incubated for 15 min on ice in the dark. After the incubation 400 µl of FACS buffer was added to each staining and the samples were centrifuged at 300 g for 5 min at 4°C. The supernatant was discarded and the cell pellet was resuspended in 400 µl FACS buffer. For FACS measurement 4 µl of 1:10 PI was added to each sample and 150 µl was measured using the MACSQuant[®] Analyzer 10.

Human study cohort

The Ethics Commissions of: (i) the State Chambers of Medicine in Rhineland-Palatinate; (ii) Saarland; (iii) San Sebastian, Spain; as well as (iv) Warsaw approved the current study (approval numbers: 837.151.13 (8836-F), 167/11, PI2014187, KB/41/A/2016 and AKB/145/2014, respectively) and patients gave their informed consent. Patients with a major second or third known comorbidity that could affect immune cell activation, such as acute inflammation, chronic inflammation, autoimmune diseases or viral infections besides HBV/HCV and liver cirrhosis, were excluded. Additionally, patients who underwent chemotherapy or were receiving chemotherapy or were subjected to any other anti-tumour therapy during the time blood samples were taken were excluded as well, except for patients who participated in the R0 resection study section. The characteristics of the patients are summarized in Tables S2 and S3.

Isolation of cell derived microparticles from human serum

Blood was collected in standard S-Monovette[®] 7.5 ml, Serum Gel with Clotting Activator (Sarstedt AG&Co., Nümbrecht, Germany) and left for 30 min at 37°C to allow for clot formation followed by centrifugation at 4,000 rpm for 20 min at 4°C. Clots were carefully separated and supernatants were stored at –80°C for further MP isolation. MPs from serum samples were isolated by differential centrifugation between 2,000 and 20,000 g as described by others and us.^{10,11,14} MPs sedimenting at 20,000 g were characterized by FACS using staining for the corresponding antibodies according to Table S4 referred to Multi Antibody Mix 1 or 2 (1: AnnexinV/EpCAM/CD147; 2: AnnexinV/EpCAM/ASGPR1/CD133). Multi Antibody Mix 2 was optimized for a better detection of liver tumours. All antibodies were titrated against the matching isotype control on patient's samples prior to use. MP preparations were characterized on a MACSQuant 10 Analyser (Miltenyi Biotec, Bergisch Gladbach, Germany) and FACS raw-data was analysed with FlowJo X software for MAC OSX (Tree Star, Inc., Ashland, Oregon). To avoid non-specific antibody binding, Fc receptors on MPs and target cells were blocked with FcR Blocking Reagent (eBioscience[™], San Diego, CA, USA) and 0.05% BSA. Used BSA blocking solution was centrifuged at 20,000 g prior to FACS to avoid artefacts due to aggregation.¹⁷ All solutions except antibody containing solutions were centrifuged or filtered (0.2 µm) prior to their use to remove contaminations such as possible protein aggregates or particles with similar size as larger EVs.



Research Article

Statistical analysis

All data are means with 95% CI. Differences between independent experimental groups were characterized using one-way analysis of variances (ANOVA). As a post-hoc test, Dunn's test was applied for multiple comparisons of subgroups when one-way ANOVA was positive and succeeded Bartlett's test for equal variance. A two-tailed Wilcoxon matched pairs signed rank test was applied to assess differences between patients who underwent a total R0 tumour resection between pre-operative (pre-OP) and post-operative (post-OP) serum samples.¹⁷ To assess the diagnostic ability of the indicated taMP populations and for discriminating between individuals with the indicated tumours, inguinal hernia, cirrhosis and controls, we calculated sensitivity, specificity, positive predictive values (PPV) and negative predictive values (NPV), and area under the receiver operating characteristic curve (AUROC) values. PPV and NPV were calculated according to the published algorithms of Altman and Bland.²⁰ These calculations were performed with Prism 5 (GraphPad Software, La Jolla, USA). Overall, $p < 0.05$ was considered significant. To determine an approximate need for sera, the total experimental strength (validation study) was calculated with the G*Power program (Heinrich-Heine-Universität Düsseldorf, version 3.1.9.2) for different effects (effect size f : 0.25, 0.45 and 0.65). In addition, an α error of 0.1 was assumed, which gives a total needed experimental strength of 312 samples with an assumed effect size of $f = 0.25$ and a test strength of 0.95 (1- β err prob).

For further details regarding the materials used, please refer to the [CTAT table](#).

Results

Explorative study: Patients with HCC or CCA are associated with elevated levels of AnnexinV⁺ EpCAM⁺ CD147⁺ double-positive taMPs

Firstly, we evaluated the presence of our previously published tumour-associated antigen combination^{17,21–25} on corresponding liver tumour cell lines *in vitro*. All indicated potential surface antigens for taMPs, *i.e.* EpCAM, CD147, CD133 and ASGPR1, showed medium to high expression on human tumour cell lines (HCC: HuH7;²⁶ hepatoblastoma: HepG2;²⁷ liver adenocarcinoma: SK-HEP-1²⁸) *in vitro* with EpCAM ranging from 95 to 99% of all living cells, except on SK-HEP-1 cells; with CD147 ranging from 82 to 85%, except on HuH7 cells; with CD133 ranging from 93 to 99%, except on SK-HEP-1 cells, and with ASGPR1 ranging from 91 to 99% (Fig. 1A). Importantly, ASGPR1 was not detectable ($< 1.5\%$, $p < 0.005$, Fig. 1B) on human pancreas ductal adenocarcinoma cell lines Panc-1²⁹ and Capan1/2,^{30,31} illustrating the importance of these antigens as possible cancer antigens and confirming ASGPR1 as a liver tumour restricted antigen. From these *in vitro* data we concluded that distinct cancer specific antigen combinations, as illustrated in Fig. 2, on donor tumour cells and their tumour cell derived MPs could specifically be associated with liver tumours.

To assess the diagnostic performance of AnnexinV⁺ EpCAM⁺ CD147⁺ taMPs in HCC and CCA, we isolated MPs by differential centrifugation of serum from patients with HCC and CCA (confirmed by MRI and histology) as published earlier.^{12,13,17} Healthy study participants served as negative controls. Mean AnnexinV⁺ EpCAM⁺ taMP values were significantly elevated (one-way ANOVA with Dunn's test) in patients with CCA ($n = 26$) by 3.5-fold ($p < 0.005$, Fig. 3A) and HCC ($n = 22$) by 2.6-fold ($p < 0.005$, Fig. 3A) as compared to healthy controls. Interestingly, AnnexinV⁺ EpCAM⁺ taMPs were also found elevated in inguinal hernia patients ($n = 18$) as compared to healthy controls by 1.8-fold ($p > 0.05$, one-way ANOVA with Dunn's test, Fig. 3A). Certain exclusions factors/underlying diseases such as inguinal hernia could be expected, since *struma nodosa* serum samples were previously shown to have elevated AnnexinV⁺ EpCAM⁺ taMPs levels

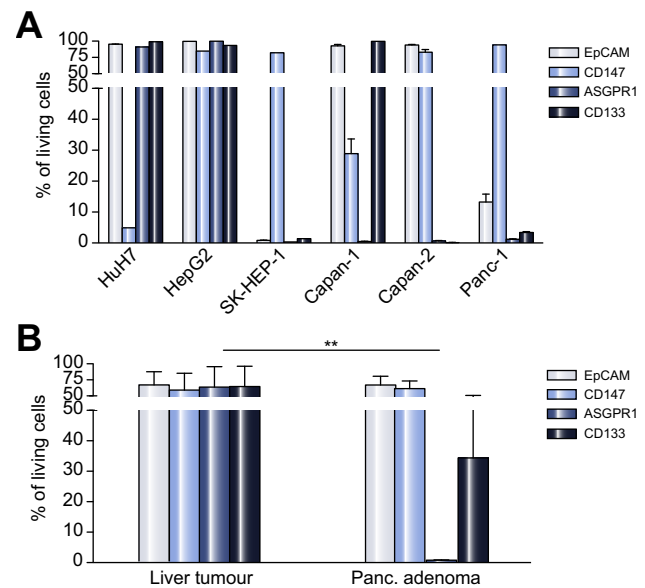


Fig. 1. Expression profiles of the surface antigens EpCAM, CD147, ASGPR1 and CD133 on human tumour cell lines. 16 to 24 h after serum starvation cells were harvested and fluorescently stained for their surface antigens, followed by FACS analysis. (A) Percentages of the antigen-bearing populations among living cells are depicted in each individual cell lines. (B) The summed marker expression present together in all three liver tumour cell lines (HuH7, HepG2 and SK-HEP-1) and the pancreatic adenoma cell lines (Capan-1, Capan-2 and Panc-1). A two-tailed Mann Whitney U test was performed to compare the antigen expressing cell populations ($*p < 0.05$, $**p < 0.005$, $***p < 0.0005$).

as well.¹⁷ The distribution of putative carcinoma-derived single positive taMPs (AnnexinV⁺ CD147⁺ EpCAM⁻) levels did not differ significantly in our study (Fig. 3B). Notwithstanding, the antigen combination of EpCAM and CD147 on taMPs successfully restored the tumour restricted detection: AnnexinV⁺ EpCAM⁺ CD147⁺ taMP values were significantly increased in liver tumour patients (HCC + CCA) by an average of 2.1-fold (Fig. 3C; Table S5) across both investigated liver tumour entities. A combination of these two antigens on taMPs seemed to efficiently separate tumour-bearing patients from healthy controls and inguinal hernia.

Explorative study: Diagnostic performance (AUROC) and predictive values of AnnexinV⁺ EpCAM⁺ CD147⁺ taMPs

Computing accompanied AUROC curves assessed the diagnostic performance (Fig. 3), sensitivity, specificity, PPV and NPV for each taMP population and investigated cancer entity. Table S5 summarizes the results, indicating that AnnexinV⁺ EpCAM⁺ taMPs were slightly superior in sensitivity and specificity. However, the accompanied PPV and NPV favoured AnnexinV⁺ EpCAM⁺ CD147⁺ taMPs over AnnexinV⁺ EpCAM⁺ taMPs (liver tumour PPV: 91% vs. 85% and NPV 45% vs. 55%). In spite of lower diagnostic performance, AnnexinV⁺ EpCAM⁺ taMPs, taken together with our previous results¹⁷ were reliable for the detection of HCC and CCA as well as NSCLC, PaCa, and CRC.

Explorative study: Correlations between AnnexinV⁺ EpCAM⁺ CD147⁺ taMPs and HCC/CCA tumour load

As previously reported,^{17,19} in general EVs and most likely certain taMP populations do not correlate with tumour load or diameter.

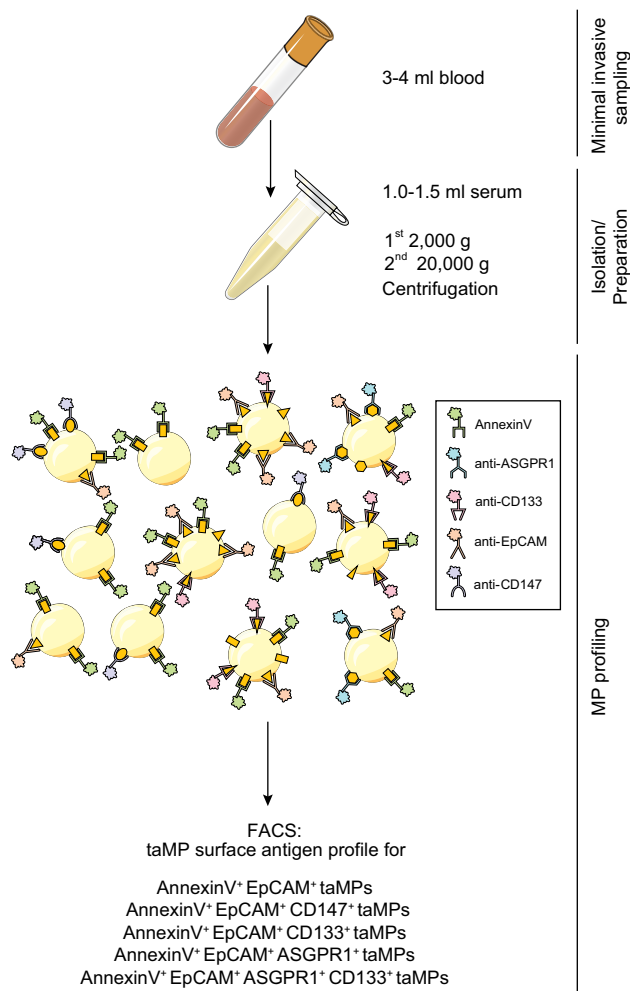


Fig. 2. taMP surface antigen profiling workflow. The schematic summary of the possible MP profiling workflow is depicted based on the availability of 1 ml serum. MPs will be enriched by sequential centrifugation as detailed in material and methods resulting in an ultrapure MP fraction. taMP profiling is performed by FACS analyses (fluorescence-activated cell scanning) for the indicated surface antigen combinations. Some of these combinations are present exclusively on taMPs associated with liver cancer (AnnexinV⁺ EpCAM⁺ CD133⁺ taMPs, AnnexinV⁺ EpCAM⁺ ASGPR1⁺ CD133⁺ taMPs) while some others are generally accompanying multiple cancer entities (AnnexinV⁺ EpCAM⁺ taMPs and AnnexinV⁺ EpCAM⁺ CD147⁺ taMPs). The most likely antigen combinations are depicted consisting of the indicated antigens e.g. CD133, ASGPR1 etc., plus AnnexinV, our general MP marker. MPs that are positive for all the listed antigen combinations will be evaluated by FACS. AnnexinV serves additionally as a general MP quantification marker.

Nevertheless, we plotted tumour volume (expressed in cm³) and diameter (in mm) against individual AnnexinV⁺ EpCAM⁺ taMP values to investigate a possible relationship. Correlations were considered ‘strong’ with a Pearson’s correlation coefficient (r) of 0.60 to 0.79, ‘moderate’ with a coefficient of 0.40 to 0.59 and ‘weak’ with a coefficient of 0.20 to 0.39.²⁰ Accordingly, Pearson analysis (two-tailed) revealed that AnnexinV⁺ EpCAM⁺ taMP values correlated ‘moderately’ with liver tumour diameter (r = 0.5144, p = 0.0290, Fig. 3D) but ‘weakly’ and non-significantly with tumour volume (r = 0.2913, p = 0.2263; data not shown).

The lower detection limit with respect to tumour size is key if taMPs are to be used as a reliable diagnostic tool. Here, the smallest detectable liver tumour by AnnexinV⁺ EpCAM⁺ taMPs was in the range of 10 and 20 mm (with exactly 11 mm) in diameter (p < 0.0005, Fig. 3E). By utilizing AnnexinV⁺ EpCAM⁺ CD147⁺ taMPs, the detection limit was set to a diameter of 17 mm. It has to be noted that due to the limitations of the currently applied methods for cancer diagnosis, there were no patients with smaller tumours available, so the lower detection limit for tumour diagnosis utilizing taMPs remains undetermined. Regarding the upper detection limit for tumour diagnosis, Annexin⁺ EpCAM⁺ as well as AnnexinV⁺ EpCAM⁺ CD147⁺ taMPs successfully detected all available tumours.

Notably, in both analyses of liver tumour entities no correlations (r < 0.3) were observed between AFP, CEA or CA19-9 concentrations and measured AnnexinV⁺ EpCAM⁺ taMPs or AnnexinV⁺ EpCAM⁺ CD147⁺ taMPs values (two-tailed Pearson’s correlation, data not shown).

Explorative study: AnnexinV⁺ EpCAM⁺ taMPs and AnnexinV⁺ EpCAM⁺ CD147⁺ taMPs levels decrease after surgical R0 resection

Consequently, in liver tumour patients with elevated AnnexinV⁺ EpCAM⁺ CD147⁺ taMPs pre-OP values above our calculated cut-off, we observed a significant decrease at day 7 post R0 resection (pre-OP blood was usually drawn the day before the resection, n = 18; day 7, post-OP day 7, n = 18; day 10, post-OP day 10, n = 5). In total, 12 out of 18 resected liver tumour patients with longitudinal blood collections showed a significant decrease from pre-OP 58.4 AnnexinV⁺ EpCAM⁺ CD147⁺ taMPs per 10³ AnnexinV⁺ MPs to 22.2 AnnexinV⁺ EpCAM⁺ CD147⁺ taMPs per 10³ AnnexinV⁺ MPs (Fig. 3F) at day 7 post R0 resection, including AnnexinV⁺ EpCAM⁺ CD147⁺ taMP values for the six patients without a decrease within the 7 day timeframe (p < 0.05, Wilcoxon matched pairs signed rank test, two-tailed). This corroborates with previous findings,¹⁷ and AnnexinV⁺ CD147⁺ EpCAM⁻ MPs did not drop after R0 resection at day 7 post-OP (p > 0.05) (data not shown).

Validation study – Step 1: taMPs based differentiation between liver disorders and other tumour entities

This retrospective study explored the possibility that certain taMP populations are characteristic for specific tumour entities. Our explorative study confirmed that EpCAM-based antigen combinations such as AnnexinV/EpCAM/CD147, detected on HCC and CCA-derived taMPs, could aid in the diagnosis of liver tumours. In our validation study, we markedly increased the cohort sizes. Confirming our explorative study results, we observed similar increased AnnexinV⁺ EpCAM⁺ taMP values for the indicated tumour entities, including HCC (n = 86), CCA (n = 38), CRC (n = 19) and NSCLC (n = 24) as well as in inguinal hernia (n = 26) and in chronic liver inflammation (stage cirrhosis, n = 49) compared to the healthy cohort (CTRL). In the liver disorders cohort, consisting of patients with cirrhosis without malignancy and HCC or CCA, AnnexinV⁺ EpCAM⁺ taMPs were in general significantly increased by 2.5-fold (p < 0.0005, one-way ANOVA with Dunn’s test, Fig. 4A), with specific increases in patients with HCC by 2.7-fold, CCA by 2.7-fold and cirrhosis by 1.8-fold (p < 0.005, p < 0.0005, respectively).

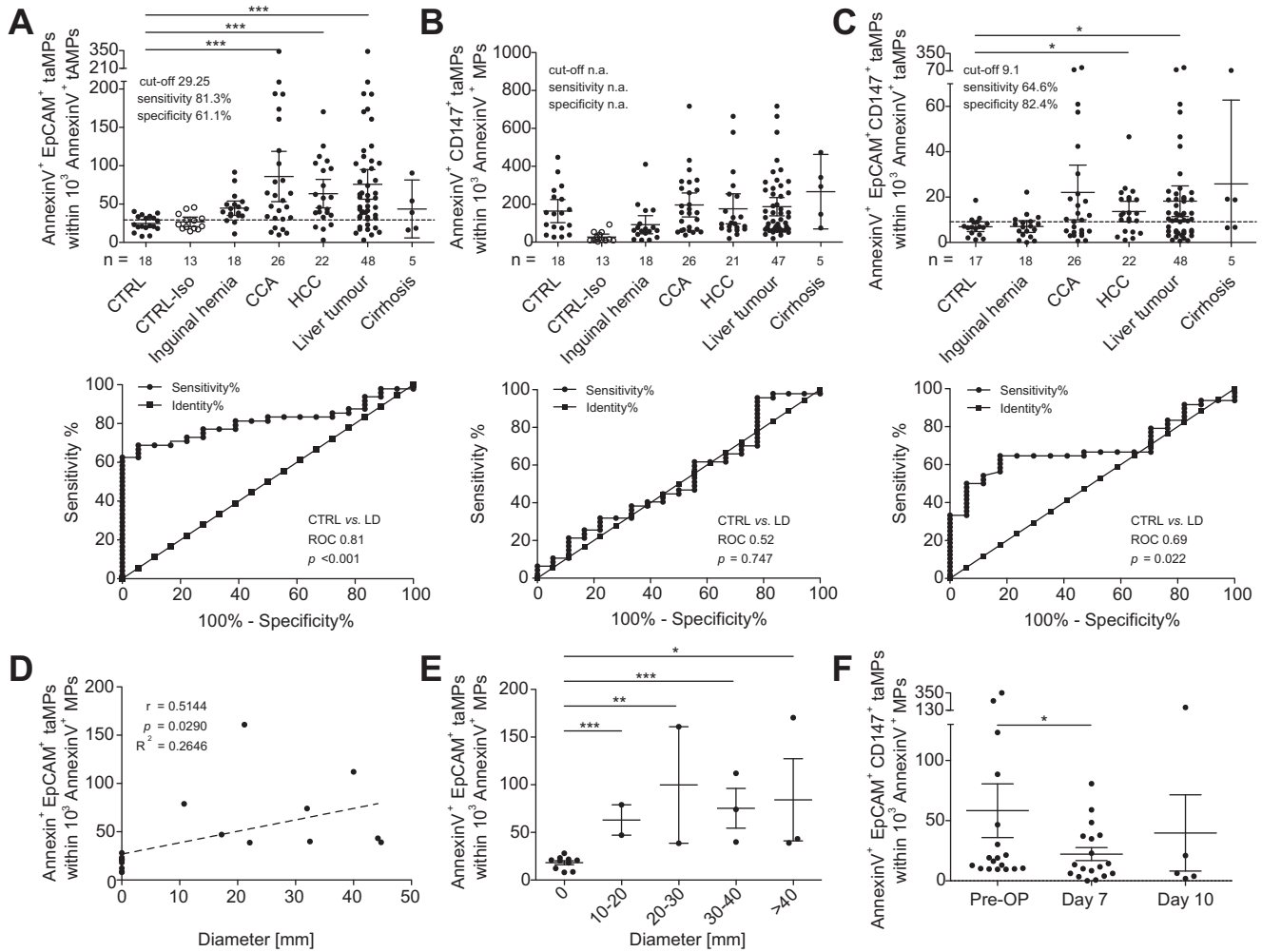


Fig. 3. EpCAM⁺ and EpCAM⁺ CD147⁺ taMPs from human serum can detect liver tumours. MPs were isolated and characterised by FACS from the sera of cancer patients bearing hepatocellular carcinoma (HCC) or cholangiocarcinoma (CCA). Healthy patients (CTRL), patients with inguinal hernia and patients with cirrhosis served as controls. Cohort ‘Liver Tumour’ combines both CCA and HCC patients. CTRL-Iso: associated CTRL sera samples incubated with the matched isotype control in exchange of the indicated antibody. (A–C) Visualises taMPs profile for each study cohort including EpCAM⁺ (A), CD147⁺ (B) and EpCAM⁺ CD147⁺ (C) taMPs populations given in mean with 95% CI. Dotted lines represent calculated cut-off values (see Table S5). Statistical significance was assessed by one-way analysis of variances (ANOVA) followed by a two-tailed unpaired *t* test. Corresponding ROC curve and AUROC value is displayed in order to analyse the diagnostic performances of the respective taMP population. Angle bisector represents line of identity that marks the lower limit for a successful diagnostic test. (D) Computed Pearson’s correlation (two-tailed) between EpCAM⁺ values and liver tumour (combined CCA and HCC) diameter given in mm. Only taMP values above the respective cut-off for liver tumours were included into the analysis and vice versa only values below the cut-off were considered for healthy controls. For each population the corresponding two-tailed Pearson’s correlation coefficient (*r*), *p* value (*p*) and coefficient of determination (*R*²) are displayed. (E) Depicted are EpCAM⁺ taMP levels separated into groups of increasing liver tumour diameter (two-tailed unpaired *t* tests). Only samples above the cut-off for liver tumours and vice versa for healthy controls were analysed. (F) Mean EpCAM⁺ CD147⁺ taMPs values of liver tumour patients before surgical R0 tumour resection (pre-OP) and day 7 and day 10 post-resection. Values above the cut-off for liver tumours and below the cut-off for healthy controls were included. Day 7 and 10 post-OP were compared to pre-OP values by a two-tailed Wilcoxon matched pairs signed rank test, resulting in significant *p* values (*p* < 0.05). (**p* < 0.05, ***p* < 0.005, ****p* < 0.0005.)

When the surface antigen combination was extended by CD133 (Fig. 4B) and AnnexinV⁺ EpCAM⁺ CD133⁺ taMP were assessed, we observed a liver disorder (cirrhosis without malignancy, HCC and CCA combined) restricted increase of AnnexinV⁺ EpCAM⁺ CD133⁺ taMPs by 2.6-fold (*p* < 0.005, one-way ANOVA with Dunn’s test), and individual increases for HCC by 2.6-fold, CCA by 3.3-fold, and cirrhosis by 2.3-fold (*p* < 0.05, *p* < 0.005, respectively). As mentioned earlier, no increased AnnexinV⁺ EpCAM⁺ CD133⁺ taMP values were noted in patients with CRC,

NSCLC and inguinal hernia as compared to CTRL. Whereas the accompanied levels of significance were not impressive for AnnexinV⁺ EpCAM⁺ CD133⁺ taMPs, the separation between CTRL and liver tumours and cirrhosis markedly increased when the staining was extended by ASGPR1. Overall, AnnexinV⁺ EpCAM⁺ CD133⁺ ASGPR1⁺ taMPs in liver disorders were increased by 3.1-fold (*p* < 0.0005, one-way ANOVA with Dunn’s test); individual increases were 3.1-fold for HCC, 3.7-fold for CCA, and 2.5-fold for cirrhosis (*p* < 0.0005, *p* < 0.0005, *p* < 0.05, respectively).

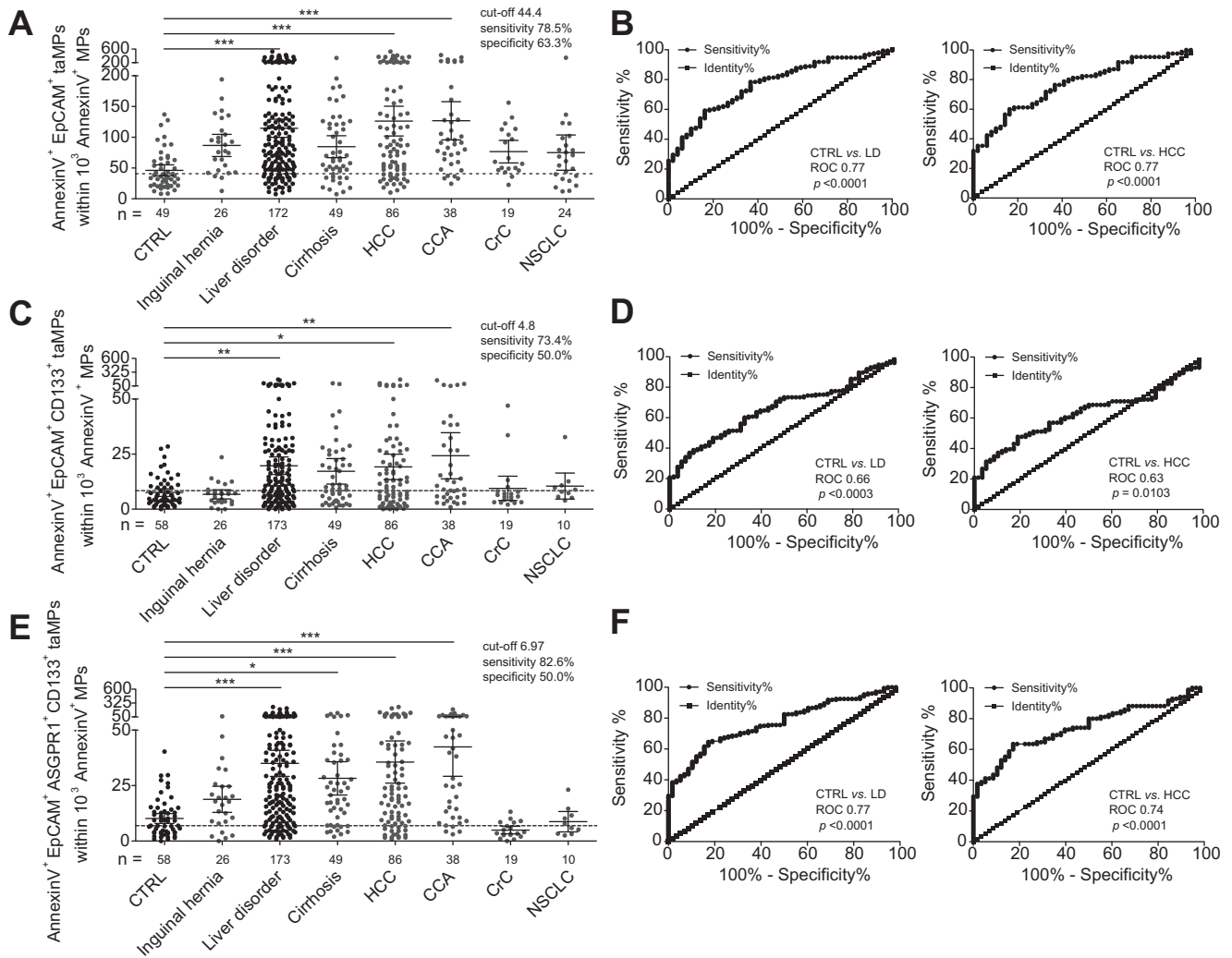


Fig. 4. By detecting EpCAM⁺ CD133⁺ and EpCAM⁺ ASGPR1⁺ CD133⁺ taMPs in human serum samples patients with indicated liver disorders can be discriminated from controls. MPs were isolated and characterised by FACS from the sera of cancer patients (HCC, CCA, CRC, NSCLC), controls (CTRL), patients with inguinal hernia and patients with cirrhosis. Cohort 'Liver Disorder' combines HCC, CCA and patients with cirrhosis. (A-C) Visualises the taMPs profile for each study cohort including EpCAM⁺ (A), EpCAM⁺ CD133⁺ (C) and EpCAM⁺ ASGPR1⁺ CD133⁺ (E) populations given in mean with 95% CI. Dotted lines represent cut-off values (see Table S6). Differences were assessed by one-way analysis of variances (ANOVA) including Dunn's test. For each population the corresponding ROC curve and AUROC value is displayed in (B), (D) and (F) in order to analyse the diagnostic performance of the respective taMP population. (**p* < 0.05, ***p* < 0.005, ****p* < 0.0005.)

Validation study: Diagnostic performance (AUROC), predictive values for liver disorder, liver tumour and liver tumour entity-specific taMPs

Analysing the accompanied AUROC assessing the diagnostic performance (Fig. 3), sensitivity, specificity, PPV and NPV clearly confirmed that the antigen combination AnnexinV/EpCAM/ASGPR1/CD133 found on AnnexinV⁺ EpCAM⁺ ASGPR1⁺ CD133⁺ taMPs was overall superior than AnnexinV⁺ EpCAM⁺ CD133⁺ taMPs regarding diagnostic performance as well as sensitivity and specificity (Table S6). However, both taMP populations are suitable to separate patients with the indicated liver disorders, i.e. cirrhosis, HCC and CCA, from other non-hepatic tumours and negative controls as healthy study subjects and patients presenting with inguinal hernia.

As previously published¹⁷ and again observed in this validation study, AnnexinV⁺ EpCAM⁺ taMPs were prone to exclusions

questioning their pan-cancer feasibility but were capable of detecting HCC and CCA. Additionally, consistent with previous observations,¹⁷ no dependence (*r* < 0.3) between measured taMP populations and AFP, CEA or CA19-9 concentrations were observed (data not shown), although the latter are widely used as serum tumour markers, even when not endorsed by clinical practice guidelines.⁶

Validation study – step 2: taMPs based differentiation between liver disorders and liver tumour entities

Since AnnexinV⁺ EpCAM⁺ CD133⁺ taMPs and AnnexinV⁺ EpCAM⁺ ASGPR1⁺ CD133⁺ taMPs could robustly separate patients suffering from liver disorders, liver cancer and cirrhosis from other tumour entities and healthy CTRL, we next evaluated if an antigen combination on taMPs could allow us to separate patients with liver disorders into liver tumour and non-liver tumour-

Research Article

bearing patients. Indeed, the antigen combination consisting of AnnexinV/EpCAM/ASGPR1 found on AnnexinV⁺ EpCAM⁺ ASGPR1⁺ taMPs was highly associated with liver tumours as compared to cirrhosis but did not allow a differentiation between HCC and CCA.

Nevertheless, AnnexinV⁺ EpCAM⁺ ASGPR1⁺ taMPs were significantly elevated by 3.0-fold in liver tumours ($p < 0.0005$, one-way ANOVA with Dunn's test, Fig. 5A), individually, HCC by 3.01-fold and CCA by 2.97-fold ($p < 0.005$, $p < 0.05$, respectively). The accompanied AUROC values were significant and indicated solid diagnostic performance (Fig. 5B; Table S6). Table S6 summarizes cut-offs, sensitivities, specificities, and NPVs and PPVs.

Validation study: Liver tumour-specific taMP levels decrease after surgical R0 resection and are dependent on liver tumour load

The surgical removal of the liver tumour load (R0 resection), which is associated with a drop of AnnexinV⁺ EpCAM⁺ ASGPR1⁺ taMPs at day 2 post-OP nicely underlined our finding of a useful antigen combination on these taMPs, separating patients with liver disorders into cirrhosis patients without a liver tumour and liver tumour patients with or without cirrhosis. In detail, mean pre-OP AnnexinV⁺ EpCAM⁺ ASGPR1⁺ taMP levels of 26.7 AnnexinV⁺ EpCAM⁺ ASGPR1⁺ taMPs per 10³ AnnexinV⁺ MPs dropped significantly at day 2 post-OP to 16.1 AnnexinV⁺ EpCAM⁺ ASGPR1⁺ taMPs per 10³ AnnexinV⁺ MPs ($p < 0.005$, two-tailed Wilcoxon matched pairs signed rank test, Fig. 5C) and remained low at day 10 post-OP at 7.7 AnnexinV⁺ EpCAM⁺ ASGPR1⁺ taMPs per 10³ AnnexinV⁺ MPs ($p < 0.05$). Even though a rebound at day 7 post-OP was observed in some patients, the overall day 7 post-

OP taMPs levels remained low at 13.1 AnnexinV⁺ EpCAM⁺ ASGPR1⁺ taMPs per 10³ AnnexinV⁺ MPs. Of note, resection serum series with pre-OP taMP values below the given cut-offs were excluded.

Validation study: Correlations between AnnexinV⁺ EpCAM⁺, AnnexinV⁺ EpCAM⁺ CD133⁺, AnnexinV⁺ EpCAM⁺ ASGPR1⁺ CD133⁺ and AnnexinV⁺ EpCAM+ASGPR1⁺ taMPs and HCC/CCA tumour load

Pearson analysis (two-tailed) revealed that AnnexinV⁺ EpCAM⁺ ASGPR1⁺ taMP values of the correctly identified liver tumour samples correlated 'moderately' with liver tumour diameters ($r = 0.56$, $p < 0.0001$, Fig. 6A), indicating a likely dependency between taMPs and tumour diameter. Additionally, we observed that AnnexinV⁺ EpCAM⁺ taMPs did perform slightly better and correlated 'moderately to strongly' with tumour diameter ($r = 0.60$, $p < 0.0001$, Fig. 6A) in line with our explorative study. No correlations were observed between AnnexinV⁺ EpCAM⁺ ASGPR1⁺ taMPs levels of liver tumour patients and AFP, CEA or CA19-9 ($r < 0.3$ or $p > 0.05$, data not shown). In particular, no significant correlation between AFP levels and tumour diameter ($r = 0.13$, $p = 0.4637$, Fig. 6C) was observed, confirming our finding that AnnexinV⁺ EpCAM⁺ ASGPR1⁺ taMP values can serve as a novel kind of liquid biopsy for tumour load.

In our validation study the smallest liver tumour detectable by taMPs was in the range of 10 to 30 mm (exactly 11 mm) in diameter (Fig. 6B). It's worth mentioning that the indicated taMP populations might be able to detect tumours even below 10 mm diameter. However, the statistical analysis for the two tumour samples in our cohort with diameters smaller than 10 mm was

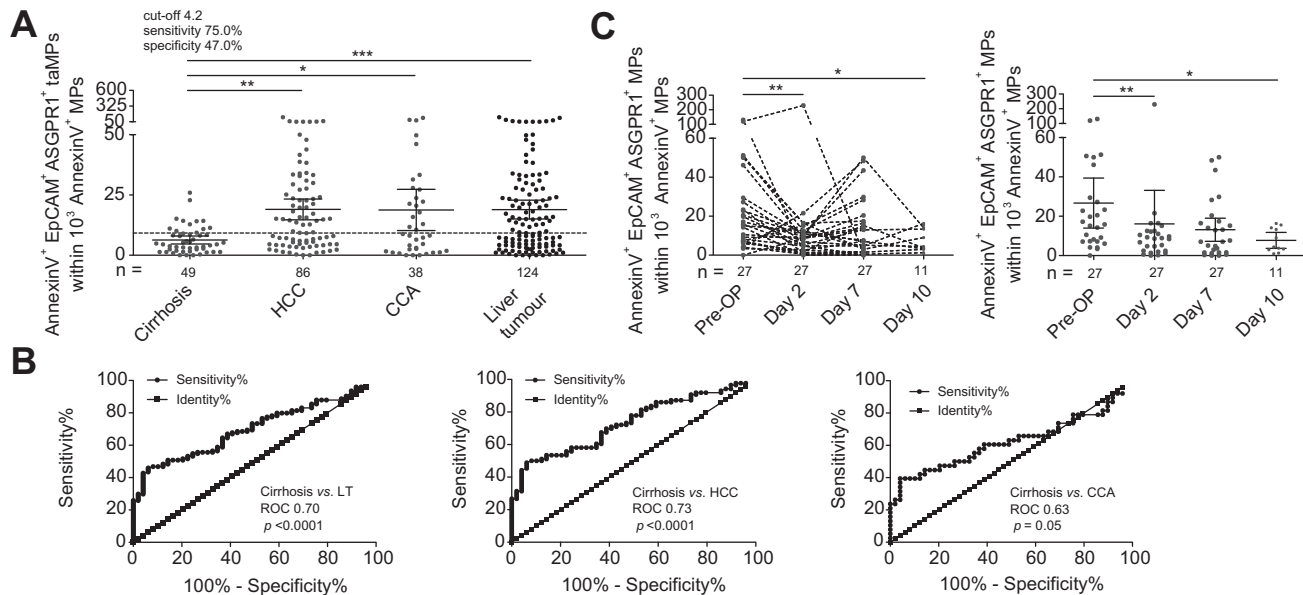


Fig. 5. EpCAM⁺ ASGPR1⁺ taMPs from human serum can separate patients with indicated liver tumours from patients with cirrhosis. MPs were isolated and characterized by FACS from the sera of cancer patients (CCA, HCC) and patients with cirrhosis. The cohort 'Liver Tumour' combines both HCC and CCA patients. (A) Visualises EpCAM⁺ ASGPR1⁺ taMP values for each study cohort given in mean with 95% CI. The dotted line represents the cut-off value for assessing the diagnostic accuracy of the population (see Table S6). Differences were assessed by one-way analysis of variances (ANOVA) including Dunn's test. For each population the corresponding ROC curve and AUROC value is displayed in (B) in order to analyse the diagnostic performance of the respective taMP population. (C) Progress of EpCAM⁺ ASGPR1⁺ taMP values of liver tumour patients before surgical R0 tumour resection (pre-OP) and day 2, day 7 and day 10 after the resection. Only pre-OP values above the respective cut-off (see Table S6) for liver tumours were included into the analysis. Right panel, mean with 95% CI values of each day are depicted. taMP levels for each post-OP day were compared to pre-OP values by applying a two-tailed Wilcoxon matched pairs signed rank test, resulting in significant p values. (* $p < 0.05$, ** $p < 0.005$, *** $p < 0.0005$.)

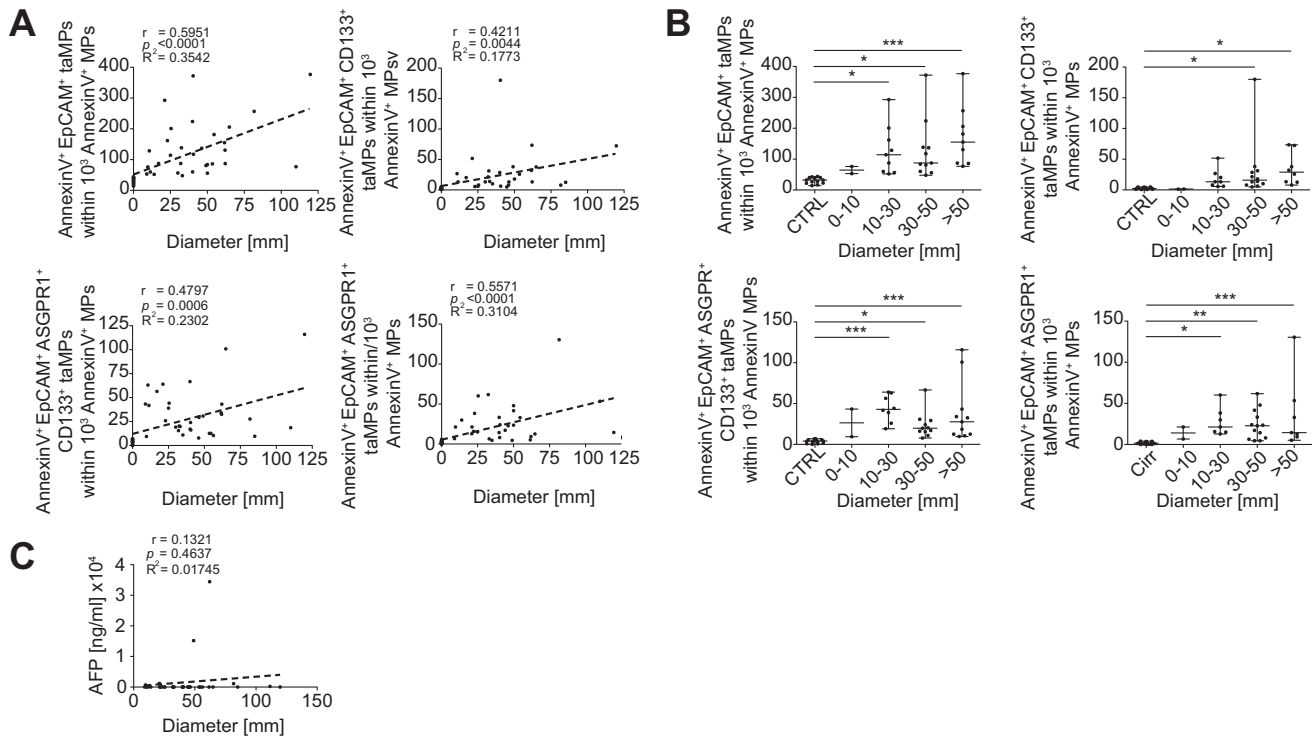


Fig. 6. taMPs from human serum correlate with tumour load and are capable of detecting small tumours. MPs were isolated and were analysed by FACS from the sera of liver cancer patients (CCA and HCC). (A) Pearson's correlations (two-tailed) between EpCAM⁺ taMP, EpCAM⁺ CD133⁺ taMP, EpCAM⁺ ASGPR1⁺ CD133⁺ taMP and EpCAM⁺ ASGPR1⁺ taMP values and liver tumour diameter [mm]. Only values above the cut-off (see Table S6) for liver tumours were included into the analysis and only values below the cut-off were considered for controls. For each population the corresponding Pearson's correlation (two-tailed) coefficient (r), p value (p) and coefficient of determination (R^2) are displayed. (B) taMP levels separated into groups of increasing liver tumour diameter for the populations shown in A. Differences were assessed by one-way analysis of variances (ANOVA) including Dunn's test. Analysis was restricted to samples with taMPs values above the cut-off for liver tumours. (C) It visualises the Pearson's correlation (two-tailed) between liver tumour diameter [mm] and corresponding AFP values [ng/ml] for each patient. For each population the corresponding Pearson's correlation coefficient (r), p value (p) and coefficient of determination (R^2) are displayed. (* $p < 0.05$, ** $p < 0.005$, *** $p < 0.0005$.)

not significant due to the low number of patients. However, we did not have access to more serum samples from patients with very small tumours.

Discussion

Here, we addressed the hypothesis that MP profiling can be extended to not only monitoring taMP subpopulations that are closely linked to cancer in general, such as AnnexinV⁺ EpCAM⁺ CD147⁺ taMPs, but to identify those that are associated specifically with liver tumours. Additionally, we asked to what extent taMP abundance correlates with liver tumour diameter/volume and with tumour resection (R0). Our work yielded a proposed strategy on how to detect a liver tumour, here HCC or CCA, in patients at risk. We conclude that our two step approach as outlined in Fig. 7 will; (i) confirm a liver disorder, e.g. cirrhosis and/or liver tumour; and (ii) detect liver tumour-specific taMP antigen combinations on HCC- and CCA-derived taMPs, allowing the separation between liver tumour-bearing vs. non-liver tumour-bearing patients. This approach is associated with a diagnostic performance consisting of AUROC values and PPV and NPV scores higher than 75%, indicating the potential for liver tumour detection. At the end of the last century scientists had tried to detect cancer traces in the periphery that might distinguish tumour-bearing patients from healthy individuals or other non-tumour-bearing controls. In 1998 an interesting study was published

utilizing PCR as a current state of the art technology.³² Circulating lung cancer cells were semi-quantitatively determined by taking the ratio of cytokeratin 19 vs. glyceraldehyde-3-phosphate dehydrogenase band intensity into account. The reported positive detection score was 40% for lung adenocarcinoma patients of all stages, 41% for squamous carcinoma patients of all stages, and 27% for small cell lung cancer patients.³²

Recent advances in antibody-based capturing methodologies in combination with molecular analysis such as quantitative PCR have allowed for the assessment of circulating tumour cell (CTC) derived from the primary tumour or from metastatic cells.³³ However, the major draw back has been the lack of truly reliable 'marker' genes, since the frequently used markers were also detectable on non-tumour cells and even tumour-related markers (for instance, AFP) were reported to be present in non-tumorous conditions without providing proof that tumour cells are reliably detectable.³³ Previously, we showed that profiling of cell-derived MPs isolated from the peripheral blood of patients with chronic liver diseases such as non-alcoholic steatohepatitis or chronic viral hepatitis in comparison to healthy controls can successfully be used not only to assess the health state of their liver, but eventually to monitor the extent of inflammation and the fibrosis stage.³⁴ Additionally, the possibility of utilizing large or small EVs for cancer surveillance has been explored but unsatisfactorily answered the question whether cancer entity-specific EV populations exist.^{17,19}

Cancer

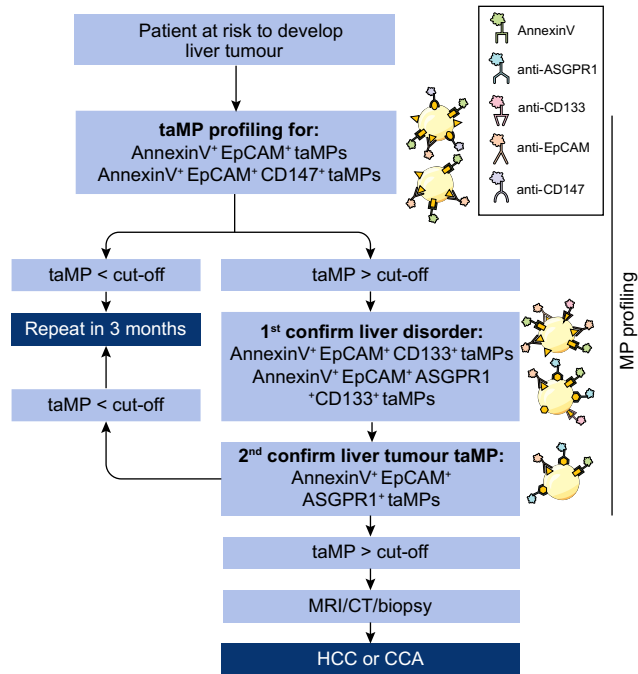


Fig. 7. Possible application as a diagnostic tool for detection of liver cancer. Overview of the application of the presented data is displayed as potential future detection guideline for non-invasive taMP liver cancer assessment in patients at risk to develop liver cancer. This approach will consist of a general screening for elevated AnnexinV⁺ EpCAM⁺ taMPs and AnnexinV⁺ EpCAM⁺ CD147⁺ taMPs indicating a liver disorder, here liver cancer or cirrhosis. Patients positively identified by elevated values above given cut-offs will follow a second step, where taMP screening will consist of a validation and a differentiation step. 1st – Validation of liver cancer or cirrhosis – using the screening for AnnexinV⁺ EpCAM⁺ CD133⁺ taMPs and AnnexinV⁺ EpCAM⁺ ASGPR1⁺ CD133⁺ taMPs. 2nd – Final discrimination between liver tumours and cirrhosis – here, the presence of AnnexinV⁺ EpCAM⁺ ASGPR1⁺ taMPs will be evaluated. Patients identified with liver cancer will undergo finally tumour assessment with MRI/CT/biopsy.

Current guidelines recommend non-invasive diagnosis of HCC.³⁵ Indeed, in most cases biopsy of the tumour is not necessary to establish the diagnosis. Given their non-invasive nature, liquid biopsy and analysis of taMPs perfectly fit to these recommendations. Our choice was based on membrane antigens that were previously successfully used¹⁷ in histopathological characterisation or FACS data, and were also supported by functional analyses for EpCAM,^{36,37} CD133,^{38,39} and ASGPR1.⁴⁰ Hence, we were confident that some combinations on taMPs might help to identify liver tumour-derived taMPs and separate them from other non-hepatic tumour entities. If the selected antigens were utilized individually, these surface antigens would not be able to distinguish between healthy controls and any type of tumour entity or tumour-derived taMP subpopulation.

Therefore, the unique combinations of these antigens on taMPs have the potential to be suitable for pinpointing the presence of a tumour or even an individual tumour entity *in vivo*. Our explorative study demonstrated that elevated numbers of blood-born AnnexinV⁺ EpCAM⁺ CD147⁺ taMPs bear a high potential to indicate the presence of tumour tissue *per se*, associated with useful PPV and NPV values. But the specific taMP surface antigen combination consisting of EpCAM, ASGPR1 and Annexin V, a general MP marker,^{2,13,34,41} became a powerful tool to identify

specifically liver tumour-derived taMPs and distinguishing them from other investigated tumour entities such as CRC and NSCLC.

A study applying EpCAM⁺ CTC-based methodology in a non-blinded HCC cohort with 123 patients demonstrated that 82 HCC patients showed elevated numbers of circulating EpCAM⁺ CTCs, yielding in a PPV of 66.66%.³⁶ It is noteworthy that our approach not only yielded higher PPV but also allowed the distinction between liver tumour-bearing vs. liver tumour-free samples in patients with cirrhosis and from other tumour entities. Additionally, current methods to detect CTCs have been discussed and raised the question whether few CTCs (usually less than 10 per ml) can reliably be detected in the peripheral blood of patients with liver cancer.²¹ In contrast, we have shown in our previous publications that even the smallest of MP subpopulations such as the one derived from invariant natural killer T (iNKT) cells and the AnnexinV⁺ EpCAM⁺ CD147⁺ MPs can be detected by FACS and be utilized to assess inflammation.³⁴

In terms of early tumour diagnosis it is of utmost importance to have knowledge about the lowest possible tumour size for detection to assess the usefulness of a novel tool as compared to other methods. Due to the lack of patients with tumours smaller than 11 mm, which represents the lower detection limit in this study, it was not possible to investigate the potential of the tool to identify even smaller tumours. This finding deserves special emphasis, since one of the major limitations in early liver cancer diagnosis is the inefficiency of the currently applied methods to reliably detect tumours below 20 mm of size (sensitivities below 50%).^{42,43} With this in mind, taMPs as an early tumour detection tool might only be limited by the stage of vascularization of the tumour, since this is a prerequisite for sufficient amounts of taMPs being present in the bloodstream. Vascularization usually occurs when the tumour exceeds a critical diameter (~2 mm).⁴⁴

In summary, we provide strong evidence that taMP screening and profiling (as proposed in Fig. 7) bears the potential not only to identify chronic liver diseases as previously published,³⁴ and acute liver failure,⁴¹ but also to trace liver tumours or even differentiate liver cirrhosis from liver tumours in patients with cirrhosis. Importantly, taMPs can potentially determine the tumour presence non-invasively, circumventing concerns in observer variability in cancer patients.^{45–47} We generated significant lines of evidence to foster our hypothesis that MP screening using the defined taMP populations could be used as a novel liquid biopsy tool to identify and discriminate liver tumours in patients with cirrhosis. Additionally, future work will focus on different sets of surface markers that can identify individual tumour entities that could lead to the development of a cancer entity-based taMP profile library in the future. Such library could provide a robust tool for non-invasive screening large cohorts.

Financial support

This work was supported by a Deutsche Krebshilfe grant (111184) to Miroslaw Kornek and by the Alexander von Humboldt Foundation, Sofja Kovalevskaja Award 2012 to Veronika Lukacs-Kornek.

Conflict of interest

No potential conflicts of interest were disclosed.

Please refer to the accompanying [ICMJE disclosure forms](#) for further details.

Authors' contributions

Conception and design: Veronika Lukacs-Kornek and Miroslaw Kornek.

Development of methodology: Henrike Julich-Haertel, Sabine Katharina Urban, Veronika Lukacs-Kornek and Miroslaw Kornek.

Acquisition of data (acquired and managed patients, provided facilities, etc.): Marcin Krawczyk, Arnulf Willms, Krzysztof Janowski, Waldemar Patkowski, Beata Kruk, Maciej Krasnodębski, Joanna Ligocka, Robert Schwab, Ines Richardsen, Angelina Klein, Sebastian Schaaf, Sebastian Gehlert, Markus Casper, Jesus M. Banales, Detlef Schuppan, Piotr Milkiewicz, Frank Lammert and Marek Krawczyk.

Analysis and interpretation of data (e.g., statistical analysis, biostatistics, computational analysis): Henrike Julich-Haertel, Sabine Katharina Urban, Marcin Krawczyk, Veronika Lukacs-Kornek and Miroslaw Kornek.

Writing, review, and/or revision of the manuscript: Henrike Julich-Haertel, Sabine Katharina Urban, Marcin Krawczyk, Hanna Sängler, Jesus M. Banales, Frank Lammert, Veronika Lukacs-Kornek and Miroslaw Kornek.

Study supervision: Veronika Lukacs-Kornek and Miroslaw Kornek.

Acknowledgements

The authors thank the leaders, patients and staff of the German Armed Forces Central Hospital for their continuous support and interest in our MP based cancer differentiation study.

Supplementary data

Supplementary data associated with this article can be found, in the online version, at <http://dx.doi.org/10.1016/j.jhep.2017.02.024>.

References

[1] Hirsova P, Ibrahim SH, Verma VK, Morton LA, Shah VH, LaRusso NF, et al. Extracellular vesicles in liver pathobiology: Small particles with big impact. *Hepatology* 2016;64:2219–2233.

[2] Kornek M, Schuppan D. Microparticles: Modulators and biomarkers of liver disease. *J Hepatol* 2012;57:1144–1146.

[3] Pan BT, Teng K, Wu C, Adam M, Johnstone RM. Electron microscopic evidence for externalization of the transferrin receptor in vesicular form in sheep reticulocytes. *J Cell Biol* 1985;101:942–948.

[4] Thery C, Ostrowski M, Segura E. Membrane vesicles as conveyors of immune responses. *Nat Rev Immunol* 2009;9:581–593.

[5] Hess C, Sadallah S, Hefti A, Landmann R, Schifferli JA. Ectosomes released by human neutrophils are specialized functional units. *J Immunol* 1999;163:4564–4573.

[6] Raposo G, Stoorvogel W. Extracellular vesicles: exosomes, microvesicles, and friends. *J Cell Biol* 2013;200:373–383.

[7] Becker A, Thakur BK, Weiss JM, Kim HS, Peinado H, Lyden D. Extracellular vesicles in cancer: cell-to-cell mediators of metastasis. *Cancer Cell* 2016;30:836–848.

[8] Wendler F, Favicchio R, Simon T, Alifrangis C, Stebbing J, Giamas G. Extracellular vesicles swarm the cancer microenvironment: from tumor-stroma communication to drug intervention. *Oncogene* 2016;36:877–884.

[9] Huber V, Fais S, Iero M, Lugini L, Canese P, Squarcina P, et al. Human colorectal cancer cells induce T-cell death through release of proapoptotic microvesicles: role in immune escape. *Gastroenterology* 2005;128:1796–1804.

[10] Costa-Silva B, Aiello NM, Ocean AJ, Singh S, Zhang H, Thakur BK, et al. Pancreatic cancer exosomes initiate pre-metastatic niche formation in the liver. *Nat Cell Biol* 2015;17:816–826.

[11] Dimuccio V, Ranghino A, Pratico Barbato L, Fop F, Biancone L, Camussi G, et al. Urinary CD133+ extracellular vesicles are decreased in kidney transplanted patients with slow graft function and vascular damage. *PLoS One* 2014;9:e104490.

[12] Kornek M, Lynch M, Mehta SH, Lai M, Exley M, Afdhal NH, et al. Circulating microparticles as disease-specific biomarkers of severity of inflammation in patients with hepatitis C or nonalcoholic steatohepatitis. *Gastroenterology* 2012;143:448–458.

[13] Kornek M, Popov Y, Libermann TA, Afdhal NH, Schuppan D. Human T cell microparticles circulate in blood of hepatitis patients and induce fibrolytic activation of hepatic stellate cells. *Hepatology* 2011;53:230–242.

[14] Masyuk AI, Huang BQ, Ward CJ, Gradilone SA, Banales JM, Masyuk TV, et al. Biliary exosomes influence cholangiocyte regulatory mechanisms and proliferation through interaction with primary cilia. *Am J Physiol Gastrointest Liver Physiol* 2010;299:G990–G999.

[15] Julich H, Willms A, Lukacs-Kornek V, Kornek M. Extracellular vesicle profiling and their use as potential disease specific biomarker. *Front Immunol* 2014;5:413.

[16] Tissota JD, Canellinia G, Rubina O, Angelillo-Scherer A, Delobela J, Prudenta M, et al. Blood microvesicles: From proteomics to physiology. *Translational Proteomics* 2013;1:38–52.

[17] Willms A, Muller C, Julich H, Klein N, Schwab R, Gusgen C, et al. Tumour-associated circulating microparticles: A novel liquid biopsy tool for screening and therapy monitoring of colorectal carcinoma and other epithelial neoplasia. *Oncotarget* 2016;7:30867–30875.

[18] D'Souza-Schorey C, Clancy JW. Tumor-derived microvesicles: shedding light on novel microenvironment modulators and prospective cancer biomarkers. *Genes Dev* 2012;26:1287–1299.

[19] Melo SA, Luecke LB, Kahlert C, Fernandez AF, Gammon ST, Kaye J, et al. Glypican-1 identifies cancer exosomes and detects early pancreatic cancer. *Nature* 2015;523:177–182.

[20] Altman DG, Bland JM. Diagnostic tests 2: Predictive values. *BMJ* 1994;309:102.

[21] Wu LJ, Pan YD, Pei XY, Chen H, Nguyen S, Kashyap A, et al. Capturing circulating tumor cells of hepatocellular carcinoma. *Cancer Lett* 2012;326:17–22.

[22] Shi B, Abrams M, Sepp-Lorenzino L. Expression of asialoglycoprotein receptor 1 in human hepatocellular carcinoma. *J Histochem Cytochem* 2013;61:901–909.

[23] Leung EL, Fiscus RR, Tung JW, Tin VP, Cheng LC, Sihoe AD, et al. Non-small cell lung cancer cells expressing CD44 are enriched for stem cell-like properties. *PLoS One* 2010;5:e14062.

[24] Cui F, Wang J, Chen D, Chen YJ. CD133 is a temporary marker of cancer stem cells in small cell lung cancer, but not in non-small cell lung cancer. *Oncol Rep* 2011;25:701–708.

[25] Sun YF, Xu Y, Yang XR, Guo W, Zhang X, Qiu SJ, et al. Circulating stem cell-like epithelial cell adhesion molecule-positive tumor cells indicate poor prognosis of hepatocellular carcinoma after curative resection. *Hepatology* 2013;57:1458–1468.

[26] Nakabayashi H, Taketa K, Miyano K, Yamane T, Sato J. Growth of human hepatoma cells lines with differentiated functions in chemically defined medium. *Cancer Res* 1982;42:3858–3863.

[27] Lopez-Terrada D, Cheung SW, Finegold MJ, Knowles BB. Hep G2 is a hepatoblastoma-derived cell line. *Hum Pathol* 2009;40:1512–1515.

[28] Heffelfinger SC, Hawkins HH, Barrish J, Taylor L, Darlington GJ. SK HEP-1: a human cell line of endothelial origin. *In Vitro Cell Dev Biol* 1992;28A:136–142.

[29] Lieber M, Mazzetta J, Nelson-Rees W, Kaplan M, Todaro G. Establishment of a continuous tumor-cell line (panc-1) from a human carcinoma of the exocrine pancreas. *Int J Cancer* 1975;15:741–747.

[30] Fogh J, Fogh JM, Orfeo T. One hundred and twenty-seven cultured human tumor cell lines producing tumors in nude mice. *J Natl Cancer Inst* 1977;59:221–226.

[31] Shiu MH, Cahan A, Fogh J, Fortner JG. Sensitivity of xenografts of human pancreatic adenocarcinoma in nude mice to heat and heat combined with chemotherapy. *Cancer Res* 1983;43:4014–4018.






[32] Peck K, Sher YP, Shih JY, Roffler SR, Wu CW, Yang PC. Detection and quantitation of circulating cancer cells in the peripheral blood of lung cancer patients. *Cancer Res* 1998;58:2761–2765.



Research Article

- [33] Paterlini-Brechot P, Benali NL. Circulating tumor cells (CTC) detection: clinical impact and future directions. *Cancer Lett* 2007;253:180–204.
- [34] Kornek T, Schafer I, Reusch M, Blome C, Herberger K, Beikert FC, et al. Routine skin cancer screening in Germany: four years of experience from the dermatologists' perspective. *Dermatology* 2012;225:289–293.
- [35] European Association for the Study of the Liver/European Organisation for Research and Treatment of Cancer. EASL-EORTC clinical practice guidelines: management of hepatocellular carcinoma. *J Hepatol* 2012;56:908–943.
- [36] Sun YF, Xu Y, Yang XR, Guo W, Zhang X, Qiu SJ, et al. Circulating stem cell-like EpCAM(+) tumor cells indicate poor prognosis of hepatocellular carcinoma after curative resection. *Hepatology* 2012;57:1458–1468.
- [37] Yoon SM, Gerasimidou D, Kuwahara R, Hytiroglou P, Yoo JE, Park YN, et al. Epithelial cell adhesion molecule (EpCAM) marks hepatocytes newly derived from stem/progenitor cells in humans. *Hepatology* 2011;53:964–973.
- [38] Hou Y, Zou Q, Ge R, Shen F, Wang Y. The critical role of CD133(+)/CD44(+/-high) tumor cells in hematogenous metastasis of liver cancers. *Cell Res* 2012;22:259–272.
- [39] Tang KH, Ma S, Lee TK, Chan YP, Kwan PS, Tong CM, et al. CD133(+) liver tumor-initiating cells promote tumor angiogenesis, growth, and self-renewal through neurotensin/interleukin-8/CXCL1 signaling. *Hepatology* 2012;55:807–820.
- [40] Zhao X, Yu Z, Dai W, Yao Z, Zhou W, Zhou W, et al. Construction and characterization of an anti-asialoglycoprotein receptor single-chain variable-fragment-targeted melittin. *Biotechnol Appl Biochem* 2011;58:405–411.
- [41] Schmelzle M, Splith K, Andersen LW, Kornek M, Schuppan D, Jones-Bamman C, et al. Increased plasma levels of microparticles expressing CD39 and CD133 in acute liver injury. *Transplantation* 2012;95:63–69.
- [42] Kim JE, Kim SH, Lee SJ, Rhim H. Hypervascular hepatocellular carcinoma 1 cm or smaller in patients with chronic liver disease: characterization with gadoteric acid-enhanced MRI that includes diffusion-weighted imaging. *AJR Am J Roentgenol* 2011;196:W758–W765.
- [43] Forner A, Vilana R, Ayuso C, Bianchi L, Sole M, Ayuso JR, et al. Diagnosis of hepatic nodules 20 mm or smaller in cirrhosis: Prospective validation of the noninvasive diagnostic criteria for hepatocellular carcinoma. *Hepatology* 2008;47:97–104.
- [44] McDougall SR, Anderson AR, Chaplain MA. Mathematical modelling of dynamic adaptive tumour-induced angiogenesis: clinical implications and therapeutic targeting strategies. *J Theor Biol* 2006;241:564–589.
- [45] Suzuki C, Torkzad MR, Jacobsson H, Astrom G, Sundin A, Hatschek T, et al. Interobserver and intraobserver variability in the response evaluation of cancer therapy according to RECIST and WHO-criteria. *Acta Oncol* 2010;49:509–514.
- [46] Ippolito D, Casiraghi AS, Talei Franzesi C, Bonaffini PA, Fior D, Sironi S. Intraobserver and interobserver agreement in the evaluation of tumor vascularization with computed tomography perfusion in cirrhotic patients with hepatocellular carcinoma. *J Comput Assist Tomogr* 2016;40:152–159.
- [47] Klein D, Jenett M, Gassel HJ, Sandstede J, Hahn D. Quantitative dynamic contrast-enhanced sonography of hepatic tumors. *Eur Radiol* 2004;14:1082–1091.

Synergistic effects of extracellular vesicle phenotyping and AFP in hepatobiliary cancer differentiation

Sabine K. Urban^{1,2} | Hanna Sanger^{2,3} | Marcin Krawczyk^{2,4} | Henrike Julich-Haertel² | Arnulf Willms⁵ | Joanna Ligocka⁶ | Mikel Azkargorta⁷ | Tudor Mocan⁸ | Christoph Kahlert⁹ | Beata Kruk⁴ | Krzysztof Jankowski¹⁰ | Waldemar Patkowski⁶ | Marek Krawczyk⁶ | Krzysztof Zieniewicz⁶ | Waclaw Hołowko⁶ | Łukasz Krupa¹¹ | Mateusz Rzucidło¹¹ | Krzysztof Gutkowski¹¹ | Wojciech Wystrychowski¹² | Robert Król¹² | Joanna Raszeja-Wyszomirska¹³ | Artur Słomka¹⁴ | Robert Schwab⁵ | Aliona Wöhler⁵ | Maria A. Gonzalez-Carmona¹ | Sebastian Gehlert¹⁵ | Zeno Sparchez⁸ | Jesus M. Banales¹⁶  | Christian P. Strassburg¹  | Frank Lammert²  | Piotr Milkiewicz^{13,17}  | Mirosław Kornek^{1,2} 

¹Department of Internal Medicine I, University Medical Center Bonn, Bonn, Germany

²Department of Medicine II, Saarland University Medical Center, Saarland University, Homburg, Germany

³Institute of Experimental Immunology, Rheinische Friedrich-Wilhelms-Universität, Bonn, Germany

⁴Laboratory of Metabolic Liver Diseases, Centre for Preclinical Research, Department of General, Transplant and Liver Surgery, Medical University of Warsaw, Warsaw, Poland

⁵Department of General, Visceral and Thoracic Surgery, German Armed Forces Central Hospital, Koblenz, Germany

⁶Department of General, Transplant and Liver Surgery, Medical University of Warsaw, Warsaw, Poland

⁷Proteomics Platform, Bizkaia Science and Technology Park, Derio, Spain

⁸Octavian Fodor Institute for Gastroenterology and Hepatology, Luliu Hațieganu University of Medicine and Pharmacy, Cluj-Napoca, Romania

⁹Department of Visceral, Thoracic and Vascular Surgery, University Hospital Carl Gustav Carus, Technische Universität Dresden, Germany

¹⁰Department of Internal Medicine and Cardiology, Medical University of Warsaw, Warsaw, Poland

¹¹Department of Gastroenterology and Hepatology with Internal Disease Unit, Specialist District Hospital in Rzeszow, Rzeszow, Poland

¹²Department of General, Vascular and Transplant Surgery, School of Medicine in Katowice, Medical University of Silesia, Katowice, Poland

¹³Liver and Internal Medicine Unit, Department of General, Transplant and Liver Surgery, Medical University of Warsaw, Warsaw, Poland

¹⁴Department of Pathophysiology, Nicolaus Copernicus University in Toruń, Ludwik Rydygier Collegium Medicum in Bydgoszcz, Poland

¹⁵Department for Biosciences of Sports, Institute of Sports Science, University of Hildesheim, Hildesheim, Germany

¹⁶Department of Liver and Gastrointestinal Diseases, Biodonostia Health Research Institute – Donostia University Hospital, University of the Basque Country (UPV/EHU), San Sebastian, Spain

¹⁷Translational Medicine Group, Pomeranian Medical University, Szczecin, Poland

Abbreviations: AnnV, Annexin V; AUC, area under the curve; CA 19-9, carbohydrate antigen 19-9; CCA, cholangiocarcinoma; CRC, colorectal carcinoma; ENS-CCA, European Network for the Study of Cholangiocarcinoma; EpCAM, epithelial cell adhesion molecule; ESMO, European Society for Medical Oncology; EVs, extracellular vesicles; FACS, fluorescence-activated cell scanning; FBS, fetal bovine serum; GbCA, gallbladder carcinoma; HCC, hepatocellular carcinoma; ISEV, International Society for Extracellular Vesicles; MISEV, minimal information for studies of extracellular vesicles; nm, nanometer; NPV, negative predictive value; NSCLC, non-small cell lung carcinoma; PPV, positive predictive value; QM, quality management; ROC, receiver operating characteristic; TICs, tumour-initializing cells.

Sabine K. Urban, Hanna Sanger, Marcin Krawczyk, Henrike Julich-Haertel and Arnulf Willms contributed equally (shared first-author).

This is an open access article under the terms of the Creative Commons Attribution-NonCommercial License, which permits use, distribution and reproduction in any medium, provided the original work is properly cited and is not used for commercial purposes.

© 2020 The Authors. *Liver International* published by John Wiley & Sons Ltd



Correspondence

Mirosław Kornek, Department of Internal Medicine I, University Medical Center Bonn, Venusberg-Campus 1, 53127 Bonn, Germany.
Email: miroslawkornek@web.de

Funding information

This work was funded by the Deutsche Forschungsgemeinschaft (DFG, German Research Foundation) to MK (project number 410853455). JMB was funded by the Spanish Carlos III Health Institute (ISCIII) [FIS PI15/01132, PI18/01075 and Miguel Servet Program CON14/00129 and CPII19/00008]] cofinanced by 'Fondo Europeo de Desarrollo Regional' (FEDER), 'Fundación Científica de la Asociación Española Contra el Cáncer' (AECC Scientific Foundation: 'Rare cancers grant 2017') and European Commission Horizon 2020 program (SEP-210503876; ESCALON project #825510).

Handling Editor: Isabelle Leclercq

Abstract

Background: Biliary cancer, comprising cholangio- and gallbladder carcinomas, is associated with high mortality due to asymptomatic disease onset and resulting late diagnosis. Currently, no robust diagnostic biomarker is clinically available. Therefore, we explored the feasibility of extracellular vesicles (EVs) as a liquid biopsy tool for biliary cancer screening and hepatobiliary cancer differentiation.

Methods: Serum EVs of biliary cancer, hepatocellular carcinoma, colorectal cancer and non-small cell lung cancer patients, as well as from healthy individuals, were isolated by sequential two-step centrifugation and presence of indicated EVs was evaluated by fluorescence activated cell sorting (FACS) analysis.

Results: Two directly tumour-related antigen combinations (AnnV⁺CD44v6⁺ and AnnV⁺CD44v6⁺CD133⁺) and two combinations related to progenitor cells from the tumour microenvironment (AnnV⁺CD133⁺gp38⁺ and AnnV⁺EpCAM⁺CD133⁺gp38⁺) were associated with good diagnostic performances that could potentially be used for clinical assessment of biliary cancer and differentiation from other cancer entities. With 91% sensitivity and 69% specificity AnnV⁺CD44v6⁺ EVs showed the most promising results for differentiating biliary cancers from HCC. Moreover using a combined approach of EV levels of the four populations with serum AFP values, we obtained a perfect separation of biliary cancer and HCC with sensitivity, specificity, positive and negative predictive value all reaching 100% respectively.

Conclusions: EV phenotyping, especially if combined with serum AFP, represents a minimally invasive, accurate liquid biopsy tool that could improve cancer screening and differential diagnosis of hepatobiliary malignancies.

KEYWORDS

biomarker, cholangiocarcinoma, diagnosis, extracellular vesicles, gallbladder cancer, hepatocellular carcinoma

1 | INTRODUCTION

Biliary tract cancers are considered rare diseases on a worldwide scale, yet incidence rates are rising. Gallbladder cancer (GbCA) and cholangiocellular carcinoma (CCA) are characterized by high mortality rates owing to the tumour's aggressiveness and lack of early diagnosing possibilities.^{1,2} Currently, no GbCA or CCA-specific serum, bile, urine or other non-invasive marker is available for reliable early detection, monitoring or screening.³ If diagnosed in time, surgical resection of the gallbladder and bile duct represents the only curative option.³ In most cases, GbCA and CCA progress asymptotically until a metastatic and inoperable stage is reached,⁴ resulting in 5-year survival rates of around 5% for GbCA and 20% for CCA.^{5,6} Despite multiple imaging techniques for staging of biliary tract malignancies, less than 10% of GbCA and only about 50% of CCA are resectable at the time of diagnosis.⁷

Recently, circulating extracellular vesicles (EVs) have been considered as a minimally invasive screening tool for early cancer diagnosis.⁸⁻¹¹ According to the MISEV2018 guidelines, circulating EVs can be classified into small EVs (sEVs), typically with a diameter

Keypoints

- No reliable diagnostic serum biomarkers for biliary cancer, that are fatal diseases with high mortality rates, are available.
- Extracellular vesicles could be a new clinically relevant serum biomarker for biliary cancer screening/diagnosis.
- Combination of extracellular vesicle levels and AFP values enhances the screening/diagnostic capacity for biliary cancer detection.

below 100 nm, and large EVs (lEVs) with typical diameters ranging between 100 and 1000 nm.¹² If not specified otherwise the term 'EVs' is subsequently used to describe large EVs throughout the manuscript. Essentially, the two types differ in size and mode of cellular release. Whereas small EVs are generated within the endomembranous system of the cell and reside within so-called multi-vesicular bodies before their release, large EVs are shed

directly from the plasma membrane of their parental cell.¹³ By isolating circulating EVs from peripheral blood and analysing them by fluorescence-activated cell scanning (FACS), it is possible to create disease-specific EV profiles. Tumour-associated EVs have been investigated in many forms of cancer, that is, glioblastoma and hepatocellular carcinoma (HCC).^{8,14} Therefore, EVs may be considered a novel type of minimally invasive liquid biopsy as highlighted recently by others and our group.^{8,11,15,16}

Considering the fatality of GbCA and CCA that is due to insufficient diagnostic measures, the need for novel early and accurate cancer diagnosis tools is omnipresent.^{16,17} By making use of circulating EV profiling, we aim to find surface antigen combinations for biliary cancer-derived EVs and for EVs associated with the tumour microenvironment that might aid in early diagnosis of GbCA and CCA.

2 | MATERIALS AND METHODS

2.1 | Mice

Animals were obtained from Charles River (Sulzfeld) and housed in pathogen-free conditions in an assigned mouse cabinet (Bioscape) at the Department of Medicine II at Saarland University. All experimental procedures were performed on male 7-9-week-old wildtype C57Bl/6 mice, fed with standard diet, with the approval of the ethics and animal care committee Homburg.

2.2 | Preparation of organ single cell suspensions and FACS measurement

Murine single cells were digested and stained for flow cytometry as described earlier.¹⁸ Briefly, mouse organs were removed, cut into pieces and enzymatically digested for 60-90 minutes at 37°C. After digestion, cells were collected and red blood cells were lysed in liver and lung using ACK lysis buffer (Life Technologies). Single cell suspensions were counted on a MACSQuant[®] Analyzer 10 (Miltenyi Biotec). For each staining, 3×10^5 (liver), 1×10^4 (gallbladder), 1×10^5 (colon) or 4×10^5 (lung) single living cells were incubated with antibodies against CD45 (103116, BioLegend), CD31 (102406, BioLegend), ASGPR1 (AF2755, R&D Systems), EpCAM (118225, BioLegend), CD133 (130-102-210, Miltenyi Biotec), gp38 (127410, BioLegend) and CD44 (130-102-904, Miltenyi Biotec). ASGPR1 was only included for liver, not for other organs. Liver cells were stained with a secondary antibody against goat IgG (A11055, Invitrogen). Detailed information about all applied antibodies can be found in Table S1. All cells were measured on a MACSQuant[®] Analyzer 10 (Miltenyi Biotec).

2.3 | Human study cohort

The Ethics commissions of (a) the State Chambers of Medicine in Rhineland-Palatinate, Germany approval number:

837.151.13 (8836-F)); (b) Saarland, Germany (167/11); (c) San Sebastian, Spain (PI2014187); (d) Warsaw, Poland (KB/41/A/2016 and AKB/145/2014) and (e) Cluj-Napoca, Romania (3042/07.03.2018) approved this study. All patients gave their informed consent.

Patients that received chemotherapy or were subjected to any other anti-tumour therapy during the time blood samples were taken were excluded. The characteristics of the patients are summarized in Table 1. GbCA patients who had undergone previous cholecystectomy were excluded from the current study.

2.4 | Isolation of extracellular vesicles and subsequent FACS analysis

Human blood samples were collected in Clotting Activator S-Monocuvettes (7.5 mL, Sarstedt) and were allowed to coagulate at RT for 30-60 minutes. Subsequently, samples were centrifuged for 20 minutes at 1500 g. Isolated serum was collected and stored at -80°C.

All large EV isolation and staining procedures were performed according to previously established and published protocols.^{8,19} Briefly, 1 mL patient serum was successively centrifuged at 2000 g and 20 000 g. Small EVs were isolated using the Total Exosome Isolation Reagent (Invitrogen by Thermo Fisher Scientific) following the manufacturer's specifications. Isolated EVs were incubated with Annexin V (AnnV)-FITC (130-093-060, Miltenyi Biotec) and were subsequently stained with antibodies against EpCAM (130-097-324), CD133 (130-107-453), gp38 (130-106-954) and CD44v6 (130-111-425, all Miltenyi Biotec). Detailed information about all applied antibodies can be found in Table S2. All samples were analysed using the MACSQuant Analyzer (Miltenyi Biotec). Cohort sizes within the progenitor cell- and tumour-associated cohorts were eventually not coherent due to flow cytometric measurement errors.

2.5 | LC-MS analysis

Details can be obtained from Supporting information.

2.6 | Human cancer cell lines

Information about the used cancer cell lines and details on staining protocols for FACS analysis can be obtained from Supporting information.

2.7 | Nanoparticle tracking analysis

Details can be obtained from Supporting information.

TABLE 1 Patient characteristics. Summary of demographic and biochemical parameters of patients with indicated diseases and healthy controls. Age, BMI, CEA, CA 19-9, ALT, AFP and bilirubin are given as mean; #: absolute number of patients in each cohort, S.D.: standard deviation, n.a.: not available

	Healthy CTRL	Cirrhosis	GbCA	CCA	HCC	NSCLC	CrC
Patients [#]	48	54	29	77	67	32	20
Female [#]	33	15	24	34	27	9	5
Male [#]	15	39	5	43	40	23	15
Age [y]	30.7	52.5	63.0	63.6	64.1	64.4	69.9
S.D.	12.3	9.5	11.1	9.9	12.3	9.6	13.8
Range	17-75	21-72	31-77	32-85	24-83	49-81	33-89
BMI [kg/m ²]	24.8	26.2	25.4	26.2	26.1	26.7	27.6
S.D.	5.0	4.8	4.3	3.9	3.9	4.4	5.7
range	18.8-38.3	20.0-38.6	18.6-36.3	18.7-37.5	18.9-42.5	20.2-44.5	20.2-44.5
CEA [ng/mL]	n.a.	3.3	14.5	7.3	3.0	3.6	4.9
S.D.		2.3	35.0	11.2	3.1	4.0	4.0
Range		0.8-8.1	0.8-177.0	0.3-50.4	0.5-18.8	0.4-13.6	0.4-13.5
CA 19-9 [U/mL]	n.a.	23.9	5,137	2,564	30.4	20.5	24.3
S.D.		27.3	9,633	11,945	54.5	11.8	29.4
Range		2.0-133.9	5.4-43,152	0.6-100,000	0.0-308.0	12.1-28.8	1.1-120.0
ALT [U/L]	n.a.	65.0	70.8	94.7	68.5	47.5	35.9
S.D.		54.4	81.8	122.0	63.0	116.7	36.6
Range		8.0-320.0	8.0-391.0	11.0-701.0	9.0-349.0	9.0-661.0	6.0-159.0
AFP [ng/mL]	n.a.	11.8	6.3	3.4	181.2	n.a.	n.a.
S.D.		42.7	11.6	2.3	216.9		
Range		0.8-293.4	1.6-60.3	0.9-16.3	1.8-820.4		
Bilirubin [mg/dL]	n.a.	4.5	6.9	16.3	3.8	0.5	1.1
S.D.		6.9	9.7	76.7	5.5	0.3	2.2
Range		0.6-33.7	0.2-31.4	0.2-644.0	0.0-23.9	0.2-1.4	0.1-10.0
T stage [%], 1/2/3/4	n.a.	n.a	10/17/69/4	31/36/19/14	54/25/14/7	n.a.	n.a.
N stage [%], 0/1/2	n.a.	n.a	28/65/7	63/37/0	95/5/0	n.a.	n.a.
M stage [%], 0/1	n.a.	n.a	55/45	67/33	57/43	n.a.	n.a.
Underlying cirrhosis [%]	n.a.	n.a	n.a	6	69	n.a	n.a

2.8 | Data processing and analysis

FACS data were analysed using FlowJo 10 for MAC OSX (Tree Star Inc). Statistical analysis was performed using GraphPad Prism 5 (GraphPad Software Inc). Figures were created using GraphPad Prism 5 and Adobe Illustrator (Adobe Systems Inc).

2.9 | Statistical analysis

All EV profiles depict the population median with interquartile range (IQR) and whiskers representing $1.5 \times$ IQR according to Tukey. Multiple cohorts (>2) were assessed by Kruskal-Wallis non-parametric tests followed by Dunn's multiple comparison post hoc tests. Each degree of freedom (*df*) is indicated in the corresponding figure legend. To assess the diagnostic benchmarks of EV populations, we calculated sensitivity, specificity, positive predictive values (PPV) and negative predictive values (NPV), and area

under ROC curve (AUC) values. Overall, $P < .05$ was considered significant. The total experimental strength was calculated with the G*Power program (Heinrich-Heine-Universität Düsseldorf, version 3.1.9.2) for different effects (effect size *f*: 0.25, 0.45 and 0.65). An α error of 0.05 was assumed. In detail, our validation study (Figure 3A,C) were associated with a test strength of >0.98 ($1-\beta$ err prob) ($f = 0.25$, 3 *df*) each and (Figure 3E,G) with 0.85 ($1-\beta$ err prob) ($f = 0.25$, 3 *df*) each respectively.

3 | RESULTS

3.1 | Selecting potential biomarkers for biliary cancer diagnosis

As published by us 2017 in the *Journal of Hepatology*, where we provide several useful large EV surface antigen combinations allowing us to differentiate liver tumour entities from other non-hepatic

malignancies,⁸ now we had aimed to distinguish hepatobiliary cancer entities from each other, in particular biliary cancers (CCA and GbCA) from HCC. As a starting point we used our published hepatobiliary EV antigen combination consisting of AnnV, CD133 (Prominin-1), CD326 (EpCAM) but minus ASGPR1. Furthermore, we added CD44v6 to the combination, acknowledging several reports that had indicated that CCA might be associated with CD44v6 expression.²⁰ Besides quantifying EVs derived directly from biliary cancer cells, we addressed the question if EVs shed from podoplanin⁺ (gp38) liver progenitor cells, as published by us, could indirectly indicate biliary cancer presence.²¹

Podoplanin (gp38) and Prominin-1 (CD133) are both transmembrane glycoproteins that are typically expressed on progenitor cells in the liver tumour microenvironment, whereas CD44 variant 6 (CD44v6) and epithelial cell adhesion molecule (EpCAM, CD326) are both transmembrane cell adhesion proteins that can be found on the surface of various carcinomas.

First, we compared *in vitro* expression levels of the selected markers EpCAM, CD44v6, CD133 and gp38 by FACS on CCA tumour cell lines (TFK-1, EGI-1 and CCC-5) and HCC tumour cell lines (HuH7, HepG2 and Hep3B), addressing the question if our selection of surface EV antigens could separate CCA from HCC at the cellular level (Figure 1A,B). Unfortunately, to our knowledge no GbCA cell line is commercially available. Gating strategy, performance of antibodies and their corresponding isotype controls are depicted in Figure S2. The expression profiles of the three tumour cell lines within each cohort (HCC or CCA) were similar, with EpCAM being universally present on all investigated tumour cell lines in relatively high levels (Figure 1A). Gp38 could not be detected on any tumour cell line, which is in agreement with available data since it is rather expressed on cancer stem cells and several types of squamous cell carcinomas, malignant mesothelioma and brain tumours.^{22,23} So far no expression of gp38 was reported on HCC cell lines.²⁴ With exception of the CCA tumour cell line EGI-1, high CD133 expression was almost exclusively limited to HCC cell lines. CD133 was significantly ($P \leq .001$) higher expressed by 6.6-fold in HCC than CCA cell lines (HCC: mean of $92\% \pm 3.625$ SEM and CCA: mean of $14\% \pm 6.665$ SEM). On the contrary, all three CCA cell lines expressed CD44v6 in high levels, CD44v6 expression was significantly ($P \leq .001$) elevated in CCA cell lines by 58.5-fold (HCC: mean of $1.3\% \pm 0.223$ SEM and CCA: mean of $76\% \pm 5.117$ SEM, respectively), whereas no expression on HCC cell lines could be detected arguing strongly for being a suitable biliary cancer antigen that could be very likely utilized in our EV biliary cancer related surface antigen combination. Even though EpCAM was highly expressed on all cell lines, the cohort comparison revealed a significantly ($P \leq .001$) lower EpCAM expression on CCA cell lines, with a mean of $99\% \pm 0.389$ SEM and a mean of $96\% \pm 0.542$ SEM on HCC and CCA cells respectively (Figure 1B).

Our *in vitro* tumor cell line data was supported by already published data that was upon our request analysed for EpCAM, CD133 and CD44 in EVs extracted from CCA tumour cell lines (TFK-1 and EGI-1, each $n = 3$), additionally complemented by EVs derived from

human primary cholangiocytes (NHC; $n = 3$) and analysed by liquid chromatography–mass spectrometry.¹⁰ Corresponding statistics are provided in Table S3. In detail, EpCAM was detected in EVs derived from tumour cell lines and primary cholangiocytes, but was shown to be significantly ($P \leq .01$) more abundant in CCA-derived EVs than in non-malignant primary cell EVs. CD133 was particularly enriched in EVs derived from EGI-1 cells, whereas CD44 was predominantly restricted to TFK-1-derived EVs. Importantly, CD133 and CD44 were less abundant in EVs derived from non-malignant primary cholangiocytes. Unfortunately, it was not possible to analyse any CD44 variants retrospectively.

3.2 | Identifying possible parental cell populations expressing the candidate markers

After verifying the presence and differential expression of our candidate markers on malignant cells *in vitro*, we aimed to identify possible physiological donor cell populations *in vivo* that express one or more of the markers simultaneously on their surface and could thus be a source for circulating EVs presenting the respective markers. For FACS analysis, wild type C57Bl/6J mouse organs were enzymatically digested to single cell suspensions and subsequently stained with a panel of antibodies (CD45, CD31, ASGPR1 (liver only), CD133, gp38, EpCAM and CD44). Corresponding isotype performances are depicted in Figure S3. The general gating strategy applied to all organs is exemplarily summarized in Figure 1C. In short, after excluding cellular debris, cell clusters, dead cells (PI), nucleated hematopoietic cells (CD45⁺), endothelial cells (CD31⁺) and hepatocytes (ASGPR1⁺, liver only), mesothelial cells were additionally excluded based on their high gp38 expression profile. Double positive CD133⁺gp38⁺ progenitor cells were detected in every organ except for the colon (Figure 1D, upper panel). Additionally, triple positive CD133⁺gp38⁺EpCAM⁺ cells could be found to various degrees in all organs except for the colon (Figure 1D, lower panel). CD44 could clearly be detected in colon but was weakly expressed in liver, gallbladder and lung (Figure 1E, upper panel). Accordingly, double positive CD44⁺CD133⁺ cells were rare in all mouse organs with a slightly increased abundance in murine gallbladder cells (Figure 1E, lower panel). In sum, our marker selection comprising the combinations CD133⁺gp38⁺, CD133⁺gp38⁺EpCAM⁺, CD44⁺ and CD44⁺CD133⁺ were found to be expressed under steady state conditions in wild type mice.

3.3 | Quality management (QM) for FACS analysis of EVs

We thoroughly tested the quality of every reagent used for EV analysis and could not detect any accountable contamination (Figure S4A). In agreement with the guidelines provided by the International Society for Extracellular Vesicles (ISEV),²⁵ typically, fractions of large EVs isolated by centrifugation result in cross-contaminations

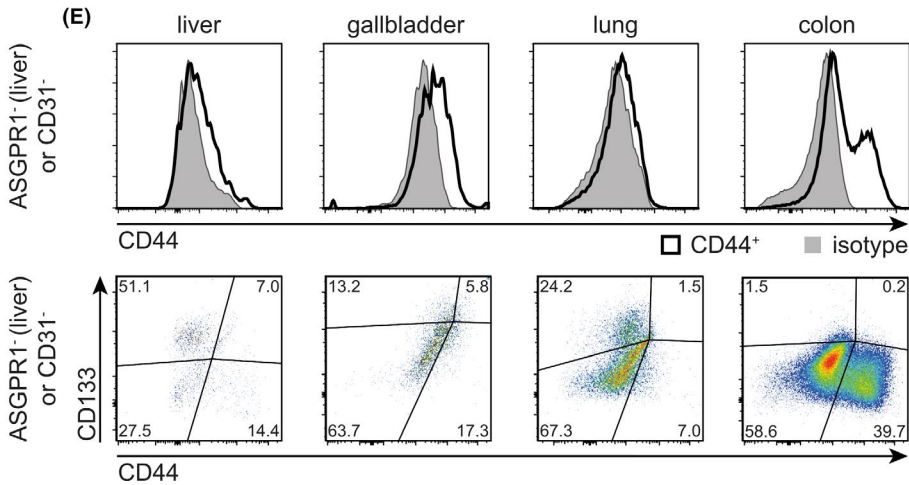
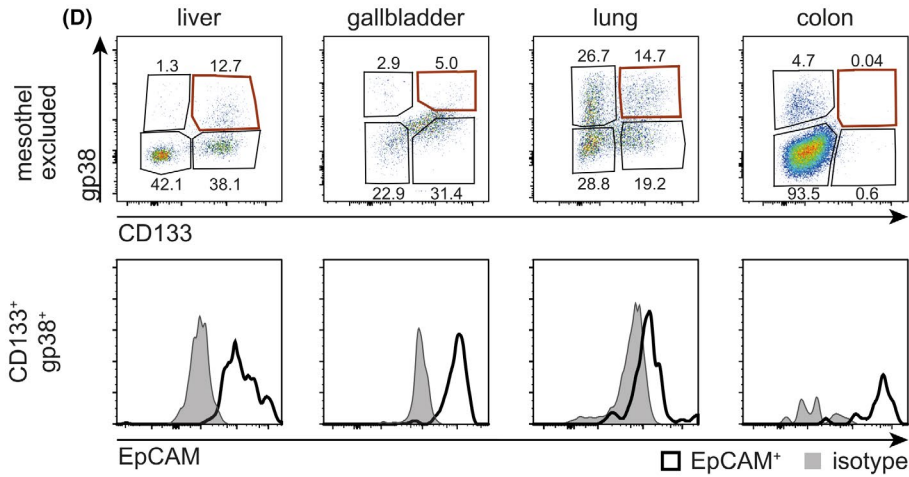
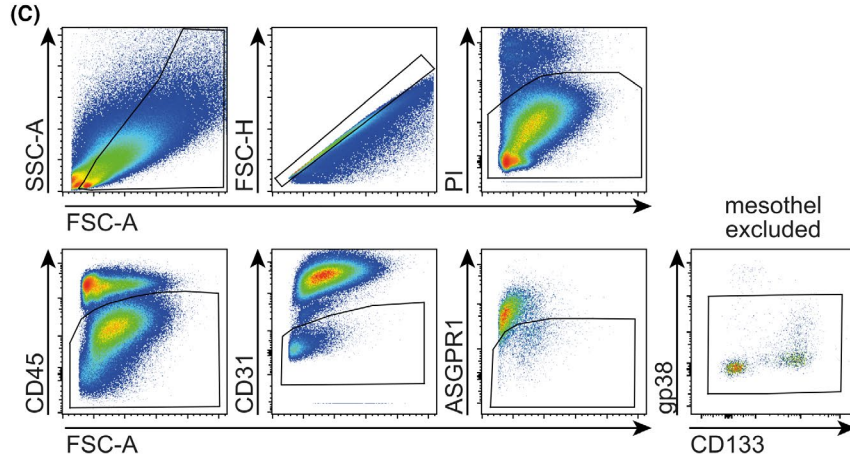
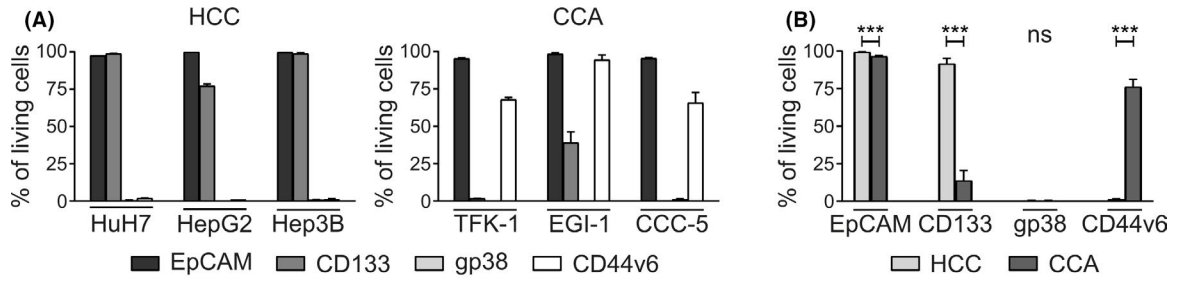


FIGURE 1 EpCAM, CD133, gp38 and CD44v6 are potential biomarkers for biliary cancer detection. Surface expression of the marker selection among living cells on CCA (TFK-1, EGI-1 and CCC-5, each $n = 3$) and HCC (HuH7, HepG2 and Hep3B, each $n = 3$) cell lines was analyzed by FACS. Graphs show means (percentage of living cells) with SEM of all HCC and CCA cell lines individually (A) and of CCA and HCC cell lines combined (B, each $n = 9$). For statistics a two-tailed Mann-Whitney U test was performed with $P \leq .05$ considered statistically significant ($* = P \leq .05$, $** = P \leq .01$). Corresponding gating strategy and isotype controls are provided in Figure S2. C-E, Single cell suspensions were prepared from wild type C57Bl/6J liver, gallbladder, lung and colon. Cells were stained with a panel of surface markers: CD45, CD31, ASGPR1 (liver only), gp38, CD133, EpCAM and CD44. Propidium iodide was used for dead cell exclusion. Corresponding gating strategy and isotype controls are provided in Figure S3. All depicted dot plots and histograms are representative of three independent experiments. C, Representative dot plots of the general gating strategy for all organs are exemplarily depicted for murine liver. ASGPR1 was only included for liver, not for other organs. D, CD133⁺gp38⁺ populations are depicted in the upper panel. Numbers indicate percent of parent population (mesothel excluded). Double positive cells were additionally tested for EpCAM positivity (white) as compared to corresponding isotype controls (grey) in the lower panel. E, Histograms of CD44⁺ cells (white) as compared to isotype (grey) are depicted in the upper panel. The lower panel represents dot plots of double positive CD44⁺CD133⁺ cells. Numbers indicate percent of parent population (ASGPR1⁺ for liver or CD31⁺ for other organs). A, area; FSC, forward scatter; H, height; SSC, sideward scatter

with small EVs and vice versa.²⁶ Complying with our QM, we tested the sensitivity of our FACS analysis assessing the numeric effect of a given small EV cross-contamination on our FACS-based large EV phenotypic analysis. In short, staining and FACS measurement parameters including gating strategy as utilized for large EV analysis (see Figure S5A) were applied to serum small EVs (Figure S4B). They were counted and confirmed in size by nanoparticle tracking analysis (NTA) prior to FACS, revealing a median diameter of 87.4 nm (D50), ranging from 35.7 (D10) to 139.8 nm (D90) (Figure S4C). The FACS sensitivity was set and confirmed by an initial number of employed small EVs for FACS measurement of 1.175×10^9 , from which only a total of 130 events were positive for AnnV, an established EV marker, ruling out any substantial influence of small EV cross-contaminations on large EV quantification in this explicit experimental setting (Figure S4B). Large EVs that were employed to conduct the following diagnostic experiments were confirmed in size by NTA and revealed a median diameter of 209.0 nm (D50), ranging from 153.8 (D10) to 323.9 nm (D90) (Figure S4D). Note: small EVs were only used for QM. The whole study is based on large EVs. Thus, if not specified otherwise the term 'EVs' is subsequently used to describe large EVs throughout the manuscript.

3.4 | Explorative study – EVs discriminate biliary cancer from healthy controls

With our selection of surface antigens proven present in vivo, we aimed to confirm their pertinence in a pathophysiologically relevant setting. Serum EVs were isolated from 10 patients with biliary cancer (5 CCA and 5 GbCA) and from 10 healthy controls by differential centrifugation and stained using antibodies against CD133, gp38, EpCAM and CD44v6. All stainings included AnnV, a common EV marker. Stained samples were subsequently analysed by flow cytometry (FACS) using the gating strategy described in Figure S5A. For every combination of surface markers, the gates for each antibody were applied successively (Figure S5B,C). Importantly, all antibodies were titrated against their matching isotype prior use (Figure S5D). Statistical analysis by two-tailed Mann-Whitney U tests revealed that EVs from patients with biliary cancer were significantly elevated

as compared to healthy controls in all four investigated EV populations (Figure 2A-D). In detail, AnnV⁺CD133⁺gp38⁺ EV levels of biliary cancer patients showed a 7.1-fold increase as compared to healthy donors ($P \leq .01$; biliary CA: median 20.9, healthy CTRL: median 3.0) (Figure 2A). AnnV⁺EpCAM⁺CD133⁺gp38⁺ EV levels of biliary cancer patients were 5.7-fold increased compared to healthy controls ($P \leq .001$; biliary CA: median 13.6, healthy CTRL: median 2.4) (Figure 2B). AnnV⁺CD44v6⁺ EV levels of biliary cancer patients showed a 2.5-fold elevation as compared to healthy donors ($P \leq .05$; biliary CA: median 93.4, healthy CTRL: median 37.7) (Figure 2C) and AnnV⁺CD44v6⁺CD133⁺ EV levels of biliary cancer patients were 2.3-fold elevated compared to healthy controls ($P \leq .01$; biliary CA: median 28.4, healthy CTRL: median 12.3) (Figure 2D).

3.5 | Validation study – progenitor cell-associated and tumour-associated EVs for biliary cancer diagnosis

Based on the results of our explorative study we next evaluated EV levels of the four surface antigen combinations on EVs in a large validation study, additionally including several cancer cohorts as negative control, that is, hepatocellular carcinoma (HCC), colorectal carcinoma (CRC) and non-small cell lung carcinoma (NSCLC) and patients with cirrhosis. Patient characteristics can be obtained from Table 1. Sample preparation of patient serum and analysis of EV surface antigens were performed as described in the explorative study. EV levels of the individual cohorts can be obtained from Figure S6. The group analysis between healthy donors, patients with cirrhosis, biliary cancer (GbCA and CCA), HCC and non-biliary cancer (HCC, CRC and NSCLC) entities revealed that EV levels were significantly elevated in biliary cancers as compared to every control group in all four EV populations (Figure 3A,C,E,G). In detail, AnnV⁺CD133⁺gp38⁺ EV levels of biliary cancer patients were 3.0-fold increased compared to healthy controls ($P \leq .01$; biliary CA: median 24.3, healthy CTRL: median 8.2), 3.2-fold increased compared to HCC subjects ($P \leq .001$; HCC: median 7.7) and 3.6-fold increased compared to non-biliary cancer patients ($P \leq .001$; non-biliary CA: median 6.7) (Figure 3A). AnnV⁺EpCAM⁺CD133⁺gp38⁺ EV levels of biliary cancer

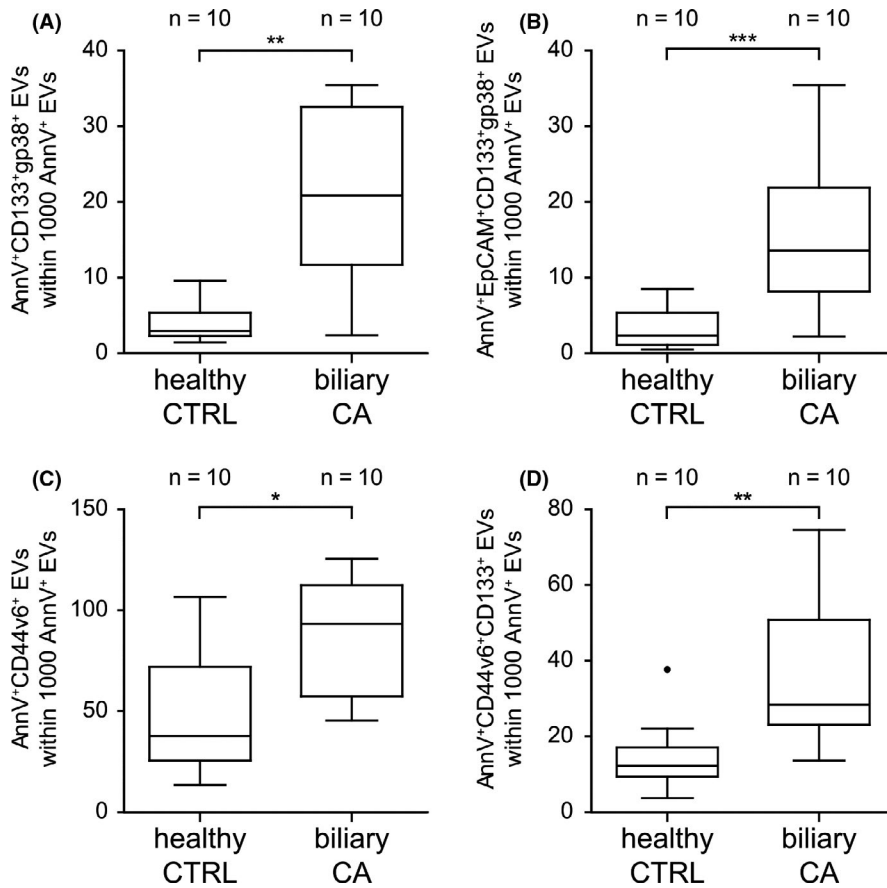
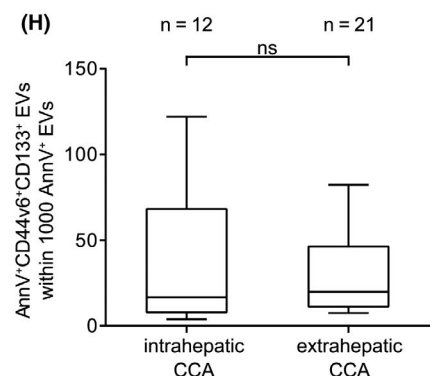
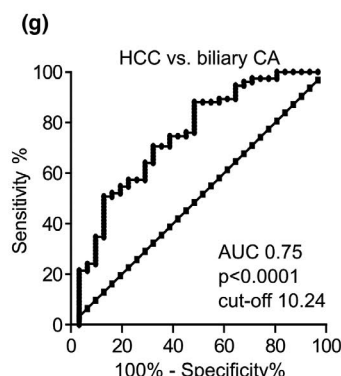
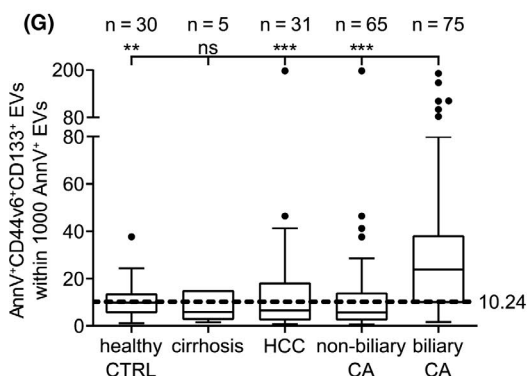
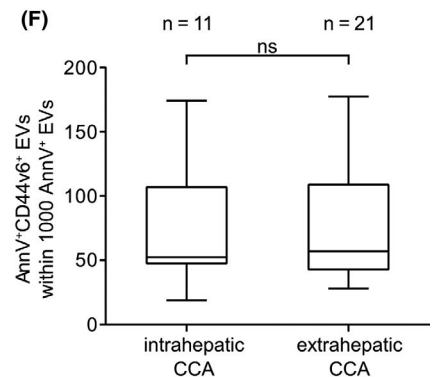
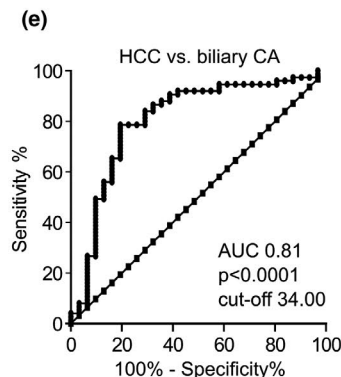
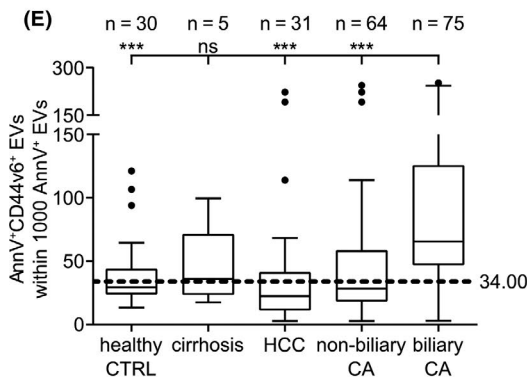
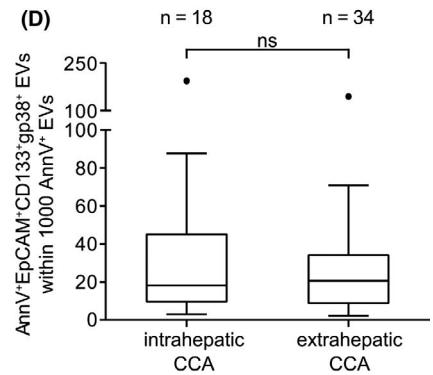
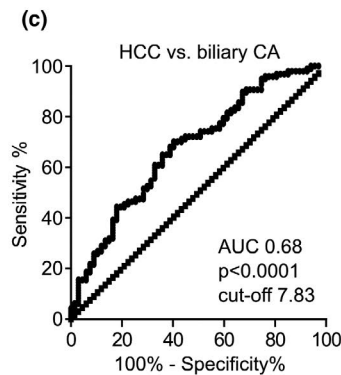
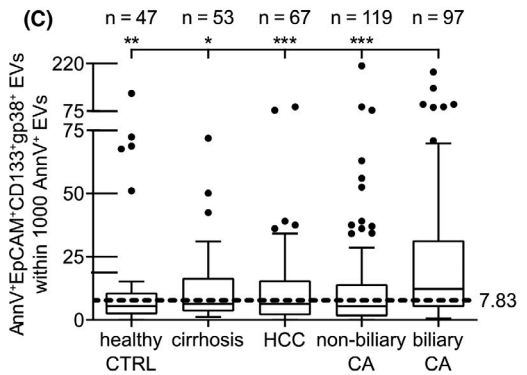
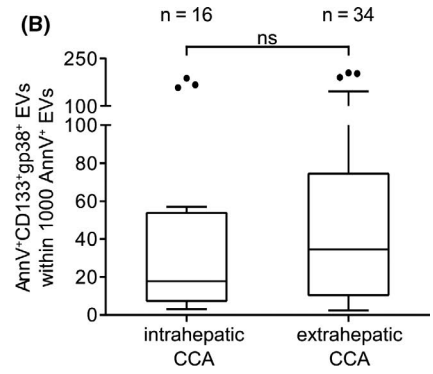
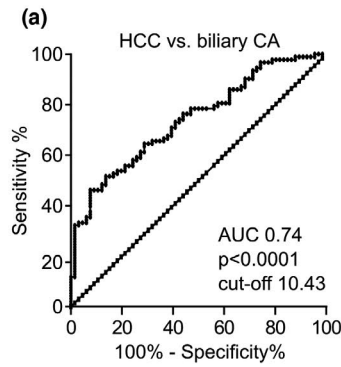
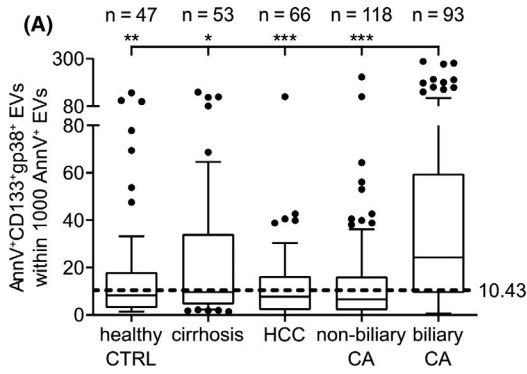


FIGURE 2 Explorative study – CD133, gp38, EpCAM and CD44v6 positive extracellular vesicles discriminate biliary cancer from healthy controls. EVs were isolated and characterized by FACS from serum of indicated biliary cancer patients (biliary CA, comprising GbCA and CCA patients) and healthy donors (healthy CTRL). Corresponding gating strategy and isotype controls are provided in Figure S5. Data shown represent medians with interquartile range (IQR), whiskers represent $1.5 \times$ IQR (Tukey) with outliers plotted as dots. (A–D) EV profiles for the populations $\text{AnnV}^+\text{CD133}^+\text{gp38}^+$ (A), $\text{AnnV}^+\text{EpCAM}^+\text{CD133}^+\text{gp38}^+$ (B), $\text{AnnV}^+\text{CD44v6}^+$ (C) and $\text{AnnV}^+\text{CD44v6}^+\text{CD133}^+$ (D) are depicted. Statistical significance was assessed by two-tailed Mann-Whitney *U* tests with $P \leq .05$ considered statistically significant (* = $P \leq .05$, ** = $P \leq .01$, *** = $P \leq .001$)

patients showed a 2.2-fold elevation as compared to healthy controls ($P \leq .01$) and non-biliary cancer patients ($P \leq .001$), respectively (biliary CA: median 12.3, healthy CTRL and non-biliary CA: median 5.5, respectively), and a 1.9-fold elevation as compared to HCC patients ($P \leq .001$; HCC: median 6.4) (Figure 3C). $\text{AnnV}^+\text{CD44v6}^+$ EV levels of biliary cancer patients were 2.2-fold elevated compared to healthy controls ($P \leq .001$; biliary CA: median 65.4, healthy CTRL: median 29.5), 2.9-fold elevated compared to HCC subjects ($P \leq .001$; HCC: median 22.4) and 2.3-fold elevated compared to non-biliary cancer patients ($P \leq .001$; non-biliary CA: median 28.5) (Figure 3E). $\text{AnnV}^+\text{CD44v6}^+\text{CD133}^+$ EV levels of biliary cancer patients showed a 2.4-fold increase as compared to healthy controls ($P \leq .01$; biliary

CA: median 23.8, healthy CTRL: median 9.9), a 3.7-fold increase as compared to HCC subjects ($P \leq .001$; HCC: median 6.5) and a 4.2-fold increase as compared to non-biliary cancer patients ($P \leq .001$; non-biliary CA: median 5.7) (Figure 3G). Considering the clinical importance of differential HCC/CCA diagnosis, ROC curves for all four EV populations were computed showing diagnostic AUC values ranging from 0.68 to 0.81 for biliary CA vs HCC (Figure 3A,C,E,G). We additionally evaluated the potential of EV profiling to differentially diagnose the biliary cancers GbCA and CCA (data not shown) but obtained no discriminatory findings. Furthermore, EV profiling did not yield a significant discrimination between CCAs of intra- or extrahepatic origin (Figure 3B,D,F,H).

FIGURE 3 Validation study – CD133, gp38, EpCAM and CD44v6 positive extracellular vesicles are comprehensive biomarkers for biliary cancer. EVs were isolated and characterized by FACS from serum of indicated cancer patients and healthy donors. Corresponding gating strategy and isotype controls are provided in Figure S5 and summarized patient characteristics can be found in Table 1. A, $\text{AnnV}^+\text{CD133}^+\text{gp38}^+$ EV profile for biliary (biliary CA) and non-biliary cancer patients (non-biliary CA) as well as for negative controls (HCC, cirrhosis and healthy CTRL). 'Biliary CA' combines GbCA and CCA patients. 'Non-biliary CA' comprises the cancer cohorts HCC, CRC and NSCLC. EV values for the individuals cohorts can be found in Figure S6. Data shown represent medians with interquartile range (IQR), whiskers represent $1.5 \times$ IQR (Tukey) with outliers plotted as dots. (a) depicts the corresponding ROC curve for $\text{AnnV}^+\text{CD133}^+\text{gp38}^+$ EVs including AUC and *P* values as well as the diagnostic cut-off for biliary CA vs HCC. EV profile for the populations $\text{AnnV}^+\text{EpCAM}^+\text{CD133}^+\text{gp38}^+$ (C), $\text{AnnV}^+\text{CD44v6}^+$ (E) and $\text{AnnV}^+\text{CD44v6}^+\text{CD133}^+$ (G) and their corresponding ROC curves (c, e, g, respectively) are depicted. Dotted lines indicate diagnostic cut-offs for discrimination between biliary CA and HCC for the respective EV population (see Table 2). Statistical significance was assessed by Kruskal-Wallis nonparametric test with 3 *df* followed by Dunn's Multiple Comparison post hoc test ($P \leq .05$). $\text{AnnV}^+\text{CD133}^+\text{gp38}^+$ (B), $\text{AnnV}^+\text{EpCAM}^+\text{CD133}^+\text{gp38}^+$ (D), $\text{AnnV}^+\text{CD44v6}^+$ (F) and $\text{AnnV}^+\text{CD44v6}^+\text{CD133}^+$ (H) EV profiles of intra- and extrahepatic CCA within the total CCA cohort are shown. Statistical significance was assessed by two-tailed Mann-Whitney *U* tests with $P \leq .05$ considered statistically significant (* = $P \leq .05$, ** = $P \leq .01$, *** = $P \leq .001$)



3.6 | Combining AFP and EV surface screening yields a diagnostically powerful biomarker for biliary cancer diagnosis as compared to HCC

Next, we addressed the question if our antigen combinations could be of diagnostic benefit when combined with other serum tumour markers that are already under investigation, especially in the context of differential HCC and CCA diagnosis. Therefore, we correlated serum AFP values, a serum tumour marker widely investigated in HCC diagnosis and surveillance, with serum EV levels of all four combinations for HCC and biliary cancer patients. Computed *r*-values (Spearman) ranging from -0.17 to 0.24 for HCC subjects and from -0.13 to 0.08 for biliary cancer patients revealed no significant correlation ($P > .05$) between the two parameters (Figure 4A). Consequently, AFP and EV levels can be considered as

two independent biomarkers. In a following step we evaluated the diagnostic performance of the two markers separately and in a combined approach by calculating sensitivity, specificity and positive and negative predictive values (Table 2). To assess the diagnostic potential of progenitor cell-derived EV populations ($\text{AnnV}^+\text{CD133}^+\text{gp38}^+$ and $\text{AnnV}^+\text{EpCAM}^+\text{CD133}^+\text{gp38}^+$ EVs) and tumour-associated EV populations ($\text{AnnV}^+\text{CD44v6}^+$ and $\text{AnnV}^+\text{CD44v6}^+\text{CD133}^+$ EVs) for detecting biliary cancers individually, we combined the respective EV populations into two separate cohorts and compared the results to serum AFP levels for each cohort. For combined analysis of AFP and EV populations biliary cancer patients were considered positive if they fulfilled the requirements for at least one of the parameters, for example, AFP below 20 ng/mL or EV levels above the respective cut-off or both, and vice versa for patients with HCC. Twenty ng/mL represents the screening cut-off for HCC surveillance as

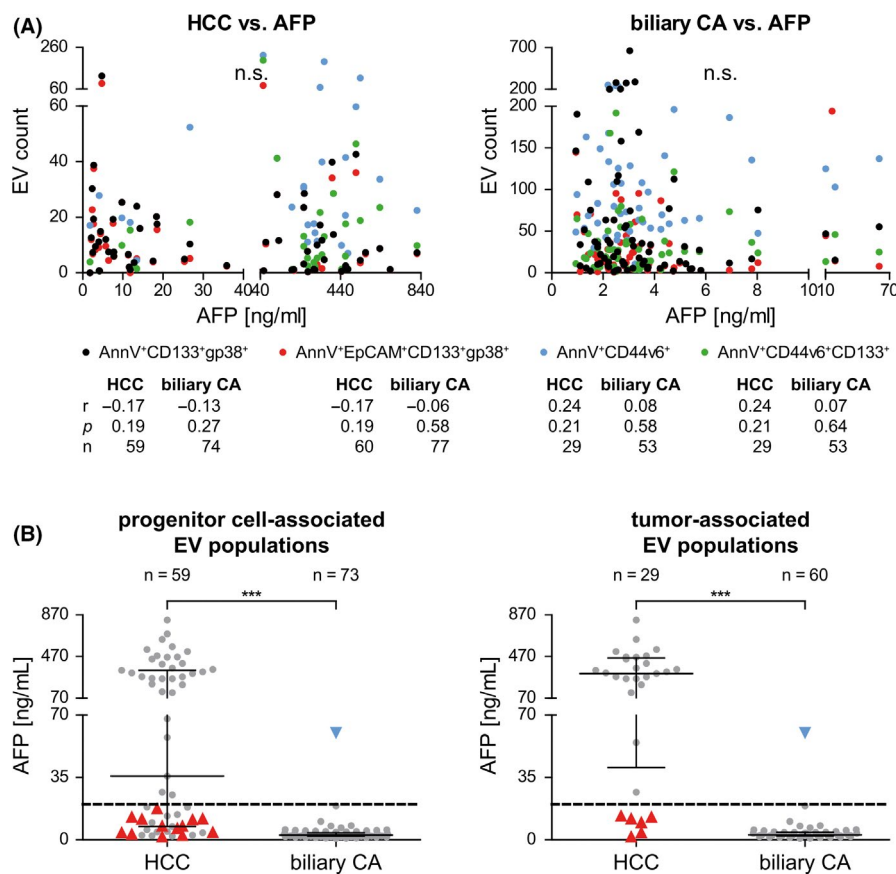


FIGURE 4 Combined analysis of AFP levels and EV profiling reliably discriminates HCC from biliary cancer. A, Correlation between AFP levels and EV counts from different populations for HCC (left panel) or biliary CA patients (right panel) are depicted. Two-tailed Spearman's correlation (*r*), *P* values and cohort sizes (*n*) are indicated for each population. B, Displayed are AFP values for HCC and biliary CA patients. In the left panel all patients with EV profiles for progenitor cell-associated EV populations ($\text{AnnV}^+\text{CD133}^+\text{gp38}^+$ and $\text{AnnV}^+\text{EpCAM}^+\text{CD133}^+\text{gp38}^+$) are included, whereas in the right panel all patients with EV profiles for tumour-associated EV populations ($\text{AnnV}^+\text{CD44v6}^+$ and $\text{AnnV}^+\text{CD44v6}^+\text{CD133}^+$) are included. Indicated in red are patients that based on AFP levels are not classified as HCC patients (AFP $< 20\text{ ng/mL}$) but can positively be identified as HCC by $\text{AnnV}^+\text{CD133}^+\text{gp38}^+$ EVs (left panel, EVs < 10.43) or $\text{AnnV}^+\text{CD44v6}^+$ EVs (right panel, EVs < 34). Indicated in blue are biliary CA patients that are not classified as such according to AFP levels (AFP $> 20\text{ ng/mL}$) but can be identified as biliary CA by $\text{AnnV}^+\text{CD133}^+\text{gp38}^+$ EVs (left panel, EVs > 10.43) or $\text{AnnV}^+\text{CD44v6}^+$ EVs (right panel, EVs > 34). Corresponding diagnostic values can be found in Table 2. Dotted line indicates diagnostic cut-off of 20 ng/mL for AFP. Statistical significance was assessed by two-tailed Mann-Whitney *U* tests with $P \leq .05$ considered statistically significant ($* = P \leq .05$, $** = P \leq .01$, $*** = P \leq .001$, n.s. = non significant)

TABLE 2 Diagnostic performance of the indicated EV populations individually and combined with AFP in biliary cancers (GbCA and CCA) as compared to HCC. Depicted are diagnostically relevant cut-offs (AFP: ng/mL, EVs: number per 10^3 AnnV⁺ EVs) as well as sensitivities, specificities, positive (PPV) and negative predictive values (NPV). n indicates cohort size, (*combined AUROC were not calculated)

Progenitor cell-associated EVs (biliary CA: n = 73, HCC: n = 59)	AUROC	P-value	Cut-off	Sensitivity [%]	Specificity [%]	PPV [%]	NPV [%]
AnnV ⁺ CD133 ⁺ gp38 ⁺	0.74	<.0001	10.43	72.6	59.3	68.8	63.6
AnnV ⁺ EpCAM ⁺ CD133 ⁺ gp38 ⁺	0.68	<.0001	7.83	71.2	59.3	68.4	62.5
AFP	0.89	<.0001	20.00	98.6	54.2	72.7	97.0
AFP and AnnV ⁺ CD133 ⁺ gp38 ⁺	*	*	20.00 and 10.43	100.0	76.3	83.9	100.0
AFP and AnnV ⁺ EpCAM ⁺ CD133 ⁺ gp38 ⁺	*	*	20.00 and 7.83	100.0	76.3	83.9	100.0
Tumour-associated EVs (biliary CA: n = 60, HCC: n = 29)	AUROC	P-value	Cut-off	Sensitivity [%]	Specificity [%]	PPV [%]	NPV [%]
AnnV ⁺ CD44v6 ⁺	0.81	<.0001	34.00	91.7	69.0	85.9	80.0
AnnV ⁺ CD44v6 ⁺ CD133 ⁺	0.75	<.0001	10.24	81.7	58.6	80.3	60.7
AFP	0.95	<.0001	20.00	98.3	79.3	90.8	95.8
AFP and AnnV ⁺ CD44v6 ⁺	*	*	20.00 and 34.00	100.0	100.0	100.0	100.0
AFP and AnnV ⁺ CD44v6 ⁺ CD133 ⁺	*	*	20.00 and 10.24	100.0	96.6	98.4	100.0

recommended by the AASLD and EASL Clinical Practice Guidelines for the Management of Hepatocellular Carcinoma.^{27,28} For biliary cancer diagnosis, progenitor cell-associated EV populations showed sensitivities ranging from 71%-73% and positive predictive values (PPVs) of 68%, respectively, while specificities (59%, respectively) and negative predictive values (NPVs; 63%-64%) were less diagnostically relevant. AFP as a tumour marker by itself achieved very good diagnostic values with 98.6% sensitivity and a NPV of 97%, although lacking in specificity (54.2) and PPV (72.7%). Interestingly, by combining AFP and progenitor cell-associated EV levels, sensitivity and NPV were increased to 100%, respectively, while simultaneously increasing specificity to 76.3% and PPV to 83.9%. In respect to tumour-associated EV populations in biliary cancer diagnosis, they showed a better diagnostic performance than progenitor cell-associated EVs (sensitivities: 81.7%-91.7%, specificities: 58.6%-69.0%, PPVs: 80.3%-85.9%, NPVs: 60.7%-80.0%) and were only slightly surpassed by the diagnostic values for AFP in this cohort (sensitivity: 98.3%, specificity: 79.3%, PPV: 90.8%, NPV: 95.8%). Interestingly, sensitivity and NPV could be increased to 100%, when combining AFP levels with AnnV⁺CD44v6⁺CD133⁺ EVs, while simultaneously specificity and PPV reached very good diagnostic values of 96.9% and 98.4% respectively. Most importantly, sensitivity, specificity, PPV and NPV all achieved 100%, when combining AFP levels with AnnV⁺CD44v6⁺ EVs.

In Figure 4B AFP values of HCC and biliary cancer patients are displayed, separated into the two EV population cohorts (progenitor cell- or tumour-associated). It represents an illustration of the diagnostic values obtained in Table 2 and indicates patients that, based on AFP values, could additionally be identified as patients with HCC (red) or as biliary cancer patients (blue) by AnnV⁺CD133⁺gp38⁺ EVs (left panel) and AnnV⁺CD44v6⁺ EVs (right panel), thus highlighting the benefit of a combined analysis. Furthermore, we investigated, if

combining CA19-9, a proposed tumour marker for bilio-pancreatic cancer diagnosis,²⁹ and our EV populations in the same manner as with AFP could be of diagnostic benefit but did not obtain better results (data not shown). Additionally, we evaluated if EV levels correlated with TNM stage or extent of metastatic spread of HCC and biliary tumours but did not observe any significant correlations (data not shown).

4 | DISCUSSION

Recently, we showed that a minimally invasive, liquid biopsy-based approach involving large EVs is advantageous for detecting hepatobiliary malignancies, however, without being able to discriminate between them.⁸ Here, in this subsequent study the potential of large EVs as a diagnostic biomarker for biliary cancer was investigated, in order to detect and differentiate between those malignancies. Except for ultrasonography (US) in patients suffering from gallstones as a possible indication for a given GbCA risk, early detection presents difficult.²⁹⁻³² Furthermore, GbCA diagnosis often only occurs incidentally during pathological assessment of routine cholecystectomy specimens due to benign diseases such as gallstones.³³ Hence, biliary cancers are highly fatal diseases, characterized by high mortality and poor 5-year survival rates.^{5,6} Therefore, several specialist societies such as ENS-CCA and ESMO are strongly in favour of developing new tools for (early and specific) biliary cancer diagnosis.^{3,29}

Podoplanin, alias gp38, is a novel yet not completely understood player in tumour immunology, tumour progression and recurrence besides being a liver progenitor cell marker.^{21,22,34,35} Since hepatic progenitor cells are activated in most chronic liver diseases and apparently are associated with hepatic carcinogenesis,³⁶ increasingly appearing liver progenitor cells during chronic hepatic inflammation

could potentially reveal the presence of hepatobiliary cancers. These liver progenitor cells were typically identified as double positive for CD133 and podoplanin.²¹ Furthermore, podoplanin is regarded as a potential marker for tumour-initializing cells (TICs) with stem cell-like properties, defined by their self-renewal, differentiation and tumour initiation capacities.³⁷ EpCAM is highly overexpressed and associated with various cancer entities in regard to cancer prognosis and cancer targeting.³⁸ We reported its feasibility as part of a diagnostic biomarker combination on large EVs.^{8,9,39} Moreover simultaneous expression of EpCAM and CD133 has been found to be strongly increased in biliary cancer and to be related to progression, invasive and metastatic behaviour and prognosis.⁴⁰

Since both CD44v6 as well as CD133 are well-established tumour stem cell and cancer markers for gallbladder carcinoma, CCA and other cancers, their single as well as combined expression on EVs was additionally of interest.⁴¹⁻⁴⁴ Antigen expression analyses on CCA cell line-derived EVs and CCA and HCC cell lines supported our hypothesis of gp38, CD133, EpCAM and CD44v6 being suitable markers (Figure 1A,B; Figure S1), hence we tested the indicated EV antigen combination being simultaneously positive for these. The human cancer cell line expression profiles indicated that CD44v6 might be of interest for CCA and HCC differentiation, since CD44v6 was highly differentially expressed on the investigated CCA and HCC cell lines (Figure 1B). The murine data suggested that CD133⁺gp38⁺ and EpCAM⁺CD133⁺gp38⁺ progenitor cell subsets as well as CD44⁺ and CD44⁺CD133⁺ tumour-associated subsets in fact were detectable under steady state conditions in varying amounts in murine liver, gallbladder, lung and colon (Figure 1D,E). Interestingly, murine gallbladder showed the highest expression of double positive CD44⁺CD133⁺ cells, which is consistent with the finding that these double positive primary human gallbladder carcinoma cells displayed cancer stem cell-like characteristics, highlighting their important role in gallbladder carcinogenesis.⁴⁵ Although not every marker combination was detectable in every organ, one has to keep in mind that a lack of expression in a healthy mouse model does not necessarily correlate with expression levels in a tumour environment. Our hypothesis of the benefit of the proposed progenitor cell-associated and tumour-associated EV populations for hepatobiliary cancer diagnosis was further supported by our explorative study, revealing significantly elevated EV levels in 10 patients with biliary cancer as compared to 10 healthy controls for all four combinations (Figure 2A-D). In a next step, we verified our preliminary results in a large validation study associated with the needed power to be conclusive and additionally including several cancer cohorts as negative controls, namely HCC, CRC and NSCLC. The group analysis between healthy donors, HCC, non-biliary cancer and biliary cancer entities showed that AnnV⁺CD133⁺gp38⁺, AnnV⁺EpCAM⁺CD133⁺gp38⁺, AnnV⁺CD44v6⁺ and AnnV⁺CD44v6⁺CD133⁺ EVs all were significantly elevated in biliary cancers and remained low in the indicated negative controls (Figure 3A,C,E,G). Except for CD44v6 singular expression profile analysis of CD133, EpCAM and gp38 on EVs were not beneficial (data not shown). With an AUC value of 0.81 AnnV⁺CD44v6⁺ EVs were the most powerful biomarker for biliary

cancer detection in this study. Our observation that patients with biliary cancer display elevated levels of AnnV⁺CD44v6⁺ EVs is consistent with previous findings that demonstrated by immunohistochemistry and real time PCR, that CD44v6 is not detected in healthy gallbladder mucosa, but strongly expressed in GbCA.⁴⁶ High CD44v6⁺ EV levels in both GbCA and CCA concur with observations that linked increased CD44v6 expression in biliary epithelium of both gallbladder and bile ducts to cancer progression.⁴⁷ We have to note that our selected EV antigens were not capable of distinguishing between intra- and extrahepatic CCA and between GbCA and CCA. This might be due to the fact that there exists a more optimal EV antigen combination for these discriminations, but we doubt that any EV surface antigen or antigen combinations will have the needed sensitivity to differentiate between intra- and extrahepatic CCA. From the surface antigenic view we do not expect any differences caused by a different location of the primary CCA tumour. We suppose that intra-vesicular differences on protein, mRNA or miRNA levels might be noticeable due to an environment-dependent interaction of the EV donor CCA cells.

Next the question arose, if our EV-based phenotyping could be improved and if synergistic effects could be observed by taking advantage of other serological screening markers such as AFP (Figure 4). AFP is a widely investigated serum tumour marker for HCC, whose use for diagnostic purposes is not recommended by the AASLD and EASL Clinical Practice Guidelines for the Management of Hepatocellular Carcinoma, whereas it has proven beneficial for HCC surveillance at a cut-off of 20 ng/mL.^{27,28} In contrast to the recommendations of the AASLD/EASL guidelines, serum AFP levels by itself, at a cut-off of 20 ng/mL, showed a diagnostic capacity for differentially diagnosing HCC and biliary cancers in this study, surpassing the performance of our investigated EV populations (Table 2). However, importantly, the diagnostic performance of AFP could be enhanced, when combined with EV levels, especially when combining it with the tumour-associated EV populations AnnV⁺CD44v6⁺ and AnnV⁺CD44v6⁺CD133⁺. Remarkably, the combination of AnnV⁺CD44v6⁺ EVs and AFP values led to a perfect separation of biliary cancer and HCC patients, with sensitivity, specificity, PPV and NPV all achieving 100%. Biliary cancers are commonly associated with low AFP levels. Except for one patient, this observation was confirmed in our study. The patient in question might display a mixed hepatocellular cholangiocarcinoma, which would explain the slightly elevated AFP levels. According to the AASLD and EASL Clinical Practice Guidelines HCCs cannot reliably be detected by AFP values alone,^{27,28} which was confirmed in our study. However, depending on the EV population added to the analysis, all or almost all previously undetected HCCs with low AFP values could be correctly diagnosed. Thus, our synergistic approach illustrates the benefit of adding EV levels to AFP-based diagnosis. It might have particular clinical relevance for differential hepatobiliary cancer detection and should be followed up by a large multi-centre study. A current alternative serum biomarker for biliary cancer diagnosis as proposed by the ESMO Clinical Practice Guidelines is CA 19-9²⁹ but it is associated with low sensitivity and specificity of 62% and 63%,

respectively,^{32,48} and is not suitable to discriminate between cancer entities. Several serum biomarkers and metabolites have been identified as potential candidates for minimal invasive discrimination of HCC and intrahepatic CCA^{10,49} but until now no liquid biopsy marker achieving a better clinically useful performance exists underlining the relevance of our study in terms of hepatobiliary cancer management. Moreover screening EVs offers a cheap, minimally invasive technique to detect cancer, while causing minimum distress to the patient. To perform an EV liquid biopsy screen only a small blood sample is required. For most patients, drawing blood is an uncritical and acceptable procedure. It requires minimum equipment and is performed quickly without special need for long medical observation afterwards. Therefore, EV profiling represents a potent tool for early cancer screening as discussed by others and us.^{9,16,49}

5 | CONCLUSION

In summary, our study provides valuable data arguing that EV phenotyping together with AFP assessment is a powerful diagnostic biomarker in detection and differentiation of hepatobiliary cancers. We presented four EV surface antigen combinations that confidently differentiated between patients with biliary cancer and HCC and whose performance could even be enhanced by combined AFP measurements. Considering the results of this and other studies, liquid biopsy-based differential diagnosis of hepatobiliary cancers might be in reach.

ETHICS APPROVAL AND CONSENT OF PARTICIPATION

The Ethics commissions of (i) the State Chambers of Medicine in Rhineland-Palatinate, Germany approval number: 837.151.13 (8836-F); (ii) Saarland, Germany (167/11); (iii) San Sebastian, Spain (PI2014187); (iv) Warsaw, Poland (KB/41/A/2016 and AKB/145/2014) and (v) Cluj-Napoca, Romania (3042/07.03.2018) approved this study. All patients gave their informed consent.

ACKNOWLEDGEMENTS

The authors thank the organizers of the EASL HCC Summit 2018 in Geneva, the EASL ILC 2018 in Paris and the ENS-CCA II Biennial Congress 2018 in Rome for the possibility to present parts of this work in invited talks. Additionally, the authors thank Björn Zapke from Dr Lukacs-Kornek's lab, University of Bonn, for his valuable inputs and assistance during the Nano Tracking Analysis (NTA) of EVs.

CONFLICT OF INTEREST

The authors declare that they have no conflict of interests.

AUTHORS' CONTRIBUTIONS

M.Ko contributed to conceptualization and supervision. SKU, HJ-H., HS and M.Ko contributed to methodology. M.Kr, A.Wi., JL, MA, TM, CK, BK, KJ, WP, Marek K., KZ, WH, Ł.K., MR, KG, WW, RK, JR-W., AS, RS, A.Wö., MG-C., SG, ZS, JMB, CPS, FL, PM and M.Ko contributed to resources. SKU, HS, HJ-H. and M.A contributed to investigation. SKU,

HS, M.Kr, MA HJ-H. and M.Ko contributed to formal analysis. M.Ko contributed to project administration. M.Ko contributed to funding acquisition. SKU, HS and M.Ko contributed to writing – original draft.

ORCID

Jesus M. Banales  <https://orcid.org/0000-0002-5224-2373>

Christian P. Strassburg  <https://orcid.org/0000-0001-7870-5359>

Frank Lammert  <https://orcid.org/0000-0003-4450-7201>

Piotr Milkiewicz  <https://orcid.org/0000-0002-1817-0724>

Mirosław Kornek  <https://orcid.org/0000-0002-1682-1765>

REFERENCES

1. Cancer.Net ASoCOA. Gallbladder cancer – medical illustrations. *CancerNet Articles*. 2012.
2. Lewis DR, Chen H-S, Cockburn MG, et al. Early estimates of SEER cancer incidence, 2014. *Cancer*. 2017;123(13):2524–2534.
3. Banales JM, Cardinale V, Carpino G, et al. Expert consensus document: cholangiocarcinoma: current knowledge and future perspectives consensus statement from the European Network for the Study of Cholangiocarcinoma (ENS-CCA). *Nat Rev Gastroenterol Hepatol*. 2016;13(5):261–280.
4. Lazcano-Ponce EC, Miquel JF, Munoz N, et al. Epidemiology and molecular pathology of gallbladder cancer. *CA Cancer J Clin*. 2001;51(6):349–364.
5. Guglielmi A, Ruzzenente A, Campagnaro T, et al. Intrahepatic cholangiocarcinoma: prognostic factors after surgical resection. *World J Surg*. 2009;33(6):1247–1254.
6. Levy AD, Murakata LA, Rohrmann Jr CA. Gallbladder carcinoma: radiologic-pathologic correlation. *Radiographics*. 2001;21(2):295–314; questionnaire, 549–255.
7. Lang H, Sotiropoulos GC, Frühauf NR, et al. Extended hepatectomy for intrahepatic cholangiocellular carcinoma (ICC): when is it worthwhile? Single center experience with 27 resections in 50 patients over a 5-year period. *Ann Surg*. 2005;241(1):134–143.
8. Julich-Haertel H, Urban SK, Krawczyk M, et al. Cancer-associated circulating large extracellular vesicles in cholangiocarcinoma and hepatocellular carcinoma. *J Hepatol*. 2017;67:282–292.
9. Julich H, Willms A, Lukacs-Kornek V, Kornek M. Extracellular vesicle profiling and their use as potential disease specific biomarker. *Front Immunol*. 2014;5:1–6.
10. Arbelaz A, Azkargorta M, Krawczyk M, et al. Serum extracellular vesicles contain protein biomarkers for primary sclerosing cholangitis and cholangiocarcinoma. *Hepatology*. 2017;66(4):1125–1143.
11. Melo SA, Luecke LB, Kahlert C, et al. Glypican-1 identifies cancer exosomes and detects early pancreatic cancer. *Nature*. 2015;523:177–182.
12. Théry C, Witwer KW, Aikawa E, et al. Minimal information for studies of extracellular vesicles 2018 (MISEV2018): a position statement of the International Society for Extracellular Vesicles and update of the MISEV2014 guidelines. *J Extracell Vesicles*. 2018;7(1):1535750.
13. Kornek M, Schuppan D. Microparticles: Modulators and biomarkers of liver disease. *J Hepatol*. 2012;57:1144–1146.
14. Shao H, Chung J, Balaj L, et al. Protein typing of circulating microvesicles allows real-time monitoring of glioblastoma therapy. *Nat Med*. 2012;18:1835–1840.
15. Mocan T, Simão AL, Castro RE, et al. Liquid biopsies in hepatocellular carcinoma: are we winning? *J Clin Med*. 2020;9(5).
16. Urban SK, Mocan T, Sanger H, Lukacs-Kornek V, Kornek M. Extracellular vesicles in liver diseases: diagnostic, prognostic, and therapeutic application. *Semin Liver Dis*. 2019;39(1):70–77.
17. Macias RIR, Kornek M, Rodrigues PM, et al. Diagnostic and prognostic biomarkers in cholangiocarcinoma. *Liver Int*. 2019;39(Suppl 1):108–122.

18. Julich-Haertel H, Tiwari M, Mehrfeld C, Krause E, Kornek M, Lukacs-Kornek V. Isolation and enrichment of liver progenitor subsets identified by a novel surface marker combination. *J Vis Exp*. 2017(120).
19. Lukacs-Kornek V, Julich-Haertel H, Urban SK, Kornek M. Multi-surface antigen staining of larger extracellular vesicles. *Methods Mol Biol*. 2017;1660:201-208.
20. Gu MJ, Jang BI. Clinicopathologic significance of Sox2, CD44 and CD44v6 expression in intrahepatic cholangiocarcinoma. *Pathol Oncol Res*. 2014;20(3):655-660.
21. Eckert C, Kim YO, Julich H, et al. Podoplanin discriminates distinct stromal cell populations and a novel progenitor subset in the liver. *American J Physiol-Gastrointestinal Liver Physiol*. 2016;310:G1-G12.
22. Astarita JL, Acton SE, Turley SJ. Podoplanin: emerging functions in development, the immune system, and cancer. *Front Immunol*. 2012;3:283.
23. Quintanilla M, Montero-Montero L, Renart J, Martín-Villar E. Podoplanin in inflammation and cancer. *Int J Mol Sci*. 2019;20(3).
24. Cioca A, Ceausu AR, Marin I, Raica M, Cimpean AM. The multifaceted role of podoplanin expression in hepatocellular carcinoma. *Eur J Histochem*. 2017;61(1):2707.
25. Lötvall J, Hill AF, Hochberg F, et al. Minimal experimental requirements for definition of extracellular vesicles and their functions: a position statement from the International Society for Extracellular Vesicles. *J Extracell Vesicles*. 2014;3:26913.
26. Ettelaie C, Collier ME, Maraveyas A, Ettelaie R. Characterization of physical properties of tissue factor-containing microvesicles and a comparison of ultracentrifuge-based recovery procedures. *J Extracell Vesicles*. 2014;3.
27. Marrero JA, Kulik LM, Sirlin CB, et al. Diagnosis, staging, and management of hepatocellular carcinoma: 2018 practice guidance by the American Association for the Study of Liver Diseases. *Hepatology*. 2018;68(2):723-750.
28. European Association for the Study of the Liver. Electronic address eee, European Association for the Study of the L. EASL clinical practice guidelines: management of hepatocellular carcinoma. *J Hepatol*. 2018;69(1):182-236.
29. Valle JW, Borbath I, Khan SA, et al. Biliary cancer: ESMO Clinical Practice Guidelines for diagnosis, treatment and follow-up. *Ann Oncol*. 2016;27(suppl 5):v28-v37.
30. Tian Y, Liu L, Yeolkar NV, Shen F, Li J, He Z. Diagnostic role of staging laparoscopy in a subset of biliary cancers: a meta-analysis. *ANZ J Surg*. 2017;87(1-2):22-27.
31. Wang W, Fei Y, Wang F. Meta-analysis of contrast-enhanced ultrasonography for the detection of gallbladder carcinoma. *Med Ultrason*. 2016;18(3):281-7.
32. Bridgewater J, Galle PR, Khan SA, et al. Guidelines for the diagnosis and management of intrahepatic cholangiocarcinoma. *J Hepatol*. 2014;60:1268-1289.
33. Dorobisz T, Dorobisz K, Chabowski M, et al. Incidental gallbladder cancer after cholecystectomy: 1990 to 2014. *Oncotargets and Therapy*. 2016;9:4913-4916.
34. Lukacs-Kornek V, Lammert F. The progenitor cell dilemma: Cellular and functional heterogeneity in assistance or escalation of liver injury. *J Hepatol*. 2017;66(3):619-630.
35. Wicki A, Lehembre F, Wick N, Hantusch B, Kerjaschki D, Christofori G. Tumor invasion in the absence of epithelial-mesenchymal transition: podoplanin-mediated remodeling of the actin cytoskeleton. *Cancer Cell*. 2006;9(4):261-272.
36. Roskams T. Liver stem cells and their implication in hepatocellular and cholangiocarcinoma. *Oncogene*. 2006;25:3818-3822.
37. Atsumi N, Ishii G, Kojima M, Sanada M, Fujii S, Ochiai A. Podoplanin, a novel marker of tumor-initiating cells in human squamous cell carcinoma A431. *Biochem Biophys Res Commun*. 2008;373(1):36-41.
38. Baeuerle PA, Gires O. EpCAM (CD326) finding its role in cancer. *Br J Cancer*. 2007;96(3):417-423.
39. Willms A, Muller C, Julich H, et al. Tumour-associated circulating microparticles: a novel liquid biopsy tool for screening and therapy monitoring of colorectal carcinoma and other epithelial neoplasia. *Oncotarget*. 2016;7(21):30867-30875.
40. Jiang S, Pei L, Yang Z-L, Liu G. Prognostic value of the stem cell markers Epcam and CD133 expression of gallbladder adenocarcinoma. *Hepatogastroenterology*. 2014;61:574-579.
41. Wang J, Wu Y, Gao W, et al. Identification and characterization of CD133(+)/CD44(+) cancer stem cells from human laryngeal squamous cell carcinoma cell lines. *J Cancer*. 2017;8(3):497-506.
42. Yu J, Tang Z, Gong W, Zhang M, Quan Z. Isolation and identification of tumor-initiating cell properties in human gallbladder cancer cell lines using the marker cluster of differentiation 133. *Oncol Lett*. 2017;14(6):7111-7120.
43. Suzuki A, Sekiya S, Onishi M, et al. Flow cytometric isolation and clonal identification of self-renewing bipotent hepatic progenitor cells in adult mouse liver. *Hepatology*. 2008;48(6):1964-1978.
44. Ashida K, Terada T, Kitamura Y, Kaibara N. Expression of E-cadherin, alpha-catenin, beta-catenin, and CD44 (standard and variant isoforms) in human cholangiocarcinoma: an immunohistochemical study. *Hepatology*. 1998;27:974-982.
45. Shi C, Tian R, Wang M, et al. CD44+ CD133+ population exhibits cancer stem cell-like characteristics in human gallbladder carcinoma. *Cancer Biol Ther*. 2010;10(11):1182-1190.
46. Yanagisawa N, Mikami T, Mitomi H, Saegusa M, Koike M, Okayasu I. CD44 variant overexpression in gallbladder carcinoma associated with tumor dedifferentiation. *Cancer*. 2001;91:408-416.
47. Tsuchida A, Nagakawa Y, Kasuya K, et al. Significance of CD44s and CD44v6 expression in pancreaticobiliary maljunction. *Hepatogastroenterology*. 2011;58:1877-1881.
48. Rupesh P, Manoj P, Vijay KS. Biomarkers in carcinoma of the gallbladder. *Expert Opin Med Diagn*. 2008;2(5):511-526.
49. Banales JM, Iñarrairaegui M, Arbelaz A, et al. Serum metabolites as diagnostic biomarkers for cholangiocarcinoma, hepatocellular carcinoma, and primary sclerosing cholangitis. *Hepatology*. 2019;70(2):547-562.

SUPPORTING INFORMATION

Additional supporting information may be found online in the Supporting Information section.

How to cite this article: Urban SK, Sängler H, Krawczyk M, et al. Synergistic effects of extracellular vesicle phenotyping and AFP in hepatobiliary cancer differentiation. *Liver Int*. 2020;40:3103–3116. <https://doi.org/10.1111/liv.14585>